Geosynthetic Reinforced Soils for Bridge Approach Slab Support

Research Final Report from The University of Tennessee-Knoxville | Khalid A. Alshibli, Wadi H. Imseeh | November 15, 2021

Sponsored by Tennessee Department of Transportation Long Range Planning Research Office & Federal Highway Administration

THE UNIVERSITY OF TENNESSEE KNOXVILLE

DISCLAIMER

This research was funded through the State Planning and Research (SPR) Program by the Tennessee Department of Transportation and the Federal Highway Administration under ***RES2019-22, Research Project Title: Geosynthetic Reinforced Soils for Bridge Approach Slab Support.***

Technical Report Documentation Page

1. Report No. RES2019-22	2. Government Accession No.	3. Recipient's Catalog No.
4. Title and Subtitle *Geosynthetic Reinforced Soils for Bridge Approach Slab Support*		5. Report Date Nov. 2021
		6. Performing Organization Code
7. Author(s) Dr. Khalid A. Alshibli Dr. Wadi H. Imseeh		8. Performing Organization Report No.
9. Performing Organization Name and Address The University of Tennessee, Knoxville 422 John Tickle Building, 851 Neyland Drive Knoxville, TN, 37996-2313		10. Work Unit No. (TRAIS)
		11. Contract or Grant No. Z19RES22
12. Sponsoring Agency Name and Address Tennessee Department of Transportation 505 Deaderick Street, Suite 900 Nashville, TN 37243		13. Type of Report and Period Covered Final (12/01/2018-02/28/2022)
		14. Sponsoring Agency Code
15. Supplementary Notes		

16. Abstract

Two approach slabs are constructed at bridge ends to serve as a smooth transition from the highway pavement to the bridge deck. Motorists usually complain about a sudden change in elevation (bump) at the highway/approach slab (H/S) joint that causes a potential hazard for public safety, damage to vehicles, and riders' discomfort. Many US States conducted research to solve the problem of bridge bumps with mixed degrees of success. In this project, the finite element (FE) method was used to predict the differential settlement at the H/S joint when supported by a strip footing (sleeper slab) that sits on compacted layers of soil embankment with geogrid reinforcement. A parametric study was conducted to select the optimum design which consists of 4 geogrid layers and a layer of woven polypropylene geotextile to separate the embankment clay from the reinforced aggregate fill. The geogrid layers are equally-spaced within a depth of $2 \times B$ below the strip footing, where B is the width of the footing. The inclusion of geogrid reinforcement did not only enhance the ultimate bearing stress of the strip footing but also redistributed the vertical loads over a wider region of soil embankment and thus reduced settlement. A case study is also presented for modeling the performance of a design recommended by the Tennessee Department of Transportation (TDOT) for the retrofit of the bridge ends. The recommended design suggests replacing soil embankment underneath the approach slab with 4 biaxial geogrid layers between 9-inch thick lifts of openly-graded aggregate and a layer of woven polypropylene geotextile to separate the embankment clay from the reinforced aggregate fill. The approach slab has a length of 24 ft and a thickness of 1 ft supported by a 3 ft sleeper slab (B = 3 ft) with a thickness of 1 ft.

17. Key Words **APPROACH SLAB, GEOSYNTHETIC REINFORCEMENT, SETTLEMENT, FINITE ELEMENT ANALYSIS**	18. Distribution Statement No restriction. This document is available to the public from the sponsoring agency at the website http://www.tn.gov		
19. Security Classif. (of this report) Unclassified	20. Security Classif. (of this page) Unclassified	21. No. of Pages 101	22. Price TBD

Acknowledgment

This research was funded through the State Research and Planning (SPR) Program by the Tennessee Department of Transportation and the Federal Highway Administration, State Project number RES2019-22.

The research team would like to thank graduate student Mohammed Elnur for his valuable help in formatting the final report and graduate student Amirsalar Moslehy who monitored field implementation at the bridge site. Also, we thank Dr. Murad Abu-Farsakh for serving as a consultant for the project and his help in finite element modeling. We would like to thank the TDOT Structures Division engineers for their valuable comments, guidance, and suggestions.

Executive Summary

The United States (US) has approximately 600,000 bridges among which 25% (~150,000) suffer from bumps at their ends and about $100 million/year is spent by the US departments of transportation (DOTs) on the repair of this issue (Briaud, 1997). Identifying the causes of these bumps and feasible solutions is a very challenging task because of the many factors involved in the problem, such as soil embankment properties, bridge-to-highway joints, type of bridge abutment, compaction methods, and type of highway pavement. A typical section consists of a reinforced concrete approach slab supported by the bridge abutment from one side and compacted layers of soil embankment or select fill material at the side of the highway/approach slab (H/S) joint. The approach slab is prone to an inevitable amount of differential settlement since the bridge abutment is usually constructed using deep foundation systems that exhibit negligible settlement, while the compacted layers of highway embankment would settle. A strip footing is known as a "sleeper slab" can be constructed underneath the H/S joint to distribute the load and reduce the amount of differential settlement. According to a nationwide survey conducted by Ng, Yasrobi (2014), almost half of the responding US States were not satisfied with their current performance of bridge approaches. Therefore, many studies were funded by several US DOTs to investigate the causes of bumps at bridge approaches, and these studies have contributed to the development of several design provisions. As noted by Dupont and Allen [2006], it is also important for the cost of any improved design not to exceed the maintenance cost required throughout the life-cycle of an existing design. This report presented a summary of the research reported by other US States and lessons learned from different approaches used to eliminate or reduce differential settlement.

Reinforcing the soil embankment underneath the sleeper slab with geosynthetics would improve the soil's bearing capacity and reduce the embankment settlement by redistributing traffic loads exerted on the approach slab over a wider region. The research team conducted a finite element (FE) analysis for a typical bridge end section that consists of an approach slab, sleeper slab, bridge abutment, and compacted layer of soil embankment with or without the inclusion of geosynthetic reinforcement. The parametric study sought an optimum design of geosynthetic reinforcement that improves the ultimate bearing stress of the sleeper slab (UBSS) and reduced settlement by distributing vertical loads on a wider region of soil embankment. Several design parameters were investigated, such as the width of the sleeper, effective depth and length of geosynthetic reinforcement layers, and number/spacing between layers. A case study was then modeled for a preliminary geosynthetic reinforcement design that was proposed by TDOT for the retrofit of bridge ends. The FE analysis was utilized to predict UBSS for the proposed design by TDOT, as well as the approach slab differential settlement when subjected to service loads (i.e., dead and different types of highway traffic loads).

The design of bridge ends is specified by TDOT in standard drawing STD-5-1 and consists of a 3-foot wide sleeper slab (B= 3-ft, thickness T = 1ft) that supports a 24-foot long ($8 \times B$) by 1-foot thick approach slab at the H/S joint. Both the sleeper and approach slabs have special provisions for rebar reinforcement, the approach slab is tied to the standard integral abutment, and the sleeper slab for asphaltic highway pavement is typically constructed with a 1-foot wide mid-stem. TDOT has recently been reporting settlement issues with their current design of bridge ends, and most of the settlement occurs explicitly at the H/S joint. The settlement at the H/S joint is

randomly reported over the state and has not been attributed to a particular region with a specific type of soil embankment. This randomness has led the TDOT to suspect poor construction and compaction practices to be the major cause of settlement and has motivated the quest to develop a retrofit design to their current state of practice and just use one design for new construction and for the repair of bridges that exhibited excessive settlement at the end of the approach slab. The analysis was then used to evaluate the differential settlement of the TDOT and modified design under the effect of service loads, including dead loads and different types of traffic highway live loads.

Key Findings

- The effective depth of geogrid reinforcement reaches $2 \times B$ below the sleeper slab, where B is the width of the sleeper slab.
- Tensile strain along the geogrid layers is significant within a distance of $2 \times B$ surrounding the sleeper slab in the traffic direction.
- The geogrid manifests a peak tensile strain underneath the center of the sleeper slab when it is placed between a depth of 0.75 and $1.5 \times B$ below the sleeper slab, whereas two peak strains occur toward the sleeper slab sides when the layer is placed below $1.5 \times B$ or above $0.75 \times B$.
- An optimum design would require reinforcing the effective depth (2×B) with five layers of geogrid equally-spaced at $0.33 \times B$.
- The benefits of geogrid inclusion become less significant when B increases.
- UBSS of a preliminary design proposed by the TDOT can be improved by 30% when rearranging the geogrid reinforcement in a way that includes one additional layer but extending the reinforced depth of soil to be at least $1.25 \times B$.
- The settlement at both sides of the H/S joint was almost the same under service loads for the TDOT retrofit and recommended designs, which suggests no sudden change in elevation (bump) for crossing motorists.

Key Recommendations

Figure 4-1 in the report body presents the adopted design which is easy to implement for new construction and for repairing approach slabs for bridges in service. The proposed design suggests replacing soil embankment underneath the approach slab with 4 biaxial geogrid layers (Tensar Biaxial BX1200 or equivalent) between 9-inch thick lifts of openly-graded aggregate and a layer of woven polypropylene geotextile (Propex GEOTEX-315ST or equivalent) to separate the embankment clay from the reinforced aggregate fill. The geogrid layers are equally-spaced within a depth of $2 \times B$ below the strip footing, where B is the width of the footing.

Table of Contents

List of Tables

List of Figures

Glossary of Key Terms and Acronyms

A/S	Abutment/approach slab
ADT	Average Daily Traffic
DOT	Department of Transportation
FE	Finite Element
GRS	Geosynthetic
H/S	Highway/approach slab
HMA	Hot Mixed Asphalt
IBS	Integrated Bridge System
IM	Static load modification factor to account for dynamic impact
PCC	Portland Cement Concrete
HMA	Hot Mixed Asphalt
SS	Sleeper Slab
TDOT	Tennessee Department of Transportation
UBSS	Ultimate Bearing Stress of the Sleeper Slab

Chapter 1 Review of Literature Studies and Current Practices

1.1 Problem Description

The bridge approach slab serves as a structural transition element from the flexible highway pavement to the bridge deck. It is usually supported by a non-yielding bridge abutment on one side and the highway embankment on the other side. Referring to Figure 1-1, it is evident that the bridge approach slab is prone to an inevitable amount of differential settlement since the bridge abutment on one side is typically constructed using deep foundation systems that exhibit a very small settlement whereas the bridge adjoining pavement on the other side is constructed on multiple layers of fill embankment. The primary function of the bridge approach slab is to minimize the amount of differential settlement and to provide a smooth transition for vehicles. However, motorists usually complain about two uncomfortable bumps at the bridge ends, as illustrated in Figure 1-1. These bumps cause a potential hazard for public safety, significant damage to vehicles, and a reduction in driver's steering response.

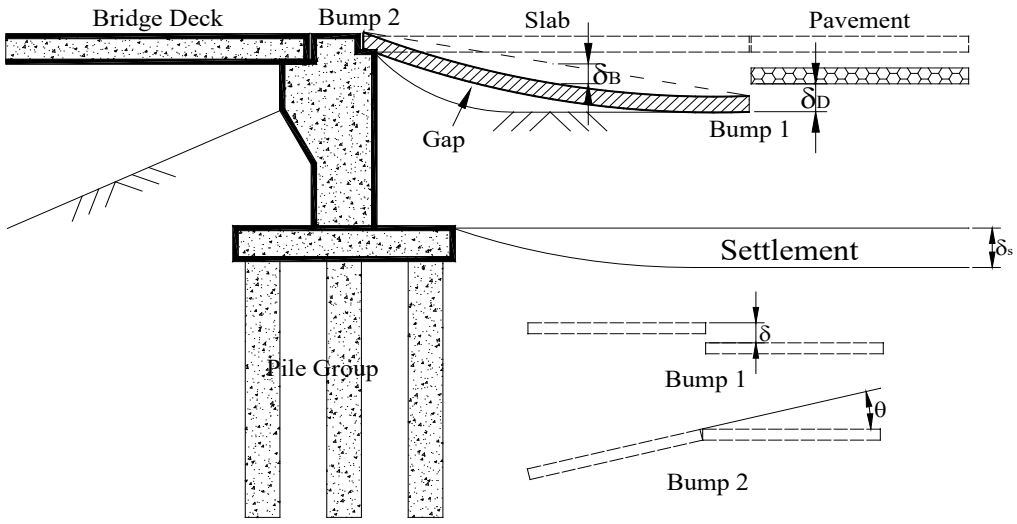

Figure 1-1. Schematic of a bridge approach slab (Abu-Farsakh and Chen 2014).

1.2 Causes of Bumps at Bridge Ends

Identifying the causes of settlement and feasible solutions for bridge approaches is a very complex task because of the many components involved in the development of the bumps at the bridge ends such as soil embankment properties, structural design of the bridge approach slab, bridge-to-highway joints, type of bridge abutment and its foundation system, highway construction methods, and the type of highway pavement. The development of the bumps at bridge ends has also been attributed to the horizontal forces exerted on the bridge abutment due to longitudinal pavement growth (Wicke and Stoelhorst 1982) or backfill soil pressure (Tadros and Benak 1989). Kramer and Sajer (1991) summarized the causes of bump development at the bridge approaches by three main

categories: differential settlement due to compression of foundation or embankment soils, vertical and horizontal movement of the bridge abutment, and poor design/construction practices such as the use of improper filling materials or lack of soil compaction. Figure 1-2 presents a summary of the major problems leading to the development of bumps at the bridge ends (Briaud 1997). Overall, the most commonly reported causes for the development of bumps at bridge ends include:

- Poor choice of embankment and backfill material.
- Improper compaction of backfill material and poor construction practices.
- Settlement of foundation soil due to extra stresses imposed by the embankment, approach slab, and traffic.
- Deflection and damage of the bridge approach slab due to its lack of flexural rigidity and the settlement of the embankment/backfill material.
- Change in the water content of backfill material, which can be caused by not choosing the optimum water content of backfill soil during construction, poor drainage, or improper protection of backfill material from surface runoff water.
- Thermal stresses of the bridge coupled with poor design of expansion joints. Improper design and lack of maintenance of expansion joints can be detrimental as they offer a path for water to seep through underlying backfill material or not enough room for bridge thermal expansion/contraction.
- Erosion of the backfill material due to poor design and construction.
- Lateral spreading of the embankment.

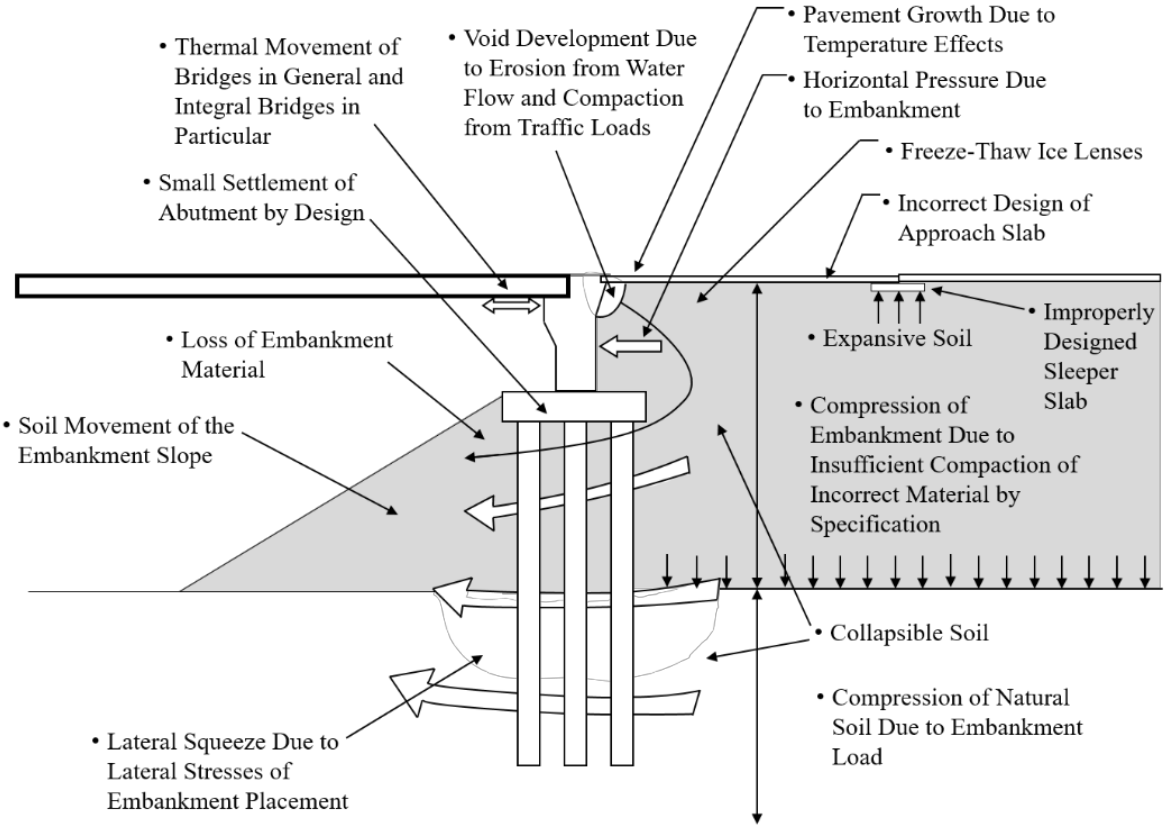

Figure 1-2. Synthesis of the main problems leading to the development of bumps at the bridge ends (Briaud 1997).

1.3 Literature Review

The United States has approximately 600,000 bridges, from which 25% (~150,000) suffer from bumps at their ends, and the amount of money spent by different DOTs on the repair of this issue is estimated to be around $100 million per year (Briaud 1997). Therefore, several comprehensive studies regarding the performance of bridge approaches have been funded by many DOTs to remedy this problem. This section summarizes the major findings of some final reports that were submitted to several DOTs regarding bridge approaches (listing is according to the alphabetic order of the States).

Colorado

- Hearn (1997) compared the settlements of bridge abutments constructed on deep versus shallow foundation systems and found no essential difference based on literature data for about 1,000 structures, including 350 bridges and 50 embankments. Hearn (1997) also reported that the median settlement of the embankments is about 3/8-inch higher than the bridge abutment and gave a relationship between the mean total and differential settlement at bridge ends: the ratio between differential to total settlement is about 1/3.
- Abu-Hejleh et al. (2006) recommended the use of mechanically stabilized earth (MSE) systems in the construction of the bridge approaches with softer (less dense) and thicker compressible (e.g., polystyrene) sheets installed in the upper zone of the abutment back wall to minimize the lateral earth pressure.

Delaware

- Talebi et al. (2014) presented details about the use of geosynthetic reinforced soil-integrated bridge systems (GRS-IBS), including their design, construction, and performance at the bridge ends. The GRS-IBS system was tested using field instrumentation to evaluate its long-term performance during the rehabilitation of an existing bridge (Br. 1-366) in New Castle County, Delaware.

Illinois

- Stark et al. (1995) examined the approaches of 1,181 bridges in Illinois and reported that 27% of the bridges exhibited severe bumps (settlement > 2 inch) at their ends. Stark et al. (1995) reported that most of the settlement occurs at the interface between the approach slab and bridge abutment, the approach slab and highway pavement, or at a crack in the approach slab due to the transition from heavy to less steel reinforcement in the approach slab structure.

Iowa

- White et al. (2005) conducted field inspections for bridge approaches in Iowa and reported that the settlement is essentially caused by the inappropriate fill of the expansion joints, lack of surface and subsurface drainage, and poor compaction of abutment backfill materials. In addition, White et al. (2005) found asphalt overlaying and expansive polyurethane grouting to be not effective as a long-term solution for the repair of settlement at bridge approaches.

Kentucky

- Hopkins (1985) provided several findings and recommendations for the Kentucky Department of Highways regarding the design and construction practices of bridge

approaches. The recommendations included implementing special compaction efforts of the filling materials within a specified distance from the back wall of the bridge abutment as well as empirical relationships for estimating the creep settlement of embankments at bridge approaches and the rate of consolidation in the foundation material.

- Dupont and Allen (2002) reviewed the practices followed by the DOTs of 50 States in regard to dealing with bridge approaches such as construction methods, bridge approach embankment, type of abutments, and drainage systems.

Louisiana

- Cai et al. (2005) conducted a finite element (FE) analysis of the embankment settlement beneath a bridge approach slab that was supported by the bridge abutment and a sleeper slab on both ends. The analysis demonstrated how the differential settlement led to losing the contact between the approach slab and embankment soil, while the sleeper slab and bridge abutment received the major portion of the load applied on the approach slab. This demonstration suggested that the embankment soil beneath the approach slab does not influence its performance, but rather the embankment beneath the sleeper slab.
- Abu-Farsakh et al. (2007) performed a parametric study using FE analysis that assessed the performance of geogrid reinforcement through embankment soils with low to medium plasticity beneath a sleeper slab supporting the highway end of the bridge approach slab. The embankment soil was modeled using the Drucker–Prager constitutive model, while the soil–geogrid interaction was modeled by the Coulomb frictional model. The FE analysis was verified using laboratory tests, then implemented to seek an optimum geogrid reinforcement for the design. The FE analysis found the effective depth of the geogrid reinforcement to be approximately 1.5 times the width of the sleeper slab.
- Abu-Farsakh and Chen (2014) confirmed the behavior reported by Cai et al. (2005) using field instrumentation on the Bayou Courtableau Bridge, St. Landry Parish, Louisiana. Abu-Farsakh and Chen (2014) have also advocated for the need to enhance the flexure strength of bridge approach slabs by increasing their thickness and rebar reinforcement as well as the importance of geosynthetic reinforcement in the embankment below the sleeper slab to minimize its settlement.
- Abu-Farsakh et al. (2018) developed 3D FE simulations for GRS-IBS that were field-instrumented earlier by Saghebfar et al. (2017) at Maree Michel Bridge, Vermilion Parish, Louisiana. The FE simulations supported that the FHWA recommendations underestimated the performance of the GRS-IBS by curbing the allowable bearing pressure to 28 psi, while the FE analysis showed that the GRS-IBS could be loaded up to 48 psi service loads.

Missouri

- Luna (2004) evaluated the performance of bridge approach slabs and identified the major causes of settlement near bridge ends to be inferior embankment/backfill materials and poor compaction practices.
- Thiagarajan et al. (2010) conducted analytical and FE analysis of the bridge approach slab. The analysis suggested a slab design moment of $40\ \text{ft.kips/ft}$ in accordance with the AASHTO requirements and loss of soil support up to 50% along the span of the approach slab. Furthermore, Thiagarajan et al. (2010) proposed an alternative solution for the repair of bridge approaches using pre-cast pre-tensioned concrete panels bonded by transverse ties. Cost analysis of this alternative appeared to be effective in both newly constructed and

rehabilitated bridge approaches.

New Hampshire

- Boisvert (2010) assessed the performance of bridge approach slabs with structural fiber replacing the top reinforcing steel, which is prone to corrosion damage due to the chloride applied to the highway for winter de-icing. The assessment defined effective performance based on laboratory experiments and three years of field evaluation of the quality of fiber-reinforcement used in the concrete approach slab at the Pembroke-Allenstown Bridge, Suncook, New Hampshire.

New Mexico

- Lenke (2006) identified geotechnical issues with natural soil foundation and embankments as the leading contributor to the development of bumps at the bridge ends. He attributed the long-term settlement of bridge approaches in New Mexico to the lack of subsurface investigation, insufficient stabilization of deep-seated foundation, poor material selection, inappropriate compaction practices, and erosion due to poor drainage.

North Dakota

- Marquart (2004) recommended special treatment of the backfill and embankment materials at bridge approaches that included a 5% slope starting from the bridge abutment, a void installation between the bridge abutment and backfill material to release lateral forces, and geotextile reinforcement within 1 foot compacted layers and a special drainage system.

Ohio

- Adams et al. (2007) examined the design, construction, and performance of GRS-IBS at Bowman Road Bridge, Defiance County, Ohio. Bowman Road Bridge consisted of prestressed concrete box beams supported on GRS abutments that were constructed using a reinforced soil foundation over clay sub-soils. The bridge did not include any approach slab in order to allow simultaneous settlement of the bridge and adjacent highway, which provided a bump-free and smooth transition for motorists. The construction cost of the bridge was about 20% less than the cost of a conventional bridge supported by pile-capped abutments, and the angular distortion of the bridge was within the AASHTO criterion for simple supported bridges.
- Greimann et al. (2008) evaluated the practice of Ohio's DOT regarding the bridge approach slab and examined the behavior and conditions of some bridge approaches in Ohio.
- Islam (2010) conducted a 3D FE analysis of the settlement at the bridge ends and reported high deflection in the bridge approach slabs when they lost contact with the underneath soil, which caused a significant decrease in the moment bearing capacity of the slab.

Oklahoma

- Zaman et al. (1995) developed a probabilistic model that predicted problematic bridge approaches (settlement > 1-inch) before construction based on several factors such as the age of the bridge approach slab, embankment height and properties, foundation soil thickness and type, skewness of the approach, and traffic volume.
- Miller et al. (2013) conducted a field investigation for 33 bridges in Oklahoma, which were identified as having moderate to severe bumps at their ends. The investigation revealed that erosion and consolidation of soil beneath the approach slab or bridge abutment are the two

main causes for the development of bumps at the ends of bridges in Oklahoma.

South Dakota

- Schaefer and Koch (1992) in South Dakota gave specific recommendations to mitigate the bumps at the bridge ends that were caused by the void development beneath the bridge approach slabs due to thermal-induced movements, particularly in bridges with integral abutments. The recommendations included asphaltic capping of the shoulder areas for the embankments beneath the bridge approaches, mud jacking the voids that extend more than 10 feet from the backwall of the bridge abutment, or if the void reaches a depth of 4-inch (2-inch in high traffic areas). Special reinforcement provisions were proposed for the approach slab to resist the transverse cracking that occurs at the interface between bridge abutment and the approach slab. The recommendations also included (i) a 25% or 50% slope of the cut made for backfill placement behind bridge abutments, (ii) the use of fine well-graded granular backfill behind bridge abutments; and (iii) installation of filter wrap to prevent erosion of the granular fill beneath the approach slab.

Texas

- James et al. (1991) rated 131 bridges in Texas by their end roughness and observed more severe roughness in rigid pavement than in flexible pavement highways.
- Dupont and Allen (2002) used a profilometer to assess the approaches for two bridges on a major highway in Houston and reported a decrease in some of the bumps over time. This self-recovery behavior was attributed to the dynamic conditions of bridge approaches, such as the shrinking/swelling nature of some embankment soils due to changes in the weather.
- Puppala et al. (2009) completed a survey for problems regarding the bridge approaches in 16 districts in Texas and reported 6% of bridge approaches had no problems, 61% exhibited settlement, and 33% suffered from heave.

Virginia

- Hoppe (1999) recommended pre-cambering of the bridge approach slab up to a 1/125 longitudinal gradient to accommodate the differential settlement that is inevitable to occur at bridge ends.
- Kost et al. (2014) constructed and instrumented a full-scale GRS-IBS abutment, then imposed large differential settlements at the foundation level. The instrumentation revealed a significant redistribution of the stresses within the reinforced fill and adequate support at the level of the superstructure. However, the facing units appeared vulnerable to removal and potentially exposed the reinforced fill to erosion.

Wisconsin

- Helwany and Koutnik (2007) investigated two construction methods of bridge approach slabs: geosynthetic-reinforced fill and flowable fill. The two methods were evaluated in the field for granular and compressible soil embankments.
- Al-Eis and LaBarca (2007) tested the URETEK pavement lifting technique to repair bumps at the bridge ends. It involved injecting polyurethane foam through small holes drilled into the concrete approach slab; then, the injected foam expands to fill the void beneath the approach slab and lift it.
- Oliva and Rajek (2011) examined the approach slab rotation caused by the settlement of the bridge abutment. The rotation was significantly correlated to the abutment height, span

length of the approach slab, stiffness of the backfill soil, and concrete stiffness of the approach slab.

Wyoming

- Edgar et al. (1989) investigated four different construction methods of bridge approach slabs that used selected backfill material with geotextile reinforcement. The investigation included extensive laboratory experiments as well as field instrumentation on the Ozone Bridge in Cheyenne, Wyoming. Edgar et al. (1989) found geotextile reinforcement to be an effective technique in controlling short-term deformations. Furthermore, the technique of constructing a 6-inch void between the reinforced embankment and abutment with cardboards appeared to be an easy and effective method that reduced lateral forces acting on the bridge abutment.
- Ng et al. (2014) conducted a thorough nationwide survey of the practices that are followed by the DOTs of 28 states regarding bridge approaches. The survey results showed that 46% of the 28 respondents were not satisfied with their current practices.

1.4 Current Practices by US DOTs

Over the last few decades, research studies reporting on the performance of bridge approaches have essentially contributed to the development of specifications and provisions for several DOTs regarding the design and construction practices of bridge approaches. The authors visited the official websites of nationwide DOTs and collected their current practices in dealing with bridge approaches. Out of the 50 States, the authors successfully accessed provisions and specifications for 47 States as listed in Table A-1 in the appendix. No online specifications or provisions regarding bridge approaches were found for Maryland and Montana DOTs, while Hawaii DOT does not offer open-source design data. The following sub-sections will thoroughly review and synthesize the collected material for the 47 States into Tables and Figures to identify the state-of-the-art practices in designing bridge approaches.

Details of the Bridge Approach Slab

Span Length

All 47 DOTs require the use of a reinforced concrete approach slab with various span lengths, thicknesses, and reinforcing steel provisions as summarized in Table A-2 (in the appendix) and Table 1-1. The appropriate span length of the bridge approach slab depends on the anticipated differential settlement between the bridge abutment and highway pavement. The bumps felt by motorists at the bridge ends are fundamentally caused by the differential settlement, and the span length of the approach slab should provide adequate length to deliver an acceptable gradient for riding comfort. Stark et al. (1995) reported a qualitative rating for the riding comfort across bridge approaches based on their differential settlement as summarized in Table 1-1, in which a bump at the bridge ends was recognizable by motorists when the differential settlement exceeded 2-inch. Accordingly, the recommended span length of the bridge approach slab would range between 15 to 35 feet based on the acceptable gradient of riding comfort between 0.5% (Wahls 1990) and 1.0% (Stark et al. 1995).

Table 1-1. Qualitative rating of the bump at bridge approaches (Stark et al. 1995).

Qualitative Rating	Description of Riding Comfort	Differential Settlement (in.)
0	No bump	~ 0
1	Slight bump	~ 1
2	Moderate bump - recognizable	~ 2
3	Significant bump – require repair	~ 3
4	Large bump – safety hazard	> 3

A summary of various span lengths of the bridge approach slabs as specified by the 47 DOTs are depicted in Figure 1-3 by the dark grey bars, which shows an agreement with the 15 to 35-foot span lengths required to deliver an acceptable gradient for riding comfort. In special cases where a larger amount of differential settlement is anticipated, most of the DOTs require the use of longer spans to accommodate the riding comfort gradient. Some of the DOTs also specify different span lengths for different highway conditions of the bridge approaches such as:

- Bridge skewness: several DOTs specify longer spans for bridges with larger skewness angle. For instance, Virginia DOT specifies a four-span length of 20, 22, 25, and 28-foot. for the approach slabs of bridges with skewness ≤ 20°, 20° < skewness ≤ 35°, 35° < skewness ≤ 45°, and skewness > 45°, respectively. A similar trend is also specified by Massachusetts,

Minnesota, Oregon, and Vermont DOTs. The approach slab is typically constructed with a similar skewness to the bridge in which the slab span length is measured along the highway centerline. In cases when one side of the approach slab is skewed, then the specified span length usually applies to the shortest side.

- Bridge traffic: several DOTs specify longer spans for bridges with heavier traffic. For instance, Vermont DOT specifies a 15-foot span length for highways with average daily traffic (ADT) < 1000 vehicle/day, while a 20-foot span length is required when ADT ≥ 1000 vehicles/day. Likewise, Louisiana DOT specifies 10-foot span length for off-system bridges (minor traffic) and 20-foot span length for on-system bridges (major traffic).

Thickness

From the collected material for the 47 US States (Table A-2), it can be noticed that various thicknesses between 8 and 20 in of bridge approach slabs are adopted by different DOTs. The various thicknesses are plotted in Figure 1-3 using the light grey bars on a secondary right axis and sided by the corresponding slab span length (dark grey bars). Some of the main factors determining the thickness of the approach slab are:

- Span length of the approach slab: some DOTs specify thicker slabs for bridge approaches with longer spans such as Arkansas, Ohio, Oregon, and Vermont. Other DOTs use a single slab thickness for various span lengths like Massachusetts, Nevada, New Hampshire, North Carolina, Oklahoma, and Virginia.
- Bridge skewness: some DOTs specify a thicker approach slab for bridges with larger skewness angle. For instance, Alabama DOT specifies 10, 11, and 14-inch slab thicknesses for bridges with skewness < 15^0, 15^0 ≤ skewness < 33^0, and skewness ≥ 33^0, respectively.
- Type of highway pavement: Louisiana DOT specifies an 18-inch slab thickness for highways with Portland cement concrete (PCC) pavement and a 20-inch for highways with hot mix asphalt (HMA) pavement.
- New/existing construction: Iowa DOT specifies a 12-inch slab thickness for a newly constructed bridge approach slab, whereas a 10-inch thick slab may be used to replace an existing 10-inch slab.
- Slab foundation: Minnesota DOT specifies a 12-inch standard thickness for the bridge approach slab, which can be tolerated as 10-inch if an aggregate wearing base is used but must be increased to 13-inch above the sleeper slab.

Moment Capacity

Bridge approach slabs are widely recognized to lose contact with their foundation embankment soil due to the differential settlement and develop voids at the bridge ends (Cai et al. 2005; Islam 2010; Chen and Abu-Farsakh 2016). Therefore, bridge approach slabs are prone to flexure deformation, and main steel reinforcement (bottom steel along the slab span length) is required to provide adequate moment capacity. The moment capacity of a reinforced concrete bridge approach slab is calculated as (Thiagarajan et al. 2010):

$$\phi M_n = \phi \left[A_s F_y \left(d - \frac{A_s F_y}{2 \times 0.85 \times f_c' \times b} \right) \right] \quad (1)$$

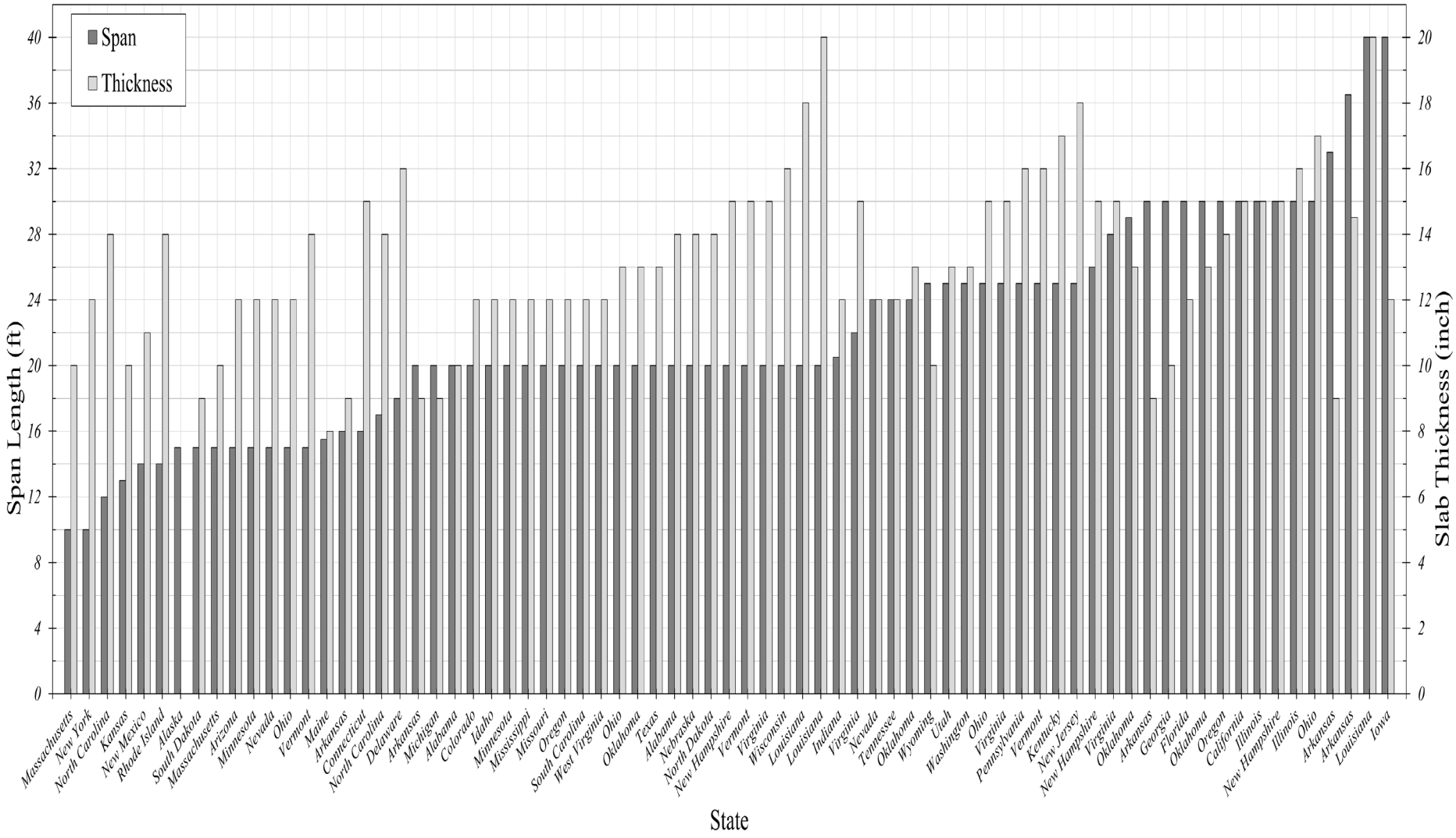

Figure 1-3. Span length and thickness of the bridge approach slabs as specified by US DOTs.

Where $\phi = 0.9$ is the moment load resisting factor, A_s is the area of the main steel reinforcement, d is the depth of the slab up to the center of the main reinforcing rebars, $F_y = 60\ ksi$ is the yielding stress of the reinforcing steel, $f_c' = 4\ ksi$ is the concrete compressive strength of the slab and b =1-ft. is a unit width. For instance, the main steel reinforcement specified by Tennessee DOT for the bridge approach slab is #6 bars spaced at 6-inch (4th column in Table A-2), which *gives* $A_s = 0.884\ in.^2/ft$. Assuming concrete cover of 2.5 in (bottom rebar cover plus rebar radius) then:

$$[\phi M_n]_{Tennessee} = 0.9\left[0.884 \times 60\left((12 - 2.5) - \frac{0.884 \times 60}{2 \times 0.85 \times 4 \times 12}\right)\right] = 422\ in.kips/ft = 35\ ft.kips/ft$$

Likewise, the moment capacity was calculated for the bridge approach slabs specified by other DOTs and displayed in Figure 1-4, which shows a moment capacity ranging between 12 and 174 ft.kips/ft. Thiagarajan et al. (2010) recommended a slab design moment of 40 ft.kips/ft. based on the AASHTO requirements and assuming a 50% loss of soil contact along the span of the approach slab. The calculated values of moment capacities in Figure 1-4 compare favorably with the 40 ft.kips/ft recommended by Thiagarajan et al. (2010). Note that higher flexure (higher bending moment) occurs with more loss of contact between the soil embankment and the approach slab along its span, and this explains the conservative practice of some DOTs that design for moment capacity up to 174 ft.kips/ft.

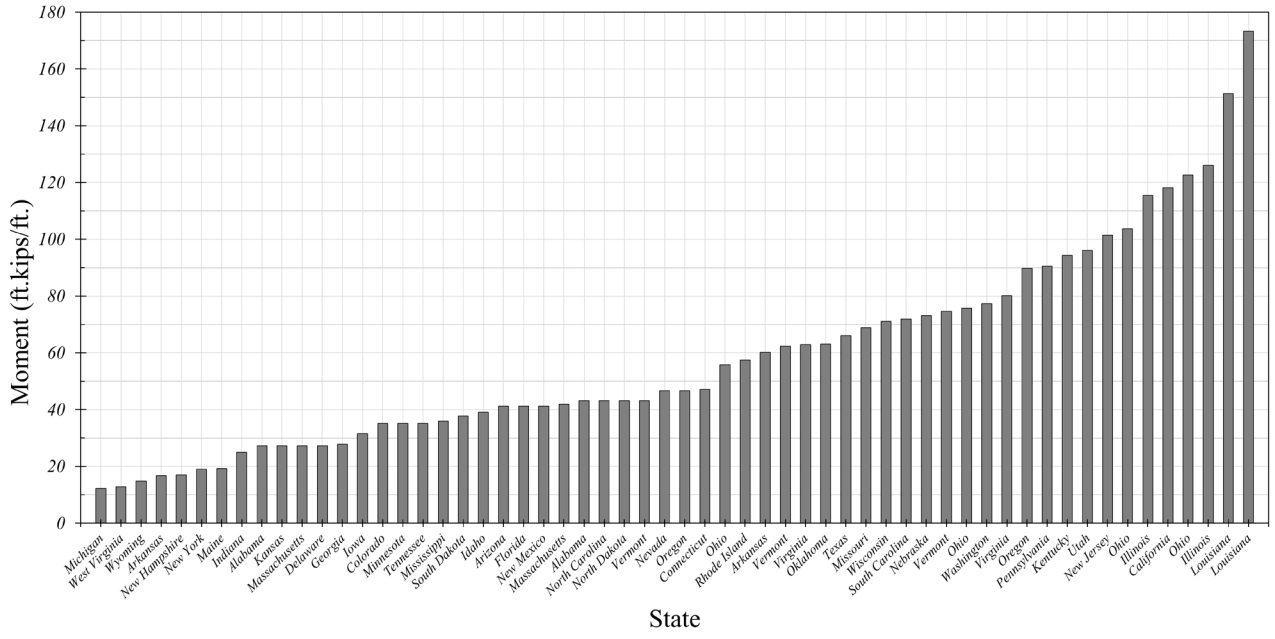

Figure 1-4. Moment capacity of the bridge approach slab as specified by different US DOTs.

Bump 1: Highway/Approach Slab (H/S) Joint

Figure 1-1 illustrates how Bump 1 at a bridge approach is developed by faulting along the highway/approach slab (H/S) joint. As the soil beneath the approach slab settles, the slab dead loads, and the traffic loads will be carried by the two ends of the slab instead of bearing along its span. From the bridge side, the approach slab end is supported by a non-yielding abutment. At the H/S joint, the other end of the approach slab rests on compacted soil prone to settlement. This differential settlement between the two ends of the approach slab leads to the development of Bump 1.

A common practice to equalize the settlement at the H/S joint is to construct a reinforced concrete strip footing known as a sleeper slab. Figure 1-5 presents the relationship between the maximum settlement at the H/S joint versus the width of the sleeper slab as reported by Seo et al. (2002). It can be seen from Figure 1-5 how the maximum settlement at the H/S joint decreases significantly with the increase of the width of the sleeper slab. Furthermore, the decrease in the maximum settlement becomes optimum at about a 5-foot wide sleeper slab. The sleeper slab is typically constructed outside the area where the soil is expected to be affected by the lateral movement of the abutment, particularly in the case of integral abutment bridges.

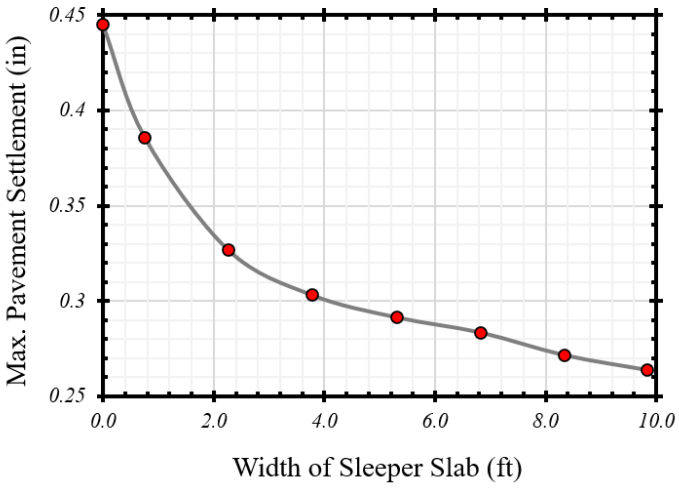

Figure 1-5. Maximum pavement settlement at bridge ends as a function of the sleeper slab width (Seo et al. 2002)

Dimension-Specifics

Based on the review and synthesis of the collected documents from 47 US States, Figure 1-6 summarizes the width (dark grey bars) and thickness (light grey bars) of the sleeper slab as specified by the 28 DOTs. The width of the sleeper slab ranges between 3 and 10 feet, with an average around 5 feet optimum width as recommended by Seo et al. (2002). The thickness of the sleeper slab varies between 9 and 24-inch. A typical example of the sleeper slab is illustrated in Figure A-1 in the appendix as specified by Pennsylvania DOT for HMA (Figures A-1(a) and (c)) and PCC pavement (Figures A-1(b) and (d)). Pennsylvania's sleeper slab design has a rectangular cross-sectional shape (5-ft. or 6-ft. by 12-inch) and supports the approach slab along its half-width while the other half extends beneath the highway pavement. Special provisions are assigned by different DOTs for the

construction of sleeper slabs, such as the horizontal dowels used to connect the approach slab and PCC pavement in Figure A-1(b) or the 12-inch pavement relief joint in Figure A-1(d). Examples of more special provisions as specified by other DOTs regarding the sleeper slab are:

- Iowa DOT specifies a 40-foot span length for the bridge approach slab that is divided into two segments: a 20-foot slab with a double layer reinforcement near the bridge followed by another 20-foot slab with a single layer reinforcement. The sleeper slab required by Iowa DOT is 6.25-foot (width) by 12-inch (thickness) and constructed between the two segments of the approach slab, as depicted in Figure A-2 in the appendix. Likewise, the approach slab specified by Arkansas DOT is divided into 15 to 20-foot segments and multiple sleeper slabs are constructed between the segments as well as beneath the H/S joint.
- South Carolina DOT specifies a 3.75-foot wide by 12-inch thick sleeper slab with a 15-inch wide mid-stem as illustrated in Figure A-3 in the appendix. Similar provisions with different dimensions are also proposed by Rhode Island DOT for bridges with span lengths exceeding 60 feet.
- Colorado DOT specifies a 3-foot wide by12-inch thick sleeper slab if the lateral movement of the bridge abutment doesn't exceed 1/2-inch. Otherwise, the sleeper slab width should be increased to 4 feet and include a 12-inch mid-stem with an expansion device, as illustrated in Figure A-4 in the appendix.
- New York DOT specifies a 6-foot wide by 12-inch thick sleeper slab that includes a 2-foot mid-stem as described in Figure A-5 in the appendix. New York DOT also specifies a 1.5-inch joint sealed with a compressible foam at the interface between the sleeper stem and the approach slab. The joint sealing material is detailed in Figure A-5.
- Tennessee DOT specifies a 3-foot wide by 12-inch thick sleeper slab as depicted in Figure A-6 in the appendix. Tennessee sleeper slab must also include a 12-inch wide mid-stem for highways with HMA pavement (Figure A-6(b)). These are similar provisions but have different dimensions than those specified by Utah DOT.
- Nevada DOT specifies two different types of sleeper slabs for highways with PCC versus HMA pavement. Both types come integrated with an approach slab, as demonstrated in Figure A-7 in the appendix. Similar provisions are also specified by Texas DOT for highways with PCC pavement.
- Michigan DOT specifies two types of sleeper slabs: 5-foot wide by 10-inch thick with a 24-inch wide mid-stem for PCC pavement (Figure A-8(a) in the appendix) and 3.5-foot wide by 12-inch thick with a 2-foot wide reversed back heal for HMA pavement (Figure A-8(b)). Similar provisions are also specified by Delaware DOT with the addition of horizontal dowels across the sleeper stem and approach slab for the PCC pavement case (Figure A-9(a) in the appendix).
- Louisiana DOT uses geotextile reinforcement in the embankment beneath the sleeper slab as illustrated in Figure A-10 in the appendix. The geotextile reinforcement enhances the rigidity of the sleeper embankment and significantly reduces its settlement.

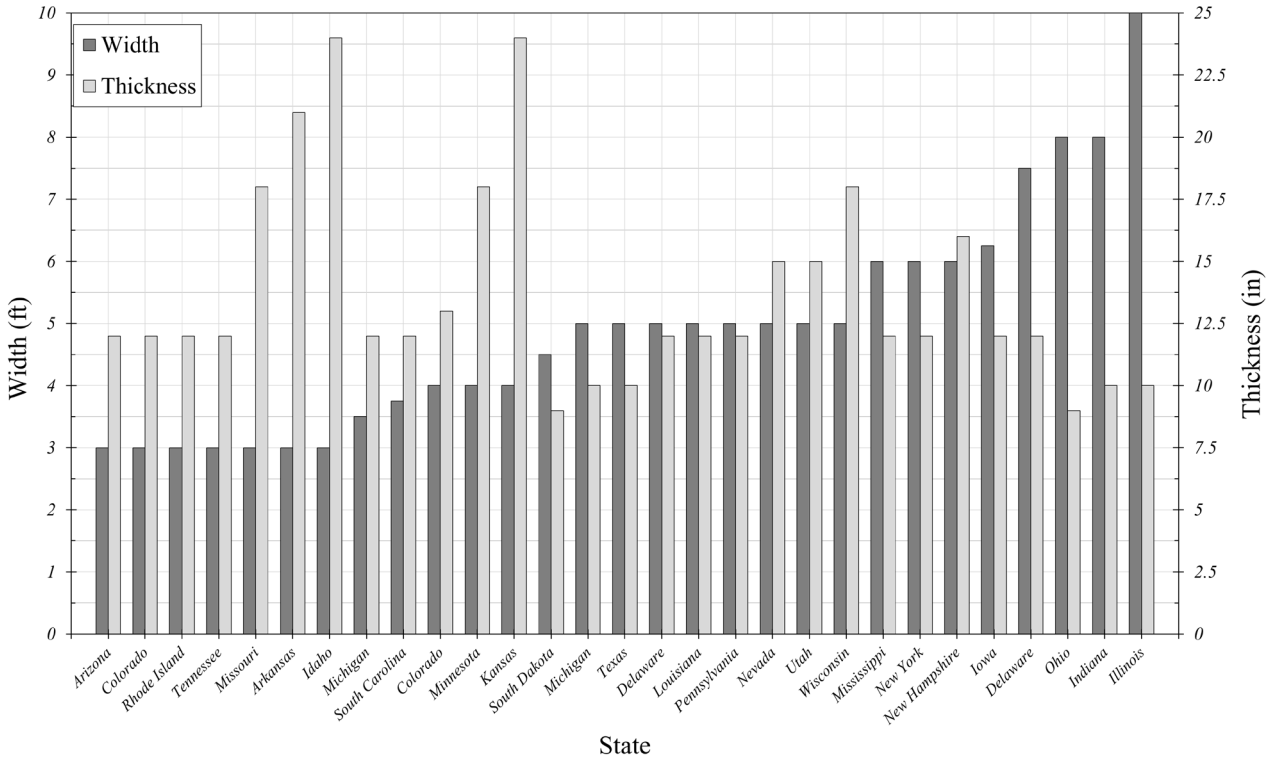

Figure 1-6. Dimensions of the sleeper slab as specified by several US DOTs.

Bump 2: Abutment/Approach Slab (A/S) Joint

Bridge approaches develop another bump at the abutment/approach slab (A/S) joint, which is labeled as Bump 2 in Figure 1-1. This bump is felt by motorists as a sudden change in slope along the highway transverse lines at the bridge entrance/exit. This sudden change in slope is fundamentally caused by the flexure deflection of the approach slab, as illustrated in Figure 1-1. The limited area of work behind the bridge abutments usually produces poor compaction and construction of the backfill material. Therefore, bridge approaches usually develop a "gap" in the embankment behind the bridge abutments as shown in Figure 1-1. This "gap" significantly contributes to the flexure deformation of the bridge approach slab and leads to the development of Bump 2 at the A/S joint.

Types of Abutments

There are two major types of bridge abutments: non-integral and integral. The non-integral abutments are the traditional type, which carries the bridge using seats and bearing supports. In integral abutments, the bridge deck and abutments are encased together by reinforced steel. The main advantage of integral abutments is the lower construction and maintenance cost since they eliminate the need for seats and bearing supports. However, integral abutments are affected by lateral thermal expansion/contraction and post-tensioning as well as creep and shrinkage deformations of the bridge superstructure. An enhanced version of the integral abutment is the semi-integral type, which seeks independent deformation of the bridge sub- and super-structure by constructing specially sealed expansion joints along the abutments.

Specific provisions and practices are assigned by different US DOTs about the connection between the approach slab and the bridge abutments in order to diminish Bump 2 at the A/S joint. Table A-4

in the appendix summarizes these provisions and practices for the 47 DOTs, which details the bridge approaches successfully found in Table A-1. Referring to Table A-4, all 47 US DOTs share a common practice of supporting the bridge approach slab on abutments by seats or brackets that vary in sizes (3 to 18-inch) and shapes. Some DOTs also tie the approach slab and abutments using structural or mechanical elements, particularly for integral abutments. The remaining part of this sub-section thoroughly discusses some common practices listed in Table A-4 with illustrative examples for each abutment type (e.g., integral, non-integral, and semi-integral).

Non-integral abutments are categorized as fixed abutments since they are isolated from the movement of the bridge superstructure. Therefore, most of the DOTs specify supporting seats with bond breakers and specially sealed expansion joints. For instance, the approach slab used by Georgia DOT (Figure 1-7(a)) is supported by an 8-inch seat on the bridge abutment with 3 layers of 30 lb. asphalt-saturation felt that prevents bonding and a sealed expansion joint that is ¾-inch wide. Pennsylvania DOT supports the approach slab using a different shape of abutment seat as illustrated in Figure 1-7(b) with 2-ply bituminous paper to break bonding and a 3/8-inch expansion joint sealed with a neoprene sponge. Other DOTs tie the bridge approach with non-integral abutments by mechanical or structural elements as illustrated in Figure 1-8. For instance, Florida DOT (Figure 1-8(a)) specifies vertical dowels into the abutment seats, Michigan DOT (Figure 1-8(b)) requires to embed the bottom rebars of the deck for a minimum of 2 feet into the approach slab, and Indiana DOT (Figure 1-8(c)) uses #5 threaded ties between the bridge approach slab and deck.

Integral abutments are categorized as movable abutments since they are designed to tolerate the movement of the bridge superstructure. The potential movability in integral abutments made most of the US DOTs require tying the approach slab with the bridge abutment or deck. Figure 1-9 presents examples for structural ties at the A/S joint as assigned by some DOTs for bridges with integral abutments:

- Arizona DOT (Figure 1-9(a)): #5 vertical tie bars spaced at 12 inches.
- Idaho DOT (Figure 1-9(b)): #4 horizontal tie bars spaced at 12 inches.
- North Carolina DOT: #4 tie bars, shape as depicted in Figure 1-9(c).
- Tennessee DOT: #6 tie bars spaced at 12 inches; shape as depicted in Figure 1-9(d).
- Colorado DOT (Figure 1-9(e)): #5 L-shape tie bars spaced at 12 inches.

Figure 1-10 shows examples of some mechanical and structural constraints that tie the approach slabs and integral abutments:

- Utah DOT uses water stops to horizontally tie the approach slab and bridge deck as shown in Figure 1-10(a).
- North Dakota utilizes #5 bars with a mechanical splicer that horizontally ties the approach slab with the bridge deck (Figure 1-10(b)).
- Texas DOT specifies to loop the vertical abutment reinforcement through the approach slab as shown in Figure 1-10(c).
- Illinois DOT has two different specifications for the ties at the A/S joint as shown in Figure 1-10(d). For cast-in-place approach slabs, #5 L-shape bars spaced at 12-inch intervals are used to tie the horizontal slab and vertical abutment. For precast-approach slabs, 1-inch ϕ by 2-foot long dowels extend vertically in the bridge abutment through 1.5-inch ϕ drilled and grouted holes.

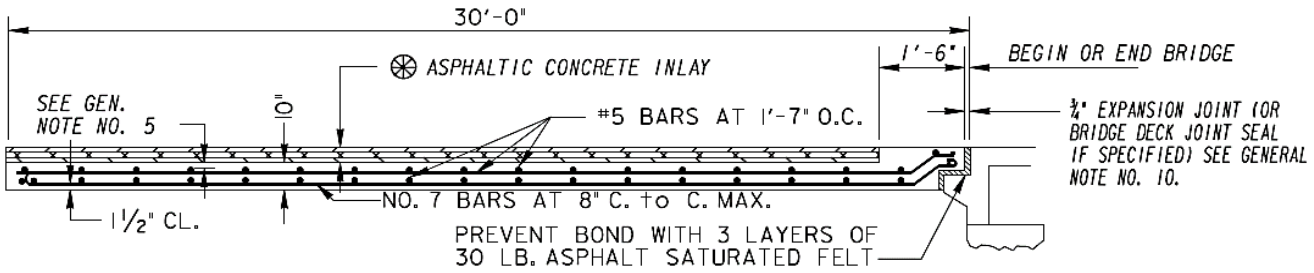

(a) Georgia DOT

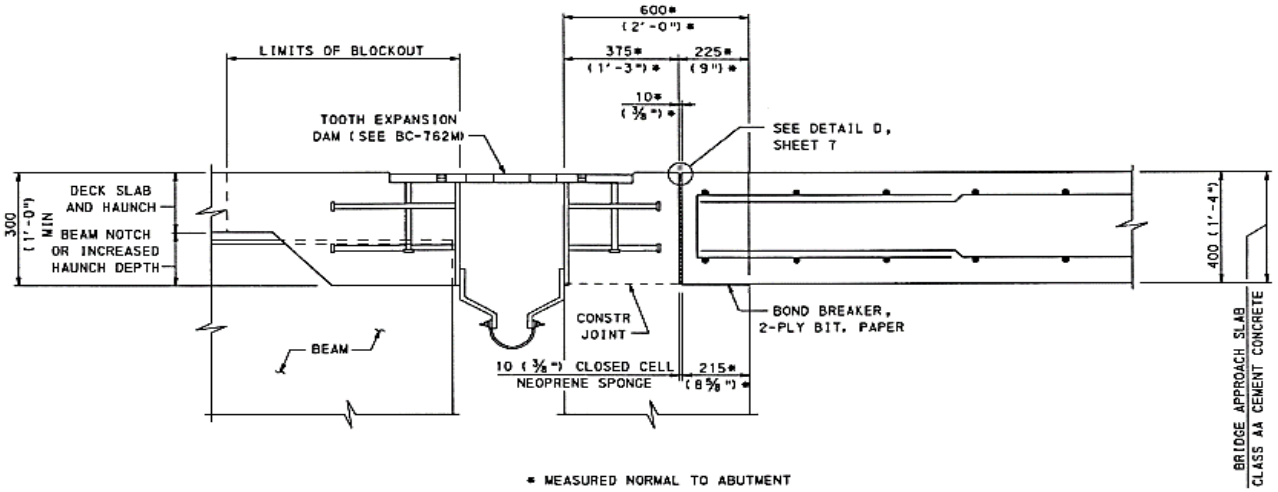

(b) Pennsylvania DOT

Figure 1-7. Examples of A/S joint for non-integral abutments without structural or mechanical ties.

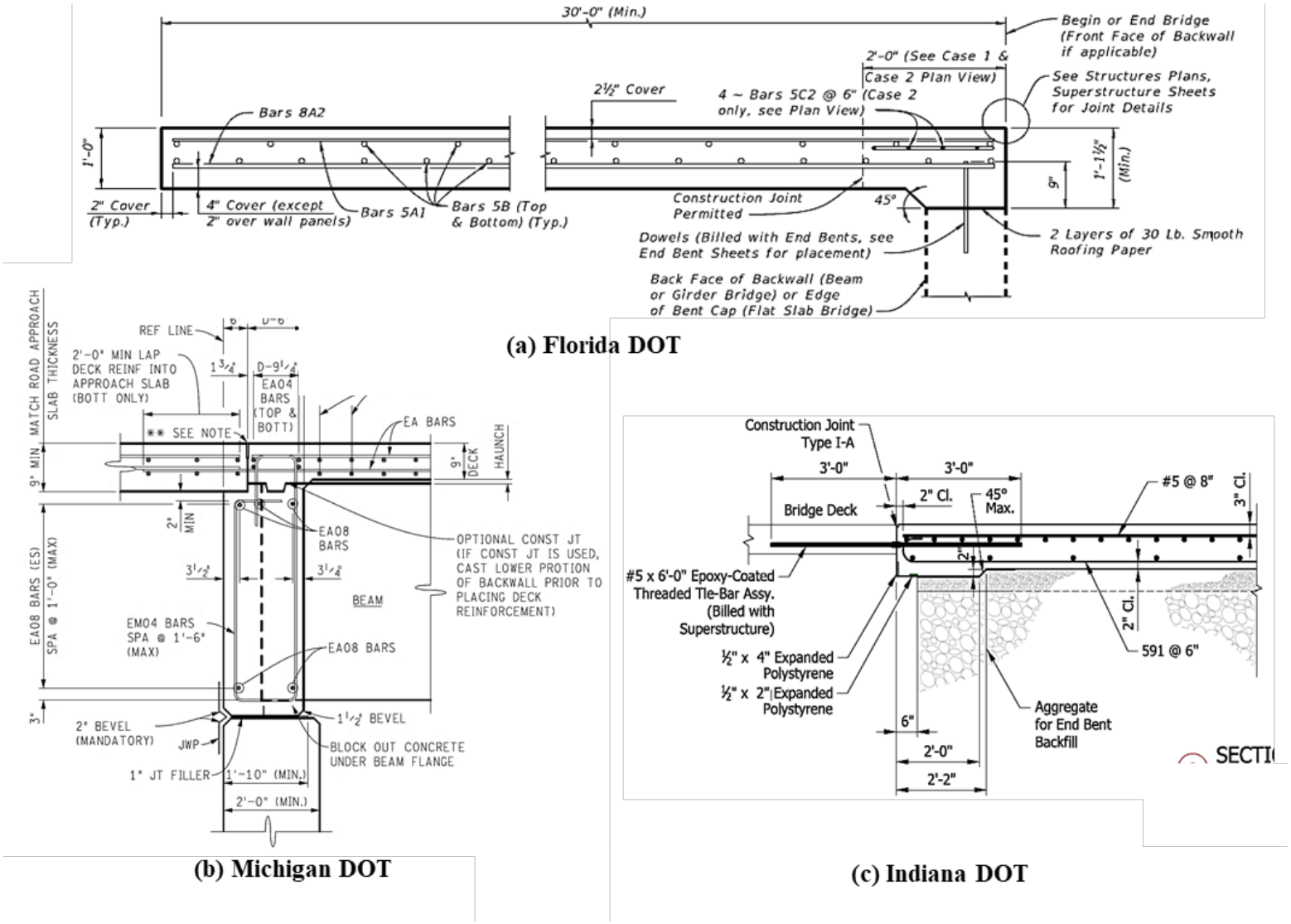

Figure 1-8. Examples of A/S joints as specified by some DOTs with structural/mechanical ties for non-integral abutments.

- California DOT specified two different tie types for seat (non-integral) and diaphragm (integral) type abutments as illustrated in Figure 1-11. In-seat type abutments, #5 bars spaced at 9 to 12-inch are used to tie the approach slab and the abutment vertically. For diaphragm-type abutments, ¾-inch ϕ by 8-inch long horizontal bolts are used to tie the approach slab and bridge deck. The bolts are spaced at 24-inch intervals.
- Iowa DOT ties the approach slab with the embankment at 10 inches away from the bridge abutment using ½-inch ϕ by 24-inch long steel rods with hooked ends, fastened into the top slab steel. Iowa DOT also specifies extra steel dowels at the A/S joint for non-integral abutments (see Figure 1-11(a)).

Some DOTs give special tie provisions at the A/S joint for a bridge with semi-integral abutments such as:

- Washington DOT specifies #5 tie bars spaced at 12-inch intervals with different shapes, as illustrated in Figure 1-12(a) for integral and non-integral abutments. For semi-integral abutment, ¾-inch ϕ anchors are used to tie the approach slab with the bridge horizontally. The anchors extend 8 to 10 inches inside the bridge abutment and 15 to 22 inches inside the approach slab.
- Wisconsin DOT uses stainless steel bars spaced at 12-inch intervals to tie the approach slab and bridge abutment. As presented in Figure 1-12(b), flat Z-shape tie bars are used with integral abutments, horizontal tie bars are used with a semi-integral abutment, and tie bars with single-bend are used with non-integral abutments.

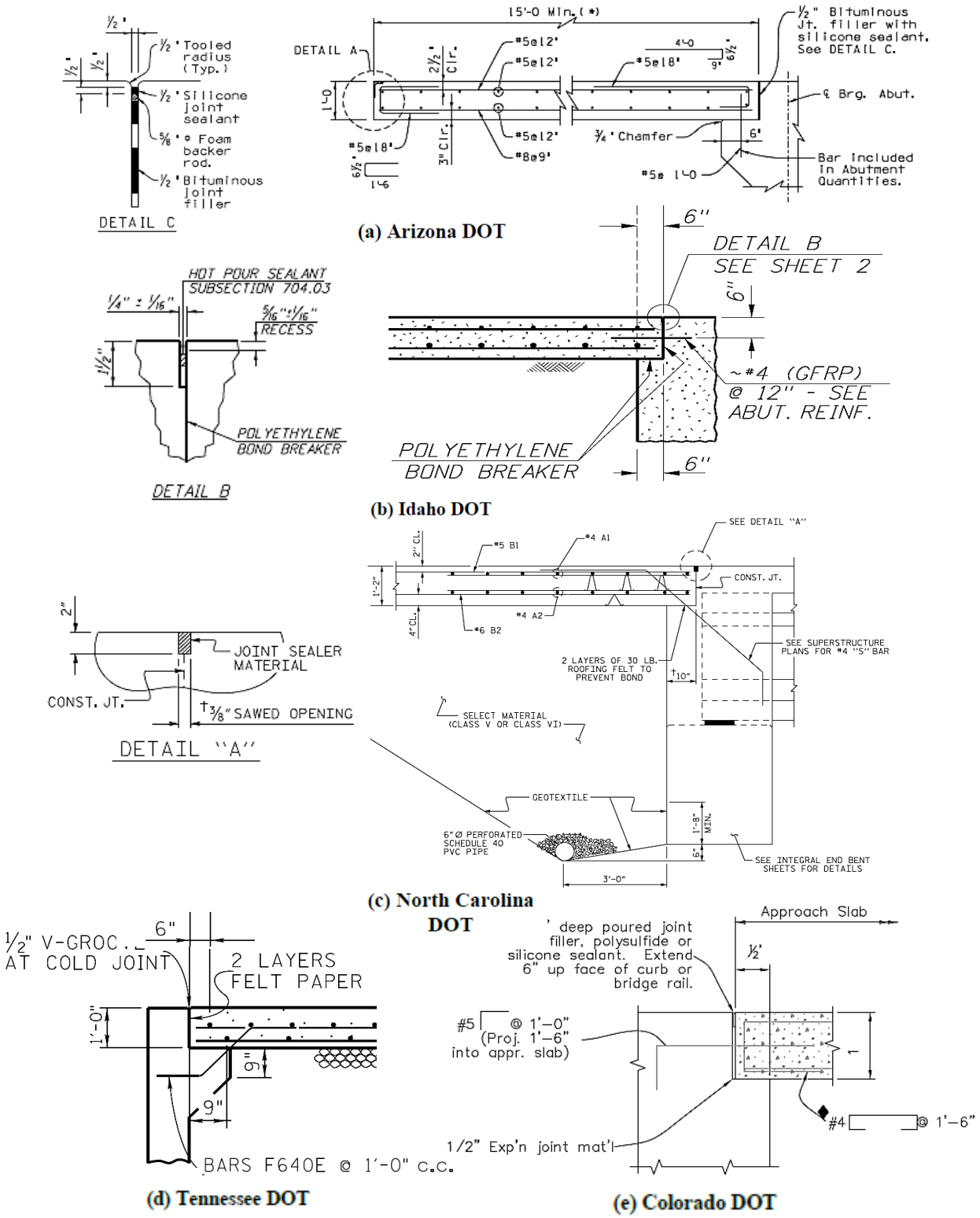

Figure 1-9. Examples for structural ties between the approach slab and integral bridge abutments.

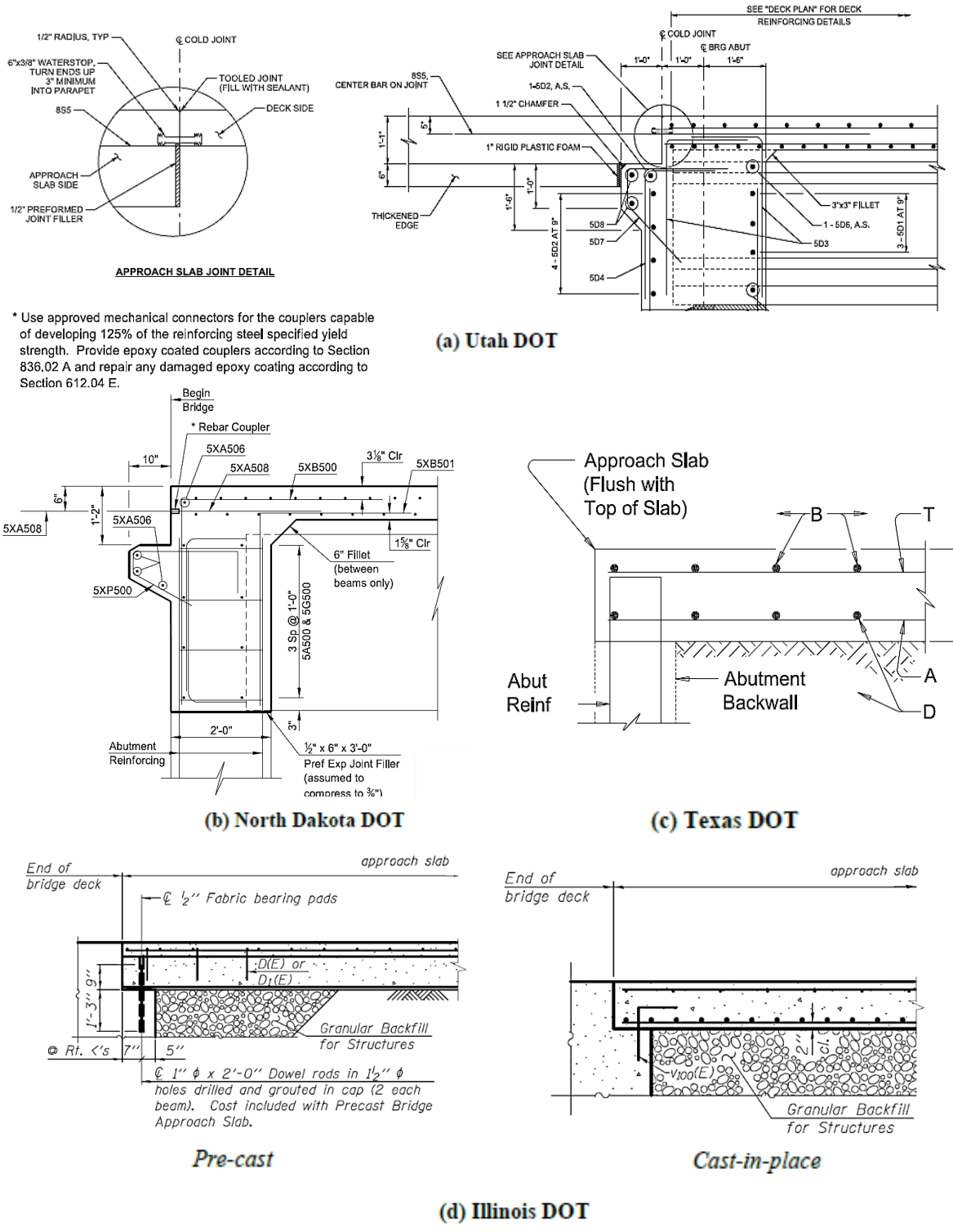

Figure 1-10. Examples of mechanical and structural ties between bridge approaches and integral abutment bridges.

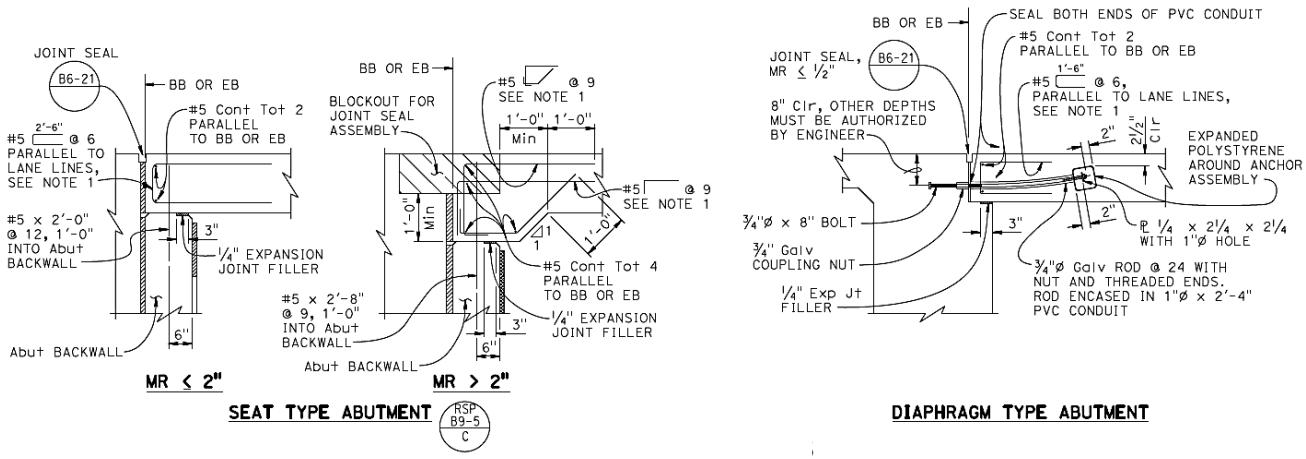

(a) California DOT

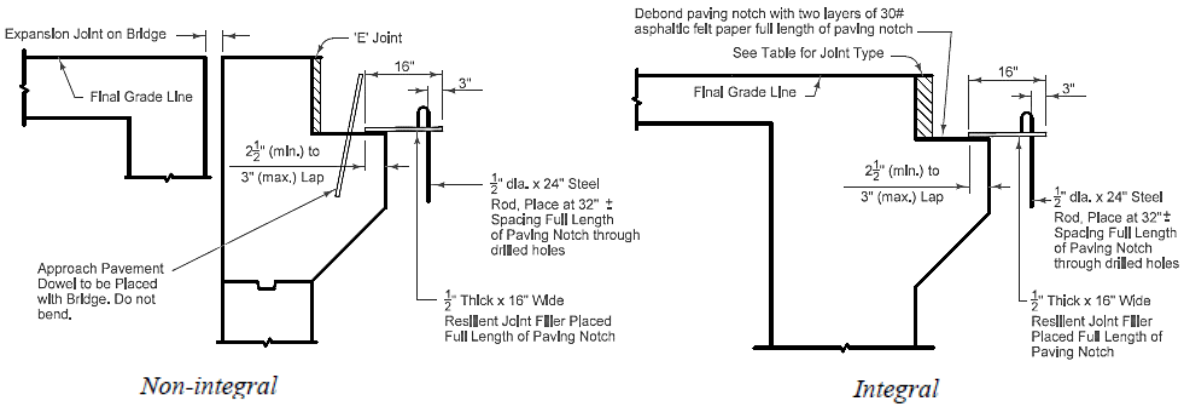

(b) Iowa DOT

Figure 1-11. Examples of special provisions reported by some US DOTs to tie the approach slab and bridges with integral and non-integral abutments.

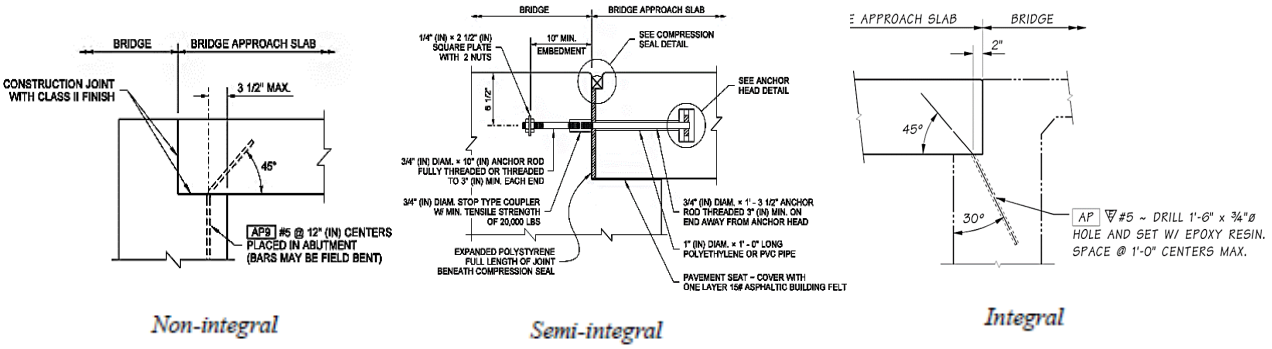

Non-integral *Semi-integral* *Integral*

(a) Washington DOT

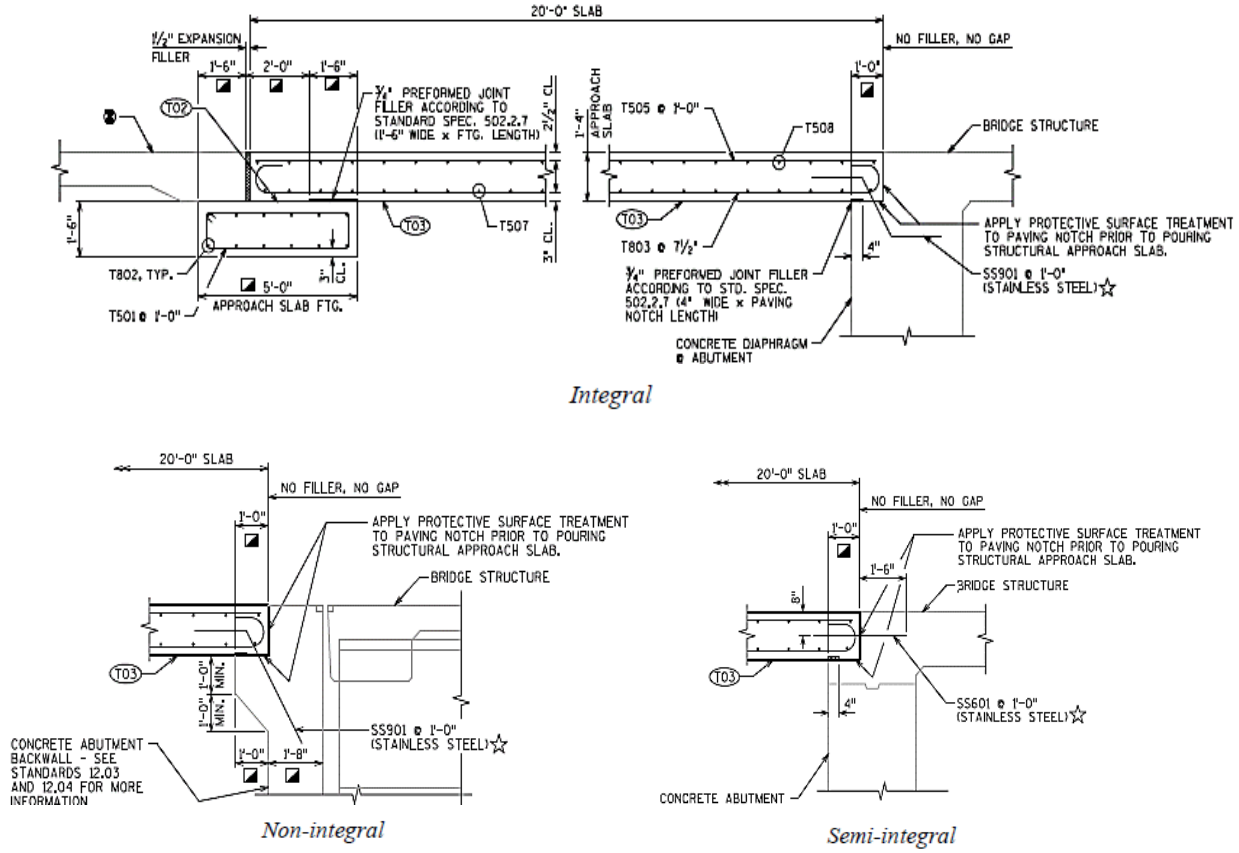

Integral

Non-integral *Semi-integral*

(b) Wisconsin DOT

Figure 1-12. Examples of provisions found for some DOTs to tie between approach slabs and bridges with integral, semi-integral, and non-integral abutments.

Backfill/Embankments at Bridge Approaches

As mentioned earlier, the development of bumps at bridge approaches is widely attributed to the poor practices in selection, construction, and compaction of the embankment and backfill materials. Some of the geotechnical properties that need to be examined for the embankment and backfill materials at bridge approaches are:

- Gradation – Embankment and backfill materials should consist of different sized particles with specified maximum particle size. Well-graded mixtures of sand and aggregate are commonly recommended for fill materials at bridge approaches. The maximum particle size controls the thickness and number of placing layers.
- Optimum moisture content and maximum dry density – Fill embankment soils are usually compacted to have an in-situ density of more than 95% of the maximum dry density obtained from an AASHTO T-99 test at a moisture content within 3% of the optimum moisture content.
- Unit weight and specific gravity – Fill materials with relatively low specific gravity offers the advantage of transmitting less dead load to the abutment and the underlying soil that supports the backfill/embankment. However, materials with very low specific gravity might be prone to erosion and the development of voids beneath the approach slab.
- Permeability – The backfill and embankment materials at bridge approaches should provide quick and sufficient drainage for excessive water.
- Shear Strength – The cohesion and/or angle of internal friction of the embankment and backfill materials should develop adequate shear strength to support highway loads and provide acceptable slope stability.
- Bearing Strength – The backfill and embankment materials at bridge approaches provide enough bearing capacity to support the dead and traffic live loads imposed upon them over the life of the bridge without undue settlement, volume change, or structural damage.
- Compressibility – Compressibility denotes the consolidation or settlement characteristics of a material under long-term loading conditions. The compressibility of a material fundamentally influences its shear strength, degree of compaction, void ratio, permeability, and degree of saturation. Low compressible materials are widely recommended for use in the embankment and backfill of bridge approaches in which most of the material settlement is preferred to occur during the construction and compaction stages.
- Corrosion resistance – Corrosion is a chemical reaction that causes damage to concrete structures, steel piles, or metal appurtenances with which the embankment or fill material may come in contact.

Most of the US DOTs specify special provisions and practices for the embankment and backfill material used in bridge approaches. Table A-5 in the Appendix summarizes these provisions and practices including the wearing base (embankment top layer) beneath the approach slab, grain size distribution of abutments backfill material, and compaction standards followed by the DOTs. All the DOTs agree on the importance of using a suitable aggregate wearing base for the bridge approach slab that reaches up to 24-inch thick, such as Wyoming DOT's specification. Tennessee DOT specifies a 6-inch mineral aggregate wearing base beneath bridge approaches, which is a common provision followed by several other DOTs. Kentucky and North Carolina specify a slope for the selected backfill material behind a bridge abutment of 1H:1V and 1.5H:1V, respectively. Geotextile is also required by these states to separate the backfill and highway embankment. This back slope and geotextile separator enhance the embankment performance and reduce settlement.

Chapter 2 Finite Element Analysis of the Differential Settlement at Bridge Ends

2.1 Introduction

The standard bridge end design specified by most of the US DOTs is composed of a reinforced concrete approach slab supported by the bridge abutment from one side and compacted layers of soil embankment from the side of the H/S joint. Therefore, the approach slab is susceptible to an inevitable amount of differential settlement where the bridge abutment on one side is usually constructed using deep foundation systems that exhibits negligible settlement, and the compacted layers of the adjoining highway embankment settles more significantly. Therefore, a strip footing, commonly known as the "*sleeper slab*", is typically constructed underneath the H/S joint to minimize the amount of differential settlement and to provide a smooth transition for vehicles crossing between the highway embankment and bridge deck.

Reinforcing the soil embankment underneath the sleeper slab with geosynthetics would improve the soil's bearing capacity and reduce the embankment settlement by redistributing the traffic loads exerted on the approach slab over a wider region. This chapter develops a finite element (FE) analysis for a typical bridge end section that consists of an approach slab, sleeper slab, bridge abutment, and compacted layers of soil embankment with or without the inclusion of geosynthetic reinforcement. An FE parametric study is conducted to evaluate the benefits of including the geosynthetic reinforcement within the soil embankment underneath the sleeper slab. The parametric study seeks an optimum design of geosynthetic reinforcement that improves the ultimate bearing stress of the sleeper slab (UBSS) and reduces settlement by distributing the vertical loads over a wider region of soil embankment. Several design parameters are investigated, such as the width of the sleeper, effective depth and length of geosynthetic reinforcement layers, and number/spacing between layers. A case study is then modeled for a preliminary geosynthetic reinforcement design that is proposed by the Tennessee Department of Transportation (TDOT) for the retrofit of the bridge ends. The FE analysis is utilized to predict the UBSS for the proposed design by TDOT as well as the approach slab differential settlement when subjected to service loads (i.e., dead and different types of highway traffic loads). Accordingly, recommendations are made for TDOT concerning how to alter their proposed geosynthetic reinforcement design in a way to achieve better performance for the approach slab settlement problem in Chapter 4.

2.2 Description of Material Models

The ABAQUS FE software was utilized to model the structural components used in the construction of a typical bridge end section. Table 2-1 summarizes these components with the appropriate material models that were selected for the FE analysis. The structural components included a reinforced concrete approach and sleeper slabs, fixed concrete abutment, and flexible layers of compacted soil embankment with the possible inclusion of geosynthetic reinforcement.

Soil Embankment and Geosynthetic Reinforcement

The soil embankment was modeled using isotropic elasto-plastic continuum meshes of 2D linear-strain triangular elements with the yielding function described by the extended Drucker-Prager

criterion as follows:

$$F = t - p\tan\beta - d = 0 \tag{2}$$

$$t = \frac{1}{2}q\left[1 + \frac{1}{K} - \left(1 - \frac{1}{K}\right)\left(\frac{r}{q}\right)^3\right] \tag{3}$$

where t is the effective mean stress, q is the equivalent von Mises stress, r is the third invariant of the deviatoric stress, and $K = 0.778$, which is the ratio of yield stress in triaxial tension to triaxial compression that would introduce dependency of the yield function on the value of the intermediate principal stress. β and d are the slope and intercept of the linear yield function in the $p - t$ stress plane, respectively, which represent the angle of friction and cohesion of the soil.

For plane strain conditions, β and d can be related to the Mohr-Coulomb angle of friction (ϕ) and cohesion (c) as:

$$\beta = \tan^{-1}\frac{\sqrt{3}\sin\phi}{\sqrt{1 + \frac{1}{3}\sin^2\phi}} \tag{4}$$

$$d = \frac{c\sqrt{3}\sin\phi}{\sqrt{1 + \frac{1}{3}\sin^2\phi}} \tag{5}$$

The geosynthetic reinforcement was modeled using 2-noded isoparametric truss elements with a yielding criterion described by von Mises and isotropic hardening. The reinforcement-to-soil interaction was modeled using a fully bonded contact interface that postulated no slippage between the geosynthetic and surrounding soil. Bridge ends are modeled as plane strain problems, and uniaxial geogrids are suitable where the geogrid strong axis would extend along the highway centerline. The geogrids are expected to enhance the bearing-settlement behavior of the soil embankment underneath the sleeper slab and are usually constructed within compacted layers of aggregate fill in which the size and aggregate angularity are assumed to develop the full interlocking behavior with the geogrid. The full interlocking behavior has been widely reported by several studies in the literature for modeling the inclusion of similar geosynthetic reinforcement close to bridge ends (Abu-Farsakh et al. 2007; Nazzal 2007). The behavior can be modeled in ABAQUS through assigning unique constraints that would tie together the soil and geogrids at their contact interfaces.

Table 2-1. Selected FE Material Models for the typical components of a bridge end section

Soil

Material	**Aggregate**	**Silty Clay**
Bridge End Component	Highway embankment	Highway embankment
Material Model	Extended Drucker Prager	Extended Drucker Prager
Element Type	3-noded triangle	3-noded triangle
Density, ρ (pcf)	165	172
Elastic modulus, E (psi)	17,400	37,700
Poisson's ratio, v	0.35	0.3
Coulomb friction angle, ϕ(°)	48	30
Coulomb cohesion, c (psi)	n/a	11.6

Concrete

Material	**Concrete**
Bridge End Component	Approach and sleeper slabs, bridge abutment
Material Model	Concrete damage plasticity
Element Type	4-noded quadrilateral
Density, ρ (pcf)	145
Tensile modulus, E (ksi)	3,370
Poisson's ratio, v	0.2
Compressive strength, f'_c (ksi)	3.5
Behavior	Uniaxial tensile and compressive behaviors are depicted in Figure 2-1(c)

Geosynthetic Reinforcement

Material	**Type I**	**Type II**	**Type III**
Bridge End Component	Uniaxial geogrid	Uniaxial geogrid	Uniaxial geogrid
Material Model	Von Mises plasticity	Von Mises plasticity	Von Mises plasticity
Element Type	2-noded truss	2-noded truss	2-noded truss
Density, ρ (pcf)	0.061	0.106	0.225
Tensile modulus, E (lb/in)	1,710	6,560	14,850
Poisson's ratio, v	0.3	0.3	0.3
Yield strength @ 2% strain (lb/in)	34	131	297
Behavior	Uniaxial tensile behavior (Fig. 2a)	Uniaxial tensile behavior (Fig. 2a)	Uniaxial tensile behavior (Fig. 2a)

Rebar Reinforcement

Material	**Rebar Reinforcement**
Bridge End Component	Approach and sleeper slabs
Material Model	Von Mises plasticity
Element Type	2-noded truss
Density, ρ (pcf)	500
Tensile modulus, E (ksi)	29,000
Poisson's ratio, v	0.28
Yield strength, σ_y (ksi)	68
Behavior	Uniaxial tensile and compressive behaviors are depicted in Figure 2-1(b)

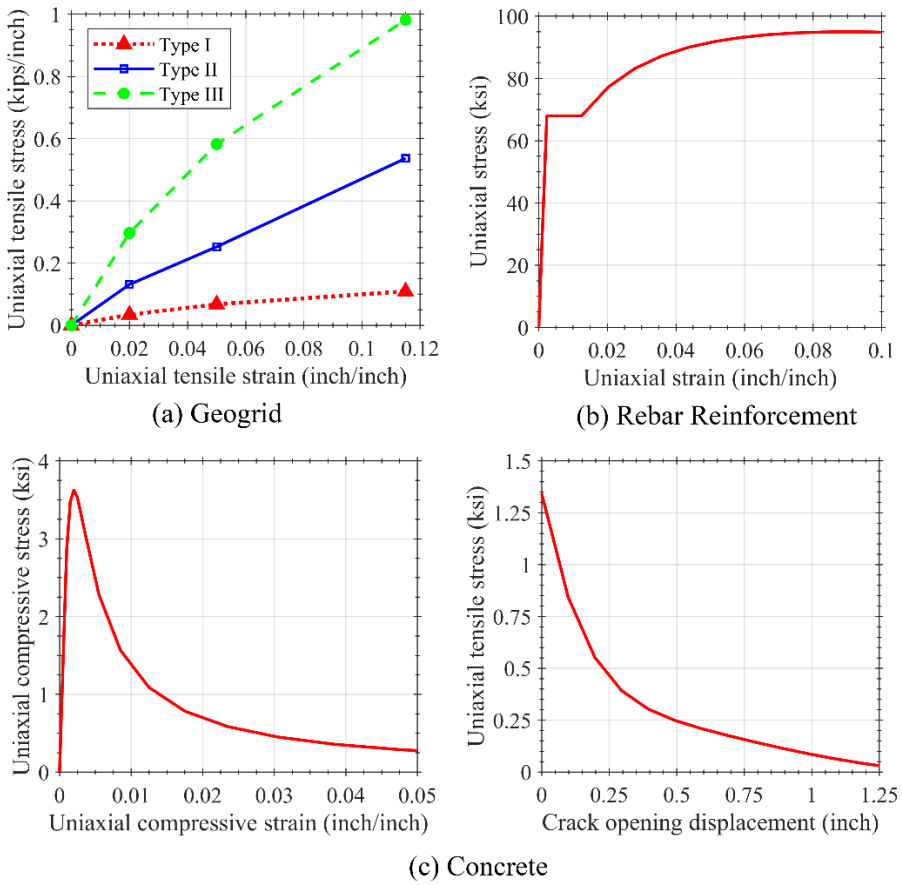

Figure 2-1. Uniaxial stress-strain relationships used to define the material models for the (a) geogrid reinforcement, (b) rebar reinforcement, and (c) concrete.

Two types of soil materials were considered in this study: crushed aggregate and medium plasticity silty clay. Table 2-1 summarizes the input parameters used for the material model of each soil type according to a study by Abu-Farsakh et al. (2012), who measured these input parameters based on large-scale direct shear tests and triaxial compression experiments. Furthermore, these input parameters were calibrated to accurately predict the relationship between the bearing stress versus the settlement for a 6-inch wide strip footing that was pushed in a laboratory-scaled setup against reinforced and unreinforced aggregate fill (Abu-Farsakh et al. 2008). Two types (I and II) of uniaxial geogrids were considered in this study, as listed in Table 2-1. The suppliers provided the material properties that were used to model the geogrid reinforcement, such as the stress-strain curves of uniaxial tension in Figure 2-1(a).

Concrete and Rebar Reinforcement

Bridge ends consist of several reinforced concrete sections, such as the approach slab, sleeper slab, and bridge abutment. The concrete was modeled using linear-strain quadrilateral elements as stress-strain behavior is determined by the "concrete damage plasticity" model available in ABAQUS. The model adopts the yield criterion proposed by Lubliner et al. (1989), and modified by Lee and Fenves (1998), to account for different softening behavior under tensile and compressive

loading within the framework of stiffness degradation and continuum damage mechanics. The stress-strain response of concrete under uniaxial compression was assumed to follow the relationship proposed by Saenz (1964),

$$\sigma_c = \frac{E_0 \varepsilon_c}{1 + \left(\frac{E_o \varepsilon_p}{\sigma_p} - 2\right)\left(\frac{\varepsilon_c}{\varepsilon_p}\right) + \left(\frac{\varepsilon_c}{\varepsilon_p}\right)^2} \tag{6}$$

where σ_c and ε_c are the uniaxial compressive stress and strain, respectively. σ_p and ε_p are the experimentally determined maximum compressive stress and corresponding strain, which represent the cylinder strength. Here, $\sigma_p = f_c' = 3.5$ ksi and $\varepsilon_p = 0.002$. E_0 is the concrete elastic modulus that was estimated according to the American Concrete Institute (ACI) Guide (2002):

$$E_0 = 57{,}000\sqrt{f_c'}\ (psi) \tag{7}$$

Under uniaxial tension, the concrete damage plasticity model involves a tensile crack opening displacement (w_t) and a required fracture energy per unit surface area for crack propagation (G_I). This chapter employed the formula proposed by Hordijk (1993) for the relationship between the tensile stress (σ_t) and crack opening displacement (w_t) as:

$$\frac{\sigma_t}{f_t} = \left[1 + \left(\frac{c_1 w_t}{w_{cr}}\right)^3\right] exp\left(-\frac{c_1 w_t}{w_{cr}}\right) - \frac{w_t}{w_{cr}}(1 + c_1^3)\, exp(-c_2) \tag{8}$$

$$w_{cr} = 5.14\frac{G_F}{f_t} \tag{9}$$

where w_{cr} is crack opening displacement at the complete loss of tensile stress, f_t is the uniaxial tensile strength of concrete, and $c_1 = 3.0$ and $c_2 = 6.93$ which are fitting constants determined from standard tensile tests of concrete. Typical values of f_t, 1.3 ksi, and G_F, 377 lb/in, were used according to the empirical correlations with f_c' that were proposed by Ceb-Fip (1990). Figure 2-1(c) illustrates the uniaxial tensile and compressive stress-strain behavior of concrete that was modeled by the FE analysis.

Rebar reinforcement was modeled using 2-noded truss elements whose yielding behavior is described by the von Mises yield criterion and isotopic hardening. Analogous to the geosynthetic reinforcement, the rebar elements were joined along their contact interface with the meshes representing the reinforced concrete sections in which no slippage is permitted. For the rebar reinforcement, Steel Grade A706 (yielding strength, σ_y equals 68 ksi) was modeled since it is the type of steel reinforcement recommended by the AASHTO Guide Specifications for LRFD seismic bridge design. Figure 2-1(b) depicts the uniaxial stress-strain relationship of the rebar reinforcement that was modeled by the FE analysis.

2.3 Parametric Study

An FE mesh was generated in ABAQUS for a typical bridge end section (Figure 2-2(a)), which is composed of a reinforced concrete approach slab that is connected at both ends to the bridge abutment and a reinforced concrete sleeper slab connected to the approach slab. While the abutment is fixed (pile-capped), the sleeper slab rests on flexible meshes of soil embankment that is assumed, for the sake of the parametric study, to be silty clay with the possible inclusion of Type II geogrid reinforcement (see Table 2-1 for material properties). The boundary conditions and problem dimensions in terms of the width of the sleeper slab (B) were adopted from a similar FE analysis for strip footing that bears against reinforced soil embankment (Abu-Farsakh et al. 2007).

The parametric study evaluated the influence of geogrid reinforcement on UBSS. As demonstrated in Figure 2-2(a), the case of full separation was assumed between the approach slab and the soil underneath it. This assumption was recently verified via field instrumentation for the Bayou Courtableau bridge in Louisiana, where the approach slab was supported by a sleeper slab that was seated on a soil embankment with geogrid reinforcement (Chen and Abu-Farsakh 2016). Namely, the geogrid reinforcement provided adequate support for the approach slab end at the H/S joint such that the approach slab exhibited flexure deformation rather than bearing against the underneath soil along its span length.

The parametric study included about 230 runs of the FE analyses for different designs of sleeper slab by means of B and the inclusion of geogrid reinforcement underneath it. In each run, dead loads were applied then the sleeper slab was assigned a displacement boundary condition of $0.12 \times B$ settlement. Both dead loads and settlement were applied incrementally in which the size of the load increments was automatically scaled by ABAQUS/Standard solver to ensure stable quasi-static analysis. At $0.12 \times B$ settlement, the vertical stress under the center of the sleeper slab was considered the default UBSS, and the influence of geogrid reinforcement on UBSS was evaluated for all runs. The runs included a design case for soil embankments at bridge ends without the inclusion of geogrid reinforcement to provide baseline estimates for normalization, a design case for a single-layered geogrid is added to determine the effective depth of reinforcement (or influence zone). Then a case for a multi-layered geogrid equally-spaced within the effective depth of reinforcement is analyzed in search of an optimum design layout.

No Geogrid Reinforcement

For baseline estimates, the FE analysis was initially conducted on the bridge end section demonstrated in Figure 2-2(a) without the inclusion of geogrid reinforcement. Several analyses were executed in which B was increased from 2 feet to 7 feet at 6-inch increments. Figure 2-2(b) depicts the bearing stress versus settlement under the center of the sleeper slab for the conducted analysis. The curves in Figure 2-2(b) show that the UBSS increased with increasing B, and this trend was clearly established when the settlement of the sleeper slab was normalized with respect to B in Figure 2-2(c).

The zone of influence is defined as the region of soil embankment that surrounds the sleeper slab and receives the majority of loads at failure ($0.12 \times B$ settlement). Figure 2-3(a) depicts a stress field within the simulated soil embankment in which the stress distribution was explored along vertical and horizontal paths below the sleeper slab. The vertical path starts from the center of the sleeper slab and extends along the depth of the soil embankment. The horizontal path crosses the vertical path at a depth of $2 \times B$ below the sleeper slab and extends along the highway centerline. Figure 2-3(b) and (d) plot the vertical stress distribution along the horizontal and vertical paths. Interestingly, unique curves were obtained in Figure 2-4(c) and (e) when normalizing the distance along the selected path by B and the corresponding stress with respect to the bearing stress at the center of the sleeper slab. Accordingly, the influence zone was determined to surround the sleeper slab at $2 \times B$ in the horizontal direction and $1.5 \times B$ in the vertical direction as demonstrated by the asymptotic lines to the unique curves in Figure 2-3(c) and (e).

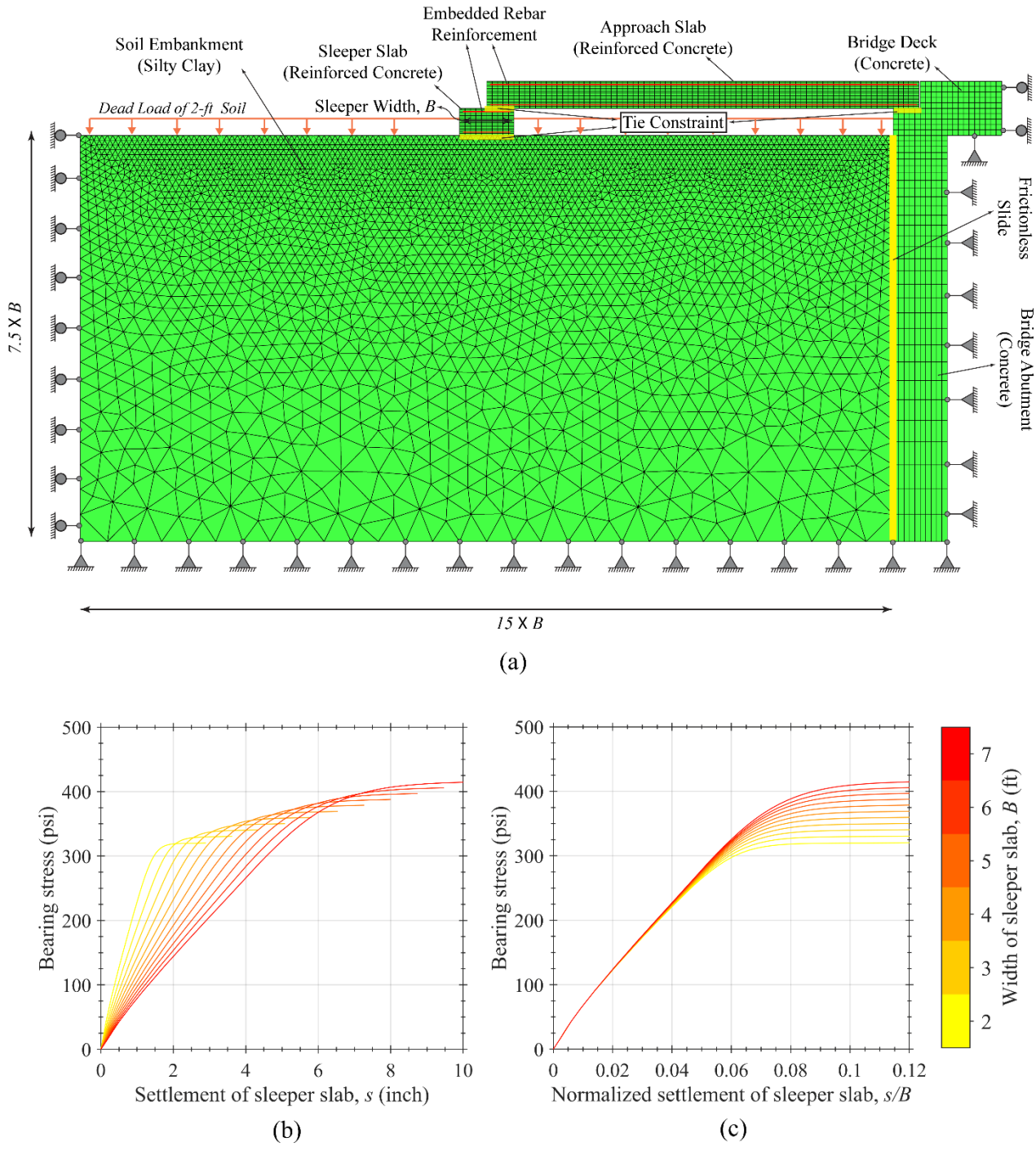

Figure 2-2. (a) Demonstration of the FE mesh generated for the bridge end section; Relationship of bearing stress versus (b) settlement and (c) normalized settlement for the sleeper slab.

Single-Layered Geogrid Reinforcement

An optimum design parameter of the geogrid-reinforced soil for the sleeper slab is the effective depth of reinforcement, below which the reinforcement inclusion has negligible benefits on the performance of the sleeper slab. In the published literature, numerical and experimental studies proposed that the effective depth of reinforcement reaches a range between 1.5 and $2 \times B$ below a strip footing, resting on geogrid-reinforced soil (Das et al. 1994; Abu-Farsakh et al. 2007). In this study, the effective depth of reinforcement was determined by executing analysis for a single-layered geogrid reinforcement within the soil embankment underneath the sleeper slab, as illustrated in Figure 2-4(a). The single-layer was placed initially at a depth of $0.4 \times B$, and then FE analyses were repeated while the geogrid layer was shifted at $0.1 \times B$ increments until reaching a depth of $4 \times B$ below the sleeper slab. Figure 2-4(b) shows the relationship between UBSS versus the depth of the single-layered geogrid, and Figure 2-4(c) plots the same relationships when normalizing the depth of the single-layered geogrid by B and UBSS with respect to that for the unreinforced soil case (Figure 2-2). Clearly, there exists a depth near $1 \times B$ for a single-layered geogrid reinforcement that would optimize the improvement in the UBSS. The optimized improvement can reach a factor of 1.3 for the case of using a sleeper slab with $B = 3$-ft, and becomes less significant for sleeper slabs with larger B. Furthermore, Figure 2-4(c) depicts an effective depth of geogrid reinforcement that reaches $2 \times B$ below the sleeper slab in agreement with results from the published literature.

The length of geogrid reinforcement is another design parameter of interest for the examined design of the bridge end section. Different lengths of geosynthetic reinforcement were recommended in the literature for the reinforced soil supporting strip footings. For instance, Adams and Collin (1997) recommended $2 \times B$ for the length of geogrid reinforcement based a series of large-scale tests on reinforced sand. The numerical FE analysis by Maharaj (2003) also advocated for $2 \times B$ as a suitable length for geogrid reinforcement within clayey soil. However, a larger length up to $2 \times B$ was suggested by Shin et al. (2002), according to laboratory-scaled tests of geogrid-reinforced clayey soil. In this study, Figures 2-4(c) and (d) display the tensile axial strain along the geogrid for the single-layered analysis with $B =$ 3-ft and 6-ft. Obviously, the geogrid exhibited insignificant axial strain beyond $2 \times B$ along each direction from the center of the sleeper slab or when the single-layer was placed below a depth of $1.75 \times B$ underneath the sleeper slab. Furthermore, the geogrid manifested a peak tensile strain at the center of the sleeper slab when the single-layer was placed between a depth of 0.75 and $1.5 \times B$, whereas two peak strains occurred toward the sleeper slab sides when the single-layer was placed below $1.5 \times B$ or above $0.75 \times B$. These relationships would be difficult to expose without the normalization procedure for the geogrid length and depth with respect to B.

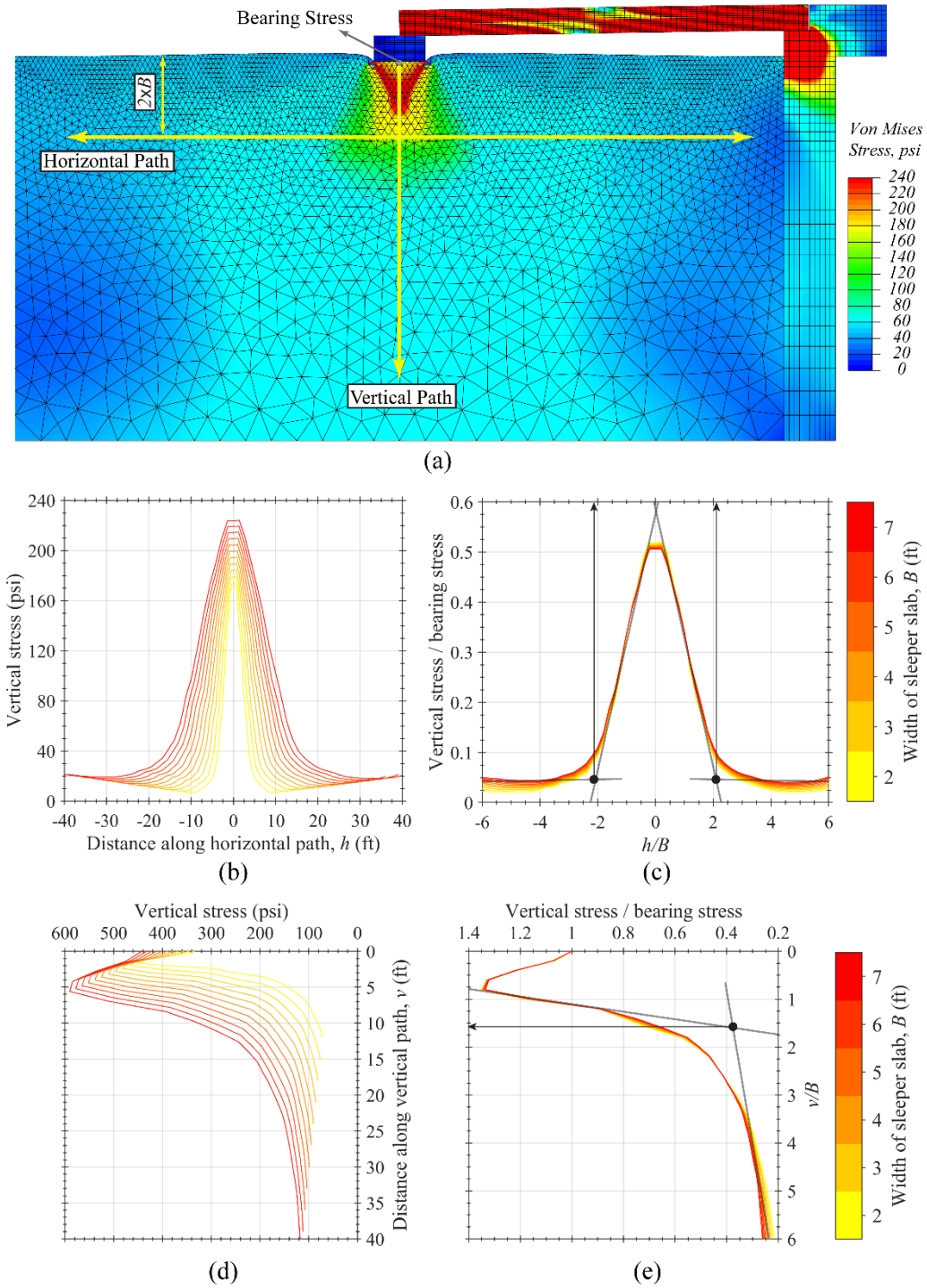

Figure 2-3. (a) Illustration of stress field within the soil embankment below the sleeper slab without the inclusion of geogrid (B=3-ft); (b)-(e) vertical stress distribution along horizontal and vertical paths.

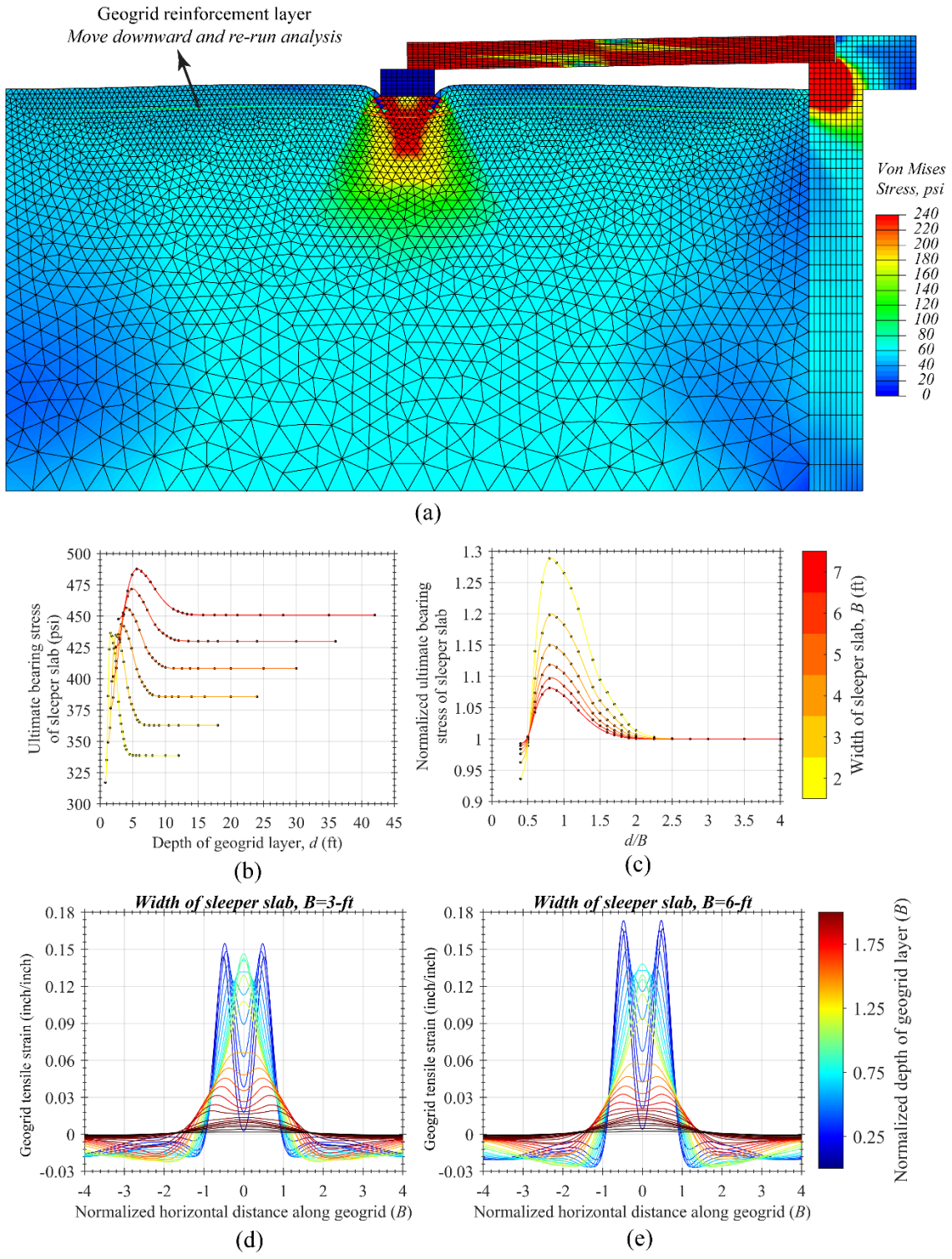

Figure 2-4. (a) Illustration of stress field within the soil embankment below the sleeper slab (B=3-ft); (b) UBSS and (c) normalized UBSS for the analysis of single-layered geogrid; Distribution of tensile strain along the single-layer of geogrid reinforcement for (d) B= 3-ft and (e) B= 6-ft.

Multi-layered Geogrid Reinforcement

The single-layered analyses have demonstrated that $2 \times B$ is the effective depth (or influence zone) below which there is no influence for the geogrid reinforcement on the bearing-settlement behavior of the sleeper slab. These geogrid reinforcements are usually constructed in multiple layers to achieve maximum improvement since the geogrid cost is low compared to the total budget for the construction of a new bridge. Therefore, the FE parametric analyses were used to investigate the effect of geogrid spacing and the number of layers on the bearing-settlement behavior of the sleeper slab. As depicted in Figure 2-5, FE analysis considered several geogrid reinforcement layouts with 1 to 8 equally-spaced layers within the $2 \times B$ effective depth of the soil embankment below the sleeper slab.

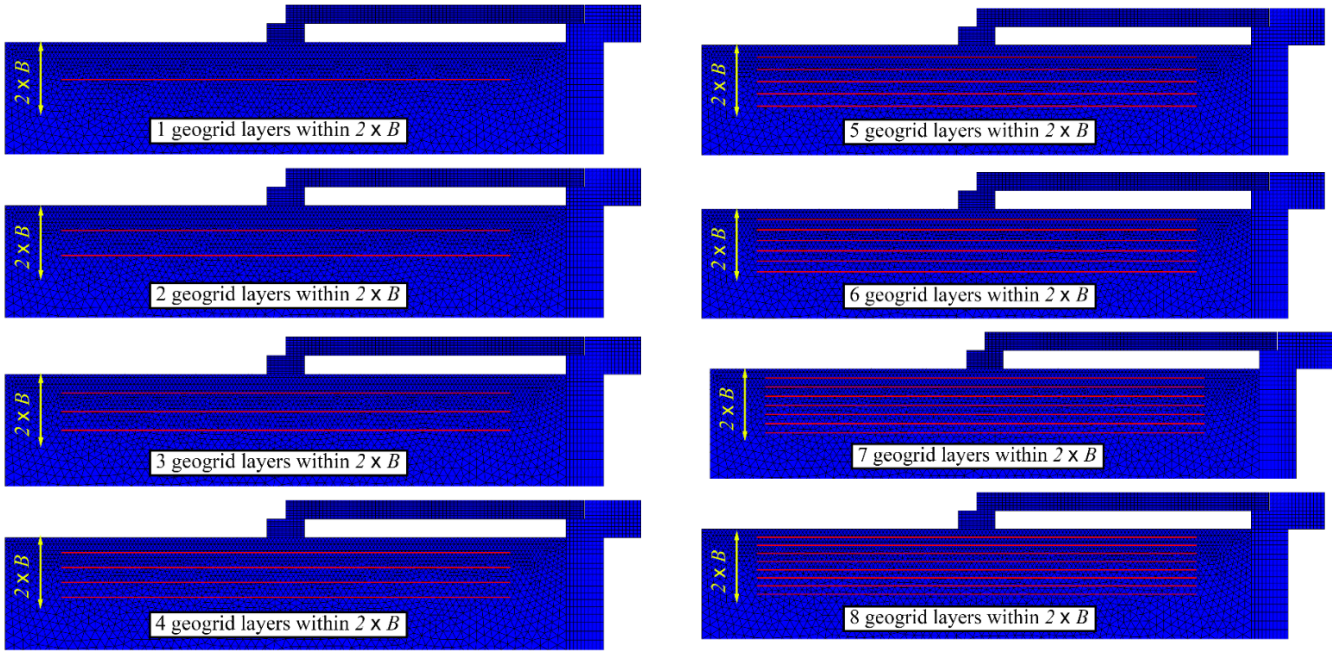

Figure 2-5. Demonstration of the design layouts that were examined in the parametric study part of multi-layered geogrid reinforcement within the effective depth $2 \times B$.

Figure 2-6(a) displays the relationship of bearing stress versus settlement for the sleeper slab in the FE analyses conducted for the multi-layered geogrid reinforcement. The dashed curves represent the relationships for sleeper slabs when supported on unreinforced soil embankment (Figure 2-2(b)). Clearly, the geogrid reinforcement improved the UBSS and prevented the ultimate settlement manifested by the dashed curves when the sleeper slab failed. For each curve in Figure 2-6(a), the UBSS value was determined at $0.12 \times B$ settlement and plotted in Figure 2-6(b) versus the number of geogrid reinforcement layers. The UBSS in Figure 2-6(c) was also normalized with respect to the UBSS displayed by the dashed curves in Figure 2-2(a) (unreinforced soil embankment with the same B). Notice that the benefits of including more reinforcement become less significant when using more than five layers of geogrid within the effective depth ($2 \times B$) below the sleeper slab. The use of five equally-spaced layers of geogrid reinforcements placed within $2 \times B$ zone would imply a geogrid spacing of $0.33 \times B$. Furthermore, more benefits for the geogrid reinforcement can be seen from Figure 2-6(c) when using a sleeper slab with a smaller B.

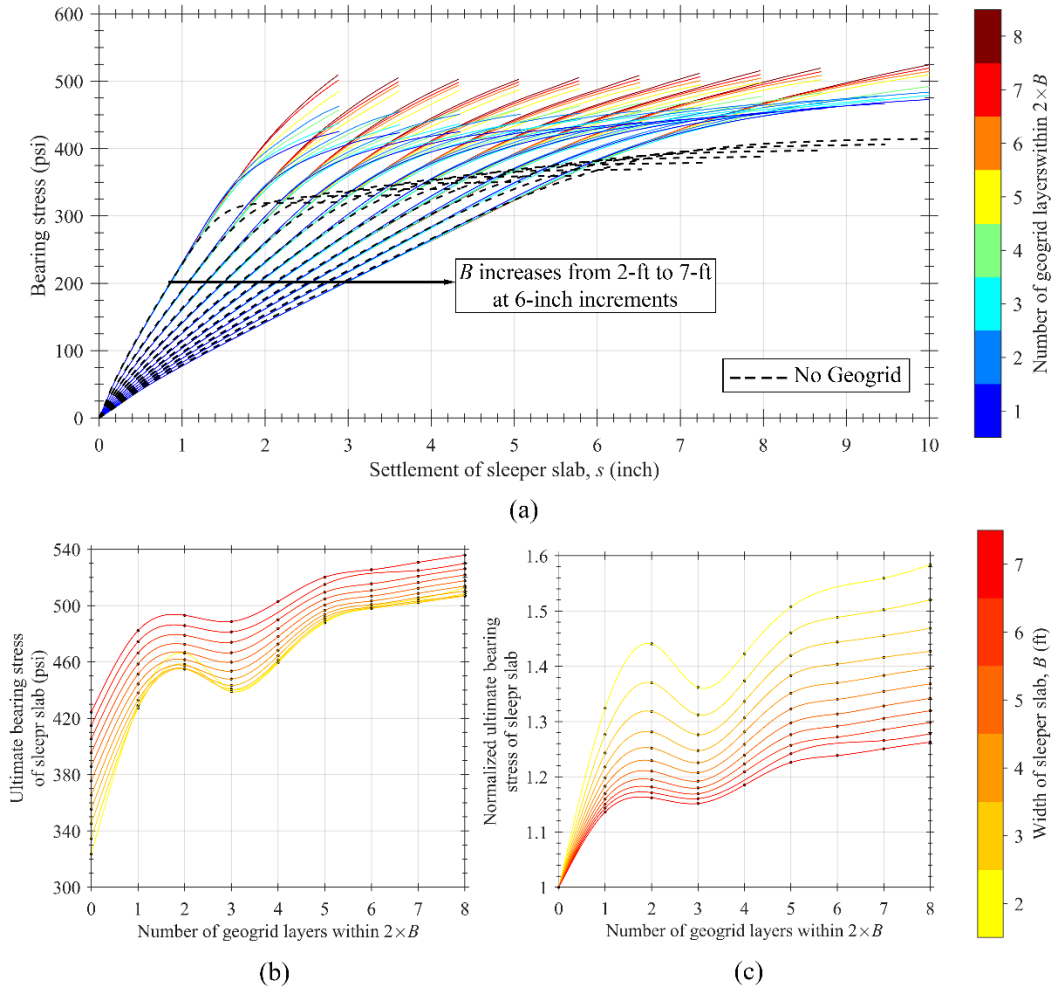

Figure 2-6. (a) Relationship of bearing stress versus settlement for the FE analysis of multi-layered geogrid within the effective depth of reinforcement ($2 \times B$) below the sleeper slab; Relationship of (b) UBSS and (c) normalized UBSS versus numbers of geogrid layers within $2 \times B$.

The geogrid reinforcement is expected to affect the distribution of vertical stress within the soil embankment below the sleeper slab that was earlier examined for unreinforced soil in Figure 2-3. In order to further assess this effect, Figure 2-7 displays the distribution curves of vertical stresses at failure ($0.12 \times B$ settlement) along similar vertical and horizontal paths that were earlier selected in Figure 2-3 for the case of unreinforced soil. The curves were also normalized with respect to the bearing stress at the center of the sleeper slab in a similar manner to the procedure followed in Figure 2-3(c) and (e). At the same failure settlement ratio, Figure 2-7(b) demonstrated how the geogrid reinforcement alleviated the peak in stress along the vertical path around a depth of $0.5 \times B$ below the sleeper slab. Conversely, the stress along the horizontal path in Figure 2-7(d) exhibited a higher peak and a wider bell shape when more geogrid layers are included. These insights indicate that the inclusion of more geogrid layers would correspond to larger bearing loads redistributing stresses within the reinforced soil over a wider area, which is expected to reduce the amount of differential settlement and hence improve the rideability at the H/S joint.

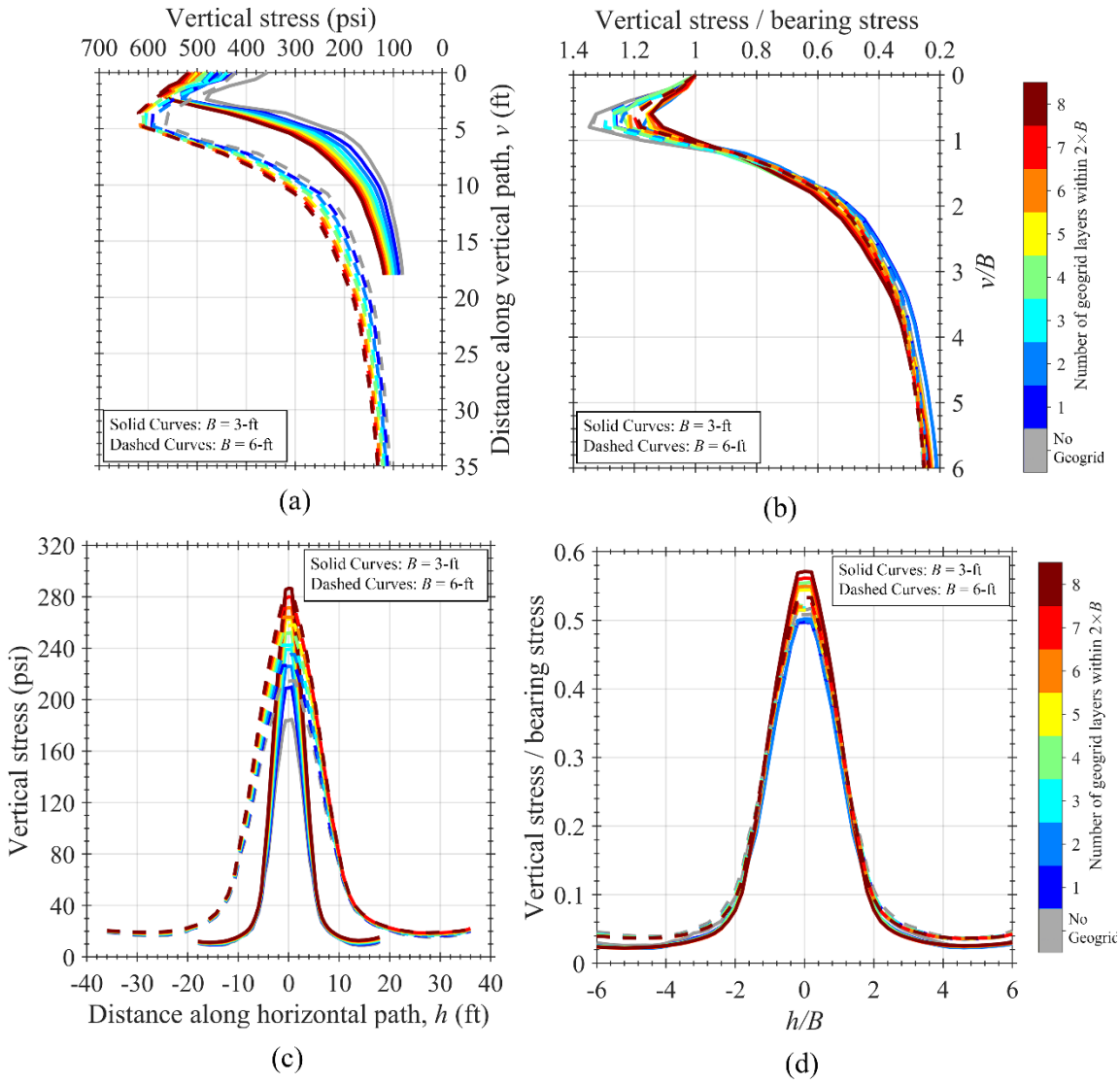

Figure 2-7. Distribution of vertical stress along similar horizontal and vertical paths presented in Figure 2-3(a), but instead for the analysis of multi-layered geogrid.

2.3 Case Study: Retrofit Design for the TDOT Bridge End Problem

The design of bridge ends is specified by TDOT in standard drawing STD-5-1 and consists of a 3-foot wide sleeper slab (B = 3-ft) that supports a 24-foot long ($8 \times B$) approach slab at the H/S joint. As detailed in Figure 2-8(a), (i) both sleeper and approach slabs have special provisions for rebar reinforcement, (ii) the approach slab is tied to the standard integral abutment, and (iii) the sleeper slab for asphaltic highway pavement is typically constructed with a 1-foot wide mid-stem. TDOT has recently been reporting settlement issues with their current design of bridge ends, and most of the settlement occurs explicitly at the H/S joint. The settlement at the H/S joint is randomly reported over the state and has not been attributed to a particular region with a specific type of soil embankment. This randomness has led the TDOT to suspect poor construction and compaction practices to be the major cause of settlement and has motivated the quest to develop a retrofit design to their current state of practice. Figure 2-8(a) presents the preliminary retrofit design proposed by TDOT, which suggests replacing the soil embankment underneath the approach slab with three compacted layers of openly-graded aggregate that are 9-inch thick and reinforced with geogrid/textile. In this case study, the FE analysis would assess the benefits of this retrofit design and suggest recommendations for a modified design version that would significantly improve the UBSS. The analysis is then used to evaluate the differential settlement of the TDOT modified design under the effect of service loads, including dead loads and different types of traffic highway live loads.

UBSS Assessment of the Retrofit Design

As demonstrated in the stress field of Figure 2-8(b), the FE analysis was upgraded to model the retrofit design proposed by TDOT, including details such as the layout of the geosynthetic reinforced aggregate, and the dimensions and rebar reinforcement of the sleeper and approach slabs. A ¼-inch separation was modeled between the approach slab and underneath soil in order to account for the experimental findings that were previously discussed by Chen and Abu-Farsakh (2016). For the sake of the case study, the material models for the soil embankment were modified to incorporate conservative strength properties of $\phi = 34^o$ for aggregate, and $\phi = 10^o$ and $c = 6.9\ psi$ for silty clay. These conservative values were recommended by TDOT in order to account for the poor compaction of soil embankment at the H/S joint due to the limited space of work behind bridge abutments, which is believed to be the major cause of settlement. The light grey curve (TDOT) in Figure 2-8(c) plots the relationship of bearing stress versus settlement for the sleeper proposed by the TDOT retrofit design in addition to six other design layouts that were examined in search of improving performance. The examined layouts are illustrated in Figure 2-9 and compared to the TDOT retrofit design as follows:

- ***Layout-1*** – Remove the geosynthetic reinforcement proposed by TDOT. The UBSS value obtained for the analysis of this layout was used as a baseline estimate for normalization of bearing stresses in Figure 2-8(d) to evaluate the improvements in UBSS as multiplying factors for each design layout.
- ***Layout-2*** – Increase B in the TDOT retrofit design from 3 feet to 4 feet in order to evaluate the benefits of using a sleeper slab that has a larger size.
- ***Layout-3 to Layout-5*** – Respectively add two, three, and four layers of 9-inch-thick reinforced aggregate below what is proposed by TDOT.

- ***Layout-6*** – Similar to Layout-4 but modified by removing the top two layers of geosynthetic reinforcement.

Figure 2-8(c) demonstrates that the TDOT retrofit design exhibited UBSS of about 55 psi, after which the soil embankment manifested indefinite settlement without any increase in bearing stress. Comparing the TDOT curve with Layout-1 shows that the inclusion of geosynthetic reinforcement as proposed by the TDOT has no significant improvement on UBSS. The geosynthetic reinforcement proposed by TDOT reaches a depth of $0.5 \times B$ below the sleeper slab, and the outcomes of the parametric study in Figure 2-4(c) clearly show no benefit from including geosynthetic reinforcement within $0.5 \times B$ depth below the sleeper slab. Furthermore, increasing B to 4 feet in Layout-2 offered little improvement to UBSS (<7%). However, the replacement of additional soil embankment by layers of reinforced aggregate appeared to be the most effective way to improve the UBSS in Layouts-3, 4, and 5, with the corresponding improvement factors of 1.15, 1.3, and 1.4, respectively. To strike a balance between construction cost and effort, including just three additional layers of geosynthetic reinforcement below what is proposed by the TDOT retrofit design is recommended, similar to Layout-4. Furthermore, the FE analysis suggested insignificant benefits from the inclusion of the top two geosynthetic layers in the TDOT design. Accordingly, the recommended design is illustrated by Layout-6 presented in Figure 2-9, which is composed of five layers of geosynthetic reinforcement equally-spaced at 9-inches below the sleeper slab. This layout implies a 3.75-foot total depth of reinforced aggregate below the sleeper slab, which is about $1.25 \times B$, and would improve the UBSS by a factor of 1.3. The compaction of an additional layer would extend the reinforced depth of soil embankment to $1.5 \times B$ below the sleeper slab and improve the UBSS by a factor of 1.4. This latter suggestion is recommended for the ends of newly-constructed embankments as it has negligible cost relative to the total budget of the bridge construction. Lastly, the FE analysis was executed for Layout-6 (recommended) using the Type I and III geogrids (see Table 2-1 for properties), which in order are weaker and stronger grades of geogrids than that considered so far (Type II). The results showed little influence from using lower/higher grade geogrids in which the improvement factor of UBSS for Layout-6 ranged from 1.3 to 1.33 when different types of geogrids were used.

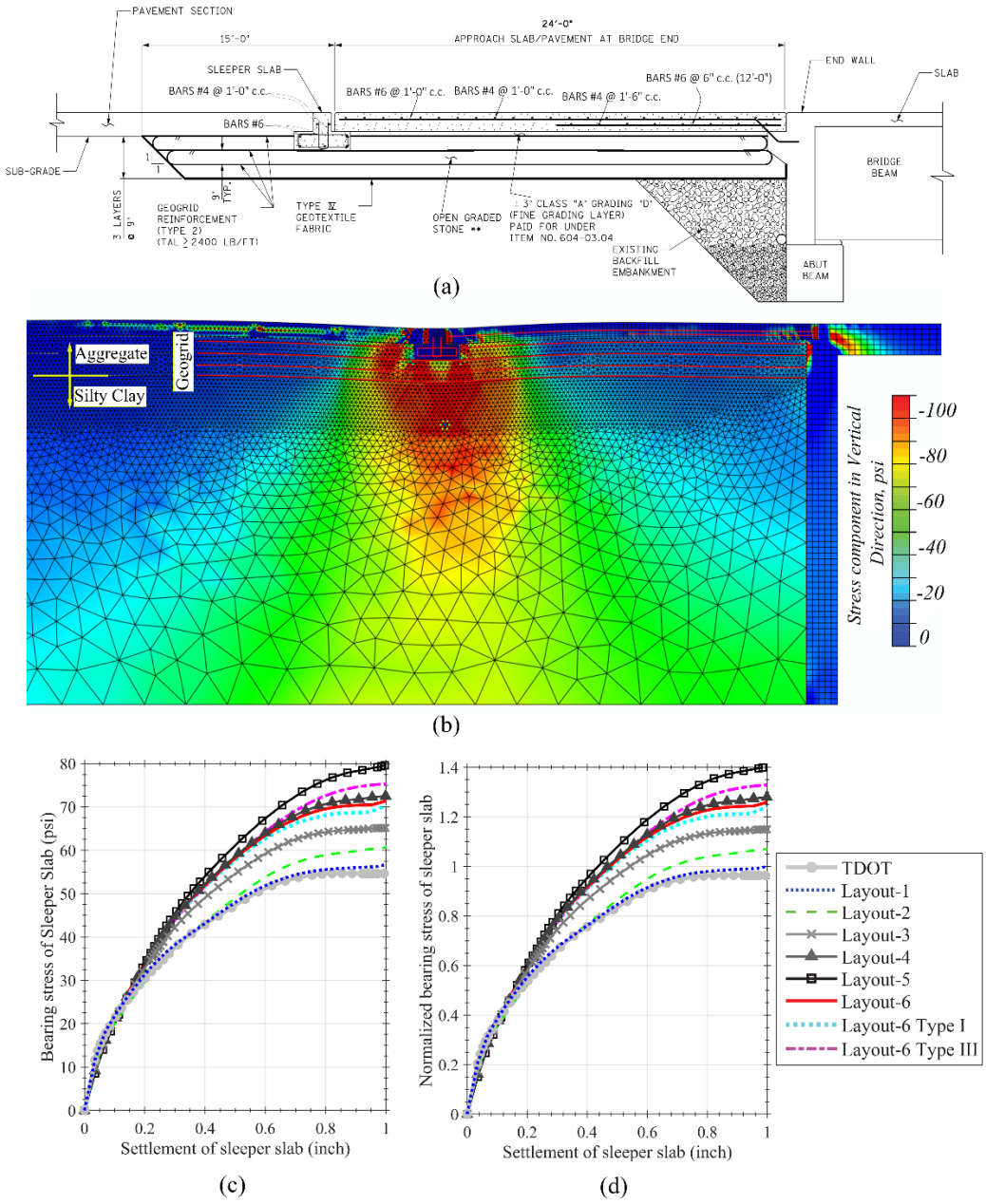

Figure 2-8. (a) Preliminary retrofit design proposed by TDOT for the geosynthetic reinforcement at bridge ends. (b) FE analysis of TDOT design (c) Relationship of bearing stress versus settlement for TDOT design and the other design layouts that were modeled using FE analysis (see Figure 2-9).

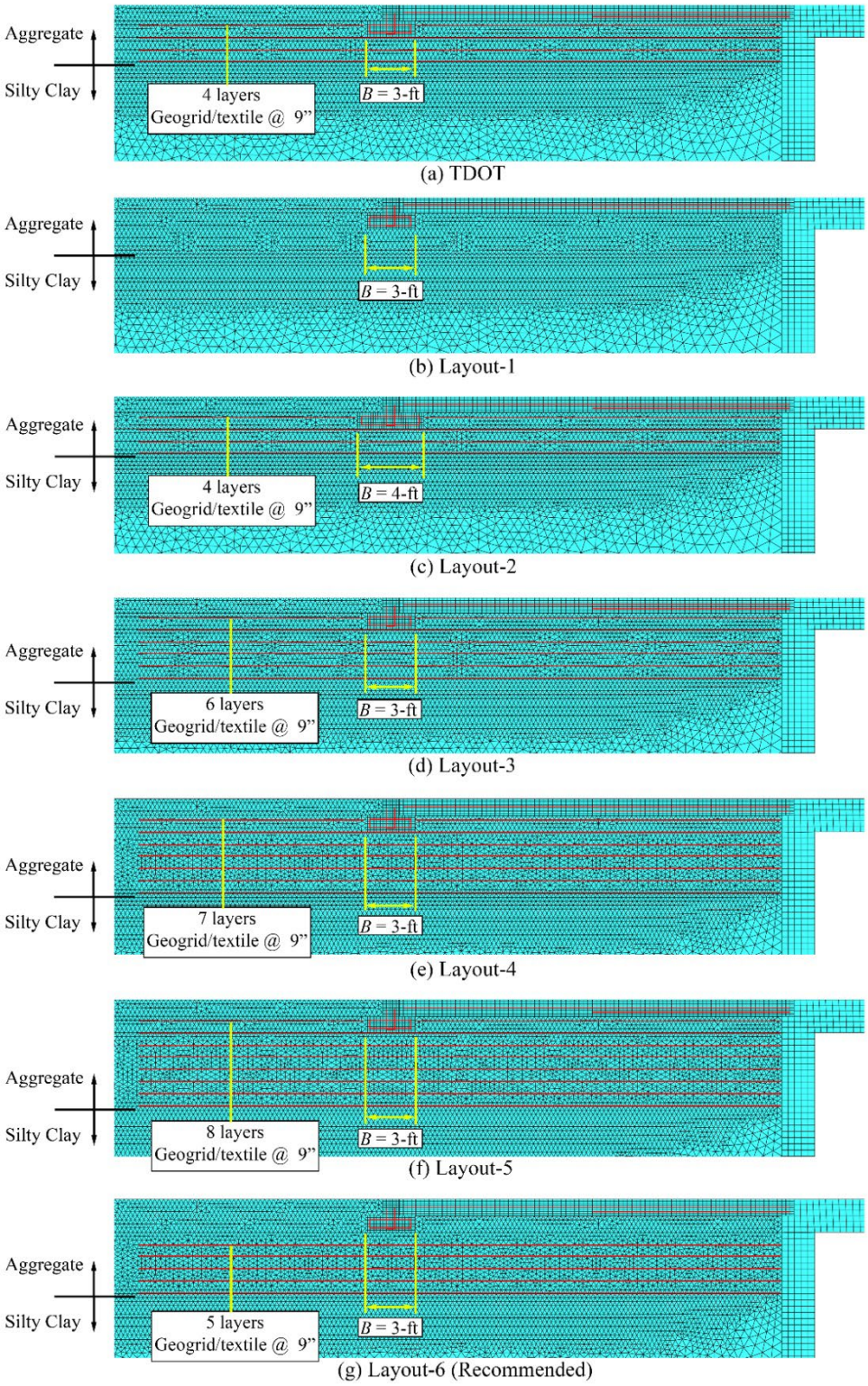

Figure 2-9. The design layouts that were examined by the FE analysis using ABAQUS in addition to the proposed retrofit design by the TDOT.

Performance under Service Loads

The FE analysis was developed to predict the differential settlement at the H/S joint under the effect of dead loads and different types of highway traffic live loads. Figure 2-10 illustrates the different types of traffic loads that were modeled, which can be summarized as:

- **Load Case-1** (Figure 2-10(a)) – A static load of 250-psf uniformly distributed over the highway pavement.
- **Load Case-2** (Figure 2-10(b)) – A static traffic lane load of 0.64 klf distributed over a standard 10-foot wide highway lane, and an AASHTO HL-93 design tandem that passes across the approach slab. The design tandem consists of two axles spaced at 4 feet, and each axle exerts a load of 25-kips.
- **Load Case-3** (Figure 2-10(c)) – A static traffic lane load of 0.64 klf distributed over a standard 10-foot wide highway lane, and an AASHTO HL-93 design truck that passes across the approach slab. The design truck consists of three axles that exert loads of 8, 32, and 32-kips; respectively. The front two axles are spaced at 14 feet, while the spacing between the rear two axles varies between 14 to 30 feet. The critical case of 14-foot spacing between the rear two axles was modeled since this case would have the two axles exist on the approach slab (24-foot length) at the same time and as near as possible.
- **Load Case-4** – Similar to Load Case-2 but with two tandems following each other and spaced at 14 feet.
- **Load Case-5** – similar to Load Case-2 but with ten tandems following each other and spaced at 125 feet.

Dead loads were incrementally applied in each case, followed by the uniformly distributed traffic loads (i.e., 250-psf or AASHTO lane load). Afterward, quasi-static frictionless sliding of a design tandem/truck across the bridge end was simulated for Load Case-2 to Load Case-5. The design axle loads were modeled using FE rigid parts (i.e., neglecting deformations) where the contact interface with the highway pavement was based on the standard shape specified by AASHTO (10-inch by 20-inch rectangle). These tire parts were assigned self-weights that would produce an equivalent load to the design axle. Furthermore, the design axle loads were factored by $IM = 1.3$ to account for dynamic impact and the lane load by the multi-lane factor $m = 1.2$.

Figure 2-11 displays the settlement at the H/S joint that is predicted by the FE analysis for the TDOT retrofit design under the five load cases. As demonstrated in Figure 2-10(a), two settlement values were recorded at the H/S joint from the approach slab side (H/S joint AS) and the sleeper slab (H/S joint SS). Both settlement values were almost the same, which indicates no differential settlement and no sudden change in the slope at the H/S joint for crossing motorists. Analysis of service loads was also conducted for the recommended design (Layout-6), and the settlement results were included in Figure 2-11. The contributions of service loads were very low relative to UBSS (55 psi for TDOT and 70 psi for Layout-6). Therefore, little settlement (<¼-inch) occurred which caused a very small difference in settlement for both design layouts.

Figure 2-12 presents the settlement at the middle of the approach slab for the TDOT and Layout-6 designs under the six load cases. The settlements are displayed at two points taken within the approach slab and underneath the soil embankment, as demonstrated by Figure 2-10(a). The unequal settlement between the two points was caused by the ¼-inch separation modeled between

the approach slab and underneath soil. This separation would make the approach slab deflect under service loads before pushing against the underneath soil embankment. Therefore, the approach slab must have adequate flexure rigidity to support the service loads by means of thickness and rebar reinforcement. The FE analysis predicted less than $^{2}/_{5}$-inch settlement at the center of the approach slab for both the TDOT and recommended designs when subjected to the five load cases. This amount of settlement is considered small (<0.15%) with respect to the span length of the approach slab (24-ft).

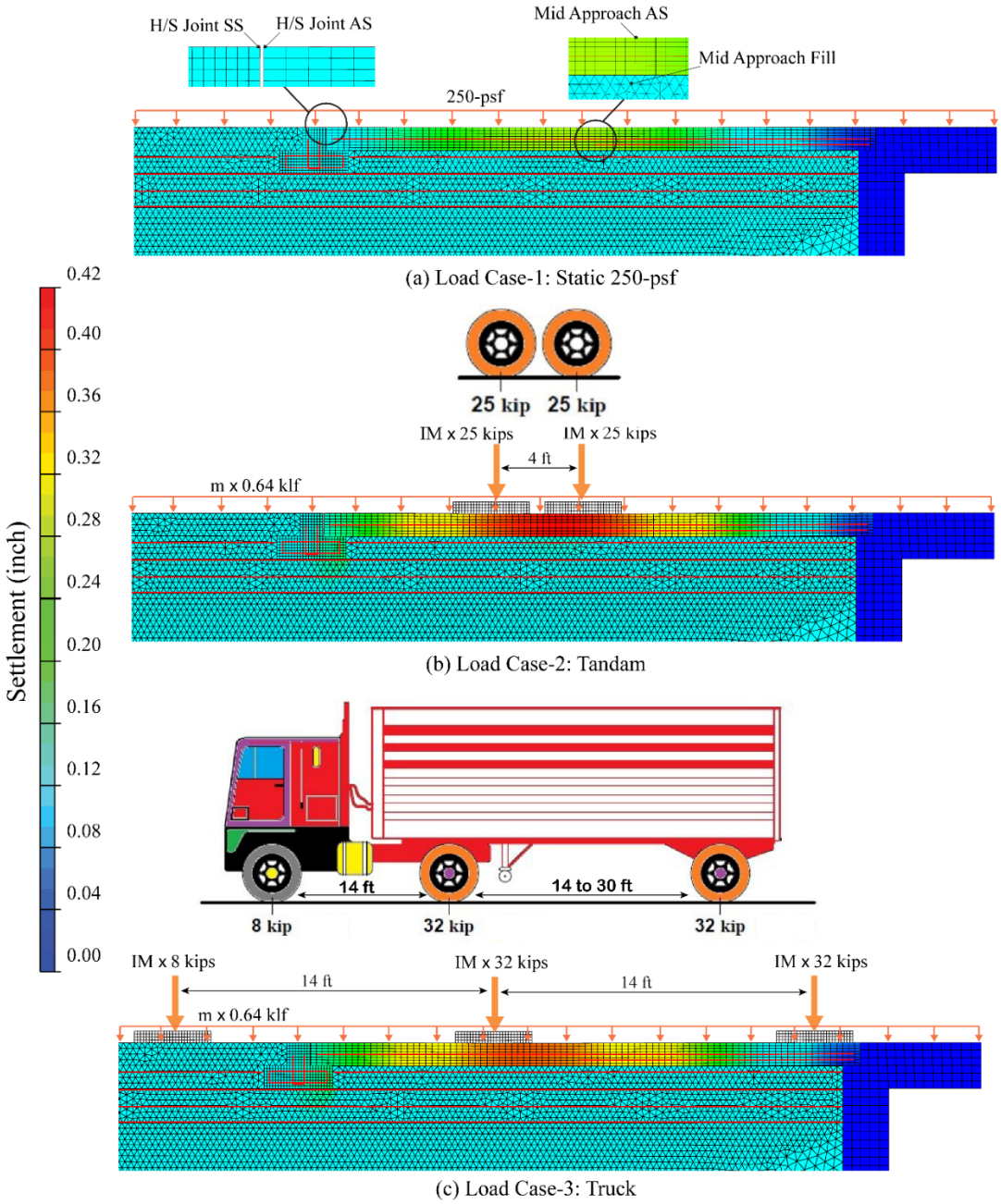

Figure 2-10. Settlement at bridge end for the retrofit design proposed by TDOT under service loads, including different types of traffic highway loads.

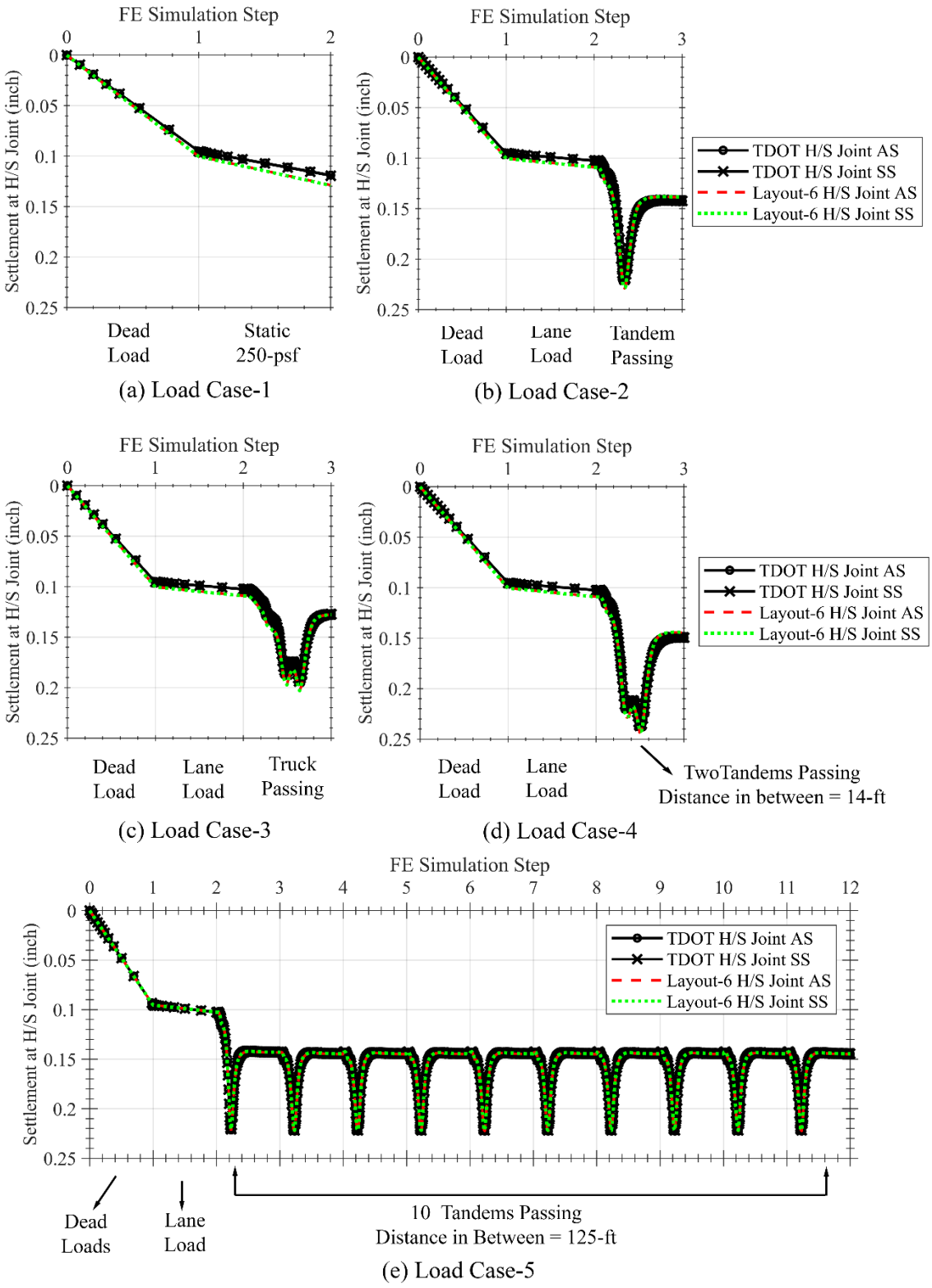

Figure 2-11. Predicted settlement at the H/S joint for the TDOT and Layout-6 (recommended) designs under the effect of service loads.

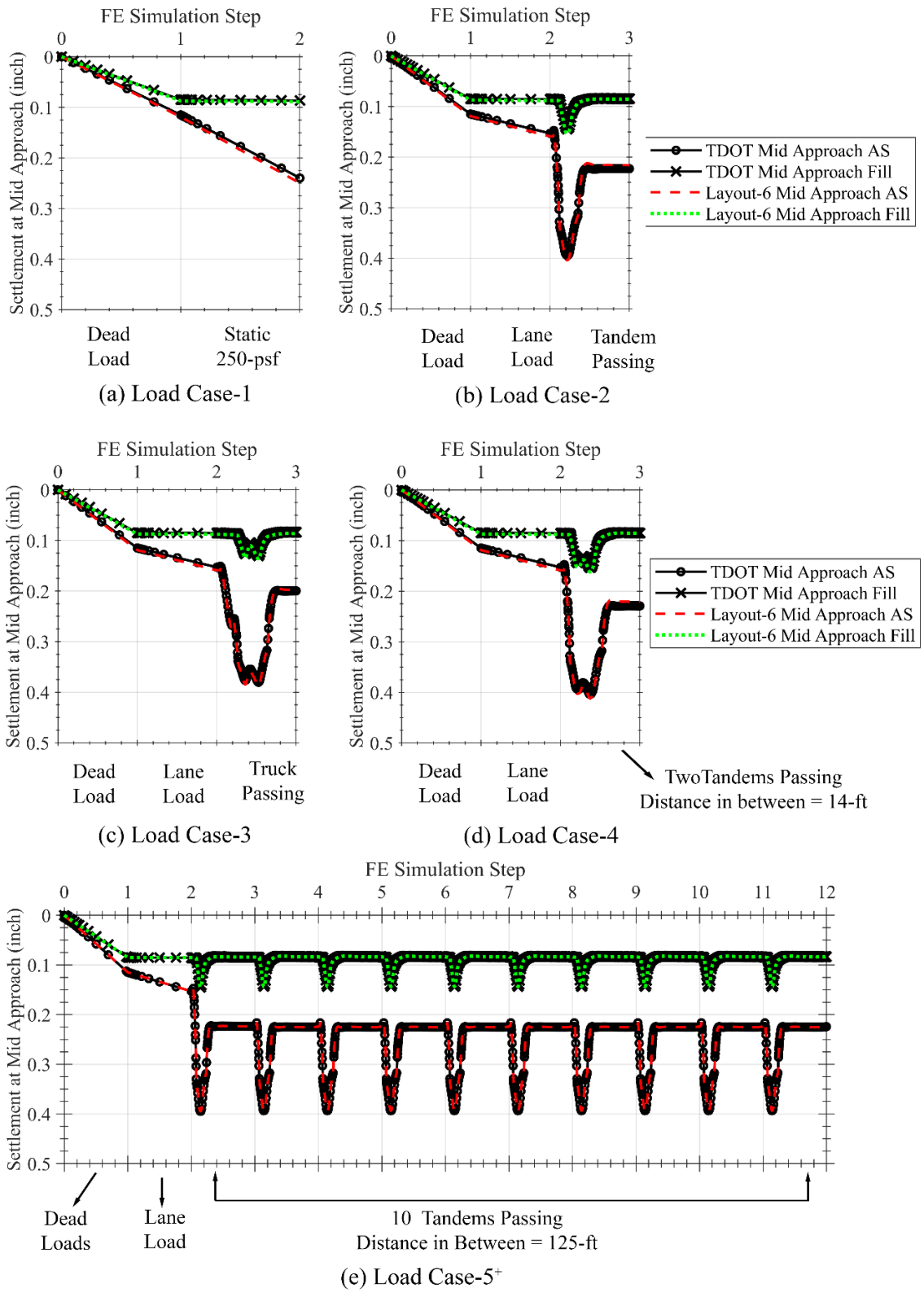

Figure 2-12. Predicted settlement at the middle of the approach slab for the TDOT and Layout-6 (recommended) designs under the effect of service loads.

2.4 Conclusions

This chapter developed FE analysis for a typical bridge end section that is composed of an approach slab, bridge abutment, sleeper slab, and soil embankment with the possible inclusion of uniaxial geogrid reinforcement. These components were modeled using the ABAQUS software, assuming plane-strain conditions and using the appropriate material models. A FE parametric study was conducted in search of an optimum geogrid design that would increase the ultimate bearing stress of the sleeper slab (UBSS) and minimize the approach slab settlement. Additionally, the FE analysis modeled the performance of a preliminary design proposed by TDOT for the retrofit of bridge ends. Detailed conclusions and recommendations from the parametric study and the case study are found in Chapter 4.

Chapter 3 Field Implementation of Recommended Design

State Route 115 over State Route 168, Knox County, Tennessee (Bridge I.D. No. 47SR1150023) was selected to implement the proposed design of the approach slabs (Figure 3-1). It is part of expanding Alcoa Highway (State Route 115). Figure 3-2 shows the face of the abutment before excavating the soil to reinforce the backfill underneath the approach slab. Then, a length of 37 feet was excavated to a depth of ~5.0 feet below the bottom of the approach slab elevation and lined with Propex GEOTEX-315ST woven polypropylene geotextile to separate the embankment clay from the reinforced aggregate fill (Figure 3-3). The geotextile sheets have a minimum of 6-inch overlap and were secured using metal pins. Then, a 9-inch layer of #57 aggregate was placed on the top of the geotextile before placing Tensar Biaxial BX1200 geogrid (Figure 3-4). A total of 4 layers of BX1200 geogrid were constructed with 9-inch thick #57 aggregate fill between them. The sleeper footing and approach slab were cast in place (Figure 3-5). TDOT decided to add a new lane on the west side of the bridge which was completed after this project.

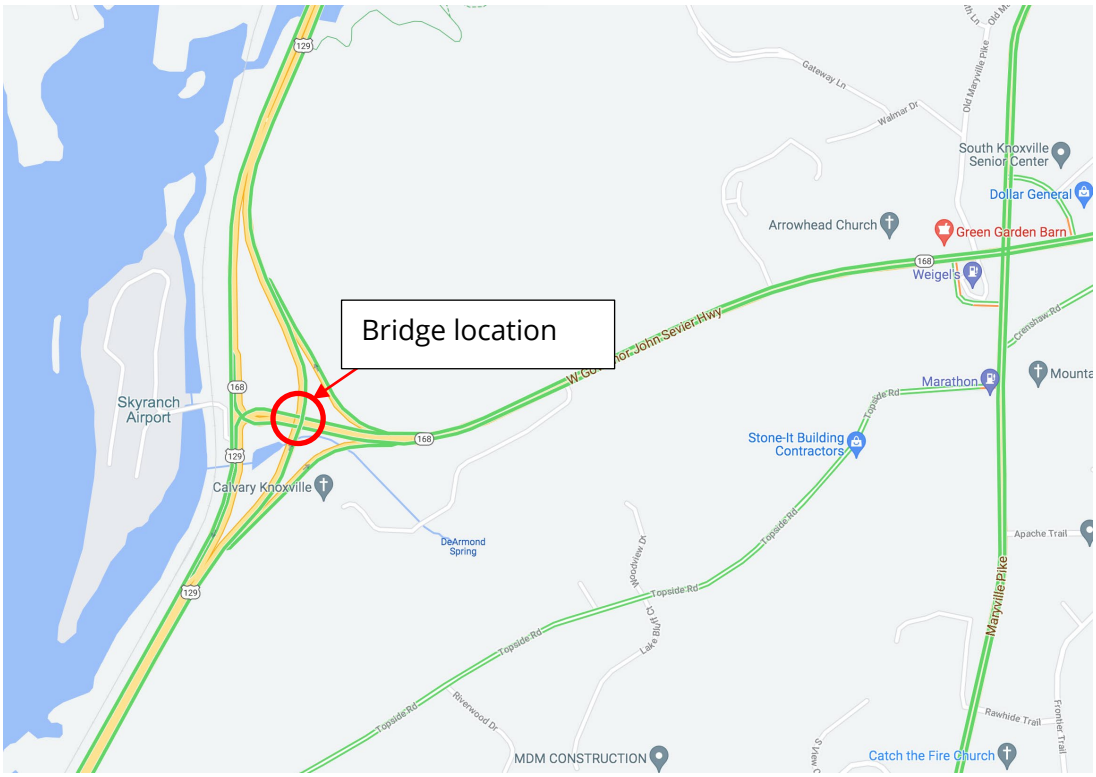

Figure 3-1. Map shows the location of the bridge in Knox County, TN

Figure 3-2. Photo of the face of the south abutment before constructing the approach slab.

Figure 3-3. Propex GEOTEX-315ST Geotextile fabric laid at the bottom before placing the fill for the north approach slab.

Figure 3-4. Tensar Biaxial BX1200 geogrid placed over #57 stone 9-in. fill.

Figure 3-5: Side view of the north approach slab and sleeper footing. A new lane was added to the bridge after this project ended.

Chapter 4 Conclusions & Recommendations

4.1 Conclusions

Chapter 2 developed FE analysis for a typical bridge end section that is composed of an approach slab, bridge abutment, sleeper slab, and soil embankment with the possible inclusion of uniaxial geogrid reinforcement. These components were modeled using the ABAQUS software, assuming plane-strain conditions and using the appropriate material models. A FE parametric study was conducted in search of an optimum geogrid design that would increase the ultimate bearing stress of the sleeper slab (UBSS) and minimize the approach slab settlement. The following was concluded from the parametric study:

- The effective depth of reinforcement reaches $2 \times B$ below the sleeper slab. In other words, there is no benefit of using geogrids below a depth of $2 \times B$ with respect to the bottom of the sleeper slab.
- The tensile strain distribution along the geogrid layers is insignificant beyond a distance of $2 \times B$ from the center of the sleeper slab in each highway direction. Accordingly, the geogrid layers must have a minimum of $4 \times B$ total length when centered underneath the sleeper slab.
- An optimum design would require reinforcing the effective depth of $2 \times B$ below the sleeper slab with five layers of geogrid equally spaced at $0.33 \times B$.
- The inclusion of geogrid reinforcement did not only enhance the UBSS but also redistributed the vertical loads over a wider region of soil embankment and thus reduced the approach slab settlement.
- The benefits of geogrid inclusion on UBSS become less significant as B increases.

Furthermore, the FE analysis modeled the performance of a preliminary design proposed by the TDOT for the retrofit of bridge ends. The TDOT design suggested the replacement of soil embankment underneath the approach slab by three layers of 9-inch reinforced aggregate with geogrid/textile. The performance was evaluated by means of UBSS and settlement under service loads (i.e., dead and highway traffic live load). The following was concluded from the case study:

- The UBSS of the retrofit design proposed by the TDOT can be improved by 30% when rearranging the geosynthetic reinforcement in a way that consumes one additional geogrid layer but extends the reinforced depth of soil to at least $1.25 \times B$ below the sleeper slab. Figure 4-1details the latter recommended design.
- The UBSS would increase by 40% when another layer of geogrid reinforcement is added below what is proposed by the recommended design. Therefore, it is suggested to design for this additional layer when constructing new fill embankments at bridge ends.
- The settlement at both sides of the H/S joint is almost the same under service loads for the TDOT retrofit and recommended designs, which suggests no differential settlement and no sudden change in slope (bump) for crossing motorists.
- The FE analysis executed for the recommended layout using the Type I and III geogrids, which in order are weaker and stronger grades of geogrids than that considered so far (Type II). The results showed little influence from using lower/higher grade geogrids in which the improvement factor of UBSS ranged from 1.3 to 1.33 when different types of geogrids were used.

4.2 Recommendation

The design of bridge ends consists of a 3-foot-wide sleeper slab (B= 3 ft, thickness T = 1 ft) that supports a 24-foot long (8×B) by 1-foot-thick approach slab at the H/S joint. The proposed design suggests replacing soil embankment underneath the approach slab with 4 biaxial geogrid layers (Tensar Biaxial BX1200 or equivalent) between 9-inch-thick lifts of openly-graded aggregate and a layer of woven polypropylene geotextile (Propex GEOTEX-315ST or equivalent) to separate the embankment clay from the reinforced aggregate fill. The geogrid layers are equally-spaced within a depth of $2 \times B$ below the strip footing, where B is the width of the footing.

4.3 Anticipated Benefits of Adoption

Some of current bridges have settlement underneath the approach slab which causes discomfort of riders, damage to vehicles, and potential road hazard. The proposed design will result in a safer and more economical solution than dealing with frequent maintenance to reduce the effect of the differential settlement. For new bridges, the proposed design is economical, easy to implement, and will rest in smoother rideability, less adverse impact on vehicles, and less maintenance.

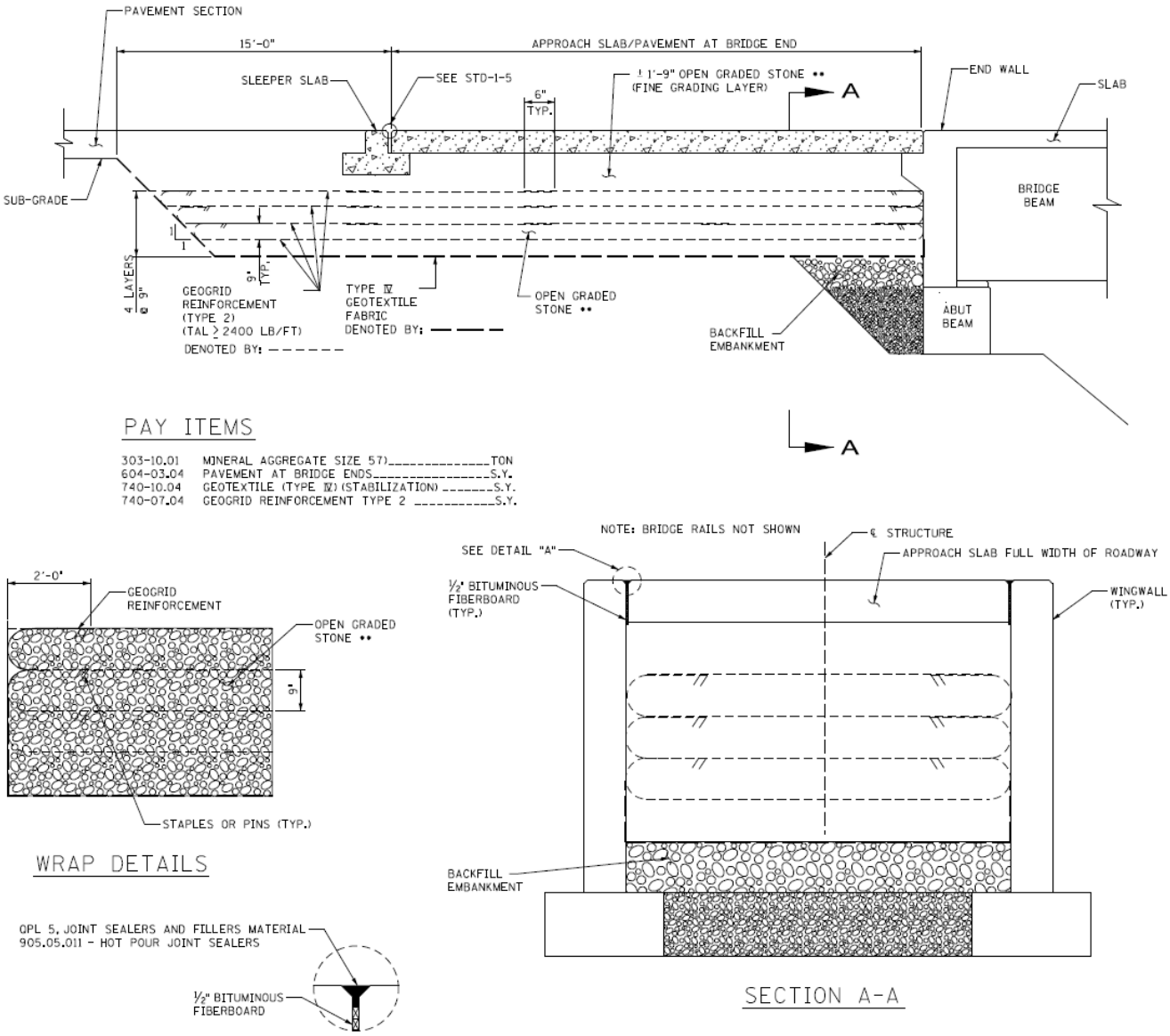

Figure 4-1. Detail drawing of recommended design.

Chapter 5 List of References

Saenz, L. P. (1964). "discussion of" Equation for the Stress-Strain Curve of Concrete" by Desayi and Krishnan." *Journal of the American Concrete Institute*, 61, 1229-1235.

Wicke, M., and Stoelhorst, D. (1982). "Problems associated with the design and construction of concrete pavements on approach embankments."

Hopkins, T. C. (1985). "Long-term movements of highway bridge approach embankments and pavements."

Edgar, T., Puckett, J., and D'Spain, R. (1989). "effects of geotextiles on lateral pressure and deformation in highway embankments. final report."

Lubliner, J., Oliver, J., Oller, S., and Oñate, E. (1989). "A plastic-damage model for concrete." *International Journal of solids and structures*, 25(3), 299-326.

Tadros, M., and Benak, J. (1989). "BRIDGE ABUTMENT AND APPROACH SLAB SETTLEMENT. PHASE 1. FINAL REPORT."

Ceb-Fip, M. C. (1990). "Design code." *Comite Euro International du Beton*, 51-59.

Wahls, H. E. (1990). *Design and construction of bridge approaches*, Transportation Research Board.

James, R., Zhang, H., Zollinger, D., Thompson, L., Bruner, R., and Xin, D. (1991). "A STUDY OF BRIDGE APPROACH ROUGHNESS. FINAL REPORT."

Kramer, S. L., and Sajer, P. (1991). "Bridge Approach Slab Effectiveness. Final Report."

Schaefer, V., and Koch, J. (1992). "VOID DEVELOPMENT UNDER BRIDGE APPROACHES. FINAL REPORT."

Hordijk, D. A. (1993). "Local approach to fatigue of concrete."

Das, B., Shin, E., and Omar, M. (1994). "The bearing capacity of surface strip foundations on geogrid-reinforced sand and clay—A comparative study." *Geotechnical & Geological Engineering*, 12(1), 1-14.

Stark, T., Olson, S., and Long, J. (1995). "Differential movement at the embankment/structure interface-mitigation and rehabilitation." *Rep. No. IABH1, FY*, 93.

Zaman, M., Laguros, J., and Jha, R. (1995). "Statistical models for identification of problematic bridge sites and estimation of approach settlements (FHWA-OK-94-02) 2188."

Adams, M. T., and Collin, J. G. (1997). "Large model spread footing load tests on geosynthetic reinforced soil foundations." *Journal of Geotechnical and Geoenvironmental Engineering*, 123(1), 66-72.

Briaud, J.-L. (1997). *Settlement of Bridge Approaches:(the Bump at the End of the Bridge)*, Transportation Research Board.

Hearn, G. (1997). "Faulted pavements at bridge abutments."

Lee, J., and Fenves, G. L. (1998). "Plastic-damage model for cyclic loading of concrete structures." *Journal of engineering mechanics*, 124(8), 892-900.

Hoppe, E. J. (1999). "Guidelines for the use, design, and construction of bridge approach slabs."

Dupont, B., and Allen, D. L. (2002). "Movements and settlements of highway bridge approaches."

Guide, A. C. (2002). "American Concrete Institute." *Detroit, MI*.

Seo, J., Ha, H., and Briaud, J.-L. (2002). "Investigation of settlement at bridge approach slab expansion joint: Numerical simulations and model tests."

Shin, E., Das, B., Lee, E., and Atalar, C. (2002). "Bearing capacity of strip foundation on geogrid-reinforced sand." *Geotechnical & Geological Engineering*, 20(2), 169-180.

Maharaj, D. K. (2003). "Nonlinear finite element analysis of strip footing on reinforced clay." *The Electronic Journal of Geotechnical Engineering*, 8, 241-256.

Luna, R. (2004). "Evaluation of bridge approach slabs, performance and design."

Marquart, M. (2004). "Fabric reinforced backfill under approach slabs." North Dakota Department of Transportation.

Cai, C., Voyiadjis, G. Z., and Shi, X. (2005). "Determination of interaction between bridge concrete approach slab and embankment settlement." Louisiana State University. Department of Civil Engieering.

White, D., Sritharan, S., Suleiman, M. T., and Chetlur, S. (2005). "Identification of the best practices for design, construction, and repair of bridge approaches." Iowa. Dept. of Transportation.

Abu-Hejleh, N., Hanneman, D., White, D. J., and Ksouri, I. (2006). *Flowfill and MSE Bridge Approaches:*

Performance, Coast, and Recommendations for Improvements, Colorado Department of Transportation, Research Branch.

Lenke, L. R. (2006). *Settlement Issues--Bridge Approach Slabs (final Report Phase 1)*, The Bureau.

Abu-Farsakh, M. Y., Gu, J., Voyiadjis, G., and Tao, M. (2007). "Numerical parametric study of strip footing on reinforced embankment soils." *Transportation Research Record*, 2004(1), 132-140.

Adams, M. T., Schlatter, W., and Stabile, T. (2007). "Geosynthetic-reinforced soil integrated abutments at the bowman road bridge in defiance county, Ohio." *Proceedings, Geo-Denver*, 01-11.

Al-Eis, K. A., and LaBarca, I. K. (2007). *Evaluation of the URETEK method of pavement lifting*, Wisconsin Department of Transportation, Division of Transportation Systems ….

Helwany, S., and Koutnik, T. E. (2007). *Evaluation of bridge approach settlement mitigation methods*, Wisconsin Highway Research Program.

Nazzal, M. D. (2007). "Laboratory characterization and numerical modeling of geogrid reinforced bases in flexible pavements."

Abu-Farsakh, M. Y., Chen, Q., and Yoon, S. (2008). "Use of reinforced soil foundation (RSF) to support shallow foundation." Louisiana Transportation Research Center.

Greimann, L., Phares, B., Faris, A., and Bigelow, J. (2008). "Integral bridge abutment-to-approach slab connection." Iowa State University. Center for Transportation Research and Education.

Puppala, A. J., Saride, S., Archeewa, E., Hoyos, L. R., and Nazarian, S. (2009). "Recommendations for design, construction, and maintenance of bridge approach slabs: synthesis report." University of Texas at Arlington.

Boisvert, D. M. (2010). "Alternate approach slab reinforcement." New Hampshire. Dept. of Transportation.

Islam, A. (2010). "On reducing bumps at pavement-bridge interface."

Thiagarajan, G., Gopalaratnam, V., Halmen, C., Ajgaonkar, S., Ma, S., Gudimetla, B., and Chamarthi, R. (2010). "Bridge approach slabs for Missouri DOT looking at alternative and cost efficient approaches." Missouri. Dept. of Transportation.

Oliva, M. G., and Rajek, G. (2011). "Toward improving the performance of highway bridge approach slabs." National Center for Freight and Infrastructure Research and Education (US).

Abu-Farsakh, M., Gu, J., Voyiadjis, G., and Chen, Q. (2012). "Finite element parametric study on the performance of strip footings on reinforced crushed limestone over embankment soil." *Electronic Journal of Geotechnical Engineering*, 17, 723-742.

Miller, G. A., Hatami, K., Cerato, A. B., and Osborne, C. (2013). "Applied approach slab settlement research, design/construction." University of Oklahoma. School of Civil Engineering and Environmental Science.

Abu-Farsakh, M. Y., and Chen, Q. (2014). "Field demonstration of new bridge approach slab designs and performance."Louisiana Transportation Research Center. FHWA/LA. 13/520.

Kost, A. D., Filz, G. M., Cousins, T., and Brown, M. C. (2014). "Full-Scale Investigation of Differential Settlements beneath a Geosynthetic-Reinforced Soil Bridge Abutment." *Transportation Research Record: Journal of the Transportation Research Board*, (2462), 28-36.

Ng, K. W., Yasrobi, S. Y., and Edgar, T. V. (2014). "Investigation of approach slab and its settlement for roads and bridges." Wyoming. Dept. of Transportation.

Talebi, M., Meehan, C. L., Cacciola, D. V., and Becker, M. L. "Design and construction of a geosynthetic reinforced soil integrated bridge system." *Proc., Geo-Congress 2014American Society of Civil Engineers*.

Chen, Q., and Abu-Farsakh, M. (2016). "Mitigating the bridge end bump problem: A case study of a new approach slab system with geosynthetic reinforced soil foundation." *Geotextiles and Geomembranes*, 44(1), 39-50.

Saghebfar, M., Abu-Farsakh, M., Ardah, A., Chen, Q., and Fernandez, B. A. (2017). "Performance monitoring of geosynthetic reinforced soil integrated bridge system (GRS-IBS) in Louisiana." *Geotextiles and Geomembranes*, 45(2), 34-47.

Abu-Farsakh, M., Ardah, A., and Voyiadjis, G. (2018). "3D Finite element analysis of the geosynthetic reinforced soil-integrated bridge system (GRS-IBS) under different loading conditions." *Transportation Geotechnics*, 15, 70-83.

Chapter 6 Appendices

Appendix (A): Data collected from several US DOTs

This appendix contains the specifications of several US DOTs about the dimensions and reinforcing details of the bridge approach slab, details of the sleeper slab, description of the connection between bridge abutment and approach slab, wearing base beneath the bridge approach slab, and wearing of the backfill material behind bridge abutments.

Table A-1: Source for the practices followed by nationwide DOTs regarding bridge approaches

State	Source
Alabama	ALDOT (https://www.dot.state.al.us), Standard and Special Drawings for Highway Construction, Section 100-199
Alaska	AlaskaDOT&PF (http://www.dot.state.ak.us), Alaska Bridges and Structures Manual 2017, Section 16.3
Arizona	ADOT (https://www.azdot.gov), Bridge Structure Detail Drawings, Sheets SD 2.01 to 2.04
Arkansas	ArDOT (https://www.arkansashighways.com), Standard Bridge Drawings, Sheets 55040
California	Caltrans (http://www.caltrans.ca.gov), Standard Plans 2018, Bridges, Structure Approach Sheets
Colorado	CDOT (https://www.codot.gov), Bridge Structural WorkSheets, Drawing WorkSheets, Sheets B601-1
Connecticut	CTDOT (https://www.ct.gov/dot), Bridge Design Manual, Section 5.8 and Division III Design Aids 6.4 Sheets
Delaware	DelDOT (https://www.deldot.gov), Bridge Design Manual, Detail No. 325.03 and 325.05
Florida	FDOT (https://www.fdot.gov), Standard plans for Bridge Construction, Sheets 400-090 and 400-091
Georgia	GDOT (http://www.dot.ga.gov), Construction Standards and Details, Sheets 9017
Hawaii	Details need Purchase
Idaho	ITD (https://itd.idaho.gov), Bridge CAAD Drawings, Sheets B2.1
Illinois	IDOT (http://idot.illinois.gov), Highway Standards, Sheets BA and BAIA
Indiana	INDOT (https://www.in.gov/indot), Bridge Plans for Spans over 20 feet, Sheet No. 21
Iowa	IOWADOT (https://iowadot.gov), Standard Road Plan, Section BR
Kansas	KDOT (http://www.ksdot.org), RD712, Bridge Approach Slab Details
Kentucky	KYTC (https://transportation.ky.gov), 2016 Standard Drawings, Bridges, BGX-017-02 Sheet
Louisiana	LaDOT (http://wwwsp.dotd.la.gov), Bridge Design Technical Memorandum No 57 (BDTM.57)
Maine	ManieDOT (https://www.maine.gov/mdot), Standard Details 2014 Edition, Sheet 502(02)
Maryland	No Details Found
Massachusetts	MassDOT (https://www.mass.gov/orgs/massachusetts-department-of-transportation), LRFD Bridge Manual Part II, Sheets 3.1.12 to 3.1.17
Michigan	MDOT (https://www.michigan.gov/mdot), SPR 1669 Final Report Part III 624877 7, Sheets R-45-I
Minnesota	MnDOT (http://www.dot.state.mn.us), Standard Plans, Bridge Approach Panel Plans
Mississippi	MDOT (http://mdot.ms.gov), Highway Design Standard Drawings, Sheet No. 6107
Missouri	MoDOT (https://www.modot.org), Bridge Standard Drawings, Sheets BAS
Montana	No Details Found
Nebraska	NDOT (https://dot.nebraska.gov), Bridge Office Policies and Procedures, Section 2.2.4
Nevada	NDOT (https://www.nevadadot.com), Standard Plans for Road and Bridge Construction, Sheet B-29.1.1
New Hampshire	NHDOT (https://www.nh.gov/dot), Bridge Design Manual Part I, Section 651
New Jersey	NJDOT (https://www.state.nj.us/transportation), Standard Bridge Construction Details, Sheet BC-505-7
New Mexico	NMDOT (http://dot.state.nm.us), Bridge Procedures and Design Guide 2018, Section 1.3.17 and 1.3.18
New York	NYDOT (https://www.dot.ny.gov), Bridge Detail Sheets, Sheets BD-SA1E to CD-SA10E
North Carolina	NCDOT (https://www.ncdot.gov), Structures, Standard Drawings, Sheets BAS
North Dakota	NDDOT (https://www.dot.nd.gov), Sheyenne Street over Sheyenne Diversion, Sheet WF-23-25
Ohio	ODOT (http://www.dot.state.oh.us), Archived Standard Drawings, Sheets AS
Oklahoma	ODOT (https://www.ok.gov/odot), Bridge Design Standards and Specifications State Bridges, Sheets B-216 and B-416
Oregon	ODOT (https://www.oregon.gov/ODOT), Standard Drawings Bridge Section, Sheet BR165
Pennsylvania	PennDOT (https://www.penndot.gov), Bridge Standard Drawings, Sheets BD-628M
Rhode Island	RIDOT (http://www.dot.ri.gov), Bridge Design Standard Details, Sheets 2.21 2.31 2.40 and 4.20
South Carolina	SCDOT (https://www.scdot.org), Standard Drawings, Sheets 702-30 to 702-32

South Dakota	SDDOT (http://www.sddot.com), Standard Plates, Sheets 380.40 and 380.41
Tennessee	TDOT (https://www.tn.gov/tdot), Standard Highway Drawings, Highway and Pavement Appurtenances, RP-J-1, Drawing STD-1-5
Texas	TxDOT (https://www.txdot.gov), Bridge Standards, Sheets BAS-A and BAS-C
Utah	UDOT (https://www.udot.utah.gov), Standard Drawing Sheets W-S17 to WS-19
Vermont	VTrans (https://vtrans.vermont.gov) - Structures Design Manual 5th Edition - Section 2.6
Virginia	VDOT (https://www.virginiadot.org), Manual of The Structure and Bridge Division Part 3, Sheets BAS
Washington	WSDOT (https://www.wsdot.wa.gov), Standard Plans, Sheet A-40.50-02
West Virginia	WVDOT (https://transportation.wv.gov), Division of Highways, Standard Details Book Vol. 1, Drawing No. PVT 5
Wisconsin	WisDOT (https://wisconsindot.gov), Bridge Manual Standard Drawings, Sheets 12.10 to 12.13
Wyoming	WYDOT (http://www.dot.state.wy.us), Bridge Application Manual, Section 4.14

Table A-2: Dimension and reinforcing details of the bridge approach slab

State	Span length: ft	Slab Thickness: in	Bottom Main Steel	Bottom Dist. Steel	Top Long. Steel	Top Trans. Steel
Alabama	20	10	#6 @ 6"	#4 @ 15"	n/a	n/a
Alabama	20	14	#6 @ 6"	#4 @ 15"	n/a	n/a
Alaska	15	designed as a simply supported slab				
Arizona	15	12	#8 @ 9"	#5 @ 12"	#5 @ 12"	#5 @ 12"
Arkansas	16	9	#5 @ 6"	#5 @ 12"	n/a	n/a
Arkansas	20	9	#5 @ 6"	#5 @ 12"	n/a	n/a
Arkansas	30	9	#5 @ 6"	#5 @ 12"	n/a	n/a
Arkansas	33	9	#5 @ 6"	#5 @ 12"	n/a	n/a
Arkansas	36.5	14.5	#7 @ 6"	#5 @ 12"	n/a	n/a
California	30	15	#10 @ 6"	#5 @ 6"	#5 @ 18"	#5 @ 18"
Colorado	20	12	#6 @ 6"	#5 @ 12"	#4 @ 18"	#5 @ 12"
Colorado	20	12	#6 @ 6"	#5 @ 12"	#4 @ 18"	#5 @ 12"
Connecticut	16	15	#6 @ 6"	#6 @ 6"	#5 @ 12"	#5 @ 12"
Delaware	18	16	#5 @ 8"	#5 @ 12"	#5 @ 12"	#5 @ 12"
Delaware	18	16	#5 @ 8"	#5 @ 12"	#5 @ 12"	#5 @ 12"
Florida	30	12	#8 @ 9"	#5 @ 9"	#5 @ 12"	#5 @ 12"
Georgia	30	10	#7 @ 8"	#5 @ 19"	#5 @ 19"	#5 @ 19"
Idaho	20	12	#8 @ 9.5"	#5 @ 12"	#4 @ 18"	#5 @ 12"
Illinois	30	15	#9 @ 5"	#5 @ 8"	#5 @ 12"	#5 @ 12"
Illinois	30	16	#9 @ 5"	#5 @ 8"	#5 @ 12"	#5 @ 12"
Indiana	20.5	12	#5 @ 6"	#5 @ 24"	#5 @ 8"	#5 @ 8"
Iowa	40	12	#8 @ 12"	#5 @ 12"	#6 @ 12"	#5 @ 12"
Kansas	13	10	#6 @ 6"	#5 @ 18"	#5 @ 12"	#5 @ 12"
Kentucky	25	17	#8 @ 6"	#5 @ 10"	n/a	n/a
Louisiana	20	18	#10 @ 6"	#8 @ 6"	#8 @ 6"	#8 @ 6"
Louisiana	20	20	#10 @ 6"	#8 @ 6"	#8 @ 6"	#8 @ 6"
Maine	15.5	8	#6 @ 6"	#5 @ 12"	n/a	n/a
Massachusetts	10	10	#6 @ 6"	#4 @ 12"	#6 @ 6"	#4 @ 12"
Massachusetts	15	10	#7 @ 5"	#4 @ 12"	#7 @ 5"	#4 @ 12"
Michigan	20	9	#6 @ 12"	#6 @ 12"	#6 @ 12"	#6 @ 12"
Michigan	20	9	#6 @ 12"	#6 @ 12"	#6 @ 12"	#6 @ 12"
Minnesota	15	12	#6 @ 6"	#5 @ 12"	#5 @ 12"	#5 @ 12"
Minnesota	20	12	#6 @ 6"	#5 @ 12"	#5 @ 12"	#5 @ 12"
Mississippi	20	12	#7 @ 8"	#5 @ 12"	#5 @ 12"	#5 @ 12"
Missouri	20	12	#6 @ 5"	#5 @ 12"	#5 @ 12"	#5 @ 12"

State	Span length: ft	Slab Thickness: in	Bottom Main Steel	Bottom Dist. Steel	Top Long. Steel	Top Trans. Steel
Nebraska	20	14	#8 @ 6"	#5 @ 9"	#5 @ 12"	#5 @ 12"
Nevada	15	12	#7 @ 6"	#4 @ 6"	#4 @ 12"	#4 @ 12"
Nevada	24	12	#7 @ 6"	#4 @ 6"	#4 @ 12"	#4 @ 12"
New Hampshire	20	15	#5 @ 12"	#5 @ 12"	#5 @ 12"	#5 @ 12"
New Hampshire	26	15	#5 @ 12"	#5 @ 12"	#5 @ 12"	#5 @ 12"
New Hampshire	30	15	#5 @ 12"	#5 @ 12"	#5 @ 12"	#5 @ 12"
New Jersey	25	18	#8 @ 6"	#19 @ 12"	#19 @ 12"	#19 @ 12"
New Mexico	14	11	#7 @ 6"	#5 @ 9"	#4 @ 9"	#4 @ 9"
New York	10	12	#5 @ 8"	#5 @ 12"	#5 @ 8"	#5 @ 12"
North Carolina	12	14	#6 @ 6"	#4 @ 12"	#5 @ 12"	#4 @ 12"
North Carolina	17	14	#6 @ 6"	#4 @ 12"	#5 @ 12"	#4 @ 12"
North Dakota	20	14	#6 @ 6"	#6 @ 6"	#5 @ 12"	#5 @ 12"
Ohio	15	12	#10@ 10"	#5 @ 9"	#5 @ 18"	#5 @ 18"
Ohio	20	13	#10 @ 8"	#5 @ 8"	#5 @ 18"	#5 @ 18"
Ohio	25	15	#10 @ 7"	#5 @ 8"	#5 @ 18"	#5 @ 18"
Ohio	30	17	#10 @ 7"	#5 @ 9"	#5 @ 18"	#5 @ 18"
Oklahoma	20	13	#9 @ 8"	#4 @ 12"	#4 @ 12"	#4 @ 12"
Oklahoma	24	13	#9 @ 8"	#4 @ 12"	#4 @ 12"	#4 @ 12"
Oklahoma	29	13	#9 @ 8"	#4 @ 12"	#4 @ 12"	#4 @ 12"
Oklahoma	30	13	#9 @ 8"	#4 @ 12"	#4 @ 12"	#4 @ 12"
Oregon	20	12	#7 @ 6"	#6 @ 12"	#6 @ 12"	#6 @ 12"
Oregon	30	14	#9 @ 6"	#6 @ 12"	#6 @ 12"	#6 @ 12"
Pennsylvania	25	16	#10 @ 9"	#6 @ 12"	#5 @ 12"	#5 @ 12"
Rhode Island	14	14	#7 @ 6"	#6 @ 12"	#6 @ 12"	#6 @ 12"
South Carolina	20	12	#9 @ 6"	#5 @ 12"	#5 @ 12"	#5 @ 12"
South Dakota	15	9	#8 @ 6”	#6 @ 12"	#4 @ 18"	#4 @ 18"
Tennessee	24	12	#6 @ 6"	#4 @ 18"	#6 @ 12"	#6 @ 12"
Texas	20	13	#8 @ 6"	#5 @ 12"	#5 @ 12"	#5 @ 12"
Utah	25	13	#10 @ 6"	#6 @ 9"	#4 @ 12"	#4 @ 13"
Vermont	15	14	#6 @ 6"	#5 @ 12"	n/a	n/a
Vermont	20	15	#9 @ 10"	#5 @ 12"	n/a	n/a
Vermont	25	16	#9 @ 9"	#5 @ 12"	n/a	n/a

State	Span length: ft	Slab Thickness: in	Bottom Main Steel	Bottom Dist. Steel	Top Long. Steel	Top Trans. Steel
Virginia	20	15	#7 @ 6"	#5 @ 9"	#5 @ 12"	#5 @ 18"
Virginia	22	15	#8 @ 6"	#5 @ 9"	#5 @ 12"	#5 @ 18"
Virginia	25	15	#8 @ 6"	#5 @ 9"	#5 @ 12"	#5 @ 18"
Virginia	28	15	#8 @ 6"	#5 @ 9"	#5 @ 12"	#5 @ 18"
Washington	25	13	#8 @ 5"	#5 @ 9 "	#5 @ 5"	#6 @ 12"
West Virginia	20	12	#5 @ 12"	#5 @ 12"	n/a	n/a
Wisconsin	20	16	#8 @ 7.5"	#5 @ 12"	#5 @ 12"	#5 @ 12"
Wyoming	25	10	#5 @ 8"	#5 @ 12"	#5 @ 12"	#5 @ 12"

Table A-3: Details of the sleeper slab as specified by several US DOTs

State	Thickness: inch	Width: ft	Comments
Arizona	12	3	n/a
Arkansas	21	3	Use between slab segments
Colorado	12	3	Bridge lateral movement ≤ 1/2-inch
Colorado	13	4	Bridge lateral movement > 1/2-inch, 12" mid-stem with an expansion joint.
Delaware	12	7.5	PCC pavement, 2-ft. wide mid-stem, horizontal dowels or tie bars between stem and approach slab
Delaware	12	5	HMA pavement, 2-ft. wide reversed back heel
Idaho	24	3	n/a
Illinois	10	10	n/a
Indiana	10	8	n/a
Iowa	12	6.25	Use between single and double reinforced slabs
Kansas	24	4	n/a
Louisiana	12	5	Geosynthetic reinforcement in the embankment beneath sleeper slab
Massachusetts	Increase the 16-inch end of the approach slab to 2-ft. thickness @ 1:1 chamfer		
Michigan	10	5	PCC pavement, 2-ft. wide mid-stem
Michigan	12	3.5	HMA pavement, 2-ft. wide reversed back heel
Minnesota	18	4	n/a
Mississippi	12	6	n/a
Missouri	18	3	Use only for major bridges
Nevada	15	5	Integrated with approach slab
New Hampshire	16	6	3-ft wide reversed back heel, expansion joint between heel and approach slab
New York	12	6	2-ft mid-stem, sealed joint between stem and approach slab
Ohio	9	8	n/a
Pennsylvania	12	5	n/a
Rhode Island	12	3	14-inch wide mid-stem, sleeper slab used for bridges with span length > 60-ft.
South Carolina	12	3.75	15-inch mid-stem, expansion joint between stem and approach slab
South Dakota	9	4.5	21-inch wide reversed back heel, 3-inch thick sealed joint between heel and approach slab
Tennessee	12	3	use a 12-inch wide mid-stem for HMA pavement with a sealed joint between stem and approach slab
Texas	10	5	Only used with PCC pavement, integrated with approach slab
Utah	15	5	Use a 2-ft. wide mid-stem for HMA pavement
Virginia	5.5	15	18-inch mid-stem with a neoprene seal between stem and approach slab
Wisconsin	18	5	n/a

Table A-4: Description of the connection between bridge abutment and approach slab

State	Abutment Type	Approach Slab Connection with Bridge Abutment
Alabama	integral/ non-integral	8-in. seat on abutment with 2 layers of graphite surfaced sheet packing non-integral abutment: add dowels, double-bend, horizontal in slab and vertical in abutment sealed joint
Alaska	non-integral	no information
Arizona	Integral	12-in seat on abutment #5 vertical bar @12-in cts. ½-in bituminous filler with silicone sealant
Arkansas	non-integral	6-in seat on abutment 1/2-in preformed joint filler
California	integral/ non-integral	6-in (seat type) or 12-in (diaphragm type) seat on abutment with 3-in expansion joint filler 1/4-in wide #5 vertical bars @ 9-in to 12-in cts., extend 2-in to 3-in in abutment (seat type) 3/4-in ϕ 8-in long horizontal bolt @ 24 cts., threaded for 28-in into approach slab (diaphragm type) joint seal
Colorado	Integral	6-in seat on abutment #5 bars @ 12-in cts., L shape, horizontal in slab and vertical in abutment, extend 18-in in slab 1/2-in expansion joint
Connecticut	non-integral	8-in seat on abutment 1.5-in sealed joint
Delaware	Integral	24-in seat on abutment with 2 sheets of polyethylene and 1-in thick polystyrene joint extend bridge deck reinforcement into approach slab bond breaker
	non-integral	10-in seat on abutment bond breaker
Florida	non-integral	18-in seat on abutment with 2 layers of 30 lb. smooth roofing paper vertical dowels in abutment 1/2-in expanded polystyrene joint
Georgia	non-integral	8-in seat on abutment prevent bond with 2 layers of 30 lb. asphalt-saturated felt 3/4-in expansion joint
Idaho	Integral	6-in seat on abutment #4 horizontal bars @12-in cts., extend from mid-slab into abutment bond breaker and 1/4-in hot pour sealant for the top 1/2-in
Illinois	integral/ non-integral	12-in seat on abutment Cast-in-place: #5 bars @ 12-in cts., L shape, horizontal in slab and extend 15.5-in vertical in abutment Pre-cast: 1-in ϕ by 2-ft long dowels, extend 15-in in 1.5-in ϕ drilled and grouted holes in vertical abutment

State	Abutment Type	Approach Slab Connection with Bridge Abutment
Indiana	non-integral	6-in seat on abutment #5 epoxy-coated threaded horizontal tie bar 6-ft long, extend 3-ft in slab and 3-ft in bridge deck construction joint
Iowa	non-integral/ integral	13-in seat on the bridge abutment 1/2-in ϕ by 24-in long steel rod hooked to slab top steel and installed vertically into subbase @ 10-in away from abutment 1-in to 2-in sealed joint add extra steel dowels to non-integral abutment
Kansas	Integral	8-in seat on abutment #5 bars @ 12-in cts., hooked to approach slab top steel and protrude the abutment in slant
Kentucky	Integral	9-in seat on abutment with 1/8-in neoprene pad 1/2-in ϕ vertical dowels
Louisiana	integral/ non-integral	12-in seat on abutment #6 vertical dowels @ 18-in cts.
Maine	non-integral	3-in roughened seat on abutment
Massachusetts	non-integral	10-in seat on the abutment #6 vertical dowels @ 18-in cts. 1/2-in preformed filler
Michigan	non-integral	18-in seat on abutment extend bridge deck bars 2-ft min. in approach slab construction joint or 1/4-in sawed sealed joint
Minnesota	integral/ non-integral	8-in seat on abutment #19 bars, single-bend, horizontal in slab and slant in abutment construction joint
Mississippi	Integral	8-in seat with metal flashing or three thickness of tar paper 1-in joint
Mississippi	non-integral	8-in seat with metal flashing or three thickness of tar paper #4 bars @ 12-in cts., double-bend, horizontal in slab and vertical in abutment no expansion joint
Missouri	integral/ non-integral	5-in seat on abutment #5 bars @ 12-in cts., L shape, horizontal in slab and vertical in abutment
Nebraska	Integral	12-in seat on abutment #6 bars @ 12-in cts., single-bend, slant in slab and vertical in abutment sealed joint
Nevada	Integral	12-in seat on abutment horizontal restrainer @ 24-in cts. Expansion joint
New Hampshire	Integral	9-in seat on abutment #5 dowels, single-bend, slant in slab and vertical in abutment expansion joint

State	Abutment Type	Approach Slab Connection with Bridge Abutment
New Jersey	Integral	15-in seat #16 horizontal bars @ 24-in cts. elastomeric joint sealer
New Mexico	non-integral	seat on abutment and 1/2-in Evazote 380 seal
New York	non-integral	6-in seat on bridge abutment construction joint
North Carolina	integral/ non-integral	10-in seat on abutment prevent bond by 2 layers of 30 lb. proofing felt integral abutments: add #4 bar, double-bend, horizontal in slab and vertical in abutment construction sealed joint
North Dakota	Integral	seat on abutment #5 horizontal bars @12-in cts. with mechanical splice
Ohio	integral/ non-integral	6-in seat on the abutment 5/8-in vertical anchors @ 3-ft cts., extend 12-in in slab seats 1-in pre-molded expansion joint filler
Oklahoma	integral/ non-integral	7-in seat on abutment #4 bars @ 12-in cts., single-bend, horizontal in slab, and extend 12-in in vertical abutment sawed and sealed construction joints
Oregon	Integral	12-in seat on abutment #5 × 3.5-ft long vertical dowels @12-in cts. hooked end in slab 2-in sealed expansion joint
Pennsylvania	non-integral	8.5-in seat on abutment with bond breaker 3/8-in closed neoprene sponge
Rhode Island	Integral	12-in seat on abutment #6 bars @ 12-in cts., single-bend, horizontal in slab and slant in abutment with a hooked end 1/2-in closed cell preformed polyethylene foam filler
Rhode Island	non-integral	6-in seat on abutment #6 vertical bars @ 12-in cts. 1/2-in closed cell preformed poly Foam filler
South Carolina	Integral	9-in seat on abutment #6 bars, single-bend, horizontal in slab and slant in abutment with a hooked end one coat of asphaltic paint
South Carolina	non-integral	18-in seat on abutment #8 vertical dowels one coat of asphaltic paint

Table A-5: Specification of the wearing base beneath the bridge approach slab and backfill material behind bridge abutments (White et al. 2005)

State	Wearing Base	GSD* Max Sieve Size (mm)	GSD % Finer Sieve #4 min.	GSD % Finer Sieve #4 max.	GSD % Finer Sieve #200 min.	GSD % Finer Sieve #200 max.	% Of Maximum Dry Density	Standard Method for Compaction
Alabama	suitable aggregate base	n/a	n/a	n/a	n/a	n/a	n/a	n/a
California	6-in of treated permeable base	75	35	100	n/a	n/a	95	AASHTO T-99 A/C
Colorado	aggregate base	50	0	100	5	20	95	AASHTO T-180
Delaware	12-in of graded aggregate base	n/a	n/a	n/a	n/a	n/a	n/a	n/a
Georgia	5-in of CS concrete or aggregate base	n/a	n/a	n/a	n/a	n/a	n/a	n/a
Idaho	3/4-in of aggregate base, increase to 12-in below sleeper	75	55	100	0	5	95	AASHTO T-99 A/C
Illinois	4-in of granular base	75	50	100	0	4	95	AASHTO T-99 C
Indiana	6-in of dense graded base	50	20	70	0	8	95	AASHTO T-99
Iowa	12-in of modified base or gravel, gradually increase to 24-in near bridge abutment, use polymer at excavation limit	n/a	n/a	n/a	n/a	n/a	n/a	n/a
Kansas	10-in of compacted aggregate base	101	0	60	0	5	95	AASHTO T-99 C/D
Kentucky	granular backfill extending at 1H:1V slope behind bridge abutment, use geotextile at excavation limit	101	0	30	0	5	n/a	n/a
Louisiana	6-in of aggregate base, increase to 12-in below sleeper	12.5	n/a	n/a	0	10	n/a	n/a
Massachusetts	2-in of controlled density backfill	12.5	40	75	0	10	95	AASHTO T-99 C
Michigan	aggregate base extend to a depth of 36-in max. below sleeper slab	25	n/a	n/a	0	7	n/a	n/a
Minnesota	4' of modified granular base, modified granular extend at 1H:1.5V behind abutment	50	0	50	0	4	95	AASHTO T-99
Mississippi	12-in of silt basins	n/a	n/a	n/a	n/a	n/a	n/a	n/a
Missouri	4-in of aggregate base	50	0	5	n/a	n/a	95	AASHTO T-99 C
Nebraska	12-in of granular base	9.5	92	100	0	3	100	AASHTO T-99
Nevada	12-in of granular base	75	35	100	0	12	n/a	n/a
New Hampshire	6-in of compacted granular base	n/a	n/a	n/a	n/a	n/a	n/a	n/a
New Jersey	6-in of base course	n/a	n/a	n/a	n/a	n/a	n/a	n/a
New Mexico	1.5-in of base course	n/a	n/a	n/a	n/a	n/a	n/a	n/a
New York	base course	101	0	70	0	15	95	AASHTO T-99 A/C

State	Wearing Base	GSD* Max Sieve Size (mm)	GSD % Finer Sieve #4 min.	GSD % Finer Sieve #4 max.	GSD % Finer Sieve #200 min.	GSD % Finer Sieve #200 max.	% Of Maximum Dry Density	Standard Method for Compaction
North Carolina	selected granular backfill extending at 1.5H:1V slope behind abutment, use geotextile at excavation limit	9.5	80	100	0	20	95	AASHTO T-99
North Dakota	4' of course selected backfill	75	35	85	0	15	95	AASHTO T-99
Ohio	aggregate base	75	-	-	0	20	100	AASHTO T-99
Oklahoma	aggregate base	75	0	45	0	10	n/a	n/a
Oregon	6-in of granular structure backfill	n/a	n/a	n/a	n/a	n/a	n/a	n/a
Pennsylvania	9-in of granular base	n/a	n/a	n/a	n/a	n/a	n/a	n/a
Rhode Island	15-in of peastone	n/a	n/a	n/a	n/a	n/a	n/a	n/a
South Carolina	12-in of base course	50	30	50	0	12	95	AASHTO T-99 A/C
South Dakota	6-in of granular base	37.5	0	20	n/a	n/a	95	AASHTO T-99
Tennessee	6-in of mineral aggregate base	37.5	35	60	5	15	100	AASHTO T-99 C
Vermont	granular base	n/a	n/a	n/a	n/a	n/a	n/a	n/a
Virginia	0.35 gal. per sq. yd. of prime aggregate base	75	16	30	4	14	n/a	n/a
Washington	2.5-in of compacted base course	50	22	66	0	5	95	AASHTO T-99
West Virginia	base course	n/a	n/a	n/a	n/a	n/a	n/a	n/a
Wisconsin	1.25-in of aggregate base	75	25	100	0	8	95	AASHTO T-99 C
Wyoming	8-in to 24-in of crushed gravel, crushed rock, or manufactured sand	n/a	n/a	n/a	n/a	n/a	n/a	n/a

*GSD – Grain Size Distribution

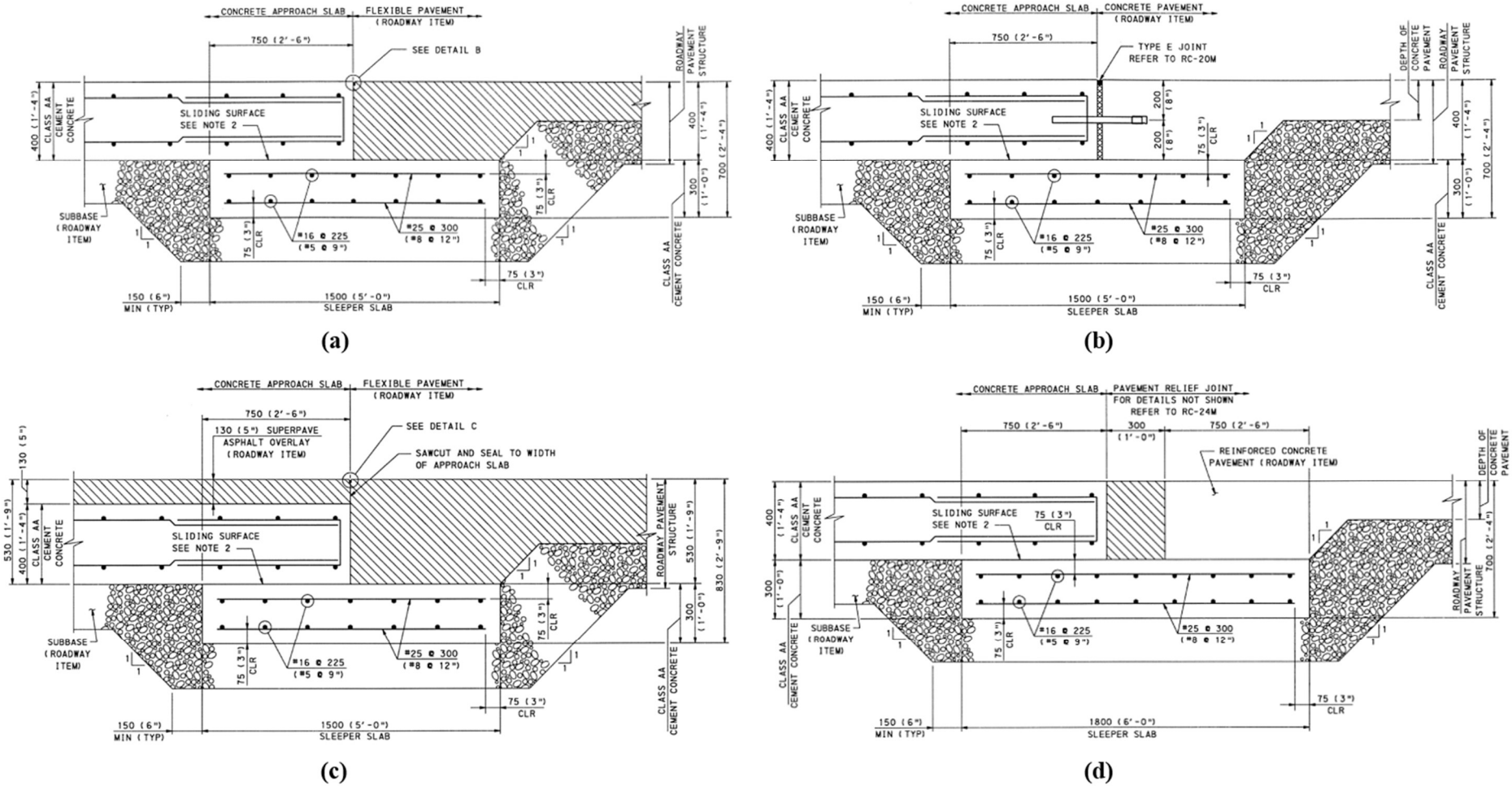

Figure A-1. Details of the sleeper slab as specified by Pennsylvania DOT for (a) HMA pavement without asphaltic overlay, (b) PCC pavement without asphaltic overlay, (c) HMA pavement with asphaltic overlay, and (d) PCC pavement with asphaltic overlay (sheet BD-628M of bridge standard drawings). Parentheses denote Imperial unit

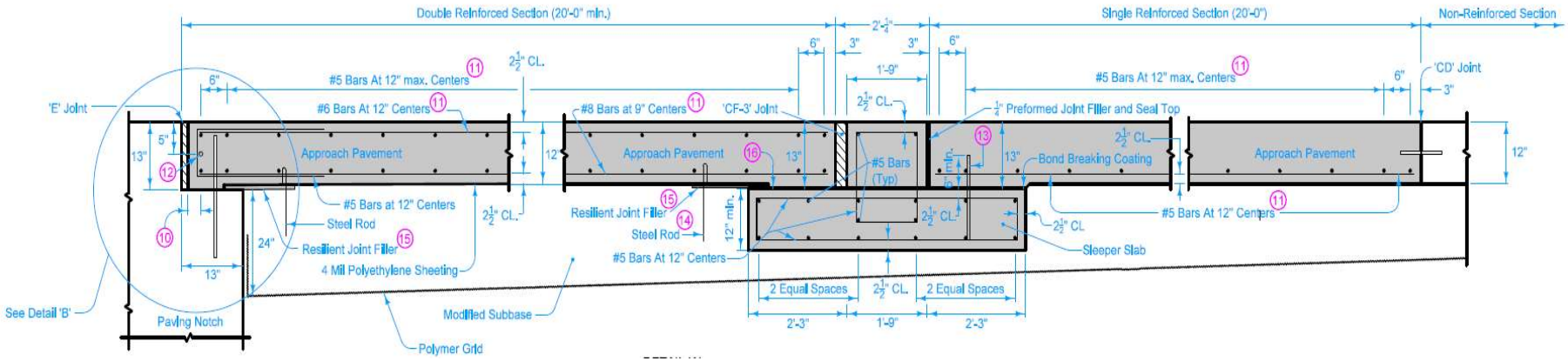

Figure A-2. Detail of the sleeper slab as specified by Iowa DOT (Sheet BR-205 of the Standard Road Plans).

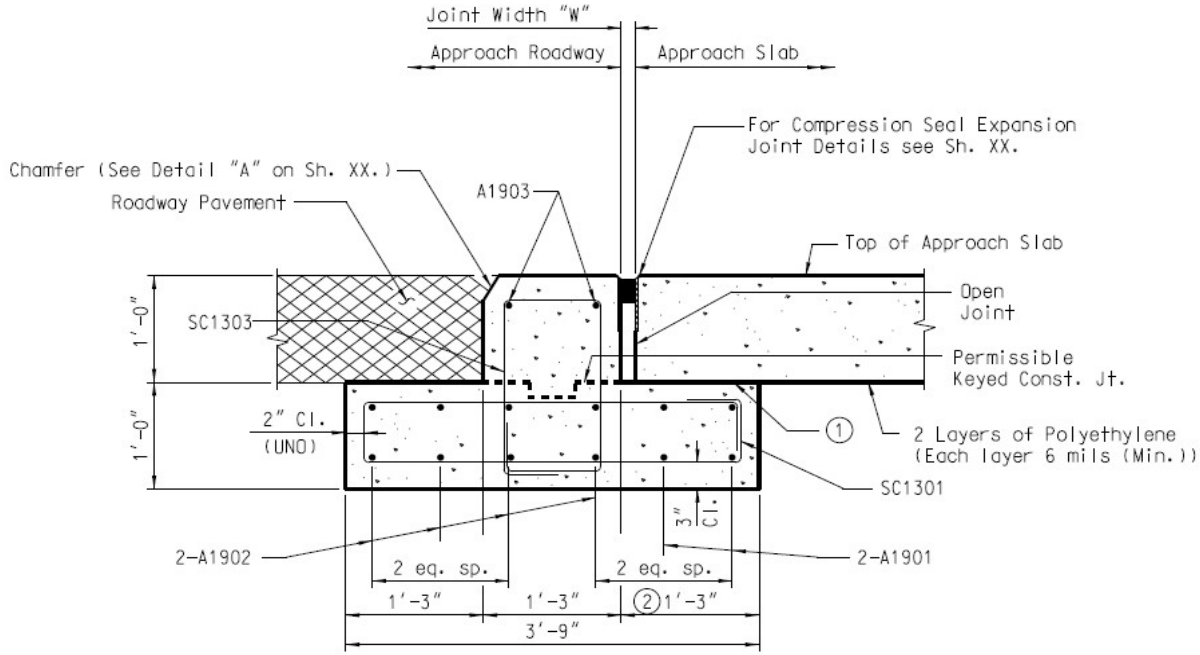

Figure A-3. Detail of the sleeper slab as specified by South Carolina DOT (Drawing 702-32b of the Standard Drawings).

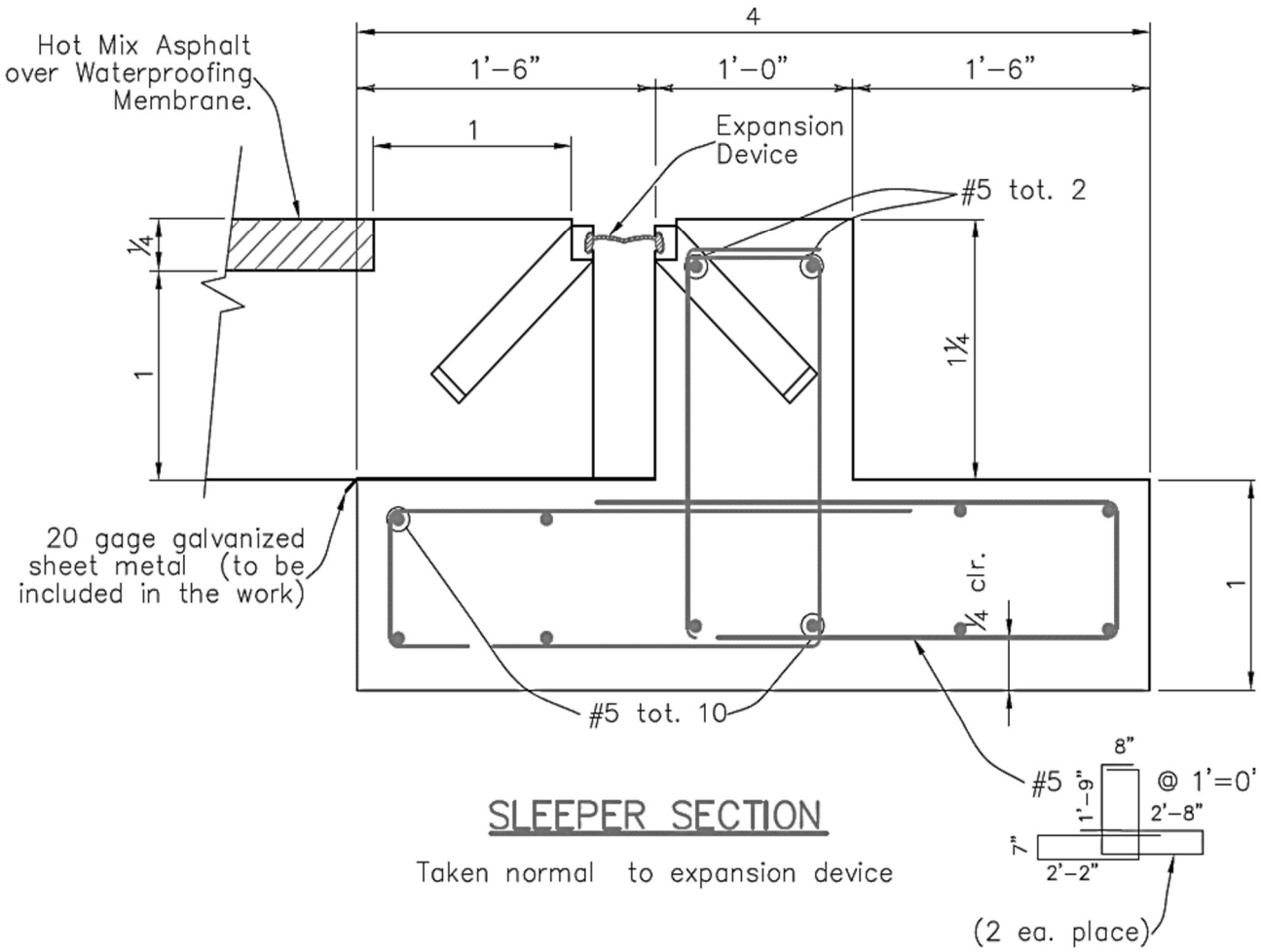

Figure A-4. . Detail of the sleeper slab and expansion device as specified by Colorado DOT for bridges with lateral movement exceeding ½-inch (Sheet B601-1 of the Bridge Structural WorkSheets).

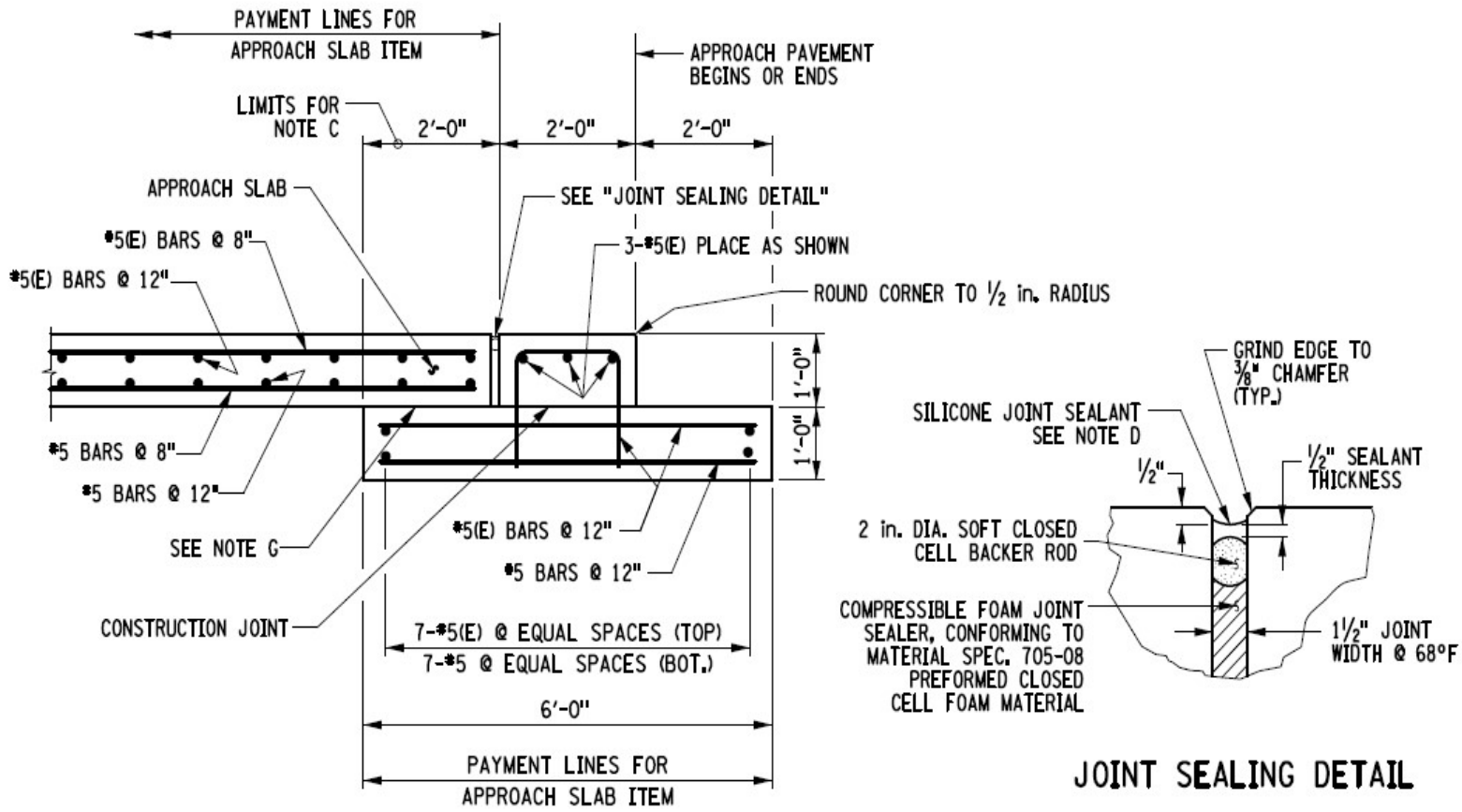

Figure A-5. Detail of the sleeper slab as specified by New York DOT (Sheet BD-SA2E of Bridge Detail Sheets).

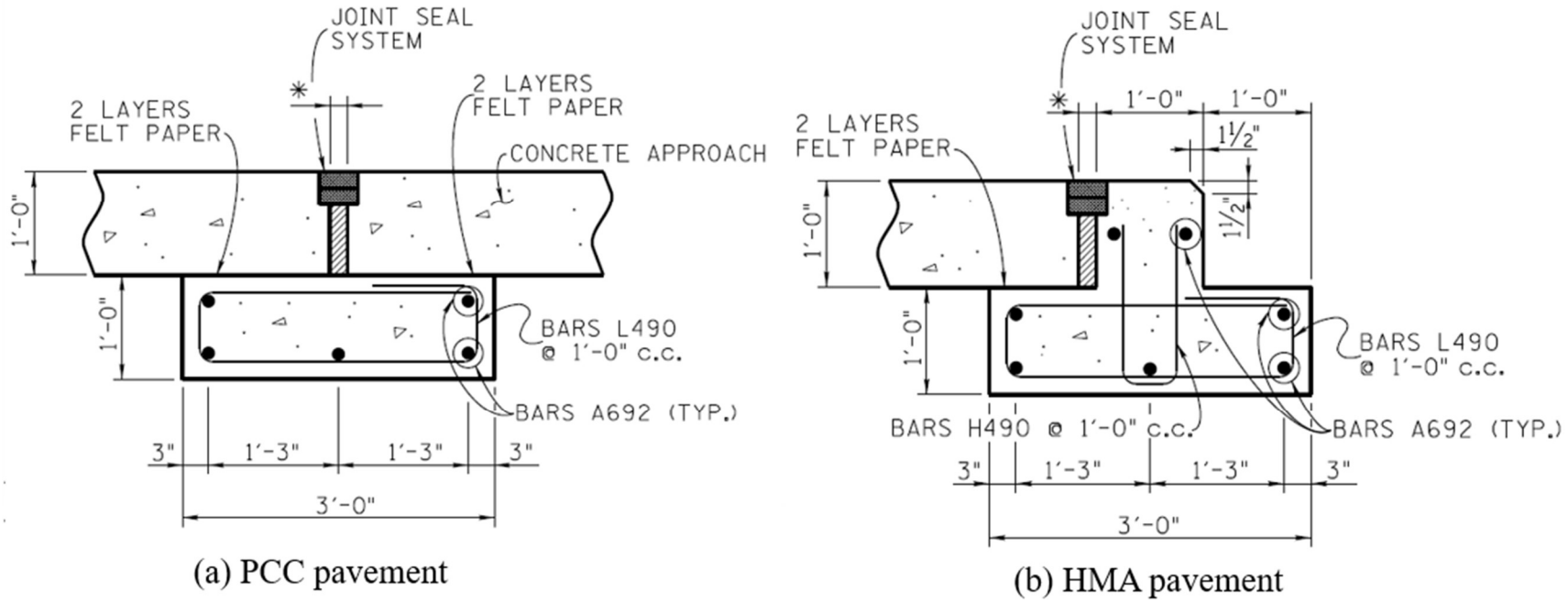

Figure A-6. Detail of the sleeper slab as specified by Tennessee DOT for highways with a pavement of (a) HMA, and (b) PCC (Sheet 5 of STD-1-5 sheets, Highway and Pavement Appurtenances, Standard Highway Drawings).

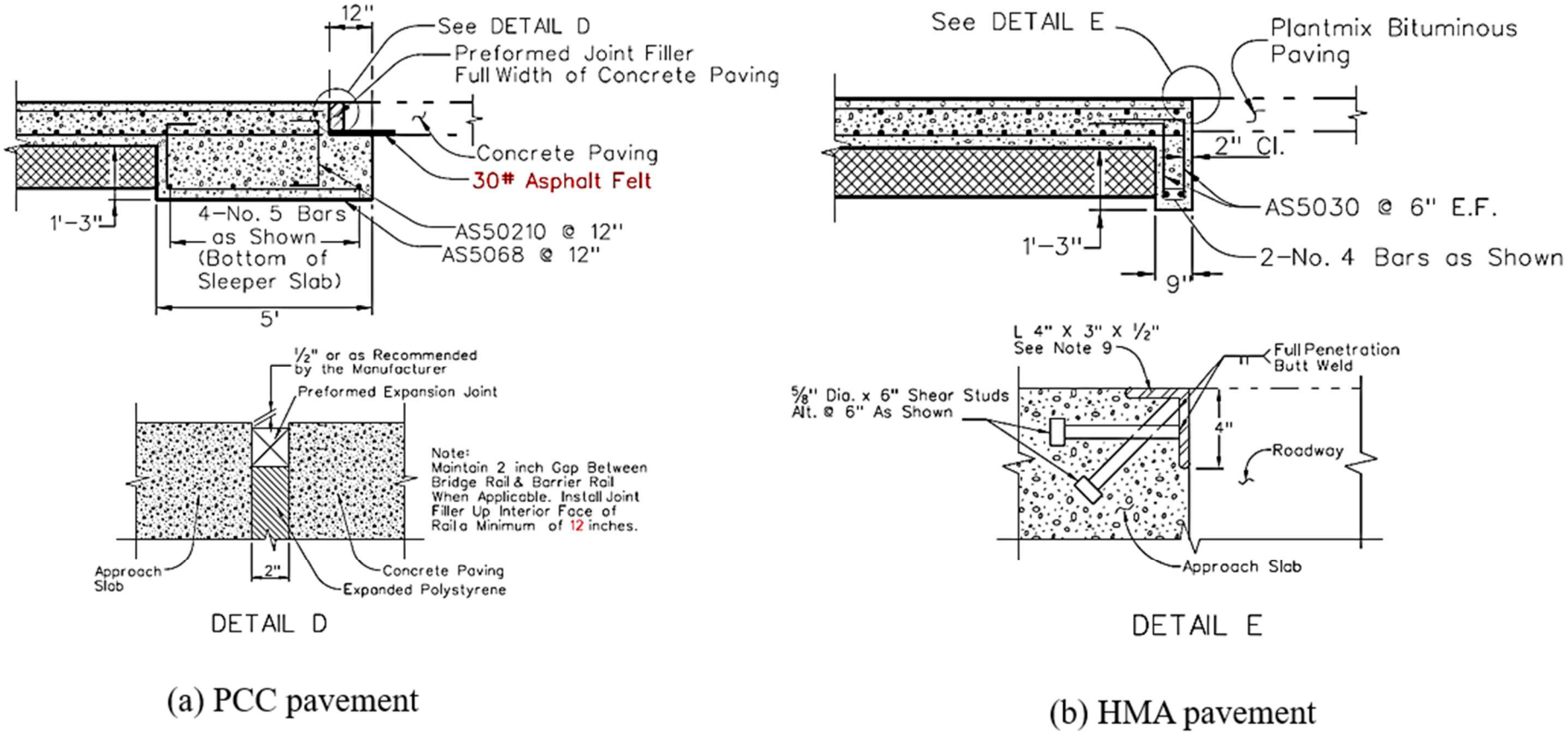

Figure A-7. Detail of the sleeper slab as specified by Nevada DOT for highways with a pavement of (a) PCC and (b) HMA (Sheet B-29.1.1 of Standard Plans for Road and Bridge Construction).

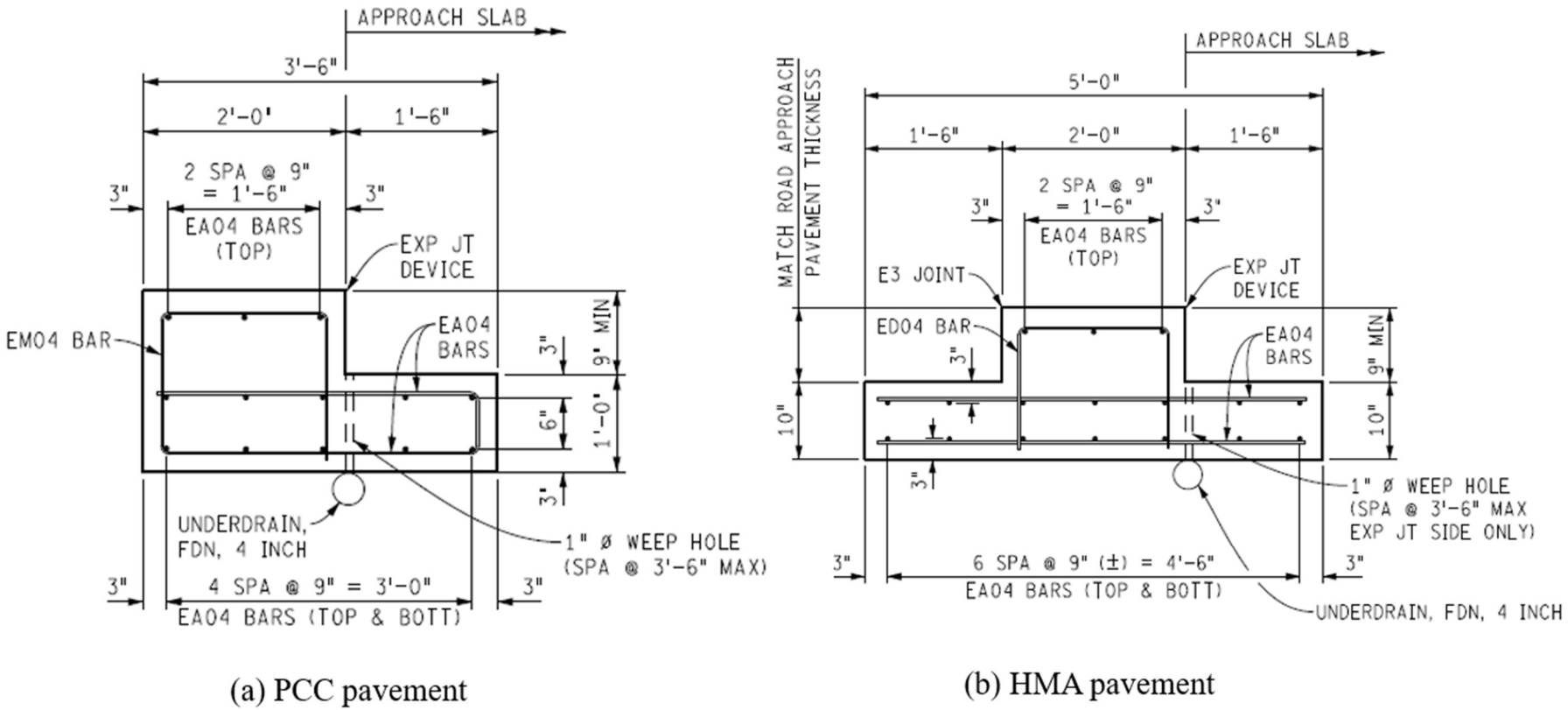

Figure A-8. Detail of the sleeper slab as specified by Michigan DOT for highways with a pavement of (a) PCC, and (b) HMA (Sheet 003 of Appendix L, SPR 1669 Final Report Part III 624877 7)

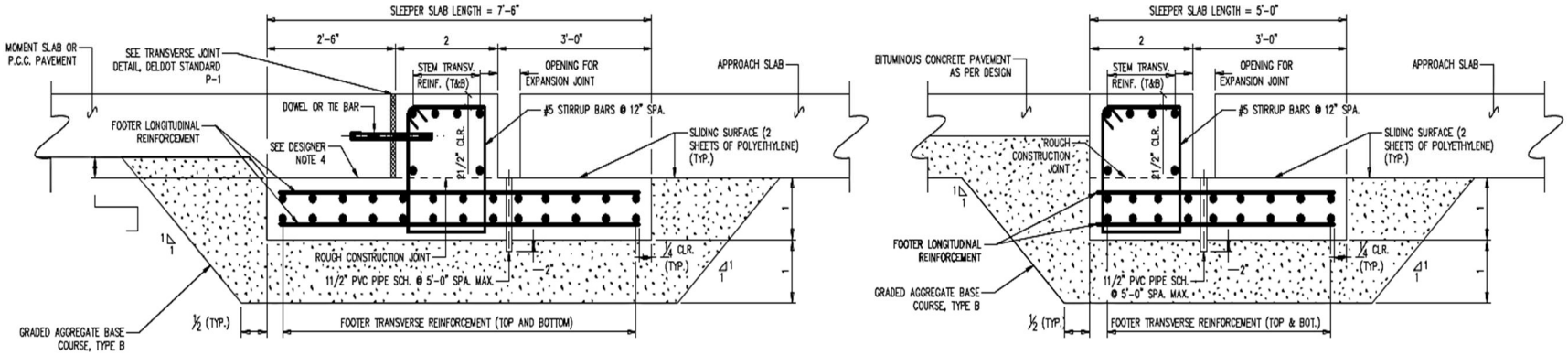

Figure A-9. Detail of the sleeper slab as specified by Delaware DOT for highways with a pavement of (a) PCC, and (b) HMA (Detail No. 325.05 of Bridge Design Manual).

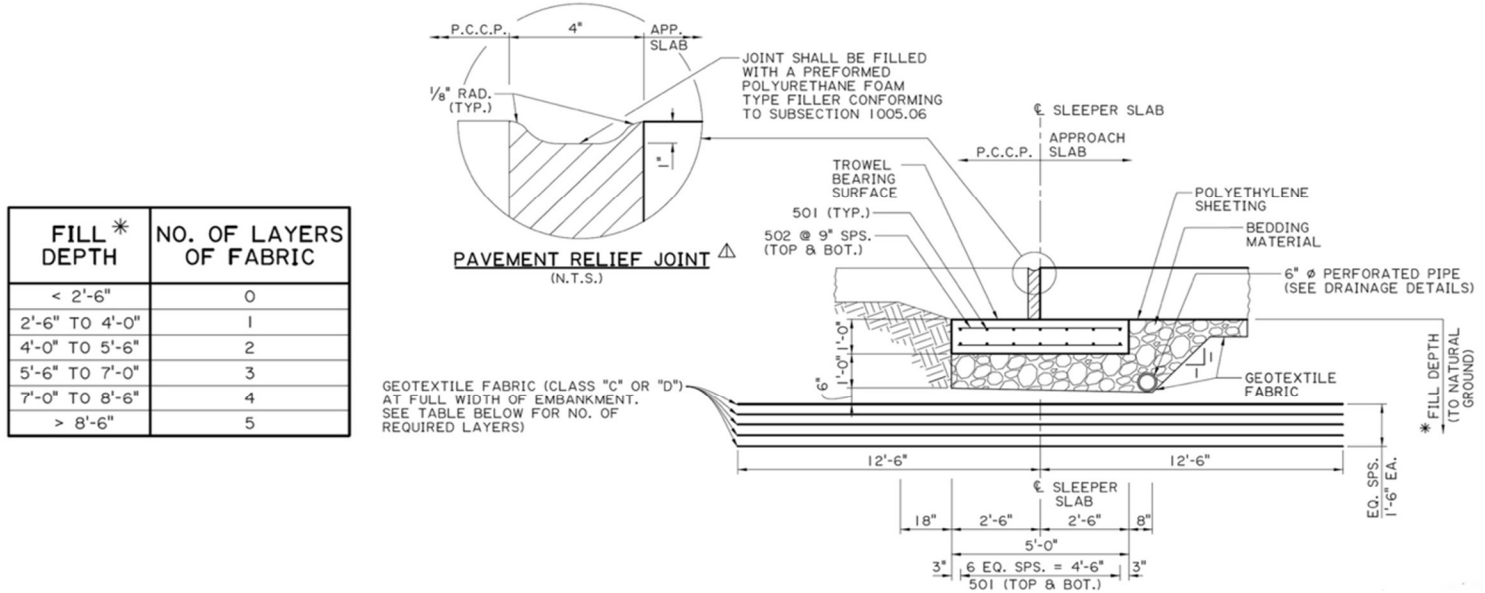

FILL * DEPTH	NO. OF LAYERS OF FABRIC
< 2'-6"	0
2'-6" TO 4'-0"	1
4'-0" TO 5'-6"	2
5'-6" TO 7'-0"	3
7'-0" TO 8'-6"	4
> 8'-6"	5

Figure A-10. Details of the sleeper slab as specified by Louisiana DOT (Bridge Design Technical Memorandum No 57).

Appendix (B): Geotex-315ST and Tensar Biaxial-MPDS_BX1200_9-20 data sheets

GEOTEX® BY PROPEX

Product Data

GEOTEX 315ST

GEOTEX 315ST is a woven polypropylene geotextile containing heavy woven tape/fibrillated yarns produced by Propex, and will meet the following Minimum Average Roll Values (MARV) when tested in accordance with the methods listed below. These characteristics make **GEOTEX 315ST** ideal for the construction of embankments over soft soils, steepened slopes, and modular block and/or wrapped-face retaining walls. The geotextile is resistant to ultraviolet degradation and to biological and chemical environments normally found in soils.

GEOTEX 315ST conforms to the property values listed below[1], as well as meets the requirements set forth by AASHTO M-288/NTPEP (Geotextile Specification for Highway Application). Propex performs internal Manufacturing Quality Control (MQC) tests that have been accredited by the Geosynthetic Accreditation Institute – Laboratory Accreditation Program (GAI-LAP). This product is NTPEP approved for AASHTO standards.

PROPERTY	TEST METHOD	MARV[2] ENGLISH	MARV[2] METRIC
ORIGIN OF MATERIALS			
% U.S. Manufactured Inputs		100%	100%
% U.S. Manufactured		100%	100%
MECHANICAL			
Tensile Strength (Grab)	ASTM D-4632	315 lbs	1401.2 N
Elongation	ASTM D-4632	15%	15%
CBR Puncture	ASTM D-6241	900 lbs	4003.4 N
Trapezoidal Tear	ASTM D-4533	113 lbs	502.7 N
ENDURANCE			
UV Resistance % Retained at 500 hrs	ASTM D-4355	70%	70%
HYDRAULIC			
Apparent Opening Size (AOS)[3]	ASTM D-4751	40 US Std. Sieve	0.425 mm
Permittivity	ASTM D-4491	0.05 sec^{-1}	0.05 sec^{-1}
Water Flow Rate	ASTM D-4491	4 gpm/ft^2	163.2 lpm/m^2

ROLL SIZES	12.5 ft x 360 ft 15.0 ft x 300 ft 17.5 ft x 258 ft	3.8 m x 109.8 m 4.6 m x 91.5 m 5.3 m x 78.6 m

NOTES:

1. The property values listed above are effective 04/2011 and are subject to change without notice.
2. Values shown are in weaker principal direction. Minimum average roll values (MARV) are calculated as the typical minus two standard deviations. Statistically, it yields a 97.7% degree of confidence that any samples taken from quality assurance testing will exceed the value reported.
3. Maximum average roll value.

Propex™ Geotextile Systems

TESTED. PROVEN. TRUSTED.
www.geotextile.com

Propex Operating Company, LLC · 1110 Market Street, Suite 300 · Chattanooga, TN 37402

ph 423 899 0444 · ph 800 621 1273 · fax 423 899 7619

Tensar International Corporation
2500 Northwinds Pkwy, Suite 500
Alpharetta, Georgia 30009
Phone: 800-TENSAR-1
www.tensarcorp.com

Product Specification - Biaxial Geogrid BX1200

Tensar International Corporation reserves the right to change its product specifications at any time. It is the responsibility of the specifier and purchaser to ensure that product specifications used for design and procurement purposes are current and consistent with the products used in each instance.

Product Type: **Integrally Formed Biaxial Geogrid**
Polymer: **Polypropylene**
Load Transfer Mechanism: **Positive Mechanical Interlock**
Primary Applications: **Spectra System (Base Stabilization, Subgrade Improvement)**

Product Properties

Index Properties	Units	MD Values[1]	XMD Values[1]
▪ Aperture Dimensions[2]	mm (in)	25 (1.0)	33 (1.3)
▪ Rib Thickness[2]	mm (in)	1.27 (0.05)	1.27 (0.05)
▪ Tensile Strength @ 2% Strain[3]	kN/m (lb/ft)	6.0 (410)	9.0 (620)
▪ Tensile Strength @ 5% Strain[3]	kN/m (lb/ft)	11.8 (810)	19.6 (1,340)
▪ Ultimate Tensile Strength[3]	kN/m (lb/ft)	19.2 (1,310)	28.8 (1,970)
Structural Integrity			
▪ Junction Efficiency[4]	%	93	
▪ Overall Flexural Rigidity[5]	mg-cm	750,000	
▪ Aperture Stability[6]	m-N/deg	0.65	
Durability			
▪ Resistance to Installation Damage[7]	%SC / %SW / %GP	95 / 93 / 90	
▪ Resistance to Long Term Degradation[8]	%	100	
▪ Resistance to UV Degradation[9]	%	100	

Dimensions and Delivery

The biaxial geogrid shall be delivered to the jobsite in roll form with each roll individually identified and nominally measuring 4.0 meters (13.1 feet) in width and 50.0 meters (164 feet) in length and 3.93 meters (12.9 feet) in width and 50.0 meters (164 feet) in length.

Notes

1. Unless indicated otherwise, values shown are minimum average roll values determined in accordance with ASTM D4759-02. Brief descriptions of test procedures are given in the following notes.
2. Nominal dimensions.
3. Determined in accordance with ASTM D6637-10 Method A.
4. Load transfer capability determined in accordance with ASTM D7737-11.
5. Resistance to bending force determined in accordance with ASTM D7748/D7748M-14.
6. Resistance to in-plane rotational movement measured in accordance with ASTM D7864/D7864M-15.
7. Resistance to loss of load capacity or structural integrity when subjected to mechanical installation stress in clayey sand (SC), well graded sand (SW), and crushed stone classified as poorly graded gravel (GP). The geogrid shall be sampled in accordance with ASTM D5818 and load capacity shall be determined in accordance with ASTM D6637.
8. Resistance to loss of load capacity or structural integrity when subjected to chemically aggressive environments in accordance with EPA 9090 immersion testing.
9. Resistance to loss of load capacity or structural integrity when subjected to 500 hours of ultraviolet light and aggressive weathering in accordance with ASTM D4355-05.

This product specification supersedes all prior specifications for the product described above and is not applicable to any products shipped prior to February 1, 2013. (7.20)

Appendix (C): Detail drawings

The following are detailed approach slab drawings and designs provided for the TDOT drawings report.

CONST. NO.:

PROJECT NO.	YEAR	SHEET NO.
- -	2020	

REVISIONS

NO.	DATE	BY	BRIEF DESCRIPTION
	- -		
	- -		
	- -		
	- -		
	- -		

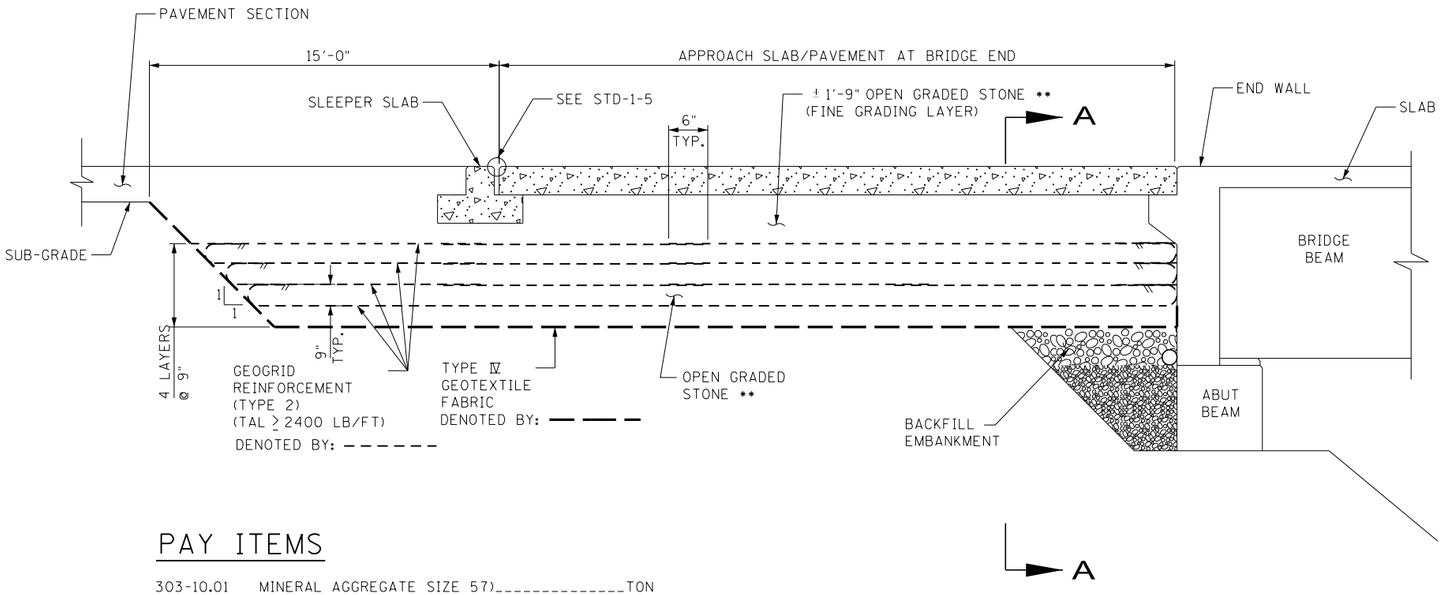

PAY ITEMS

303-10.01 MINERAL AGGREGATE SIZE 57)_____TON
604-03.04 PAVEMENT AT BRIDGE ENDS_____S.Y.
740-10.04 GEOTEXTILE (TYPE IV)(STABILIZATION) _____S.Y.
740-07.04 GEOGRID REINFORCEMENT TYPE 2 _____S.Y.

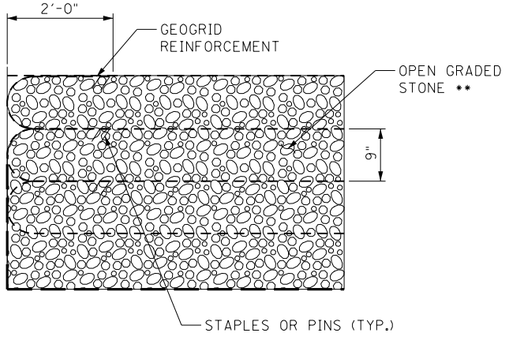

WRAP DETAILS

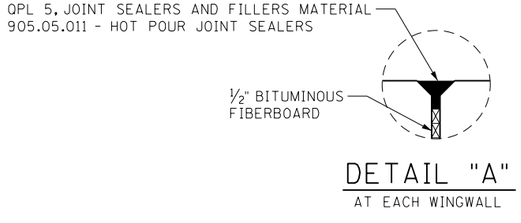

DETAIL "A"

AT EACH WINGWALL

NOTE: BRIDGE RAILS NOT SHOWN

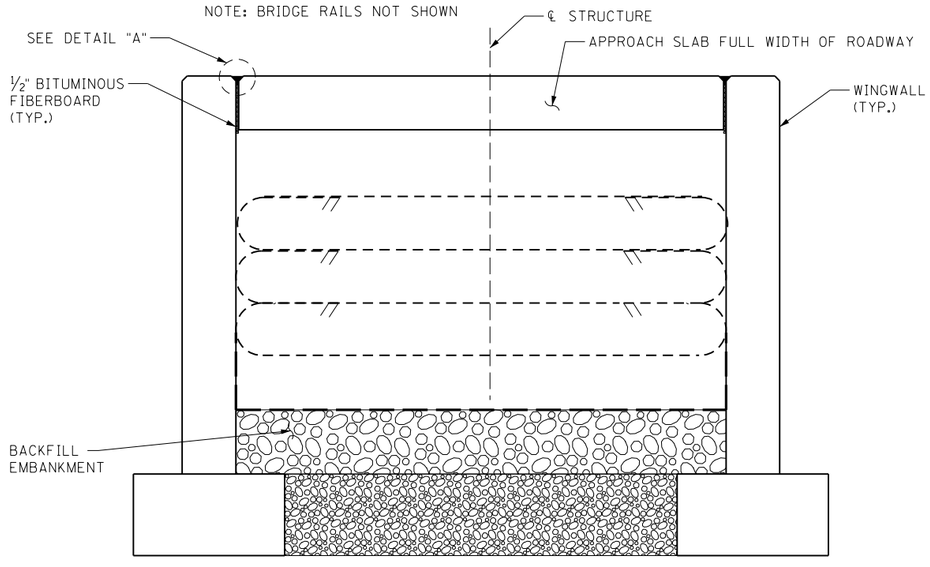

SECTION A-A

NOTES

NOTES FOR STRUCTURAL BACKFILL:

GEOTEXTILE REINFORCEMENT BETWEEN THE EMBANKMENT MATERIAL AND OPEN GRADED STONE SHALL BE TYPE IV WOVEN FABRIC WITH A TAL > 2400 LBS/FT AND MEET THE MATERIAL REQUIREMENTS OF TDOT QPL 36.

GEOTEXTILE GRID REINFORCING SHALL BE PLACED BY ALTERNATING MACHINE DIRECTION (MD) WITH CROSS MACHINE DIRECTION (XD) FROM LAYER TO LAYER.

THE GEOTEXTILE REINFORCEMENT WRAP AT FACE OF ABUTMENT AND WINGWALLS SHALL BE PULLED BACK SLACK FREE WITH ITS END ANCHORED TO OPEN GRADED STONE UNDERNEATH WITH STAPLES OR PINS.

MINIMUM SPLICE LENGTHS OF ALL GEOTEXTILES SHALL CONSIST OF 6" OF OVERLAP.

OPEN GRADED STONE SHALL BE PLACED IN LAYERS AS SHOWN ON THIS SHEET. EACH LIFT SHALL BE COMPACTED WITH A MINIMUM OF 4 PASSES WITH A THREE TON VIBRATORY ROLLER. ALL EDGES SHALL BE COMPACTED WITH A MECHANICAL TAMPER.

** ALLOWABLE GRADATIONS FOR THE OPEN GRADED STONE BACKFILL ARE #4, #5, #57, #67, #68, #7, #78, AND #8

SPECIAL NOTES FOR PAVEMENT AT BRIDGE ENDS:

CONCRETE FOR APPROACH SLAB SHALL BE CLASS "X" (3000 PSI @ 18 HOURS) WITH A MINIMUM OF 714 LBS/CY CEMENT.

CLASS "A' GRADING "D" STONE USED FOR FINAL GRADING SHALL BE COMPACTED PER THE SPECIFICATIONS AND CONFORM TO ROADWAY SLOPE AND GRADE AND COST TO BE INCLUDED IN COST OF PAVEMENT AT BRIDGE ENDS.

TWO LAYERS OF 6 MIL POLY SHALL BE PLACED BETWEEN THE COMPACTED FILL AND THE BOTTOM OF PAVEMENT AT BRIDGE ENDS WITH THE COST TO BE INCLUDED IN THE COST OF THE PAVEMENT AT BRIDGE ENDS.

THE PAVEMENT AT BRIDGE ENDS CONTROL ELEVATIONS SHALL BE ADJUSTED TO MATCH THE IN-PLACE DECK SLAB IN BOTH TRANSVERSE AND LONGITUDINAL DIRECTIONS.

THE JOINT SEAL SYSTEM AND SLEEPER SLAB ARE NOT REQUIRED WHEN THE BRIDGE HAS AN EXPANSION JOINT AT THE ADJACENT ABUTMENT. THE REINFORCED BACKFILL SHALL BE ADJUSTED AS REQUIRED FOR THIS CONDITION.

SPECIAL NOTES FOR PHASED CONSTRUCTION:

A TEMPORARY WALL OR SUPPORT SYSTEM WILL BE REQUIRED AT THE PHASE LINE DURING INSTALLATION OF THE PAVEMENT AT BRIDGE ENDS. SYSTEM TYPE SHALL BE SELECTED BY THE CONTRACTOR AND WILL BE SUBMITTED TO THE ENGINEER FOR REVIEW.

GEOGRID AND GEOTEXTILE SHALL BE TURNED UP ALONG THE SUPPORT SYSTEM TO ALLOW FOR OVERLAP DURING THE SECOND PHASE OF CONSTRUCTION. A MINIMUM OF 6 INCHES OF OVERLAP IS REQUIRED FOR THE GEOGRID OR GEOTEXTILE MATERIALS.

COST FOR SUPPORT SYSTEM IS CONSIDERED INCIDENTAL AND SHALL BE INCLUDED IN OTHER ITEMS.

DRAFT

STATE OF TENNESSEE
DEPARTMENT OF TRANSPORTATION

MISC. ABUTMENT & PAVEMENT AT BRIDGE ENDS BACKFILL DETAILS

2020

PIN NO.:

DESIGN BY:	TDOT STRUCTURES	DATE: 08/01/2020
DRAWN BY:	GARY YOUNG	DATE: 08/01/2020
SUPERVISED BY:	TED KNIAZEWYCZ	DATE: 08/01/2020
CHECKED BY:	TED KNIAZEWYCZ	DATE: 08/01/2020

8/11/2020 2:01:54 PM
P:\Structures\StandardDocuments\StandardDrawings\working files\STD-10-2 new std.dgn

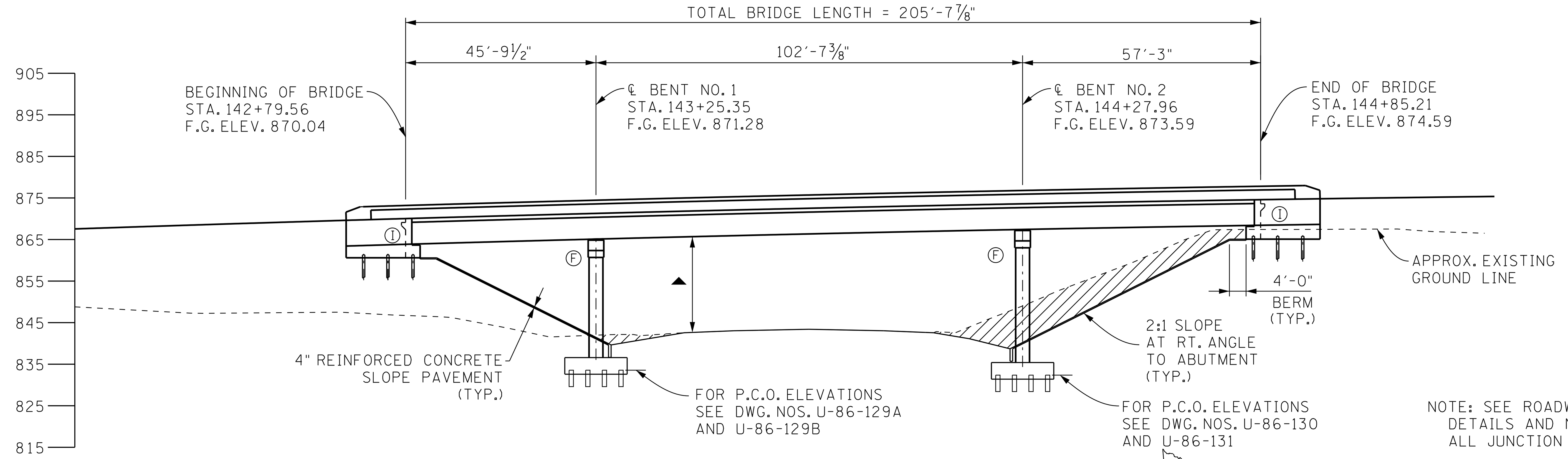

ELEVATION

(AT RT. ∆S TO ℄ SURVEY STATE ROUTE 115)
(SCALE: 1" = 20'-0")
ELEVATION VIEW IS PROJECTED
FROM PLAN VIEW BELOW. DIMENSIONS MAY
NOT BE THE SAME AS THE NOTED SCALE.

DENOTES: EXCAVATION TO BE PAID FOR AS A ROADWAY ITEM.
Ⓘ DENOTES: INTEGRAL
Ⓕ DENOTES: FIXED
▲ DENOTES: 16'-6" REQ'D. MIN. VERT. CL.
18'-0" ACTUAL MIN. VERT. CL.

NOTE: SEE ROADWAY PLANS FOR ALL LIGHTING DETAILS AND NOTES. INCLUDING LOCATION OF ALL JUNCTION BOXES AND PULL BOXES.

CURVE DATA
(STATE ROUTE 115)
PI 143+92.54
N 571,243.7685
E 2,574,934.9943
∆s 50° 16' 54" (LT)
θs 12° 42' 22"
∆c 24° 52' 09" (LT)
Dc 4° 45' 00"
Rc 1,206.23
Lc 523.56
Ts 837.78
Ls 535.00
SE 0.080 FT/FT
DESIGN SPEED 60 MPH
TRANS. LENGTH 535'

CURVE DATA
(STATE ROUTE 168)
PI 74+34.91
N 571,349.5833
E 2,574,466.9975
∆ 47° 10' 49" (LT)
D 22° 45' 00"
R 251.85
L 207.39
T 109.98
SE 0.08 FT/FT
DESIGN SPEED 40 MPH
TRANS. LENGTH 210'

CONST. NO. 47026-3281-14

PROJECT NO.	YEAR	SHEET NO.
STP/NH-115(27)	2018	

REVISIONS

NO.	DATE	BY	BRIEF DESCRIPTION
1.	4-5-19	ALP	GENERAL REVISIONS
2.	7-29-19	ALP	REVISED GRATE NOTE

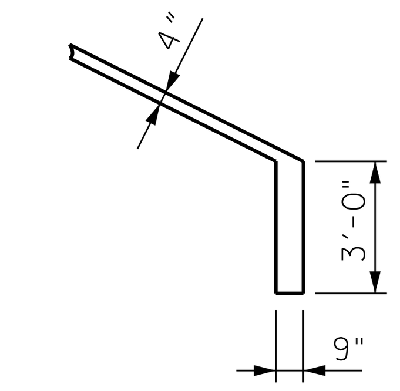

REINFORCED CONCRETE SLOPE PAVEMENT AT DITCH

PAVE SLOPES AND EXPOSED EARTH UNDER BRIDGES WITH 4" THICK CEMENT CONCRETE SLAB REINFORCED WITH NO. 4 GAGE WIRE FABRIC @ 6" CENTERS AND 58 LB. PER 100 S.F. THE WIRE FABRIC REINFORCEMENT SHALL BE PLACED AT ONE-HALF THE DEPTH OF THE SLAB AND EXTEND TO WITHIN 3" OF ITS EDGE WITH A 12" LAP REQUIRED ON ALL SHEETS. THE COST OF THE WIRE FABRIC REINFORCEMENT SHALL BE INCLUDED IN THE UNIT PRICE BID FOR ITEM 709-04, REINFORCED CONCRETE SLOPE PAVEMENT. ONE-HALF INCH PREMOLDED EXPANSION JOINTS WITHOUT LOAD TRANSFERS SHALL BE FORMED ABOUT ALL STRUCTURES AND FEATURES PROJECTING THROUGH, IN OR AGAINST THE SLAB. THE SLAB SHALL BE GROOVED PARALLEL WITH AND AT RIGHT ANGLES TO THE UNDER ROADWAY CENTERLINE AT 6' CENTERS. DEPTH OF GROOVE TO BE NOT LESS THAN 1". SEE STD. DWG. RD01-SA-1 FOR LIMITS OF SLOPE PROTECTION.

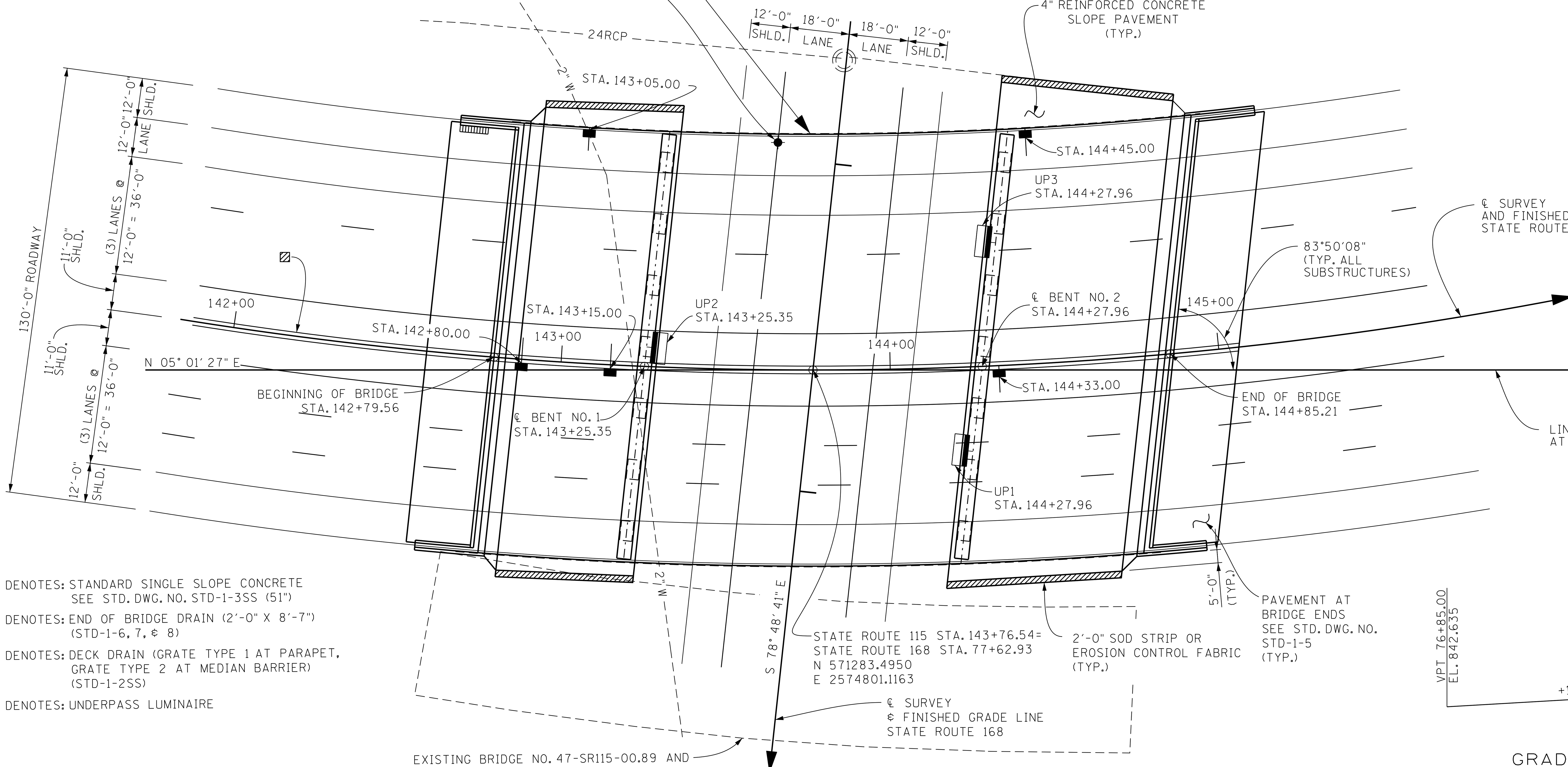

PLAN

(SCALE: 1" = 20'-0")

DENOTES: STANDARD SINGLE SLOPE CONCRETE
SEE STD. DWG. NO. STD-1-3SS (51")
DENOTES: END OF BRIDGE DRAIN (2'-0" X 8'-7")
(STD-1-6, 7, & 8)
② DENOTES: DECK DRAIN (GRATE TYPE 1 AT PARAPET, GRATE TYPE 2 AT MEDIAN BARRIER)
(STD-1-2SS)
DENOTES: UNDERPASS LUMINAIRE

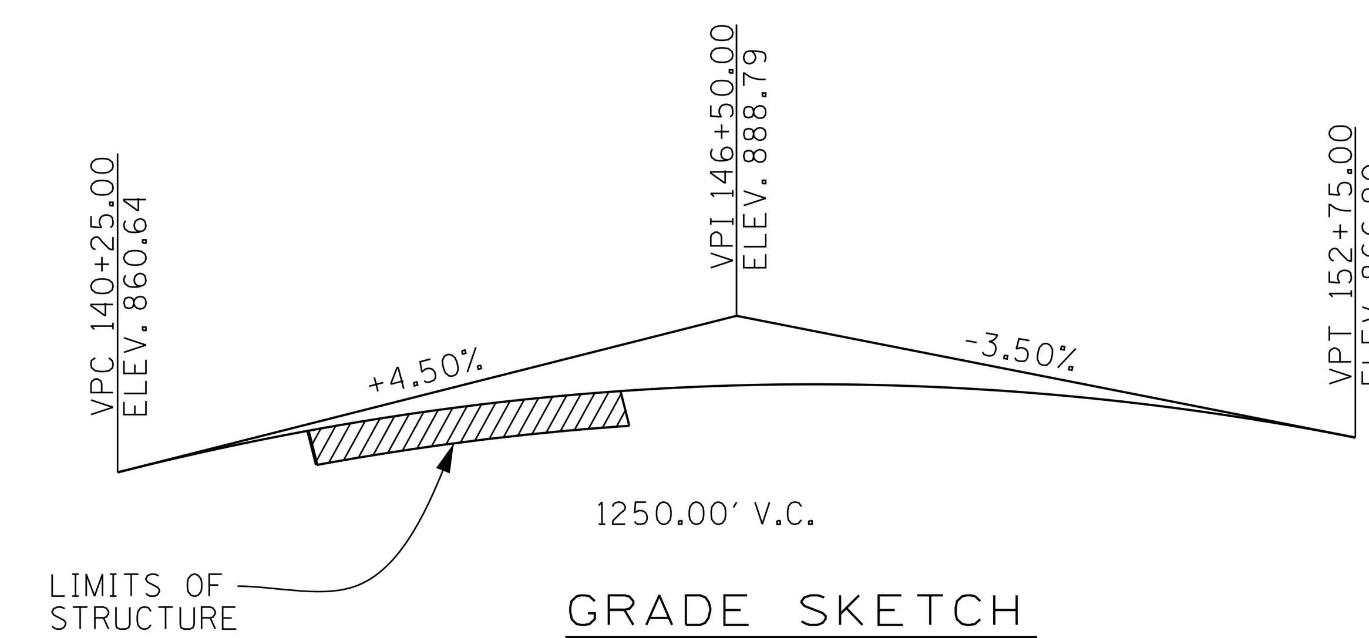

GRADE SKETCH
STATE ROUTE 115

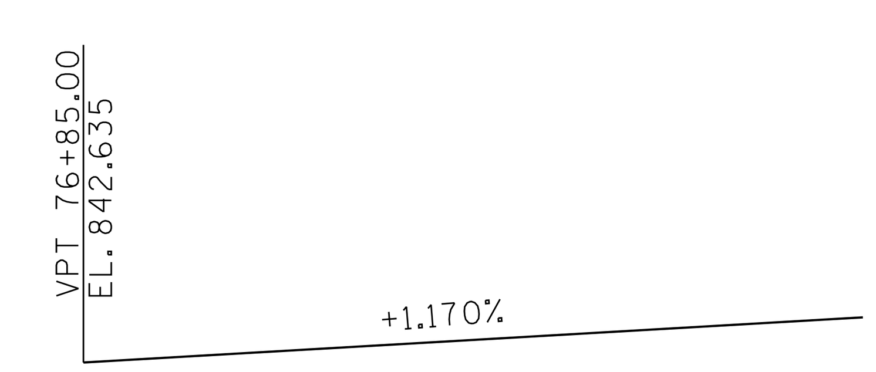

GRADE SKETCH
STATE ROUTE 168

ADAM L. PRICE — STATE OF TENNESSEE
07-29-2019

2038 ADT = 89180
130'-0" ROADWAY WITH STD-1-1SS PARAPETS
AND STD-1-3SS MEDIAN BARRIER
DESIGN SPEED = 60 MPH

STATE OF TENNESSEE
DEPARTMENT OF TRANSPORTATION

① BRIDGE NO. 2
LAYOUT OF BRIDGE
STATE ROUTE 115
OVER
STATE ROUTE 168
STATION 143+76.54
BRIDGE ID. NO. 47SR1150023
KNOX COUNTY
2018

CORRECT ______ ENGINEER OF STRUCTURES

DESIGNED BY	ALI OMAR	DATE	08-15
DRAWN BY	C. STAPLER	DATE	02-15
SUPERVISED BY	PRICE/MARTINKO	DATE	02-15
CHECKED BY	DAWOD ABDULLAH	DATE	11-17

U-86-104

INTERCONNECTED PORTABLE BARRIER RAIL (T-PBR-1) = 496 L.F.

FD1180.DGN

PIN NO. 100241.02

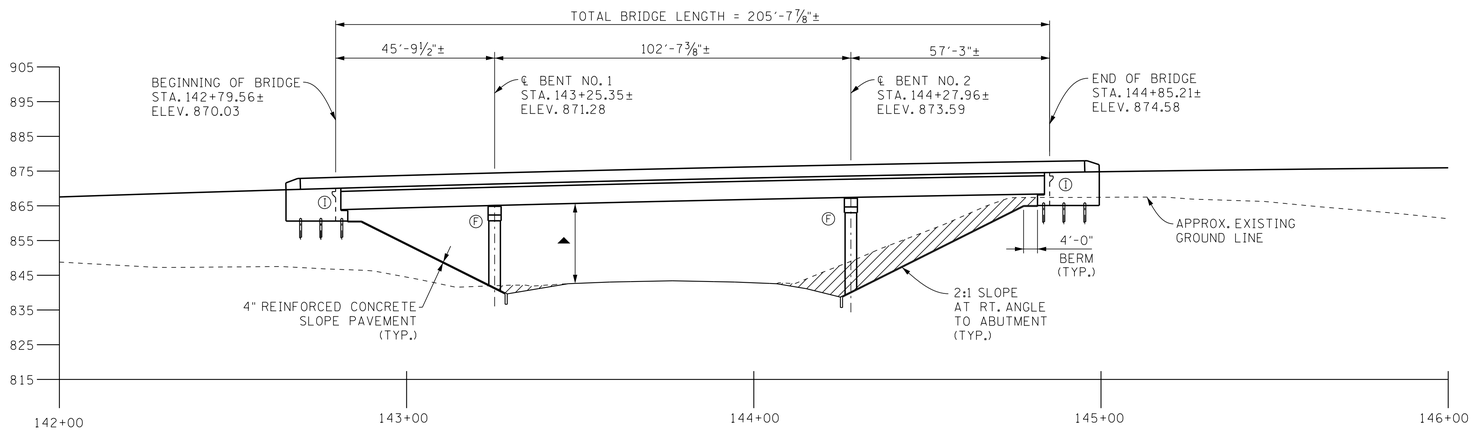

ELEVATION

(AT RT. ΔS TO ℄ SURVEY STATE ROUTE 115)
(SCALE: 1" = 20'-0")
ELEVATION VIEW IS PROJECTED FROM PLAN VIEW BELOW. DIMENSIONS MAY NOT BE THE SAME AS THE NOTED SCALE.

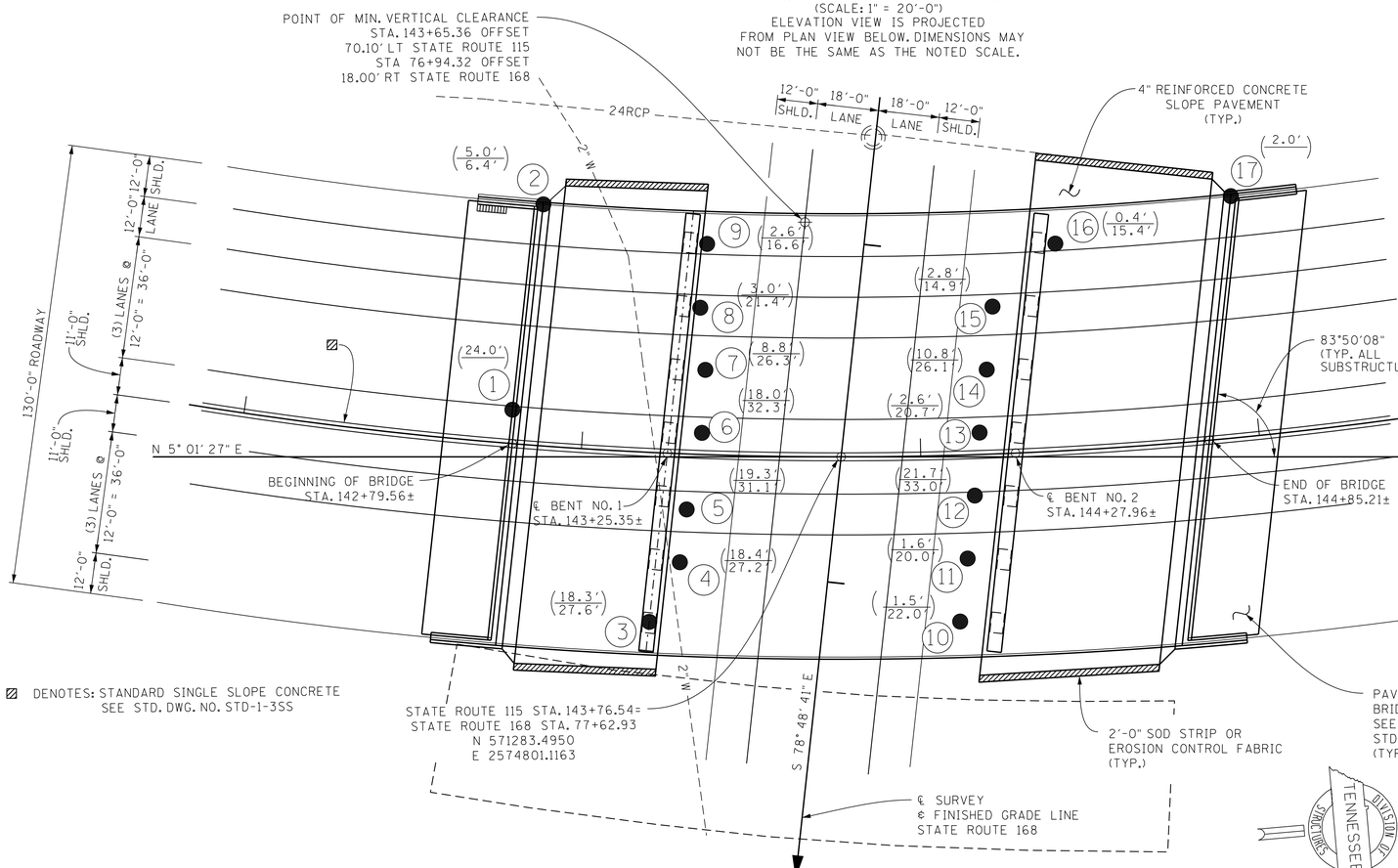

▨ DENOTES: STANDARD SINGLE SLOPE CONCRETE SEE STD. DWG. NO. STD-1-3SS

PLAN

(SCALE: 1" = 20'-0")

BENCHMARKS:

BM #S1
STA. 143+62±
OFFSET 1044.1' RT.
ELEV. = 873.96

BM #S20
STA. 144+70±
OFFSET 124.6' RT.
ELEV. = 875.76

② CONST. NO. 47026-3281-14

PROJECT NO.	YEAR	SHEET NO.
STP/NH-115(27)	2018	

REVISIONS

NO.	DATE	BY	BRIEF DESCRIPTION
1.	4-5-19	ALP	GENERAL REVISIONS
2.	5-17-19	ALP	CHANGED P.E. NO. TO CONST. NO.

NOTES:

DESIGN SPECIFICATIONS: AASHTO LRFD 7TH EDITION, 2014 WITH INTERIMS, AND THE 2011 AASHTO GUIDE SPECIFICATIONS FOR LRFD SEISMIC BRIDGE DESIGN, 2ND EDITION WITH INTERIMS.
SEISMIC CATEGORY "A" WITH AS = 0.194, SDS = 0.345, SD1 = 0.120, (1000 YEAR RETURN PERIOD).

NO.	OFFSET	STATION	GROUND ELEVATION (FT.)	ROCK ELEVATION(FT.)	BOTTOM (FT.)	TOTAL DEPTH (FT.)
1	10.0' LT	142+79.56	847.26	823.3	823.26	24.0
2	71.0' LT	142+83.21	837.47	832.5	831.07	6.4
3	49.9 RT	143+12.23	844.66	826.4	817.06	27.6
4	32.25' RT	143+23.37	843.53	825.1	816.33	27.2
5	16.6' RT	143+31.54	843.10	823.8	812.00	31.1
6	6.0' LT	143+35.2	841.53	823.5	809.23	32.3
7	24.6' LT	143+35.5	840.57	831.8	814.27	26.3
8	43.3' LT	143+33.3	840.50	837.5	819.10	21.4
9	61.9' LT	143+31.6	839.96	837.4	823.36	16.6
10	49.4' RT	144+09.7	845.27	843.8	823.27	22.0
11	30.89' RT	144+12.8	845.51	843.9	823.51	20.0
12	12.4' RT	144+15.9	845.80	823.9	812.80	33.0
13	6.0' LT	144+17.6	845.17	842.6	824.47	20.7
14	24.5' LT	144+20.6	844.00	833.2	817.91	26.1
15	42.9' LT	144+23.2	842.84	840.0	827.94	14.9
16	61.4' LT	144+42.8	839.94	839.5	824.54	15.4
17	70.0' LT	144+98.70	837.86	835.9	835.90	2.0

NOTE:
BORING DEPICTIONS SHOWN ON FOUNDATION DATA SHEET INDICATE GENEREAL SOIL AND ROCK TYPE AT SPECIFIC BORING LOCATIONS.

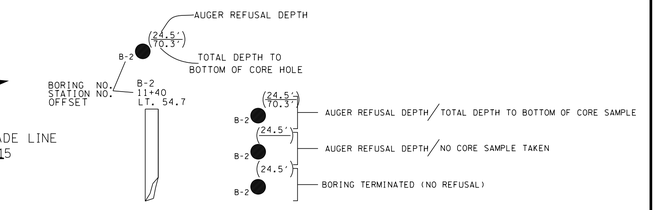

A.R. - AUGER REFUSAL
B.T. - BORING TERMINATED (NO REFUSAL)

● DENOTES DRILLING POINT LOCATION

(2) DENOTES DRILLING POINT NUMBER

REQUIRED:
1) SUFFICENT GROUND, ROCK, AND CORING INFORMATION FOR BRIDGE FOUNDATIONS.
2) APPROXIMATE EXISTING GROUND AND ROCK LINE.

☞ THIS DRAWING IS FOR FOUNDATION DATA ONLY AND IS NOT TO BE USED AS A LAYOUT.

STATE OF TENNESSEE
DEPARTMENT OF TRANSPORTATION

BRIDGE NO. 2 FOUNDATION DATA STATE ROUTE 115 OVER STATE ROUTE 168 STATION 143+76.54 KNOX COUNTY 2018

DESIGNED BY ALI OMAR DATE 08-15
DRAWN BY ALI OMAR/C. STAPLER DATE 08-15
SUPERVISED BY PRICE/MARTINKO DATE 08-15
CHECKED BY DAWOD ABDULLAH DATE 11-17

TENNESSEE DEPARTMENT OF TRANSPORTATION STRUCTURES DIVISION

CORRECT Jed A. Kniewasser
ENGINEER OF STRUCTURES

U-86-107

PREL284.DGN

CONST. NO. 47026-3281-14

PROJECT NO.	YEAR	SHEET NO.
STP/NH-115(27)	2018	

REVISIONS

NO.	DATE	BY	BRIEF DESCRIPTION
1.	4-5-19	ALP	GENERAL REVISIONS
2.	5-17-19	ALP	CHANGED P.E. NO. TO CONST. NO.

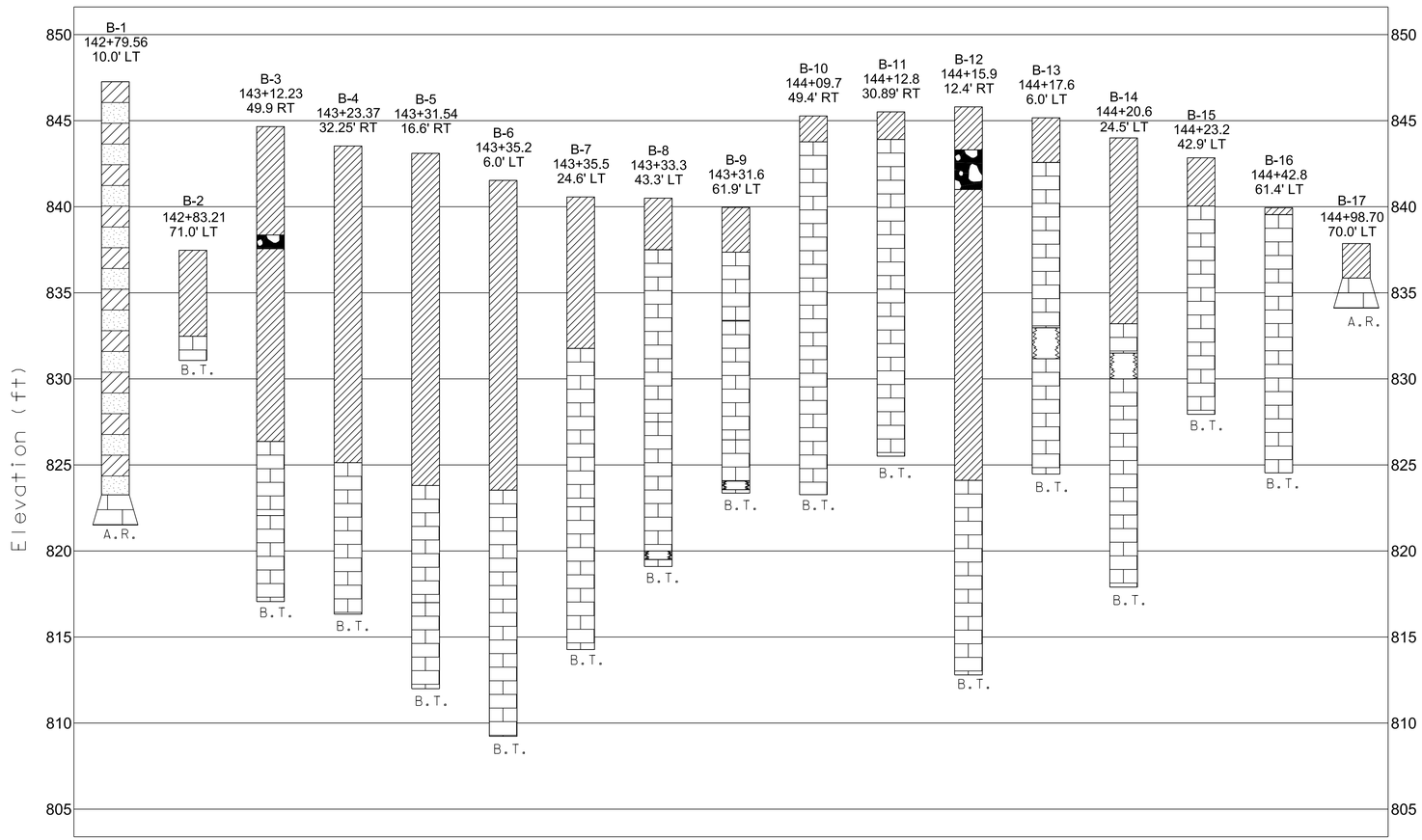

LEGEND

FILL

USCS LOW PLASTICITY CLAY

LIMESTONE

BOULDERS AND COBBLES

CAVITY OR VOID

STATE OF TENNESSEE
DEPARTMENT OF TRANSPORTATION

BRIDGE NO. 2
FOUNDATION DATA
STATE ROUTE 115
OVER
STATE ROUTE 168
STATION 143+76.54
KNOX COUNTY
2018

DESIGNED BY ALI OMAR DATE 08-15
DRAWN BY ALI OMAR/C. STAPLER DATE 08-15
SUPERVISED BY PRICE/MARTINKO DATE 08-15
CHECKED BY DAWOD ABDULLAH DATE 11-17

CORRECT
ENGINEER OF STRUCTURES

U-86-108

SP1180.DGN

CONST. NO. 47026-3281-14

PROJECT NO.	YEAR	SHEET NO.
STP/NH-115(27)	2018	

REVISIONS

NO.	DATE	BY	BRIEF DESCRIPTION
1	4-5-19	ALP	GENERAL REVISIONS

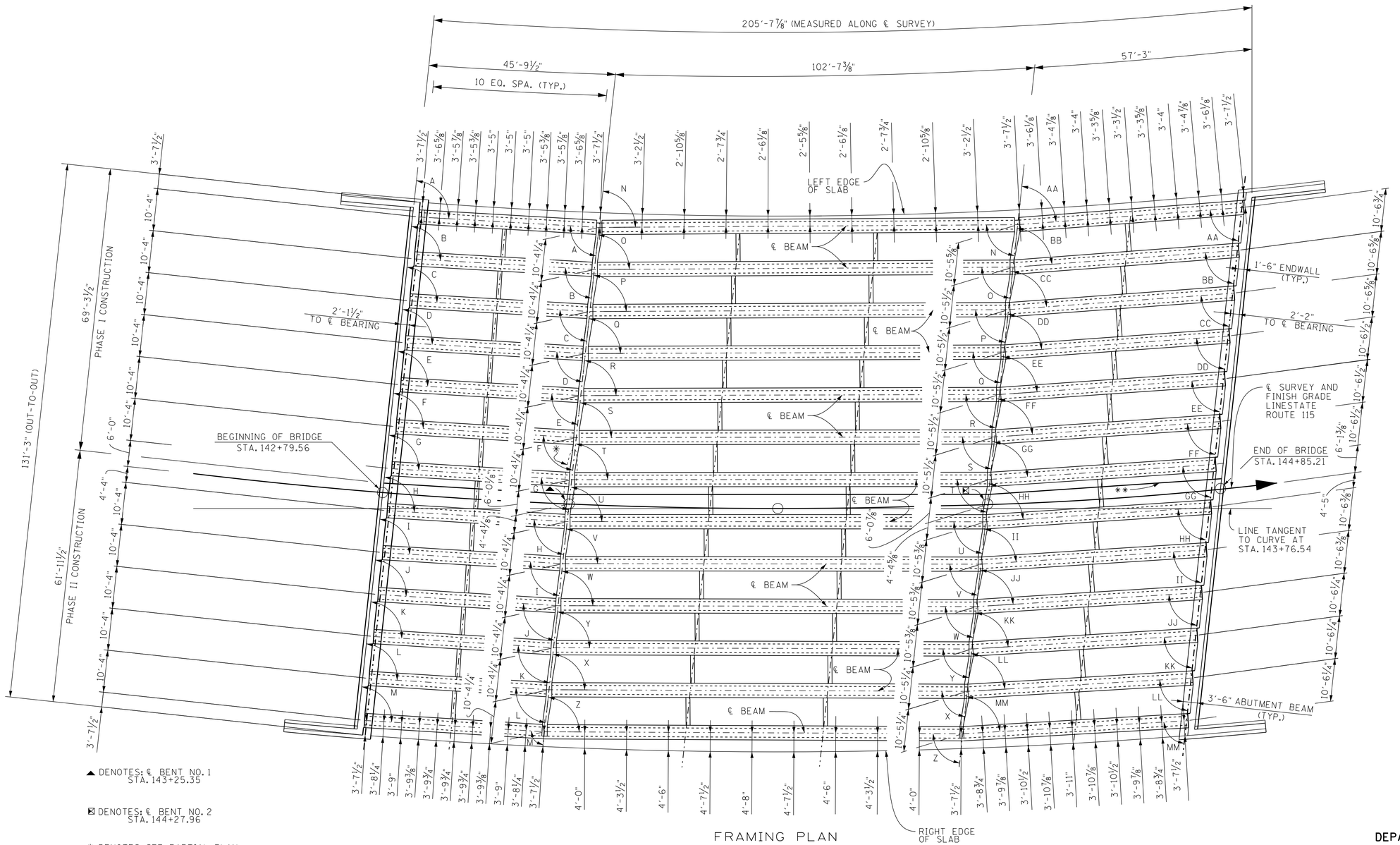

▲ DENOTES: ℄ BENT NO. 1 STA.143+25.35

⊠ DENOTES: ℄ BENT NO. 2 STA.144+27.96

* DENOTES: SEE PARTIAL PLAN OF DIAPHRAGM

** DENOTES: PHASE CONSTRUCTION JOINT

FRAMING PLAN

TABLE OF ANGLES

A	87°08′ 34"	I	87°20′ 12"	Q	83°38′ 01"	X	84°03′ 14"	GG	80°02′ 05"
B	87°10′ 07"	J	87°21′ 32"	R	83°41′ 23"	Z	84°06′ 19"	HH	80°07′ 15"
C	87°11′ 38"	K	87°22′ 51"	S	83°44′ 42"	AA	79°29′ 08"	II	80°12′ 19"
D	87°13′ 07"	L	87°24′ 05"	T	83°47′ 57"	BB	79°34′ 53"	JJ	80°17′ 18"
E	87°14′ 35"	M	87°25′ 26"	U	83°51′ 08"	CC	79°40′ 31"	KK	80°22′ 12"
F	87°16′ 02"	N	83°27′ 33"	V	83°54′ 17"	DD	79°46′ 04"	LL	80°27′ 01"
G	87°17′ 26"	O	83°31′ 06"	W	83°57′ 22"	EE	79°51′ 30"	MM	80°31′ 45"
H	87°18′ 50"	P	83°34′ 36"	Y	84°00′ 24"	FF	79°56′ 50"		

DESIGNED BY ALI OMAR DATE 08-15
DRAWN BY B. ERVIN DATE 01-18
SUPERVISED BY ADAM PRICE DATE 08-15
CHECKED BY DAWOD ABDULLAH DATE 11-17

ADAM L. PRICE — LICENSED ENGINEER — AGRICULTURE — NUMBER 117[illegible] — STATE OF TENNESSEE
04-10-2019

STATE OF TENNESSEE
DEPARTMENT OF TRANSPORTATION

BRIDGE NO. 2
SUPERSTRUCTURE DETAILS
STATE ROUTE 115
OVER
STATE ROUTE 168
STATION 143+76.54
KNOX COUNTY
2018

CORRECT Dawod A. Abdullah
ENGINEER OF STRUCTURES

U-86-110

4/8/2019
P:\Cadd User Group Regions (and 2)\Billy Ervin\180 SR 115 over SR 168, Knox Co, 2017\SP1180.dgn

SP1180.DGN

CONST. NO. 47026-3281-14

PROJECT NO.	YEAR	SHEET NO.
STP/NH-115(27)	2018	

REVISIONS

NO.	DATE	BY	BRIEF DESCRIPTION
1	4-5-19	ALP	GENERAL REVISIONS

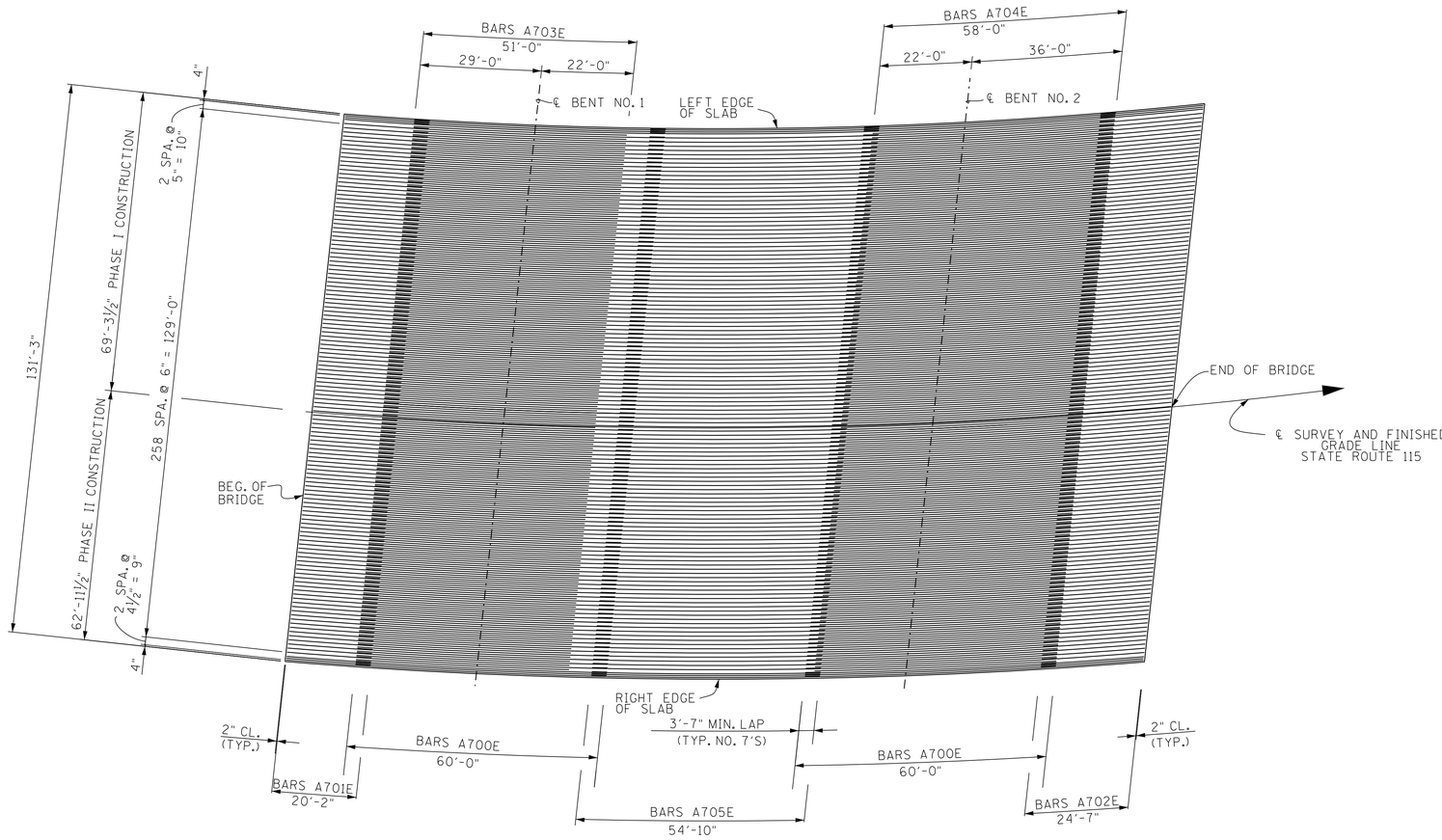

PLAN OF MAIN REINFORCEMENT

ADAM L. PRICE
LICENSED TO PRACTICE
AGRICULTURE
ARCHITECTURE
ENGINEERING
STATE OF TENNESSEE

04-10-2019

STATE OF TENNESSEE
DEPARTMENT OF TRANSPORTATION

BRIDGE NO. 2
SUPERSTRUCTURE DETAILS
STATE ROUTE 115
OVER
⚠1 STATE ROUTE 168
STATION 143+76.54
KNOX COUNTY
2018

CORRECT Jed A. Kmiyawiyas
ENGINEER OF STRUCTURES

U-86-112

DESIGNED BY ALI OMAR DATE 08-15
DRAWN BY B. ERVIN DATE 01-18
SUPERVISED BY ADAM PRICE DATE 08-15
CHECKED BY DAWOD ABDULLAH DATE 11-17

4/8/2019
P:\Cadd User Group Regions I and 2\Billy Ervin\180 SR 115 over SR 168, Knox Co. 2017\SP1180.dgn

AB1180.DGN

CONST. NO. 47026-3281-14		
PROJECT NO.	YEAR	SHEET NO.
STP-NH-115(27)	2018	

REVISIONS

NO.	DATE	BY	BRIEF DESCRIPTION
1	4-5-19	ALP	GENERAL REVISION

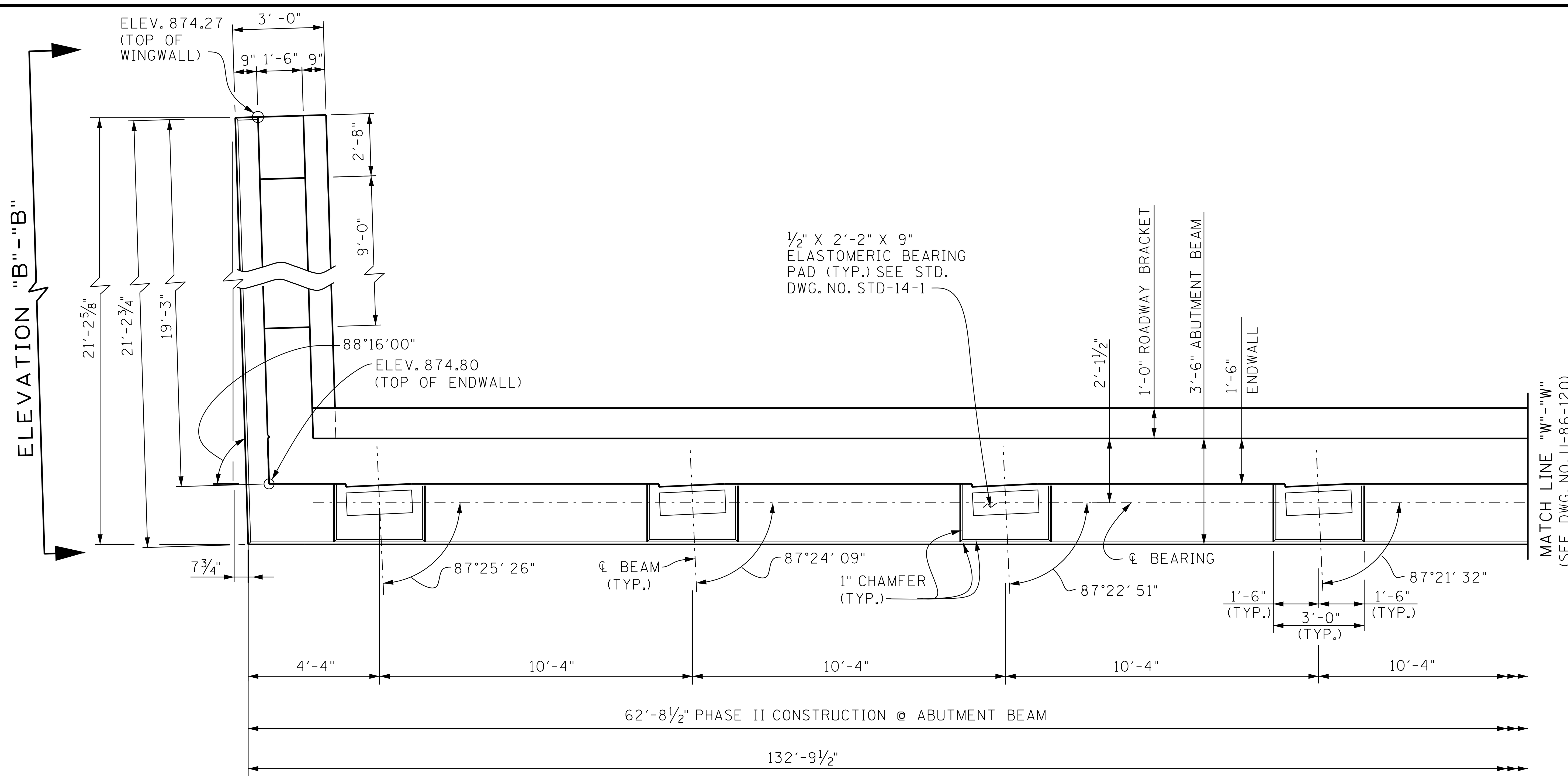

PLAN

NOTE: FOR ELEVATION "B"-"B" SEE DWG. NO. U-86-123

NOTE: FOR SECTION "C"-"C" SEE DWG. NO. U-86-121

NOTE: FOR SECTION "D"-"D" SEE DWG. NO. U-86-122

GENERAL NOTES

NOTE: RISER BLOCKS SHALL BE POURED MONOLITHICALLY WITH ABUTMENT BEAM.

NOTE: WHEN POURING WINGWALLS, PROVISIONS SHALL BE MADE FOR SETTING REINFORCING STEEL FOR WINGPOSTS AND PARAPETS. FOR DETAILS OF WINGPOSTS AND PARAPET, SEE STANDARD DRAWING NO. STD-1-1SS.

NOTE: ELASTOMERIC PADS SHALL BE IN PLACE A MINIMUM OF ONE DAY BEFORE BEING DISTURBED BY SETTING BEAMS. PLACE RUBBER BONDING CEMENT IN SUCH A WAY THAT VISIBLE CONCRETE SURFACES WILL NOT BE STAINED.

NOTE: NOT LESS THAN HALF OF THE SLAB IN THE END SPAN SHALL BE POURED PRIOR TO, OR CONCURRENTLY WITH, PLACEMENT OF ANY PART OF THE ABUTMENT BACKWALL. AT LEAST THE TOP 12 INCHES OF THE BACKWALL SHALL BE POURED CONCURRENTLY WITH THE END OF SLAB.

NOTE: COST OF BRIDGE RAIL AND POST IS TO BE INCLUDED IN THE UNIT PRICE BID FOR THE BRIDGE RAIL SYSTEM.

NOTE: WINGBEAM PILES SHALL BE DRIVEN TO THE PLANS TIP ELEVATION OR REFUSAL. SEISMIC ATTACHMENT IS NOT REQUIRED FOR WING BEAM PILES.

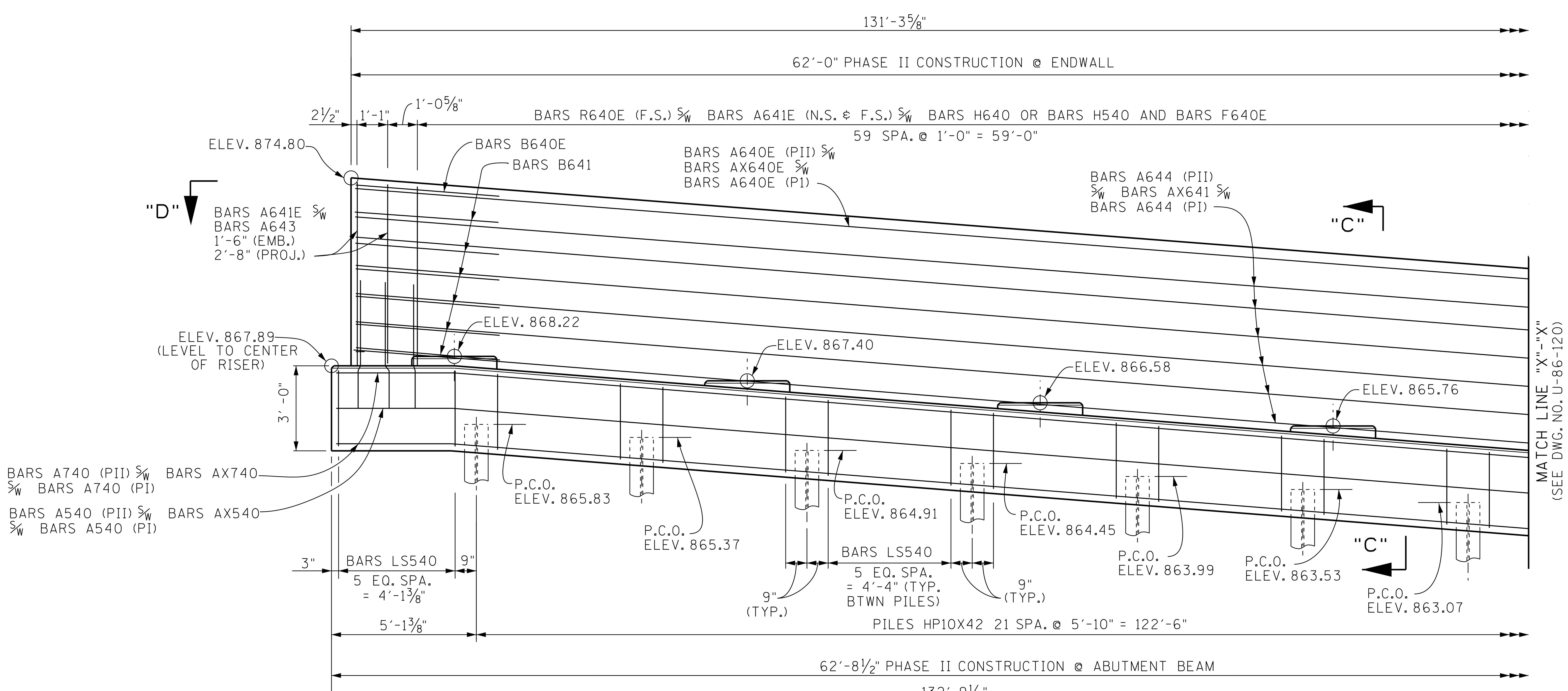

ELEVATION

(LOOKING BACK ON SURVEY)

P.C.O. DENOTES: PILE CUT-OFF
N.S. DENOTES: NEAR SIDE
F.S. DENOTES: FAR SIDE
PI DENOTES: PHASE I
PII DENOTES: PHASE II

ESTIMATED QUANTITIES

CONCRETE CLASS "A" CY.	EPOXY COATED REINFORCING STEEL LB.	STEEL BAR REINFORCEMENT (BRIDGES) LB.
133	5,137	13,705

ADAM L. PRICE
04-10-2019

STATE OF TENNESSEE
DEPARTMENT OF TRANSPORTATION

BRIDGE NO. 2
ABUTMENT NO. 1
STATE ROUTE 115
OVER
STATE ROUTE 168
STATION 143+76.54
KNOX COUNTY
2018

CORRECT ____ ENGINEER OF STRUCTURES

DESIGNED BY	ADAM PRICE	DATE	08-15
DRAWN BY	JERRY W. SIMPSON	DATE	02-18
SUPERVISED BY	MARTINKO/HASTINGS	DATE	02-18
CHECKED BY	DAWOD ABDULLAH	DATE	11-17

U-86-119

AB1180.DGN

CONST. NO. 47026-3281-14

PROJECT NO.	YEAR	SHEET NO.
STP-NH-115(27)	2018	

REVISIONS

NO.	DATE	BY	BRIEF DESCRIPTION
1	4-5-19	ALP	GENERAL REVISION

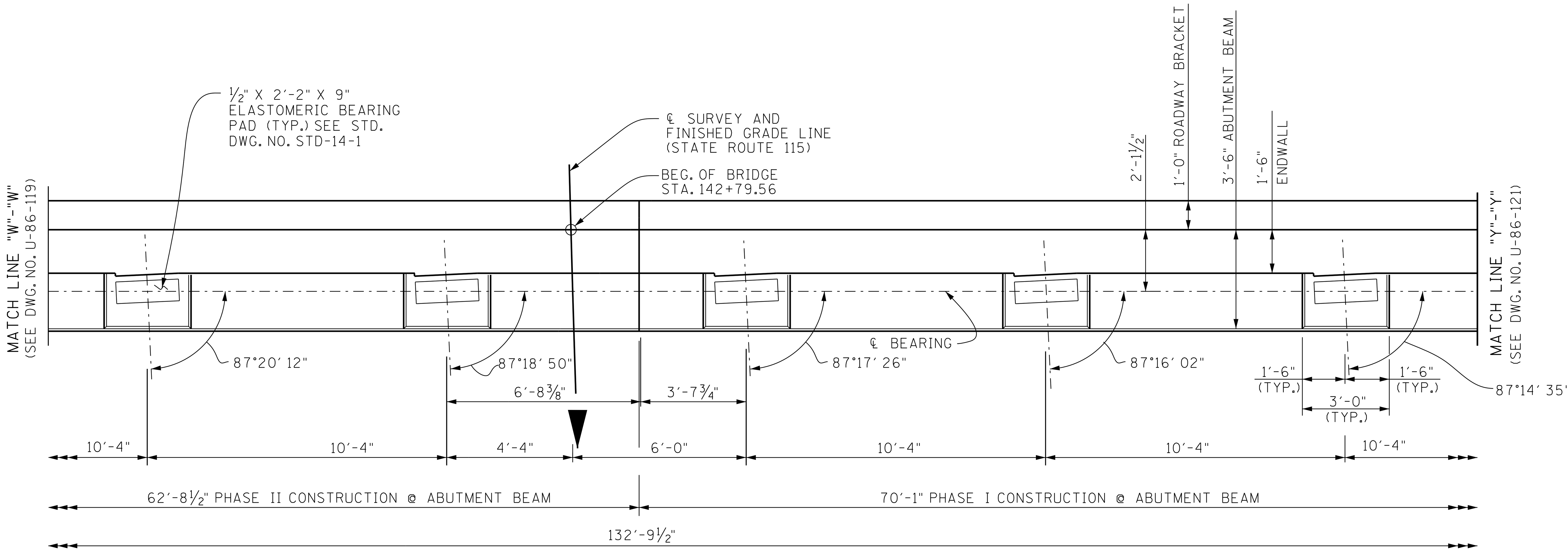

PLAN

P.C.O. DENOTES: PILE CUT-OFF
N.S. DENOTES: NEAR SIDE
F.S. DENOTES: FAR SIDE
PI DENOTES: PHASE I
PII DENOTES: PHASE II

NOTE: FOR SECTION "C"-"C" SEE DWG. NO. U-86-121

NOTE: FOR SECTION "D"-"D" SEE DWG. NO. U-86-122

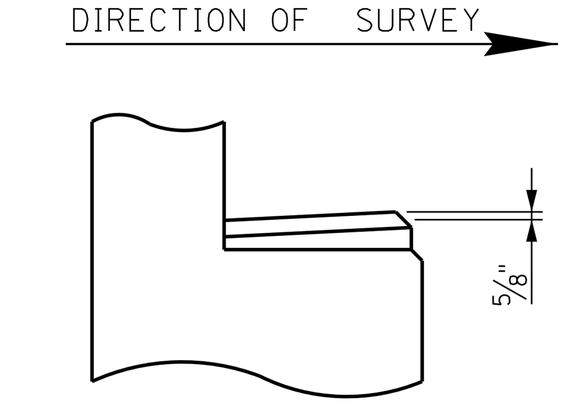

RISER BLOCK SLOPE DETAILS

NOTE: RISER BLOCK BEARING PAD SURFACES TO CONFORM TO BOTTOM OF BEAM GRADE.

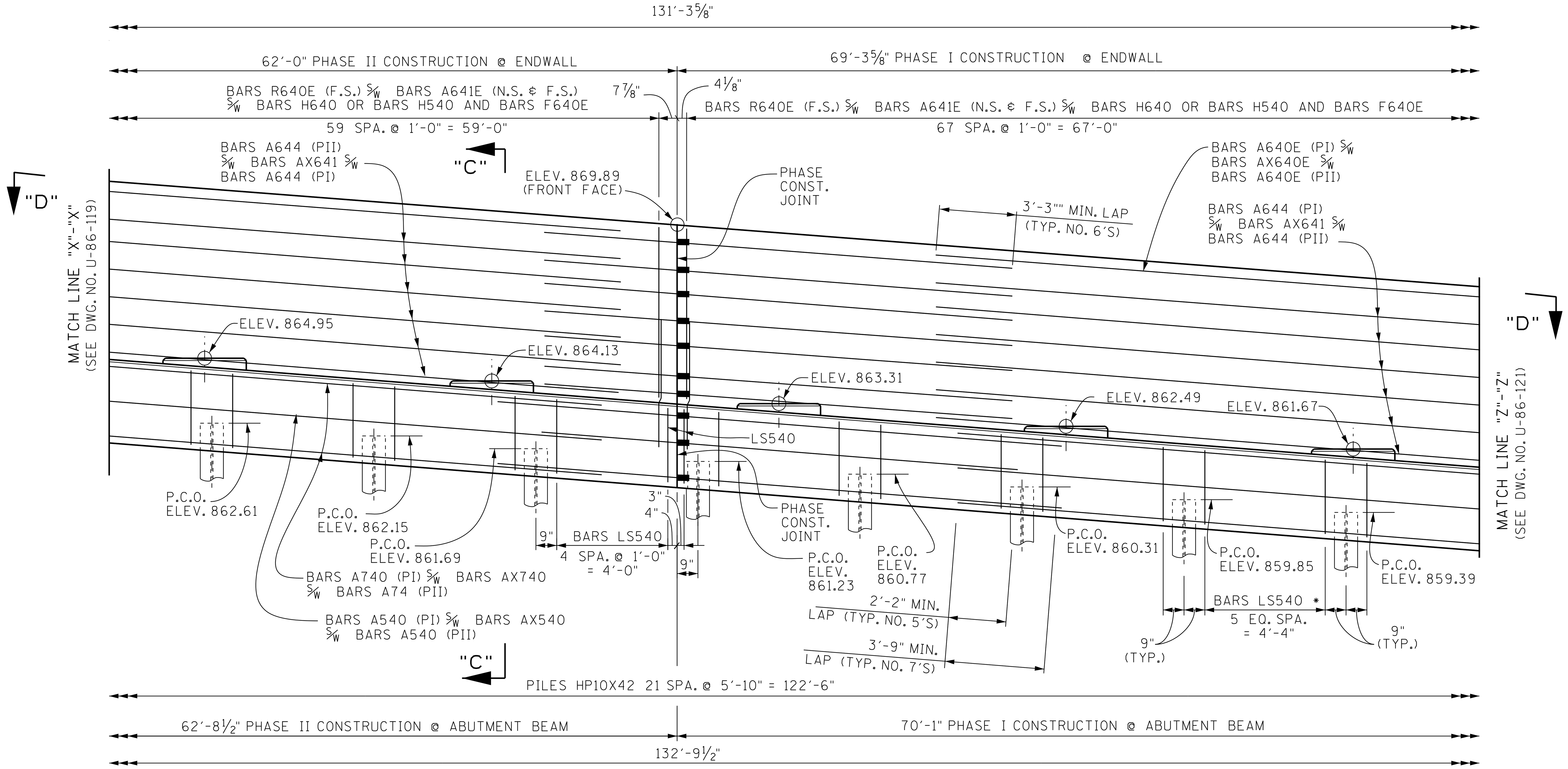

ELEVATION

(LOOKING BACK ON SURVEY)

* DENOTES: TYP. BTWN. PILES EXCEPT @ PHASE CONSTRUCTION JOINT LOCATION

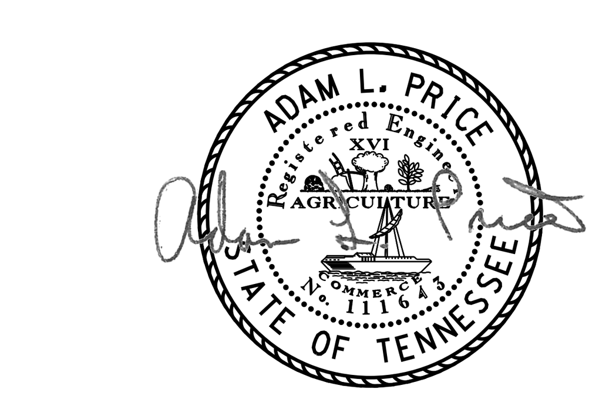

04-10-2019

STATE OF TENNESSEE
DEPARTMENT OF TRANSPORTATION

BRIDGE NO. 2
1 ABUTMENT NO. 1 DETAILS
STATE ROUTE 115
OVER
STATE ROUTE 168
STATION 143+76.54
KNOX COUNTY
2018

DESIGNED BY	ADAM PRICE	DATE	08-15
DRAWN BY	JERRY W. SIMPSON	DATE	02-18
SUPERVISED BY	MARTINKO/HASTINGS	DATE	02-18
CHECKED BY	DAWOD ABDULLAH	DATE	11-17

CORRECT ENGINEER OF STRUCTURES

U-86-120

AB1180.DGN

CONST. NO. 47026-3281-14

PROJECT NO.	YEAR	SHEET NO.
STP-NH-115(27)	2018	

REVISIONS

NO.	DATE	BY	BRIEF DESCRIPTION
1	4-5-19	ALP	GENERAL REVISION

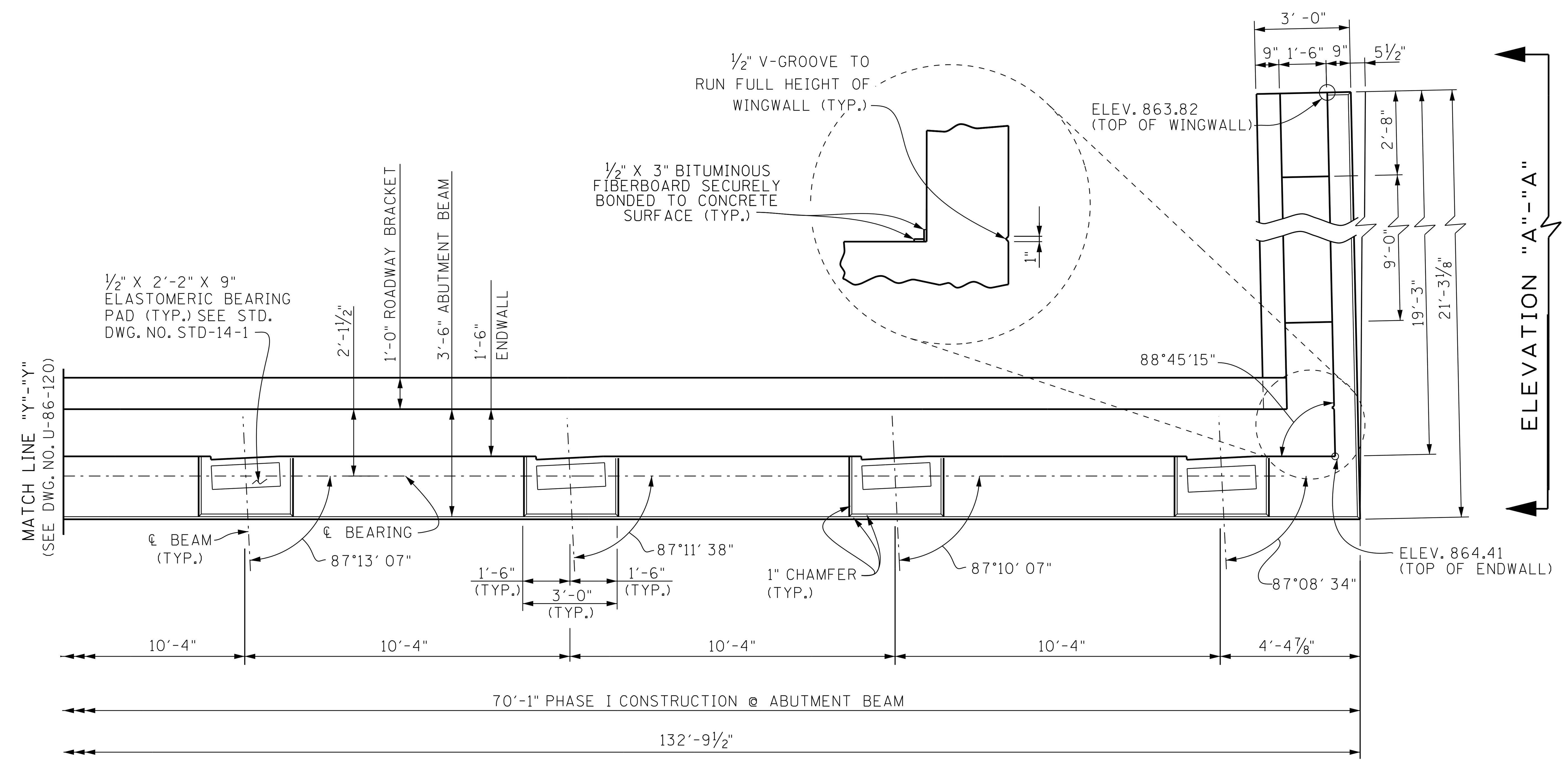

PLAN

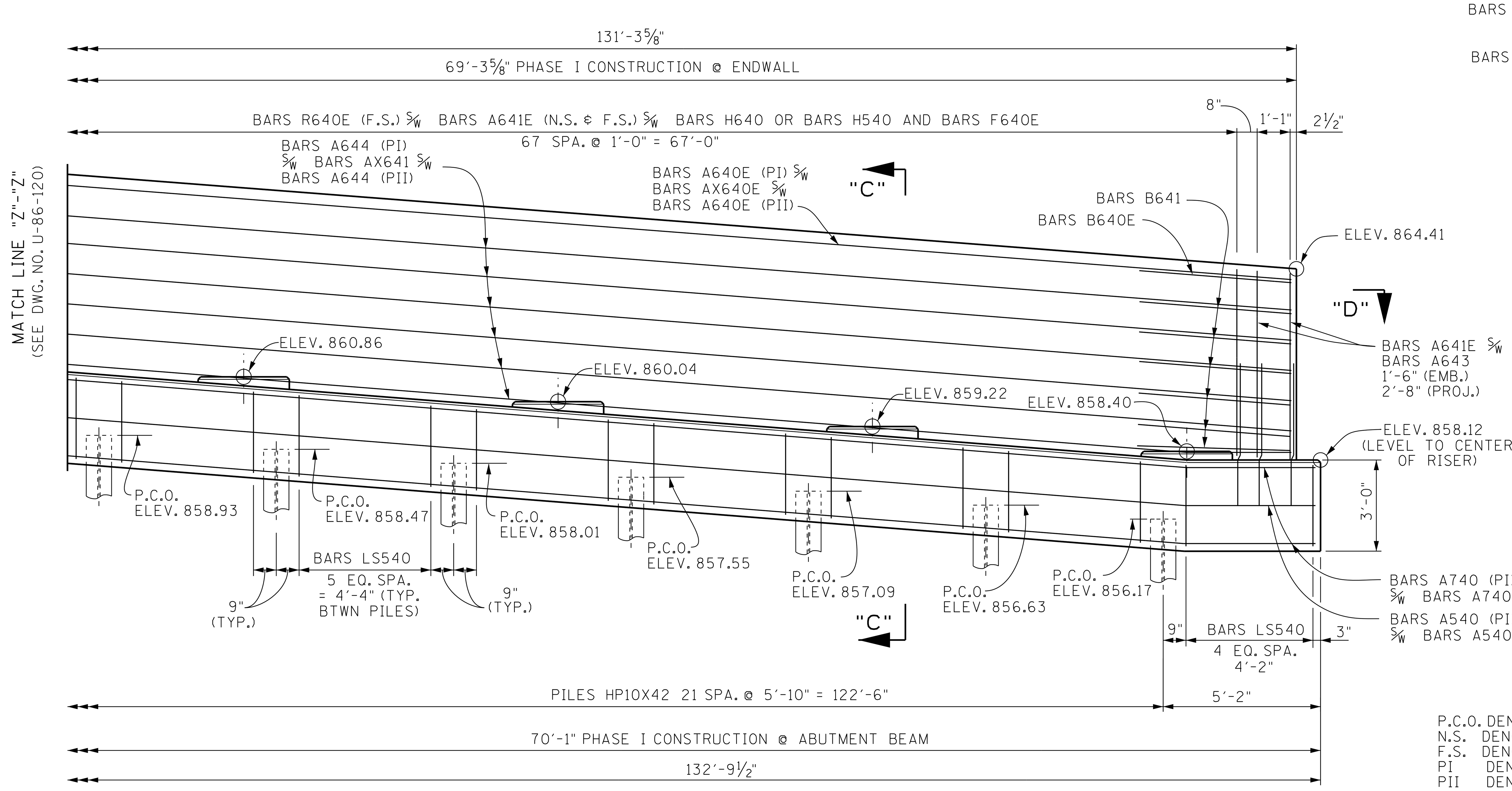

ELEVATION

(LOOKING BACK ON SURVEY)

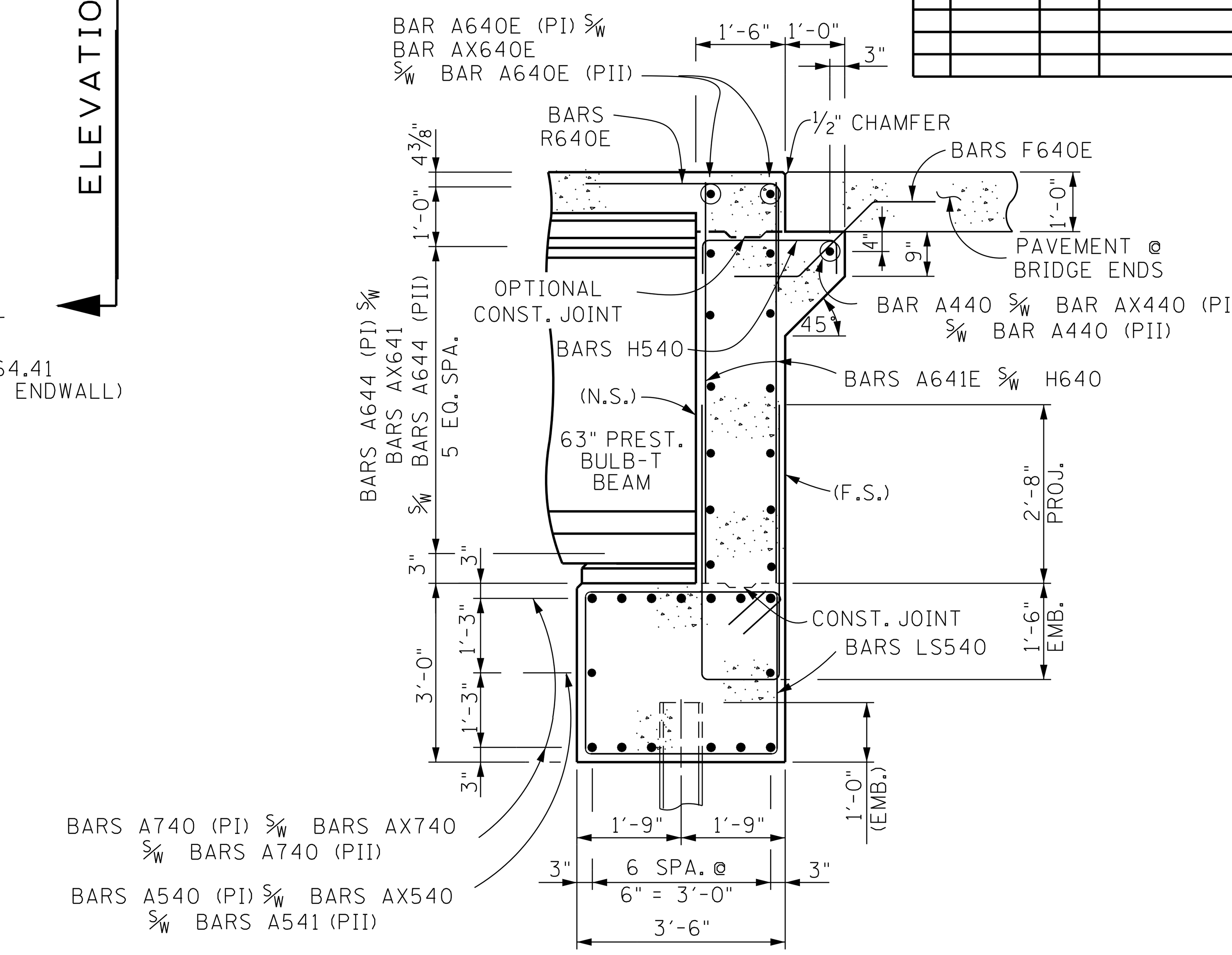

SECTION "C"-"C"

NOTE: FOR ELEVATIONS "A"-"A", SEE DWG. NO. U-86-123

NOTE: FOR SECTION "D"-"D" SEE DWG. NO. U-86-122

P.C.O. DENOTES: PILE CUT-OFF
N.S. DENOTES: NEAR SIDE
F.S. DENOTES: FAR SIDE
PI DENOTES: PHASE I
PII DENOTES: PHASE II

ADAM L. PRICE — STATE OF TENNESSEE — 04-10-2019

STATE OF TENNESSEE
DEPARTMENT OF TRANSPORTATION
BRIDGE NO. 2
1 ABUTMENT NO. 1 DETAILS
STATE ROUTE 115
OVER
STATE ROUTE 168
STATION 143+76.54
KNOX COUNTY
2018

DESIGNED BY	ADAM PRICE	DATE	08-15
DRAWN BY	JERRY W. SIMPSON	DATE	02-18
SUPERVISED BY	MARTINKO/HASTINGS	DATE	02-18
CHECKED BY	DAWOD ABDULLAH	DATE	11-17

CORRECT ______ ENGINEER OF STRUCTURES

U-86-121

AB1180.DGN

CONST. NO. 47026-3281-14

PROJECT NO.	YEAR	SHEET NO.
STP-NH-115(27)	2018	

REVISIONS

NO.	DATE	BY	BRIEF DESCRIPTION
1	4-5-19	ALP	GENERAL REVISION

N.S. DENOTES: NEAR SIDE
F.S. DENOTES: FAR SIDE
PI DENOTES: PHASE I
PII DENOTES: PHASE II

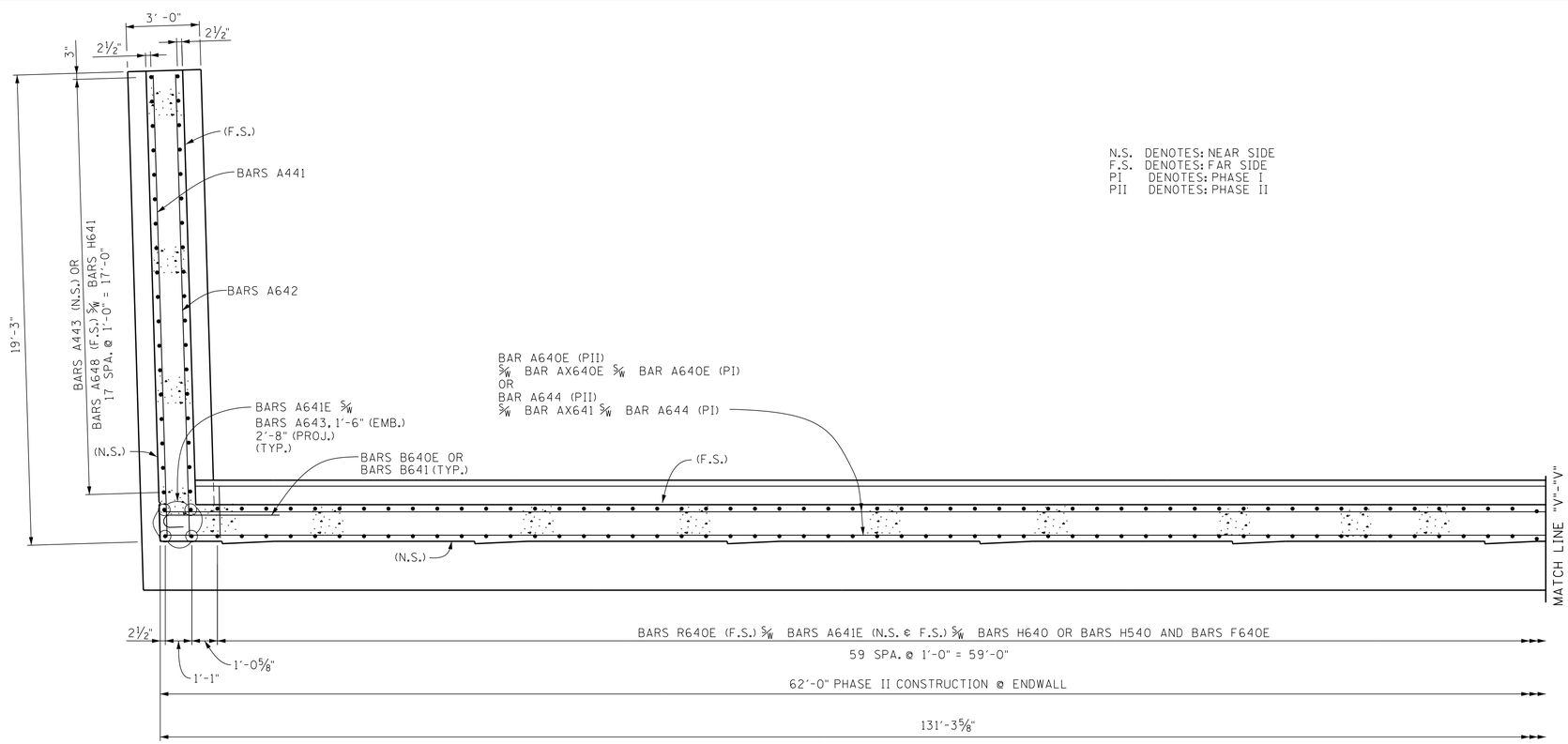

SECTION "D"-"D"

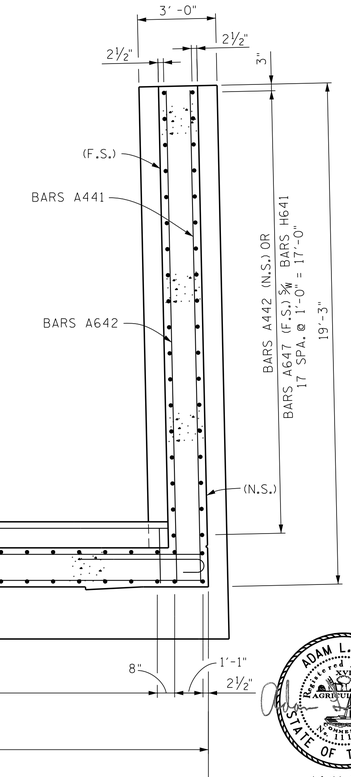

SECTION "D"-"D"

ADAM L. PRICE
LICENSED PROFESSIONAL ENGINEER
STATE OF TENNESSEE

04-10-2019

STATE OF TENNESSEE
DEPARTMENT OF TRANSPORTATION

BRIDGE NO. 2
⚠1 ABUTMENT NO. 1 DETAILS
STATE ROUTE 115
OVER
STATE ROUTE 168
STATION 143+76.54
KNOX COUNTY
2018

CORRECT _____
ENGINEER OF STRUCTURES

DESIGNED BY ADAM PRICE DATE 08-15
DRAWN BY JERRY W. SIMPSON DATE 02-18
SUPERVISED BY MARTINKO/HASTINGS DATE 02-18
CHECKED BY DAWOD ABDULLAH DATE 11-17

U-86-122

4/4/2019
jsimpson
C:\Users\jsimpson\Desktop\Regions 1 and 2\Jerry Simpson\1180-rx 02021321-sta 143+76.54-sr 115 over sr 168 - knox co\AB1180.dgn

AB1180.DGN

CONST. NO.	47026-3281-14	
PROJECT NO.	YEAR	SHEET NO.
STP-NH-115(27)	2018	

REVISIONS

NO.	DATE	BY	BRIEF DESCRIPTION
1	4-5-19	ALP	GENERAL REVISION

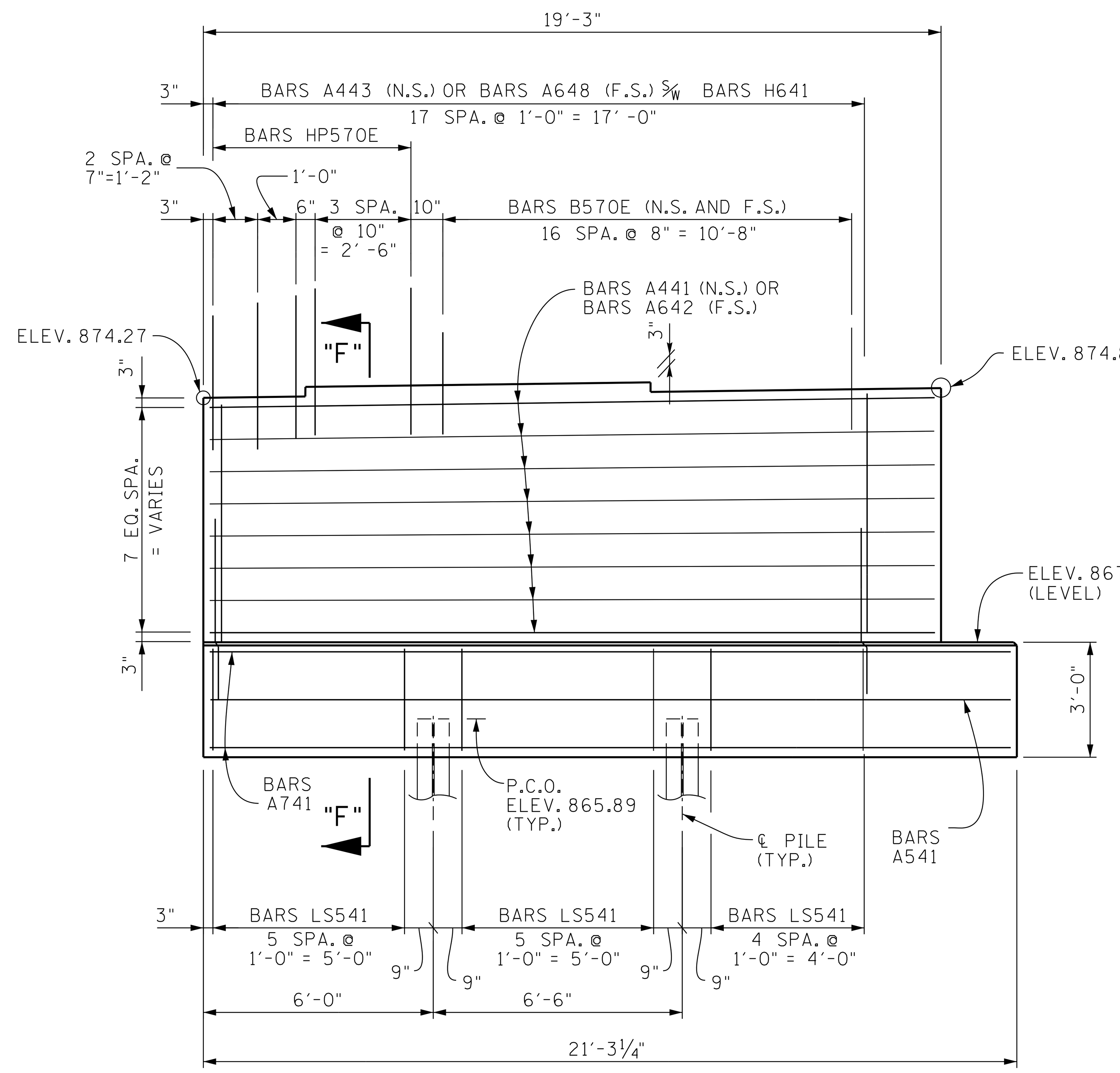

ELEVATION "B" - "B"

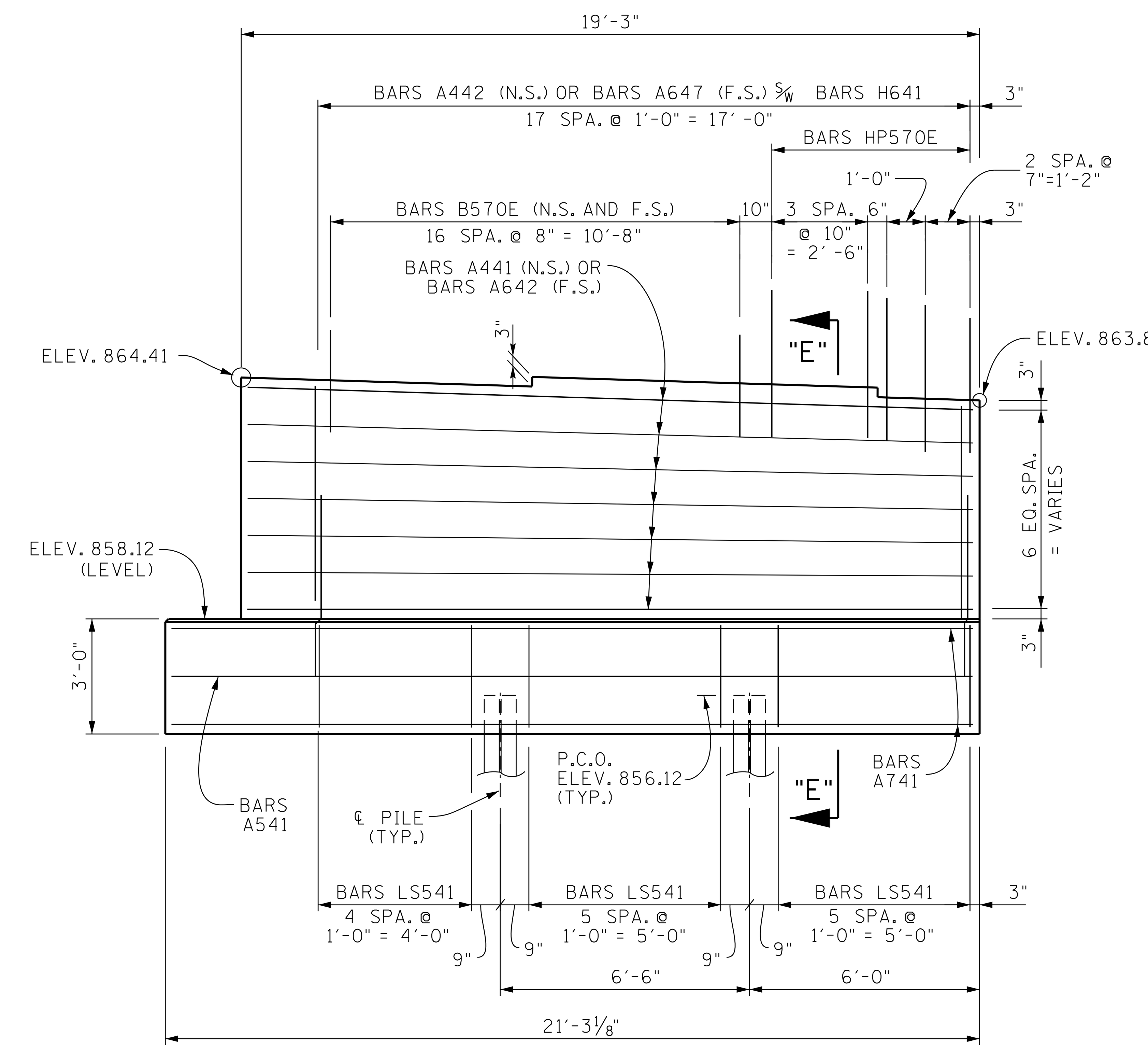

ELEVATION "A" - "A"

P.C.O. DENOTES: PILE CUT-OFF
N.S. DENOTES: NEAR SIDE
F.S. DENOTES: FAR SIDE

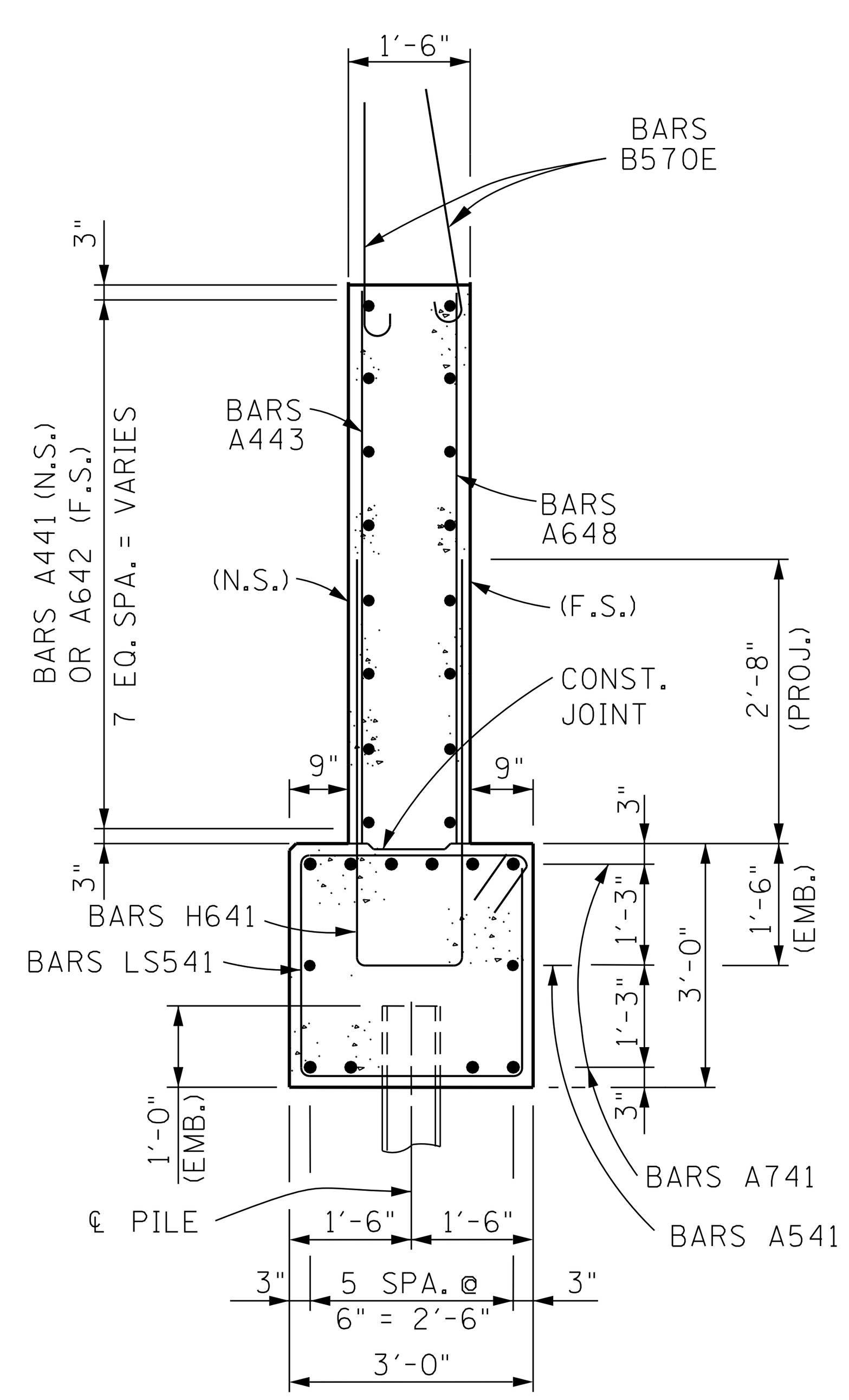

SECTION "F"-"F"

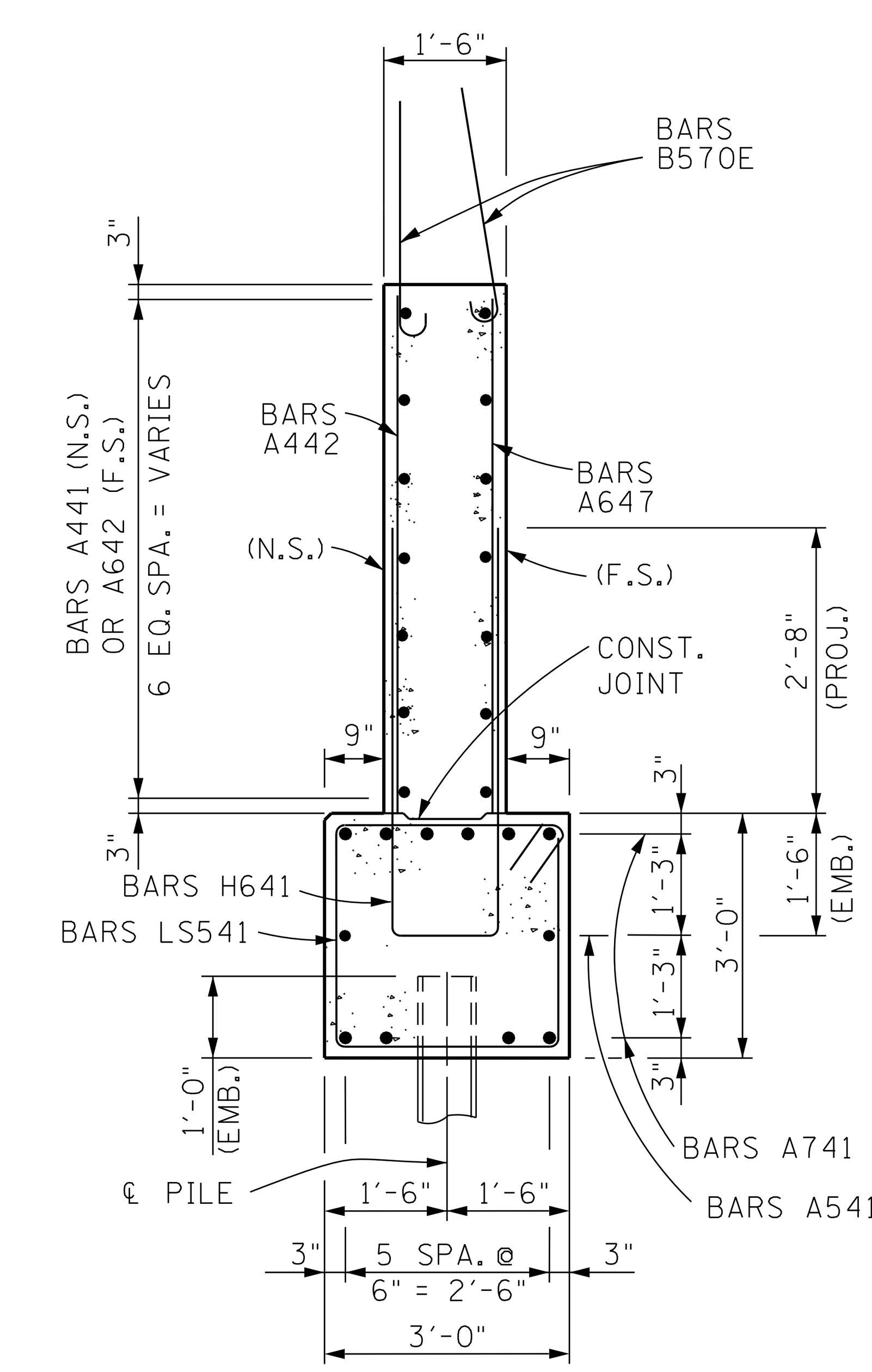

SECTION "E"-"E"

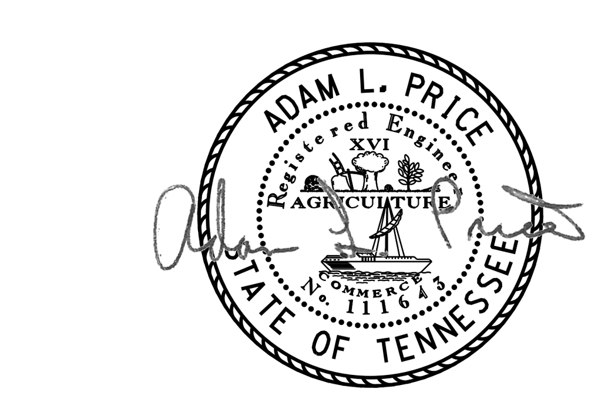

04-10-2019

STATE OF TENNESSEE
DEPARTMENT OF TRANSPORTATION

BRIDGE NO. 2
(1) ABUTMENT NO. 1 DETAILS
STATE ROUTE 115
OVER
STATE ROUTE 168
STATION 143+76.54
KNOX COUNTY
2018

DESIGNED BY	ADAM PRICE	DATE	08-15
DRAWN BY	JERRY W. SIMPSON	DATE	02-18
SUPERVISED BY	MARTINKO/HASTINGS	DATE	02-18
CHECKED BY	DAWOD ABDULLAH	DATE	11-17

CORRECT ______ ENGINEER OF STRUCTURES

U-86-123

AB1180.DGN

CONST. NO.	47026-3281-14	
PROJECT NO.	YEAR	SHEET NO.
STP-NH-115(27)	2018	

REVISIONS

NO.	DATE	BY	BRIEF DESCRIPTION
1	4-5-19	ALP	GENERAL REVISION

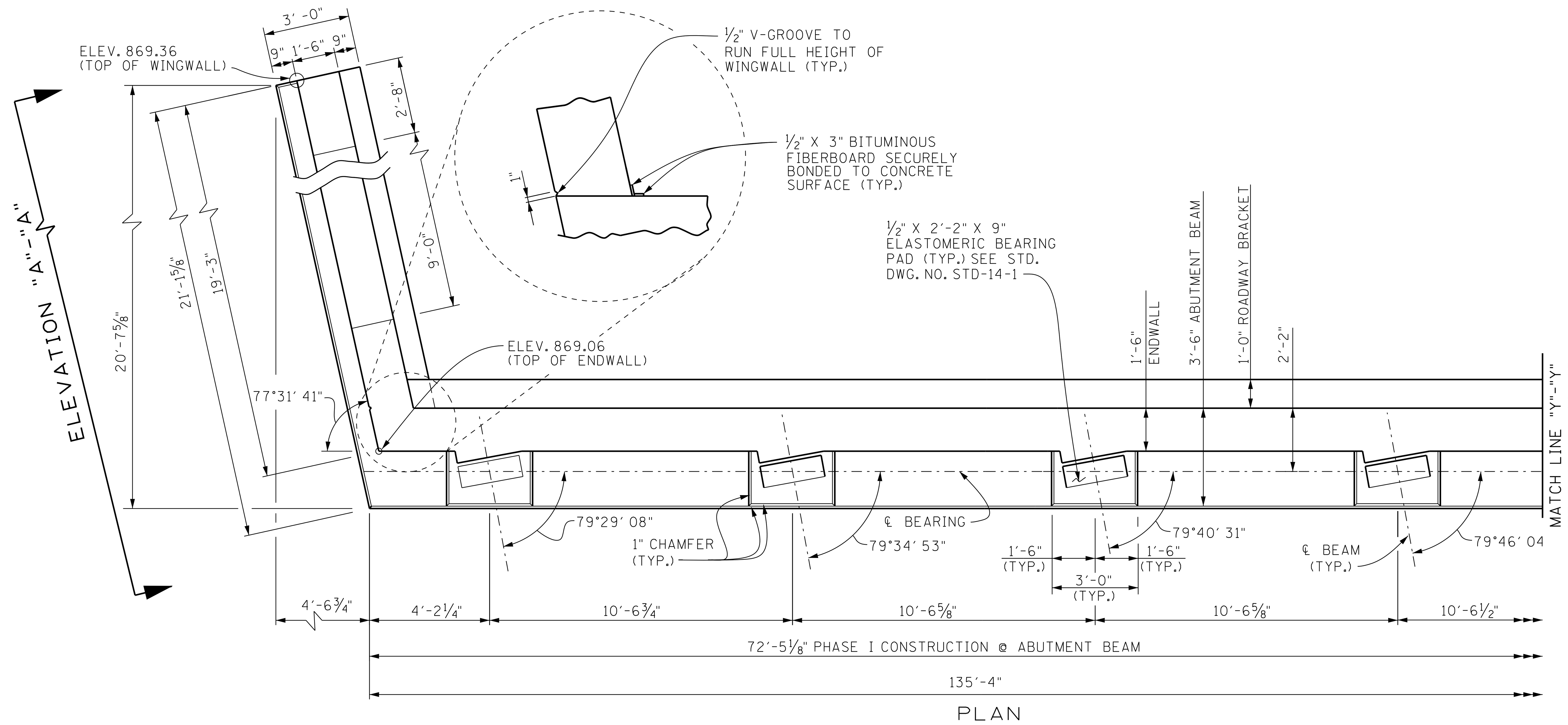

PLAN

GENERAL NOTES

NOTE: RISER BLOCKS SHALL BE POURED MONOLITHICALLY WITH ABUTMENT BEAM.

NOTE: WHEN POURING WINGWALLS, PROVISIONS SHALL BE MADE FOR SETTING REINFORCING STEEL FOR WINGPOSTS AND PARAPETS. FOR DETAILS OF WINGPOSTS AND PARAPET, SEE STANDARD DRAWING NO. STD-1-1SS.

NOTE: ELASTOMERIC PADS SHALL BE IN PLACE A MINIMUM OF ONE DAY BEFORE BEING DISTURBED BY SETTING BEAMS. PLACE RUBBER BONDING CEMENT IN SUCH A WAY THAT VISIBLE CONCRETE SURFACES WILL NOT BE STAINED.

NOTE: NOT LESS THAN HALF OF THE SLAB IN THE END SPAN SHALL BE POURED PRIOR TO, OR CONCURRENTLY WITH, PLACEMENT OF ANY PART OF THE ABUTMENT BACKWALL. AT LEAST THE TOP 12 INCHES OF THE BACKWALL SHALL BE POURED CONCURRENTLY WITH THE END OF SLAB.

NOTE: COST OF BRIDGE RAIL AND POST IS TO BE INCLUDED IN THE UNIT PRICE BID FOR THE BRIDGE RAIL SYSTEM.

NOTE: WINGBEAM PILES SHALL BE DRIVEN TO THE PLANS TIP ELEVATION OR REFUSAL. SEISMIC ATTACHMENT IS NOT REQUIRED FOR WING BEAM PILES.

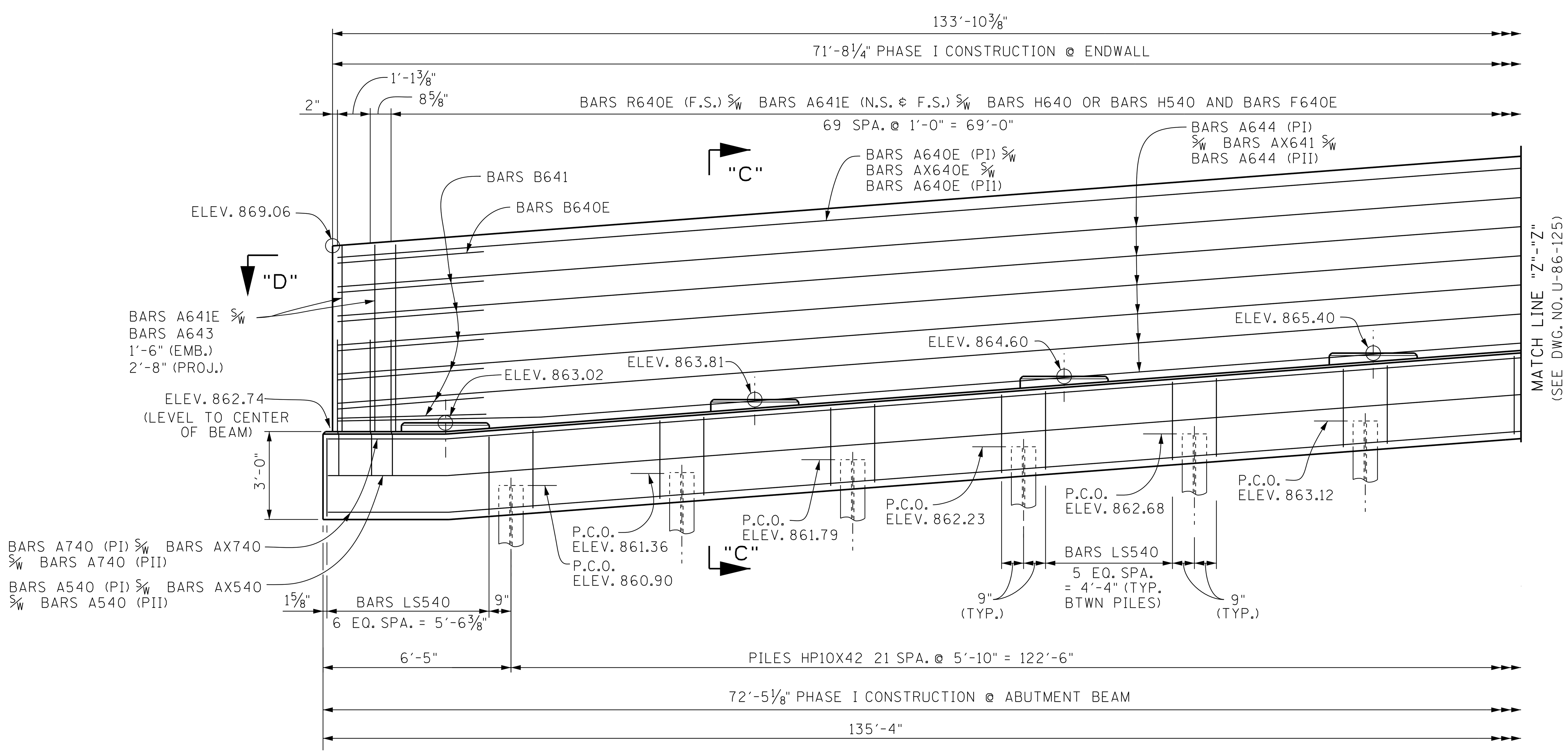

ELEVATION

(LOOKING FORWARD ON SURVEY)

ESTIMATED QUANTITIES		
CONCRETE CLASS "A"	EPOXY COATED REINFORCING STEEL	STEEL BAR REINFORCEMENT (BRIDGES)
CY.	LB.	LB.
132	5,176	13,960

NOTE: FOR ELEVATIONS "A"-"A" SEE DWG. NO. U-86-128

NOTE: FOR SECTION "C"-"C" SEE DWG. NO. U-86-126

NOTE: FOR SECTION "D"-"D" SEE DWG. NO. U-86-127

ADAM L. PRICE
04-10-2019

P.C.O. DENOTES: PILE CUT-OFF
N.S. DENOTES: NEAR SIDE
F.S. DENOTES: FAR SIDE
PI DENOTES: PHASE I
PII DENOTES: PHASE II

STATE OF TENNESSEE
DEPARTMENT OF TRANSPORTATION
BRIDGE NO. 2
ABUTMENT NO. 2
STATE ROUTE 115
OVER
STATE ROUTE 168
STATION 143+76.54
KNOX COUNTY
2018

DESIGNED BY	ADAM PRICE	DATE	08-15
DRAWN BY	JERRY W. SIMPSON	DATE	02-18
SUPERVISED BY	MARTINKO/HASTINGS	DATE	02-18
CHECKED BY	DAWOD ABDULLAH	DATE	11-17

CORRECT ________ ENGINEER OF STRUCTURES

U-86-124

AB1180.DGN

CONST. NO.	47026-3281-14	
PROJECT NO.	YEAR	SHEET NO.
STP-NH-115(27)	2018	

REVISIONS

NO.	DATE	BY	BRIEF DESCRIPTION
1	4-5-19	ALP	GENERAL REVISION

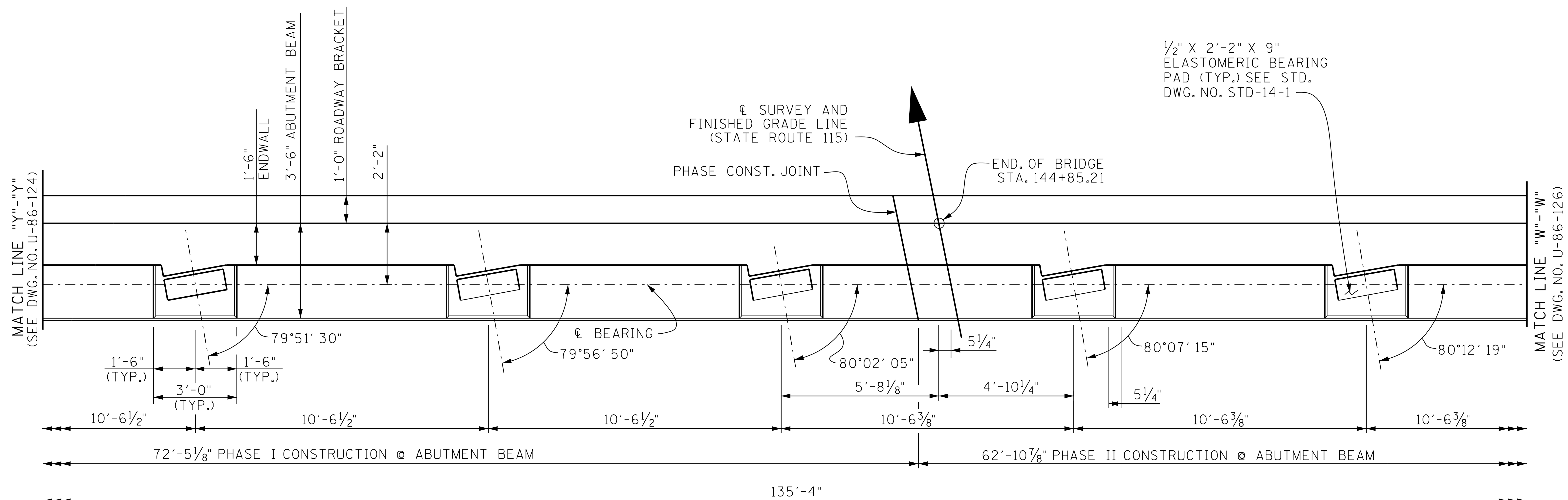

PLAN

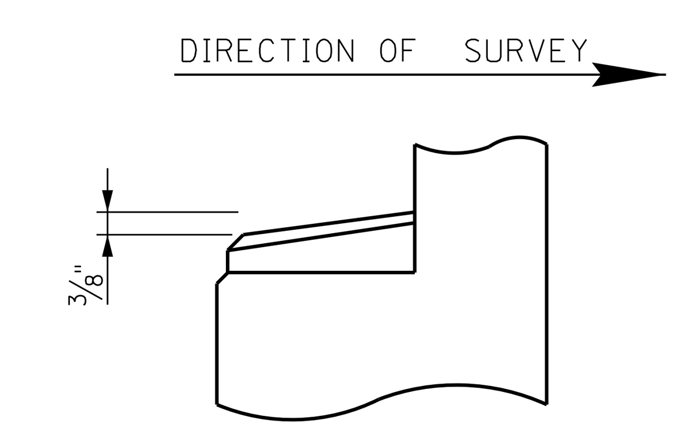

RISER BLOCK SLOPE DETAILS

NOTE: RISER BLOCK BEARING PAD SURFACES TO CONFORM TO BOTTOM OF BEAM GRADE.

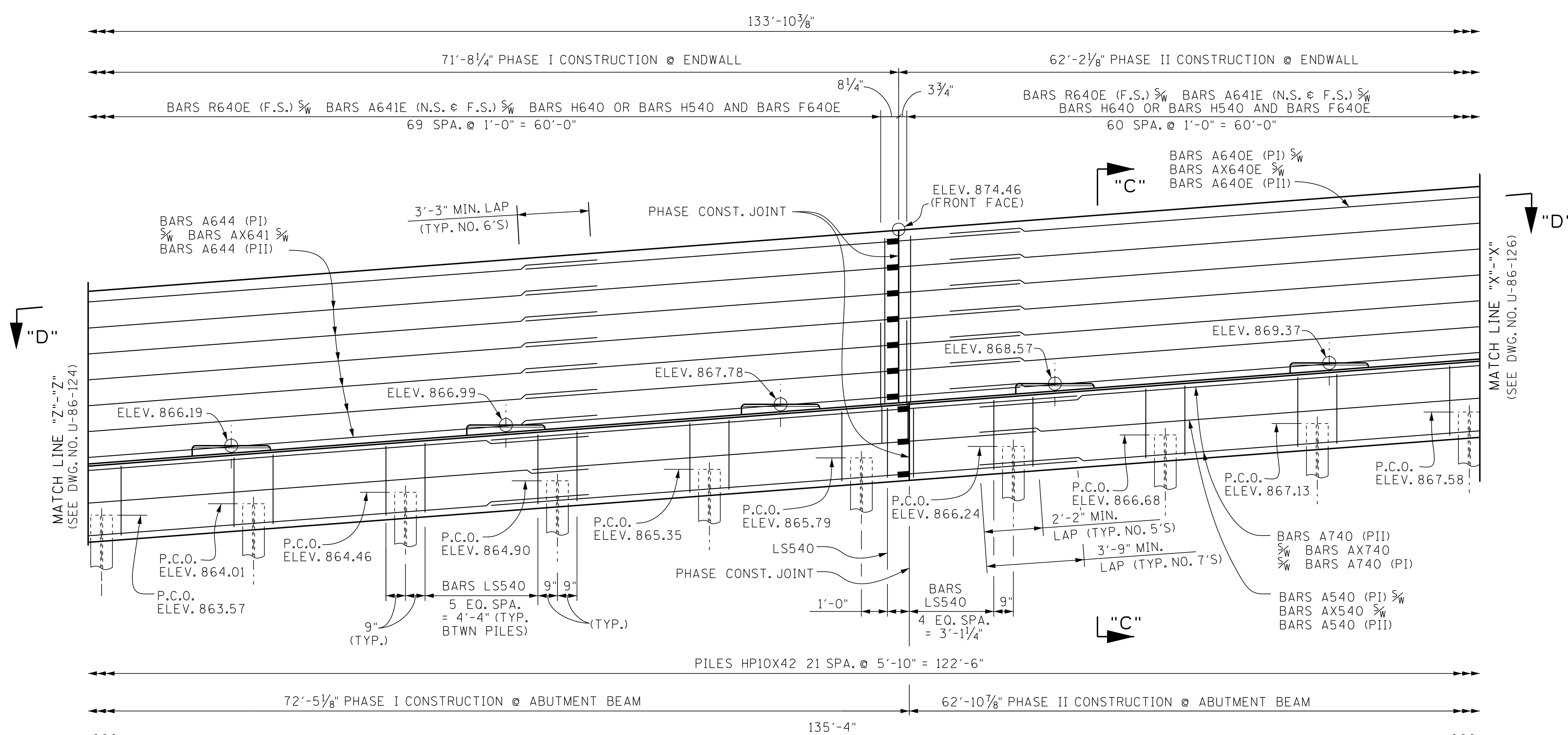

ELEVATION

(LOOKING BACKWARD ON SURVEY)

NOTE: FOR SECTION "C"-"C" SEE DWG. NO. U-86-126

NOTE: FOR SECTION "D"-"D" SEE DWG. NO. U-86-127

P.C.O. DENOTES: PILE CUT-OFF
N.S. DENOTES: NEAR SIDE
F.S. DENOTES: FAR SIDE
PI DENOTES: PHASE I
PII DENOTES: PHASE II

ADAM L. PRICE — STATE OF TENNESSEE — AGRICULTURE — COMMERCE — Registered Engineer

04-10-2019

STATE OF TENNESSEE
DEPARTMENT OF TRANSPORTATION

BRIDGE NO. 2
(1) ABUTMENT NO. 2 DETAILS
STATE ROUTE 115
OVER
STATE ROUTE 168
STATION 143+76.54
KNOX COUNTY
2018

CORRECT ______ ENGINEER OF STRUCTURES

DESIGNED BY	ADAM PRICE	DATE	08-15
DRAWN BY	JERRY W. SIMPSON	DATE	02-18
SUPERVISED BY	MARTINKO/HASTINGS	DATE	02-18
CHECKED BY	DAWOD ABDULLAH	DATE	11-17

U-86-125

AB1180.DGN

CONST. NO.	47026-3281-14	
PROJECT NO.	YEAR	SHEET NO.
STP-NH-115(27)	2018	

REVISIONS

NO.	DATE	BY	BRIEF DESCRIPTION
1	4-5-19	ALP	GENERAL REVISION

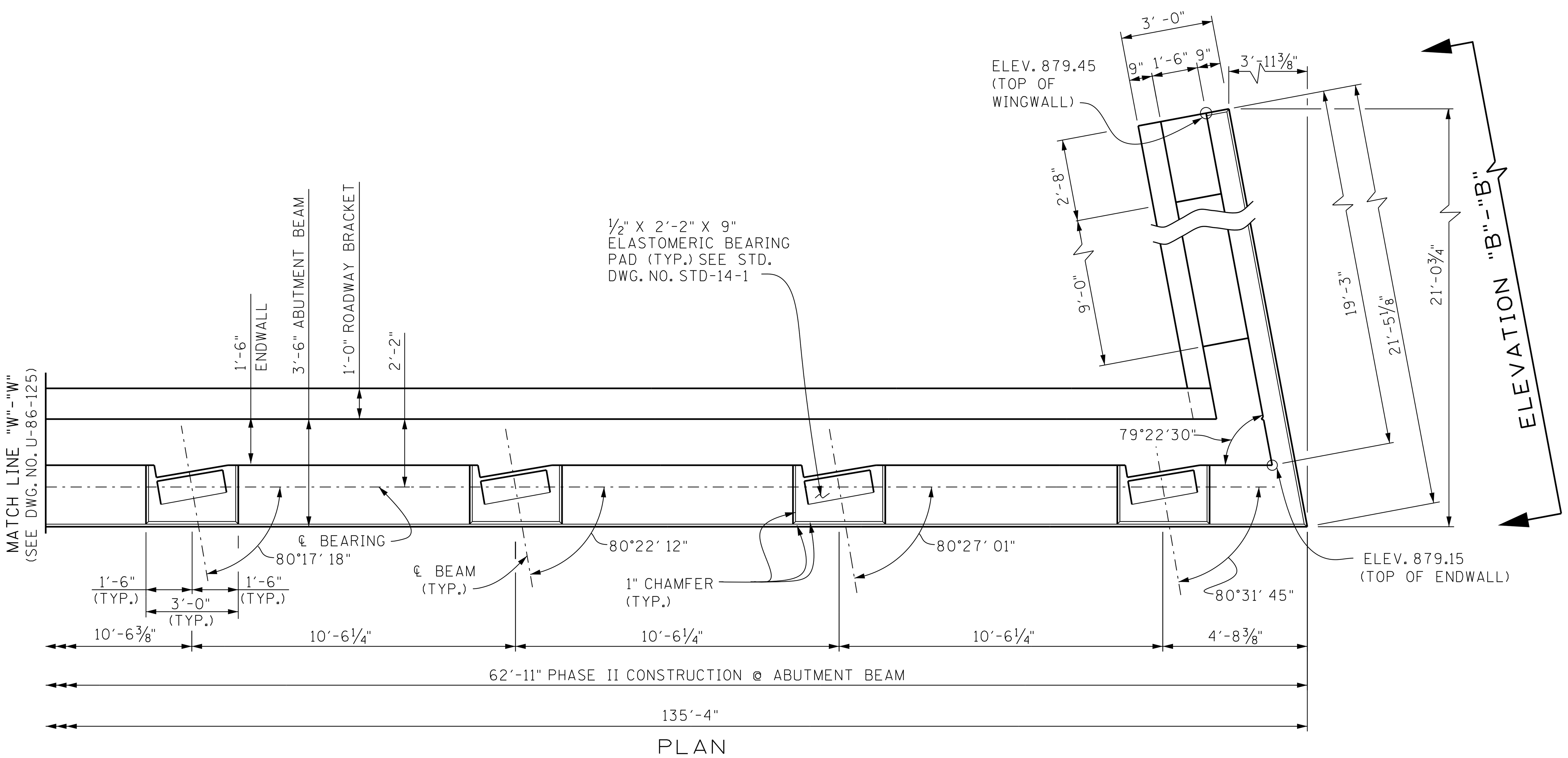

PLAN

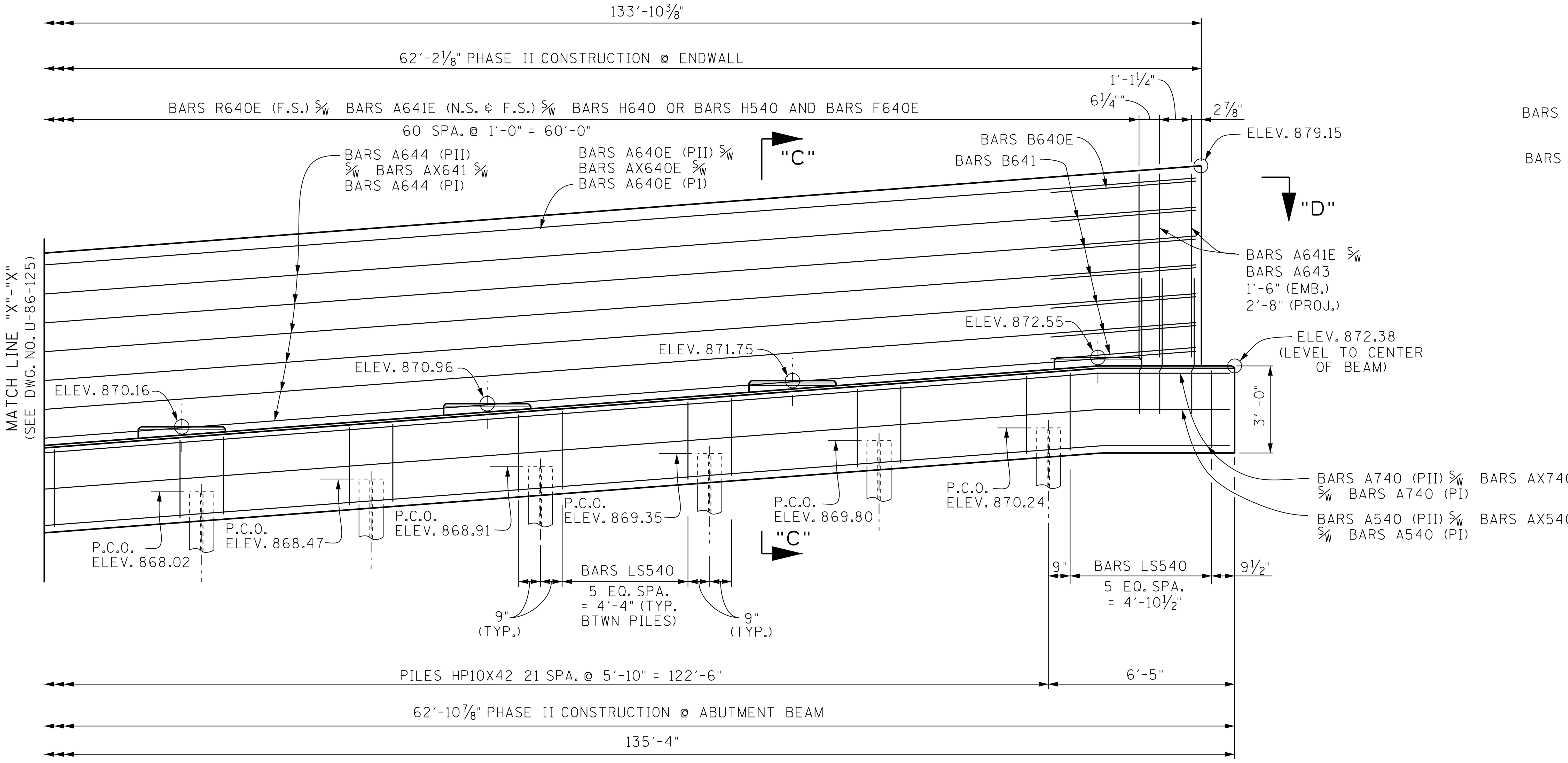

ELEVATION

(LOOKING BACKWARD ON SURVEY)

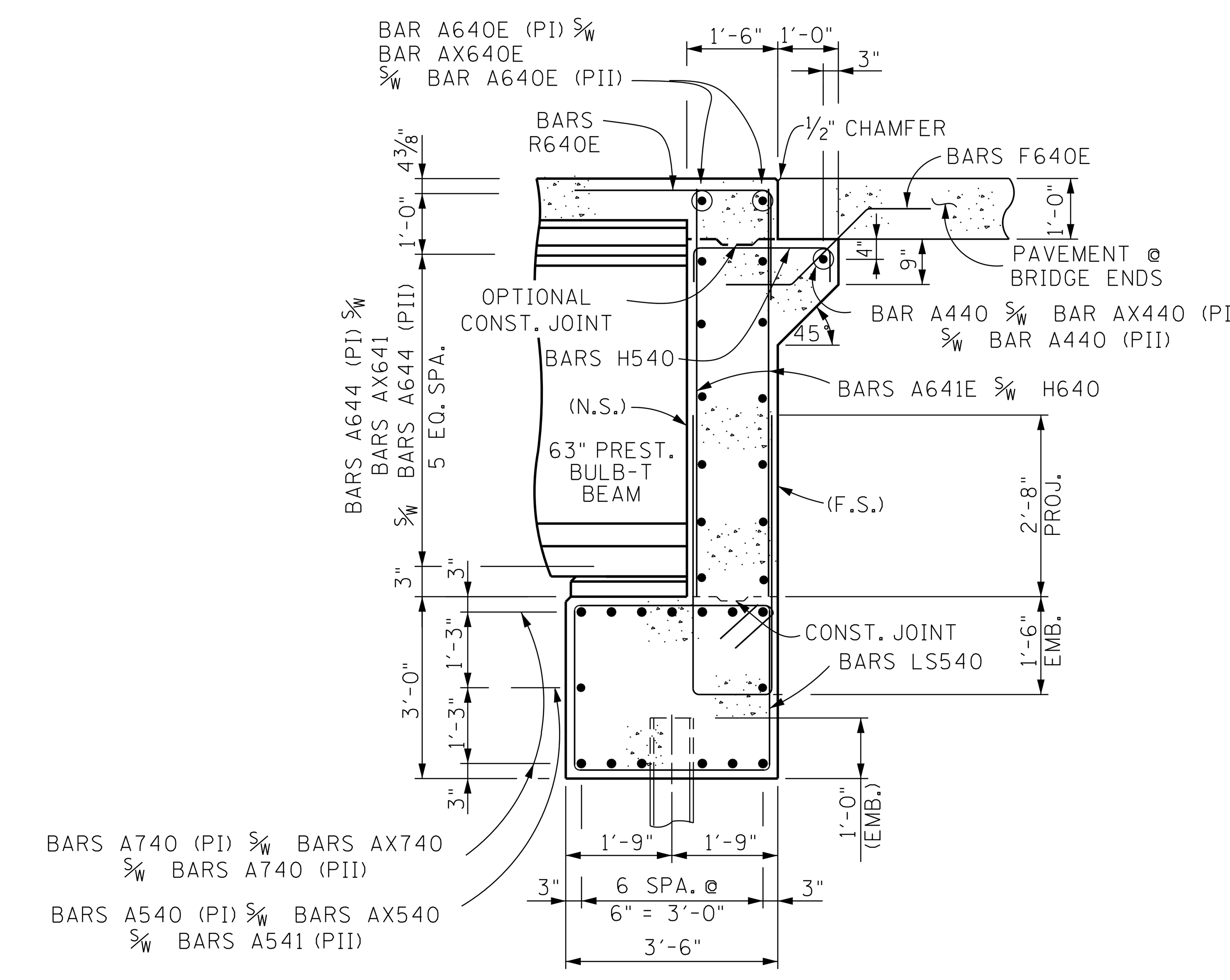

SECTION "C"-"C"

NOTE: FOR ELEVATIONS "B"-"B" SEE DWG. NO. U-86-128

NOTE: FOR SECTION "D"-"D" SEE DWG. NO. U-86-127

P.C.O. DENOTES: PILE CUT-OFF
N.S. DENOTES: NEAR SIDE
F.S. DENOTES: FAR SIDE
PI DENOTES: PHASE I
PII DENOTES: PHASE II

ADAM L. PRICE — Registered Engineer — No. 117 — AGRICULTURE COMMERCE — STATE OF TENNESSEE

04-10-2019

STATE OF TENNESSEE
DEPARTMENT OF TRANSPORTATION

BRIDGE NO. 2
1 ABUTMENT NO. 2 DETAILS
STATE ROUTE 115
OVER
STATE ROUTE 168
STATION 143+76.54
KNOX COUNTY
2018

DESIGNED BY	ADAM PRICE	DATE	08-15
DRAWN BY	JERRY W. SIMPSON	DATE	02-18
SUPERVISED BY	MARTINKO/HASTINGS	DATE	02-18
CHECKED BY	DAWOD ABDULLAH	DATE	11-17

CORRECT Ted A. Kniazewycz
ENGINEER OF STRUCTURES

U-86-126

AB1180.DGN

CONST. NO. 47026-3281-14

PROJECT NO.	YEAR	SHEET NO.
STP-NH-115(27)	2018	

REVISIONS

NO.	DATE	BY	BRIEF DESCRIPTION
1	4-5-19	ALP	GENERAL REVISION

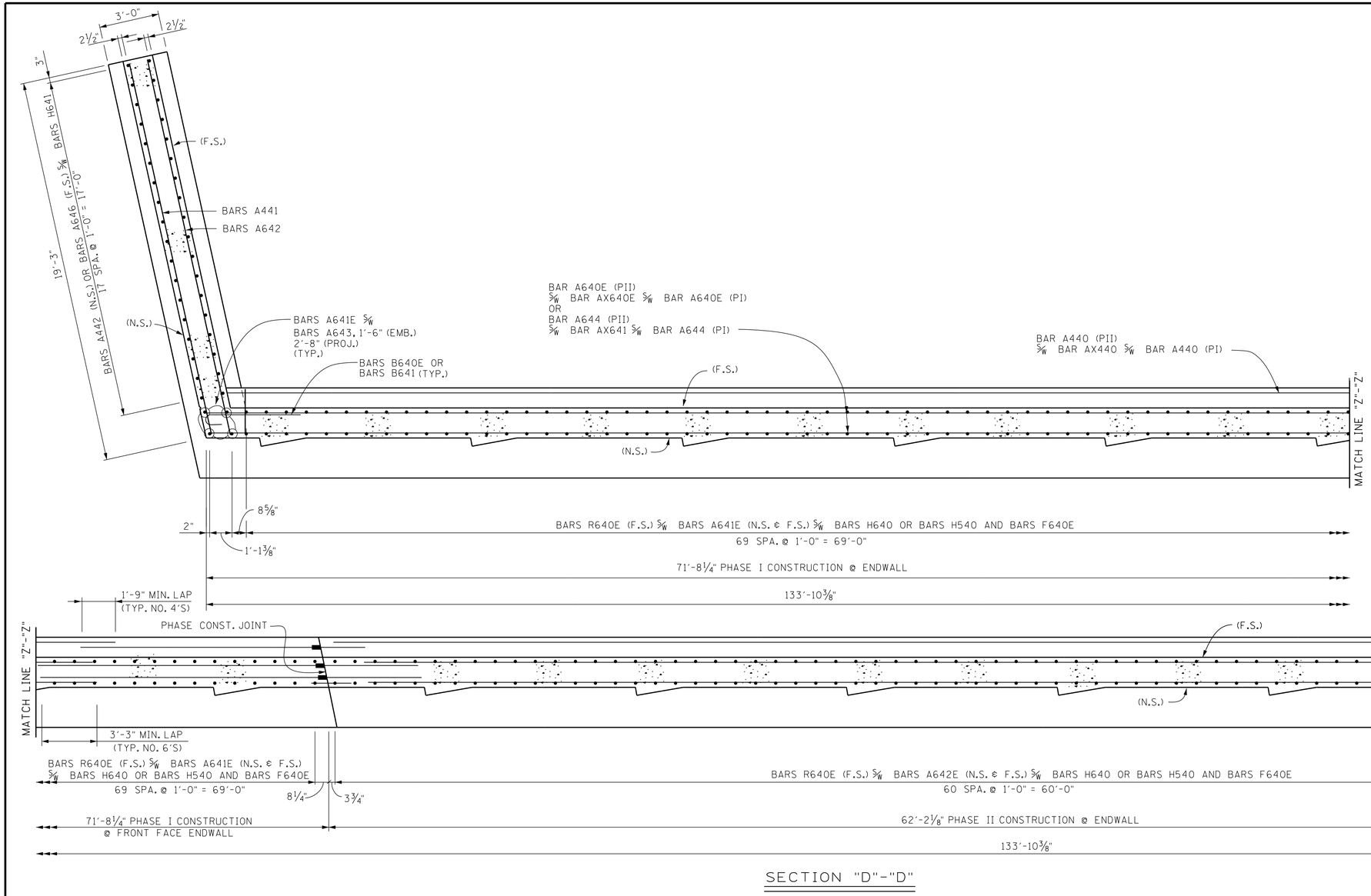

SECTION "D"-"D"

ADAM L. PRICE
LICENSED PROFESSIONAL ENGINEER
AGRICULTURE
111
STATE OF TENNESSEE

04-10-2019

STATE OF TENNESSEE
DEPARTMENT OF TRANSPORTATION

BRIDGE NO. 2
⚠1 ABUTMENT NO. 2 DETAILS
STATE ROUTE 115
OVER
STATE ROUTE 168
STATION 143+76.54
KNOX COUNTY
2018

DESIGNED BY ADAM PRICE DATE 08-15
DRAWN BY JERRY W. SIMPSON DATE 02-18
SUPERVISED BY MARTINKO/HASTINGS DATE 02-18
CHECKED BY DAWOD ABDULLAH DATE 11-17

CORRECT Jed A. Kniazewycz
ENGINEER OF STRUCTURES

U-86-127

4/8/2019 Z:\Bridge Group Regions 1 and 2\Jerry Simpson\1180-14 0021232-sta 143+76.54-pr 115 over pr 168 - knox co\AB1180.dgn

AB1180.DGN

CONST. NO. 47026-3281-14		
PROJECT NO.	YEAR	SHEET NO.
STP-NH-115(27)	2018	

REVISIONS

NO.	DATE	BY	BRIEF DESCRIPTION
1	4-5-19	ALP	GENERAL REVISION

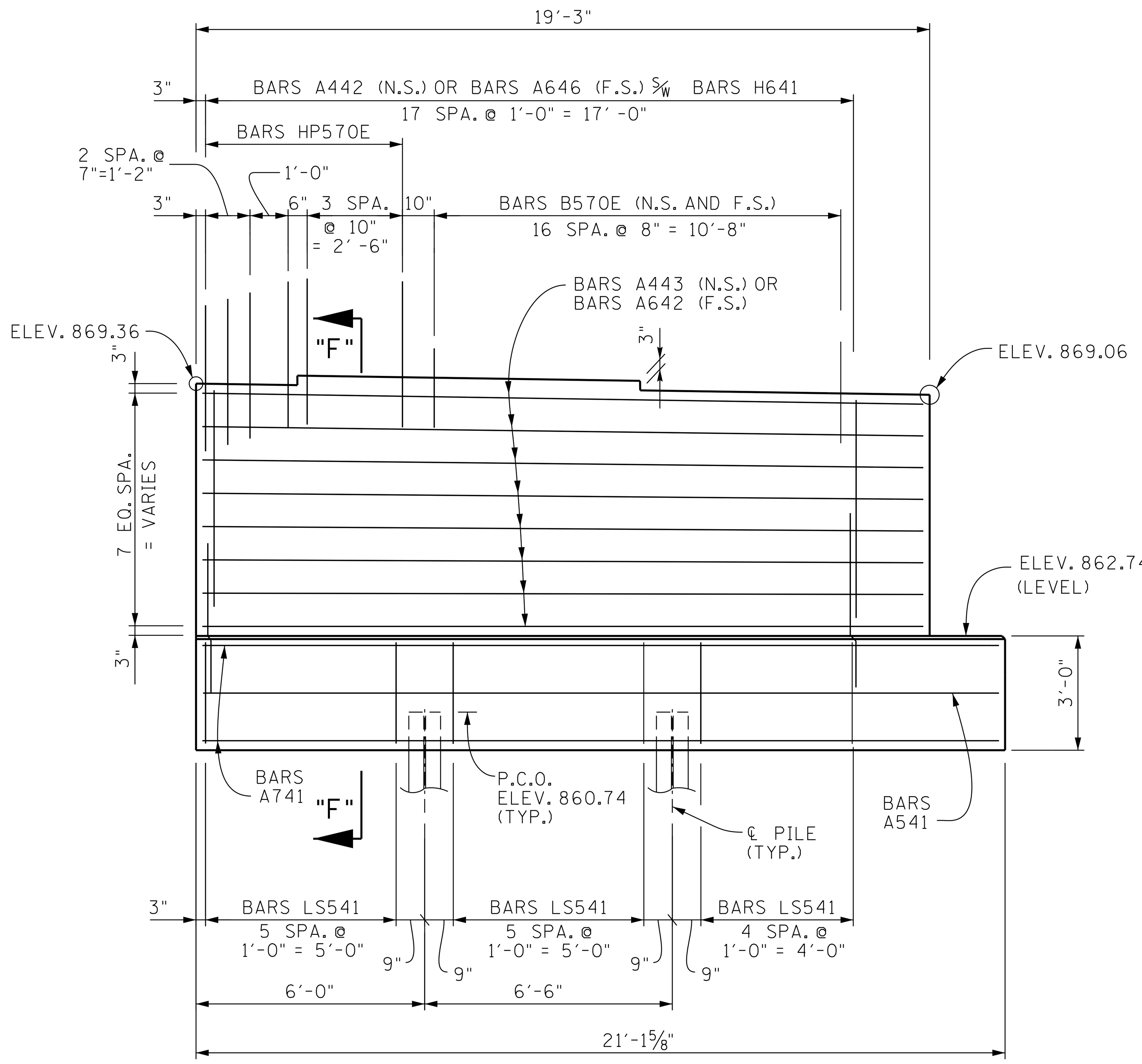

ELEVATION "A"-"A"

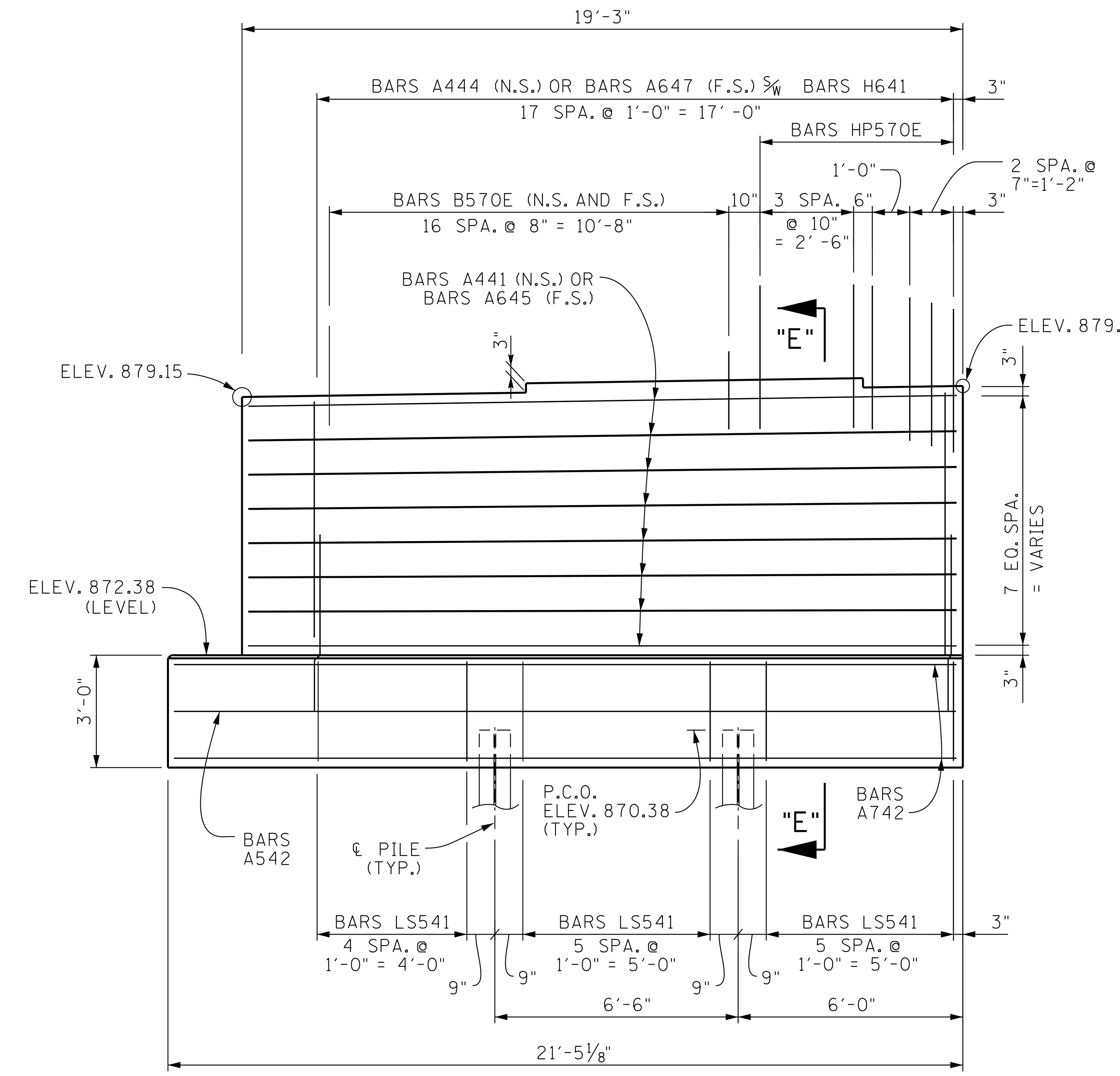

ELEVATION "B" - "B"

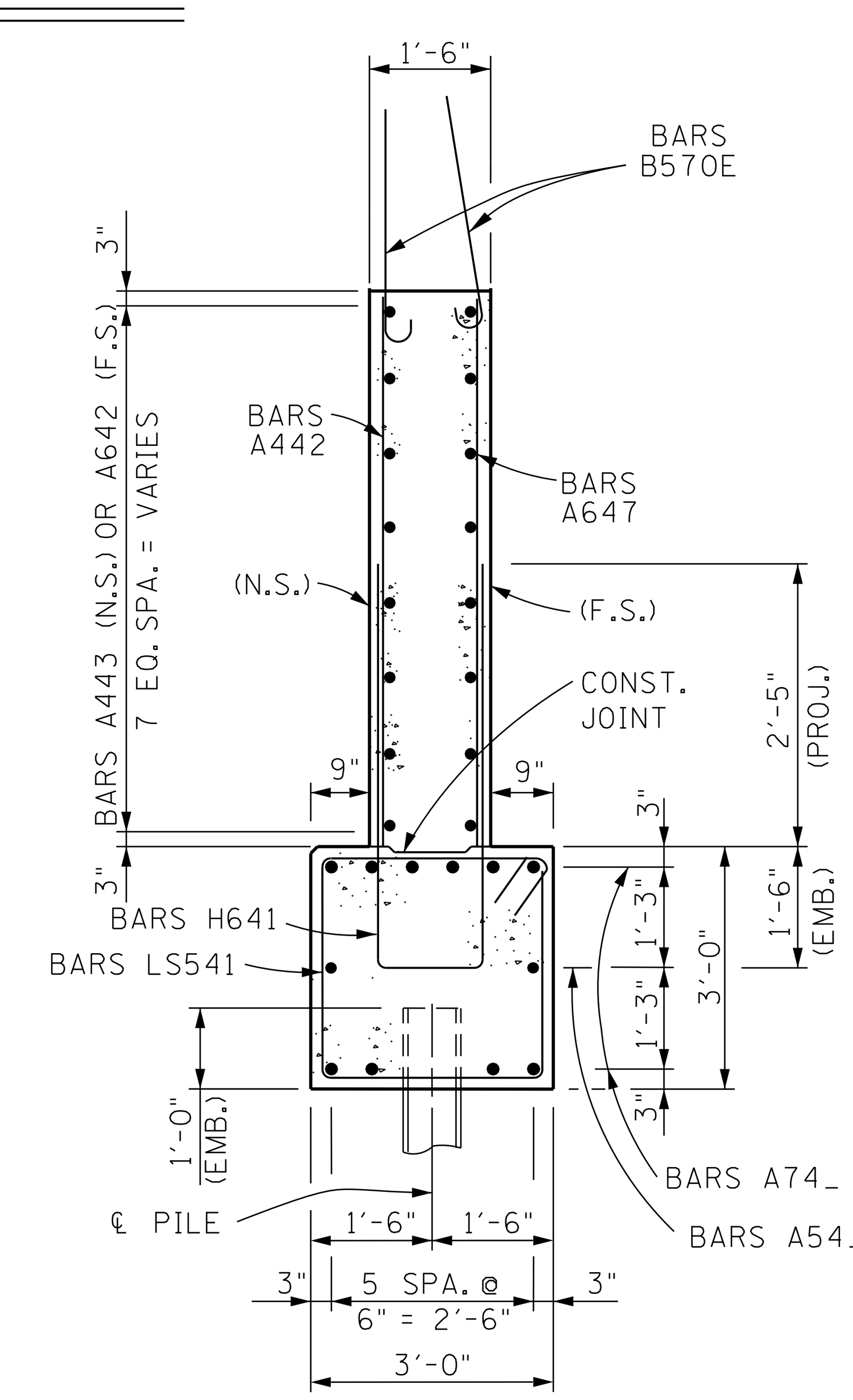

SECTION "F"-"F"

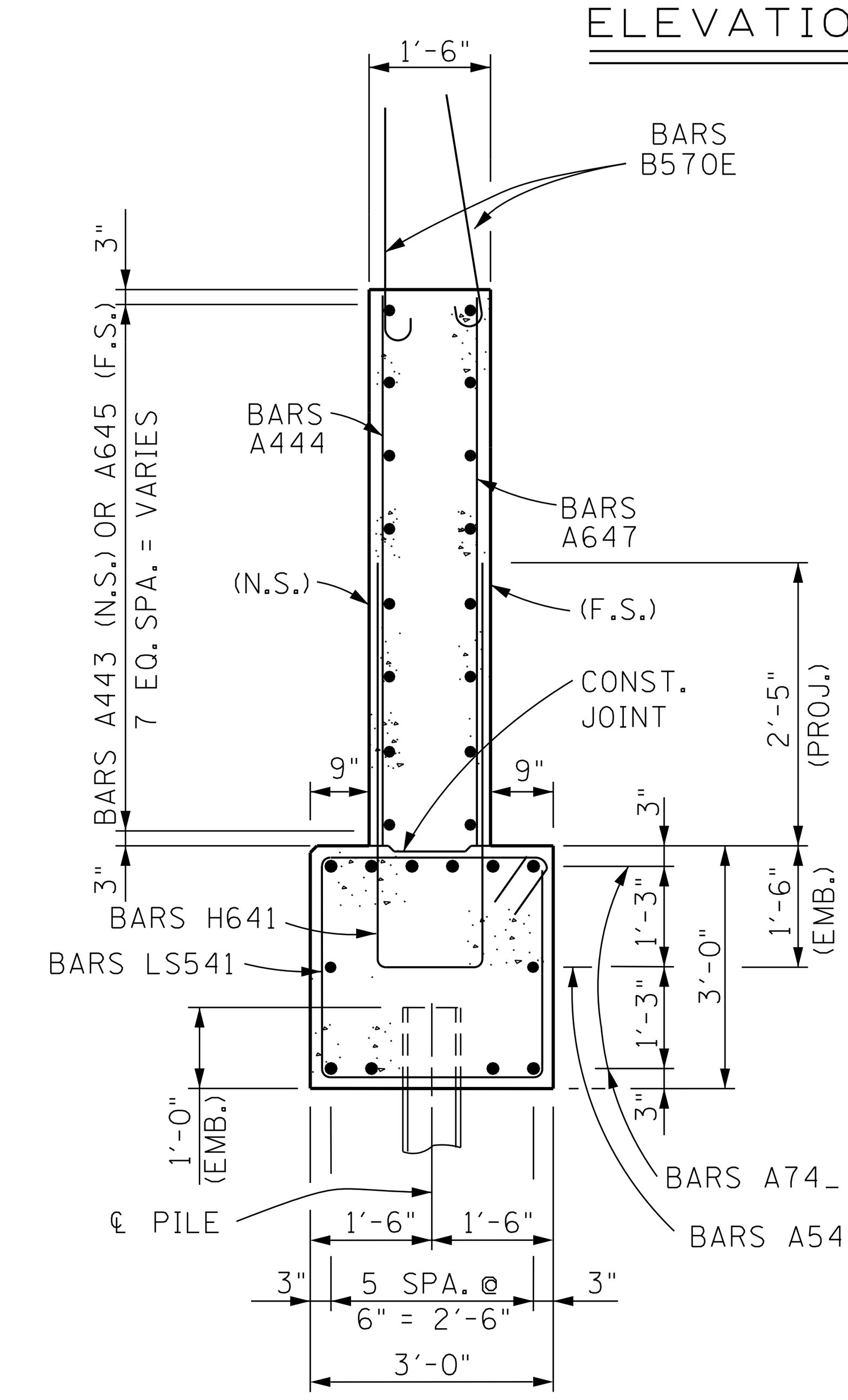

SECTION "E"-"E"

DESIGNED BY	ADAM PRICE	DATE	08-15
DRAWN BY	JERRY W. SIMPSON	DATE	02-18
SUPERVISED BY	MARTINKO/HASTINGS	DATE	02-18
CHECKED BY	DAWOD ABDULLAH	DATE	11-17

ADAM L. PRICE
04-10-2019

STATE OF TENNESSEE
DEPARTMENT OF TRANSPORTATION

BRIDGE NO. 2
(1) ABUTMENT NO. 2 DETAILS
STATE ROUTE 115
OVER
STATE ROUTE 168
STATION 143+76.54
KNOX COUNTY
2018

CORRECT
ENGINEER OF STRUCTURES

U-86-128

BP1180.DGN

CONST. NO.	47026-3281-14	
PROJECT NO.	YEAR	SHEET NO.
STP/NH-115(27)	2018	

REVISIONS

NO.	DATE	BY	BRIEF DESCRIPTION
1	4-5-19	ALP	GENERAL REVISIONS

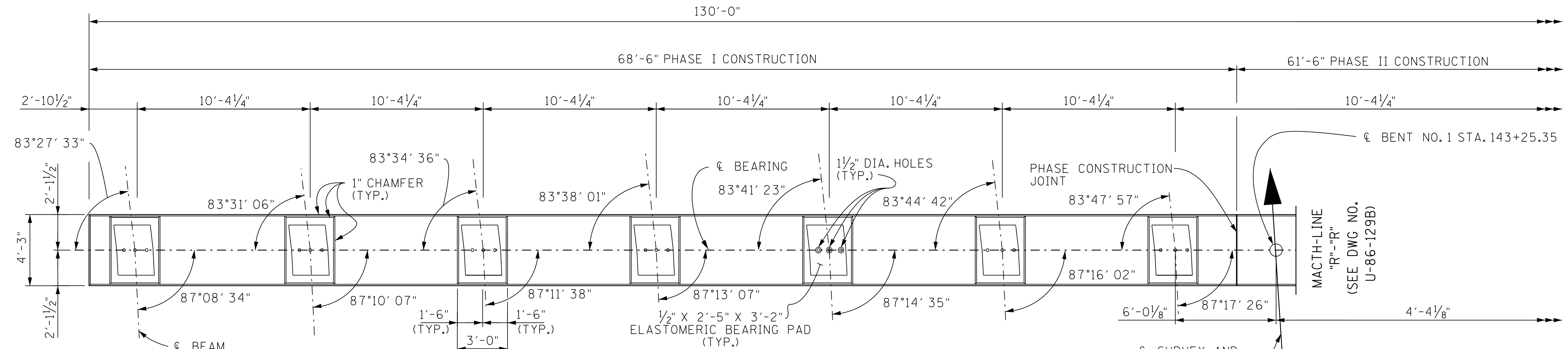

PLAN

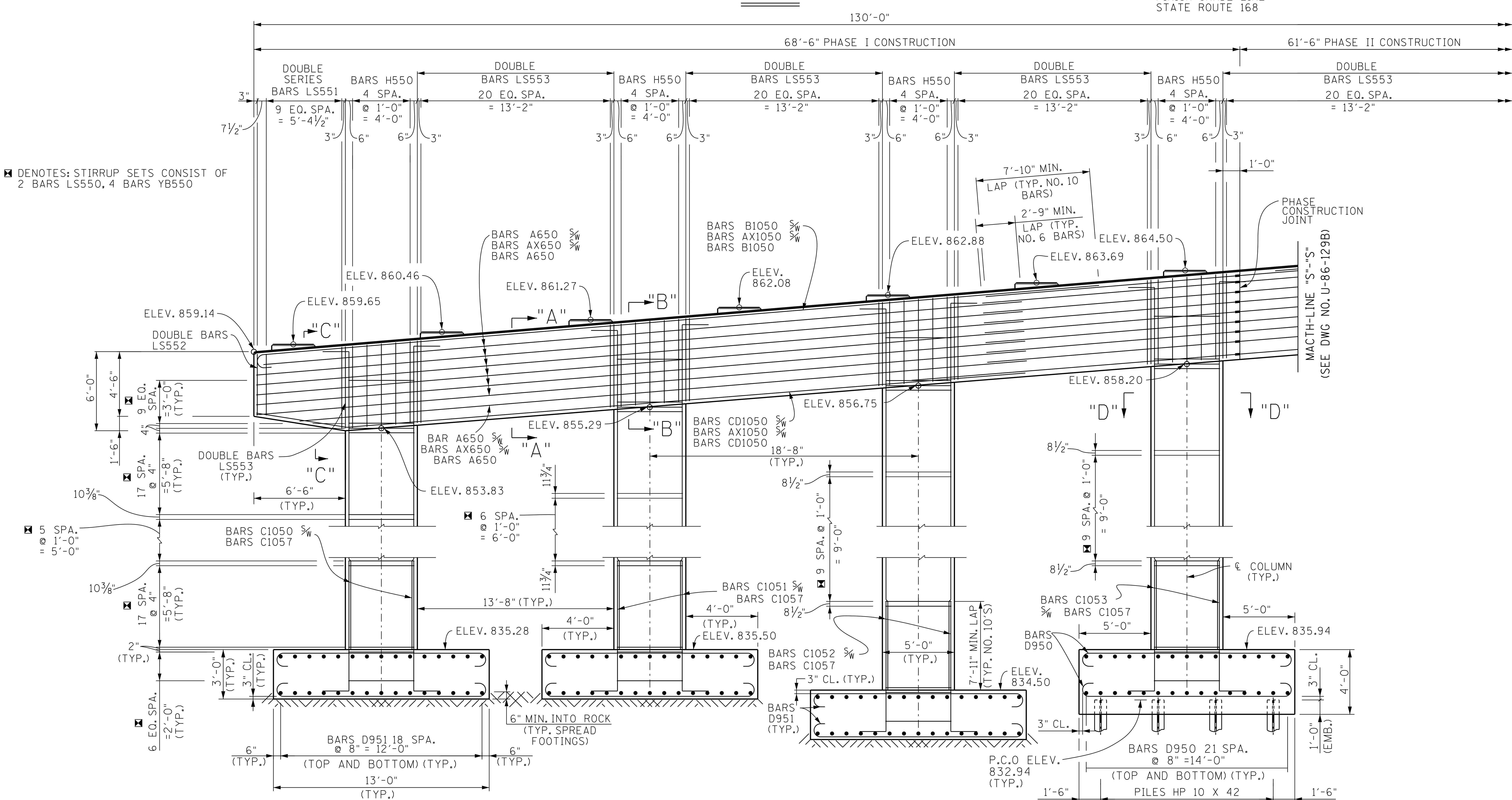

ELEVATION

(LOOKING FORWARD ON SURVEY)

GENERAL NOTES

NOTE: WHEN POURING CAP BEAM, PROVISIONS SHALL BE MADE FOR SETTING ANCHOR BOLTS. SEE STANDARD DRAWING STD-6-1. BOLT PROJECTION 11".

NOTE: RISER BLOCKS TO BE POURED MONOLITHICALLY WITH CAP BEAM.

NOTE: ELASTOMERIC PADS SHALL BE IN PLACE A MINIMUM OF ONE DAY BEFORE BEING DISTURBED BY SETTING BEAMS ON CONCRETE. PLACE RUBBER BONDING CEMENT IN SUCH A WAY THAT VISIBLE CONCRETE SUFACES WILL NOT BE STAINED.

NOTE: COLUMN STEEL TO EXTEND 5'-6" INTO CAP BEAM.

NOTE: SEE DWG. NO. U-86-132 FOR SECTIONS "A"-"A", "B"-"B", "C"-"C", "D"-"D" AND PLAN OF FOOTING.

ESTIMATED QUANTITIES		
	CLASS "A" CONCRETE (BRIDGES) C.Y.	STEEL BAR REINFORCEMENT (BRIDGES) L.B.
BENT NO. 1	414	104,318

ADAM L. PRICE — STATE OF TENNESSEE

04-10-2019

STATE OF TENNESSEE
DEPARTMENT OF TRANSPORTATION

BRIDGE NO. 2
BENT NO. 1
STATE ROUTE 115
OVER
STATE ROUTE 168
STATION 143+76.54
KNOX COUNTY
2018

CORRECT ______ ENGINEER OF STRUCTURES

DESIGNED BY	ALI OMAR	DATE	08-15
DRAWN BY	B. ERVIN	DATE	01-18
SUPERVISED BY	ADAM PRICE	DATE	01-18
CHECKED BY	DAWOD ABDULLAH	DATE	11-17

U-86-129A

4/8/2019
P:\Cadd User Group Regions I and 2\Billy Ervin\180 SR 115 over SR 168, Knox Co. 2017\BP1180.dgn

BP1180.DGN

CONST. NO. 47026-3281-14

PROJECT NO.	YEAR	SHEET NO.
STP/NH-115(27)	2018	

REVISIONS

NO.	DATE	BY	BRIEF DESCRIPTION
1	4-5-19	ALP	GENERAL REVISIONS

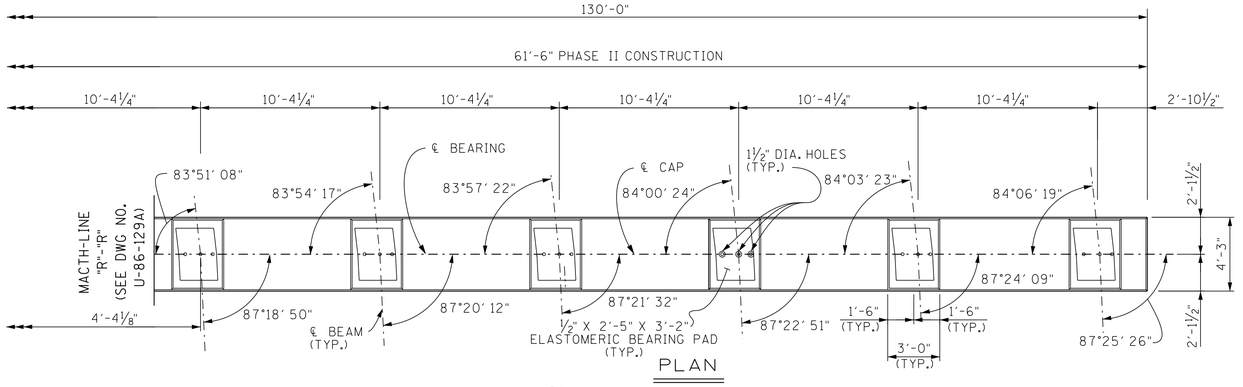

PLAN

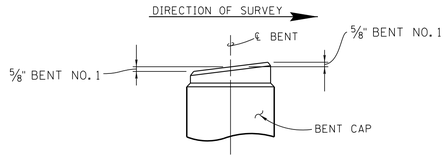

RISER BLOCK SLOPE DETAIL

(RISER BLOCK BEARING SURFACE TO CONFORM TO BOTTOM OF BEAM GRADE.)

▣ DENOTES: STIRRUP SET CONSIST OF 2 BARS LS550, 4 BARS YB550

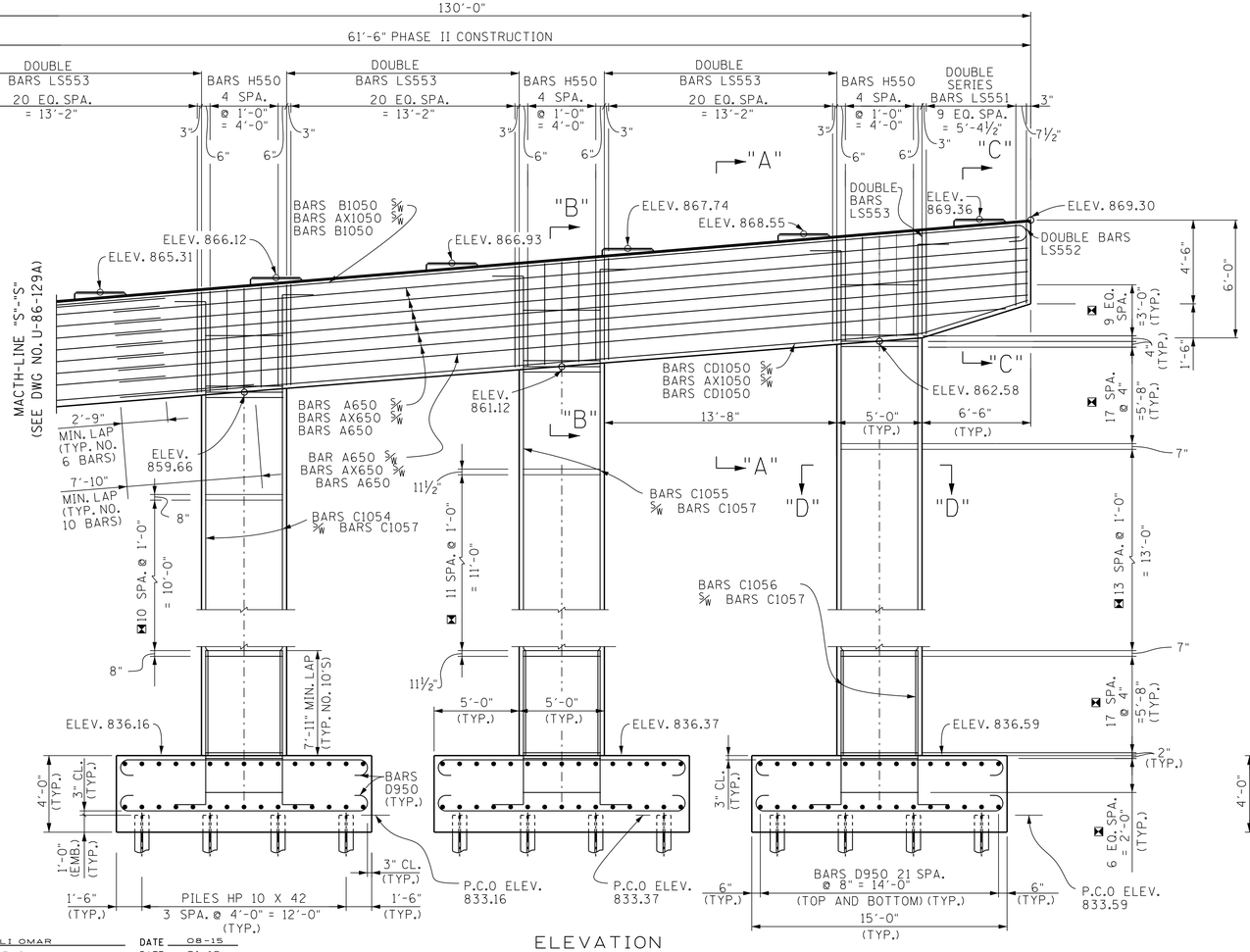

ELEVATION

(LOOKING FORWARD ON SURVEY)

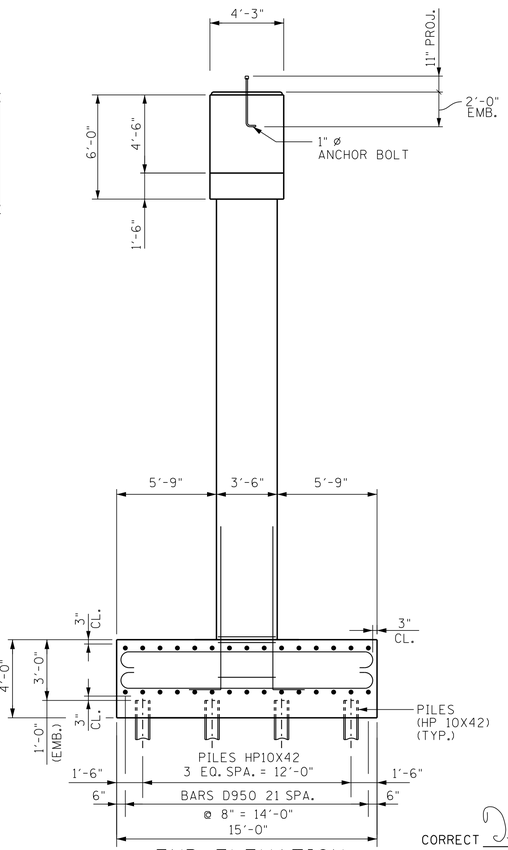

END ELEVATION

04-10-2019

STATE OF TENNESSEE
DEPARTMENT OF TRANSPORTATION

BRIDGE NO. 2
BENT NO. 1 DETAILS
STATE ROUTE 115
OVER
STATE ROUTE 168
STATION 143+76.54
KNOX COUNTY
2018

⚠1

CORRECT

ENGINEER OF STRUCTURES

DESIGNED BY ALI OMAR	DATE 08-15
DRAWN BY B. ERVIN	DATE 01-18
SUPERVISED BY ADAM PRICE	DATE 01-18
CHECKED BY DAWOD ABDULLAH	DATE 11-17

U-86-129B

4/8/2019
P:\Cadd User Group Regions (and D\Billy Ervin\180 SR 115 over SR 168, Knox Co. 2017\BP1180.dgn

BP1180.DGN

CONST. NO. 47026-3281-14

PROJECT NO.	YEAR	SHEET NO.
STP/NH-115(27)	2018	

REVISIONS

NO.	DATE	BY	BRIEF DESCRIPTION
1	4-5-19	ALP	GENERAL REVISIONS

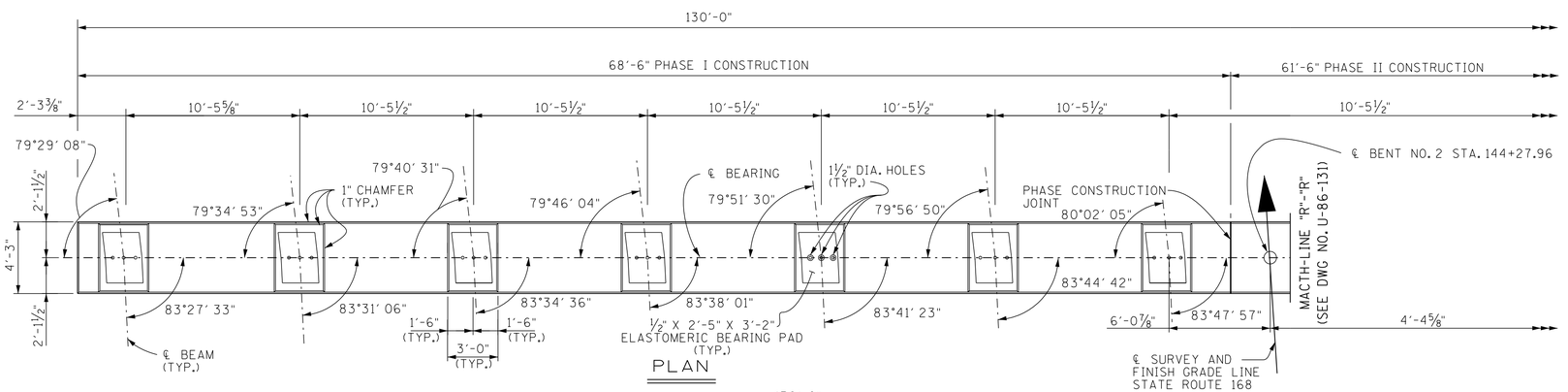

PLAN

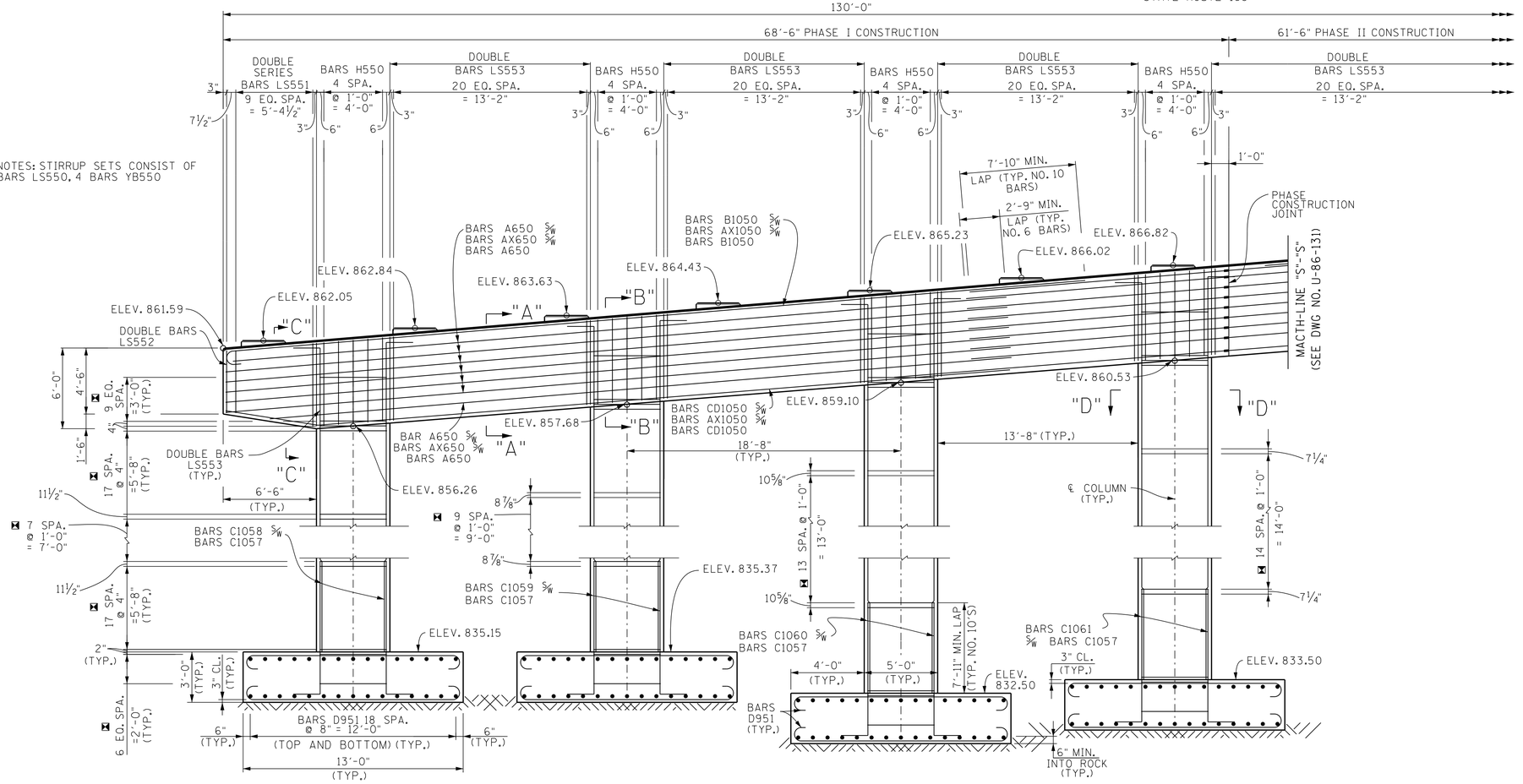

ELEVATION
(LOOKING FORWARD ON SURVEY)

GENERAL NOTES

NOTE: WHEN POURING CAP BEAM, PROVISIONS SHALL BE MADE FOR SETTING ANCHOR BOLTS. SEE STANDARD DRAWING STD-6-1. BOLT PROJECTION 11".

NOTE: RISER BLOCKS TO BE POURED MONOLITHICALLY WITH CAP BEAM.

NOTE: ELASTOMERIC PADS SHALL BE IN PLACE A MINIMUM OF ONE DAY BEFORE BEING DISTURBED BY SETTING BEAMS ON CONCRETE. PLACE RUBBER BONDING CEMENT IN SUCH A WAY THAT VISIBLE CONCRETE SUFACES WILL NOT BE STAINED.

NOTE: COLUMN STEEL TO EXTEND 5'-6" INTO CAP BEAM.

NOTE: SEE DWG. NO. U-86-132 FOR SECTIONS "A"-"A", "B"-"B", "C"-"C", "D"-"D" AND PLAN OF FOOTING.

ESTIMATED QUANTITIES

	CLASS "A" CONCRETE (BRIDGES) C.Y.	STEEL BAR REINFORCEMENT (BRIDGES) L.B.
BENT NO. 2	384	104,467

ADAM L. PRICE — 931 — STATE OF TENNESSEE — DEPARTMENT OF AGRICULTURE — REGISTERED LANDSCAPE ARCHITECT
04-10-2019

STATE OF TENNESSEE
DEPARTMENT OF TRANSPORTATION
BRIDGE NO. 2
BENT NO. 2
STATE ROUTE 115
OVER
STATE ROUTE 168
STATION 143+76.54
KNOX COUNTY
2018

CORRECT — ENGINEER OF STRUCTURES

DESIGNED BY ALI OMAR DATE 08-15
DRAWN BY B. ERVIN DATE 01-18
SUPERVISED BY ADAM PRICE DATE 01-18
CHECKED BY DAWOD ABDULLAH DATE 11-17

U-86-130

4/8/2019
P:\Cadd User Group Regions I and 2\Billy Ervin\180 SR 115 over SR 168, Knox Co. 2017\BP180.dgn

BP1180.DGN

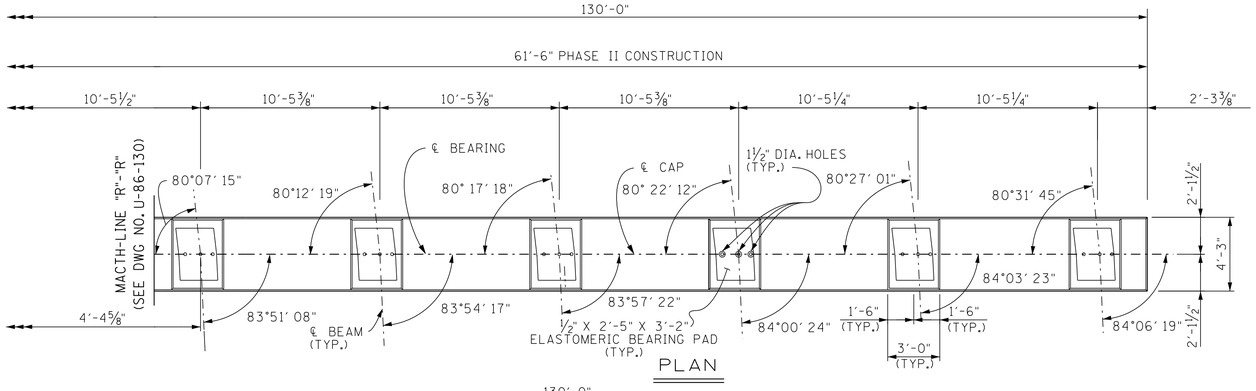

PLAN

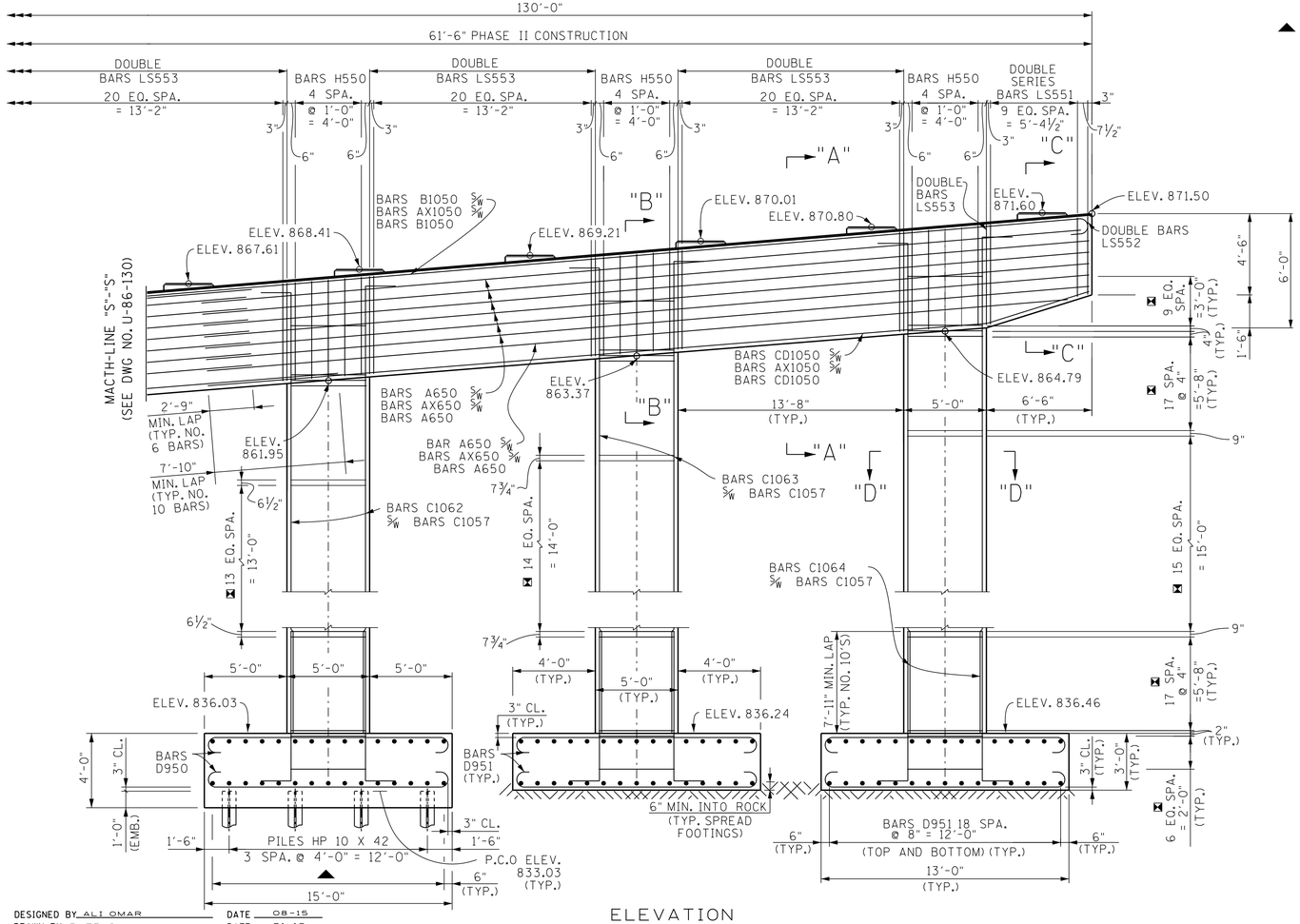

ELEVATION

(LOOKING FORWARD ON SURVEY)

▣ DENOTES: STIRRUP SET CONSIST OF 2 BARS LS550, 4 BARS YB550

▲ DENOTES: BARS D950 21 SPA. @ 8" = 14'-0" (TOP AND BOTTOM) (TYP.)

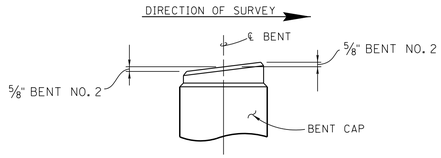

RISER BLOCK SLOPE DETAIL

(RISER BLOCK BEARING SURFACE TO CONFORM TO BOTTOM OF BEAM GRADE.)

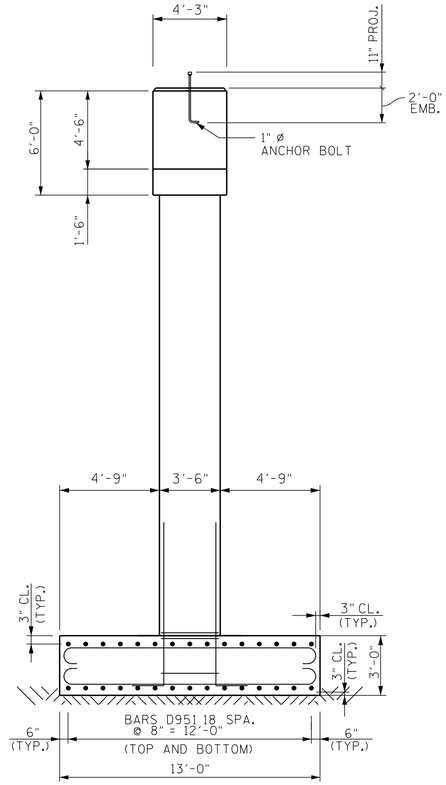

END ELEVATION

CONST. NO. 47026-3281-14

PROJECT NO.	YEAR	SHEET NO.
STP/NH-115(27)	2018	

REVISIONS

NO.	DATE	BY	BRIEF DESCRIPTION
1	4-5-19	ALP	GENERAL REVISIONS

ADAM L. PRICE — LICENSED PROFESSIONAL ENGINEER — STATE OF TENNESSEE

04-10-2019

STATE OF TENNESSEE
DEPARTMENT OF TRANSPORTATION

BRIDGE NO. 2
BENT NO. 2 DETAILS
STATE ROUTE 115
OVER
STATE ROUTE 168
STATION 143+76.54
KNOX COUNTY
2018

1

CORRECT Jed A Kmiazewyz
ENGINEER OF STRUCTURES

DESIGNED BY ALI OMAR DATE 08-15
DRAWN BY B. ERVIN DATE 01-18
SUPERVISED BY ADAM PRICE DATE 01-18
CHECKED BY DAWOD ABDULLAH DATE 11-17

U-86-131

4/8/2019
P:\Cadd User Group Regions I and 2\Billy Ervin\180 SR 115 over SR 168, Knox Co. 2017\BP1180.dgn

BP1180.DGN

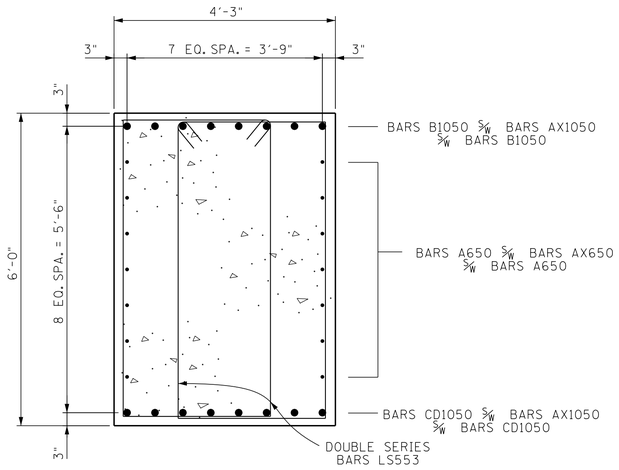

SECTION "A"-"A"

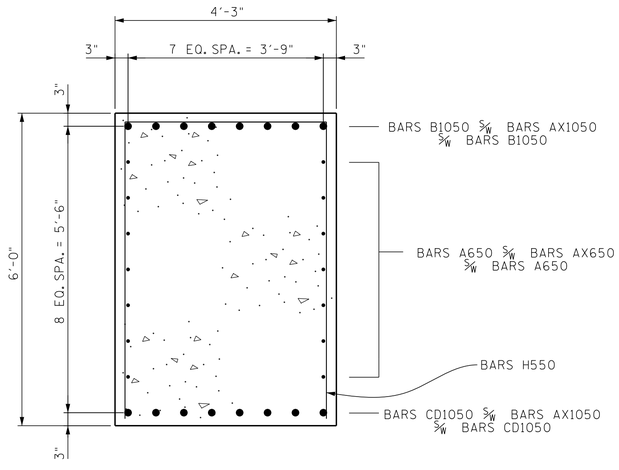

SECTION "B"-"B"

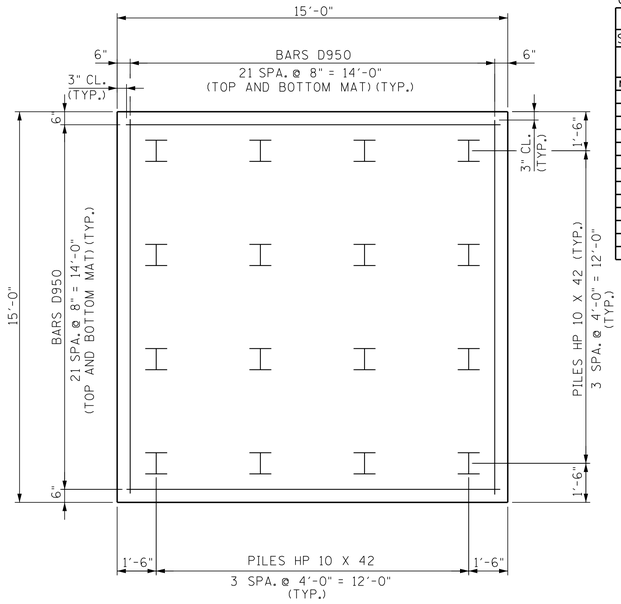

PLAN OF PILE FOOTING

CONST. NO. 47026-3281-14

PROJECT NO.	YEAR	SHEET NO.
STP/NH-115(27)	2018	

REVISIONS

NO.	DATE	BY	BRIEF DESCRIPTION
1	4-5-19	ALP	GENERAL REVISIONS

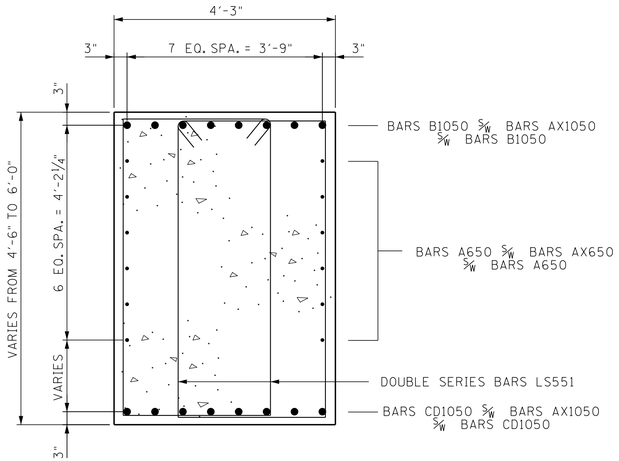

SECTION "C"-"C"

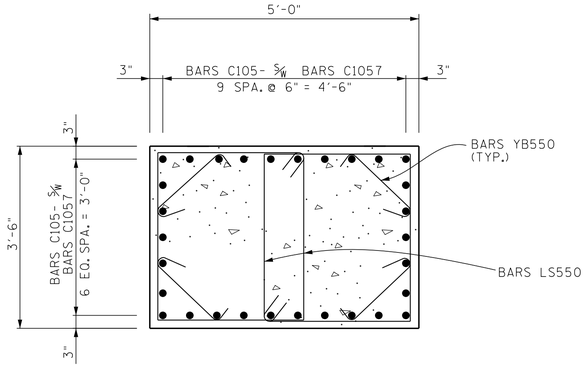

SECTION "D"-"D"

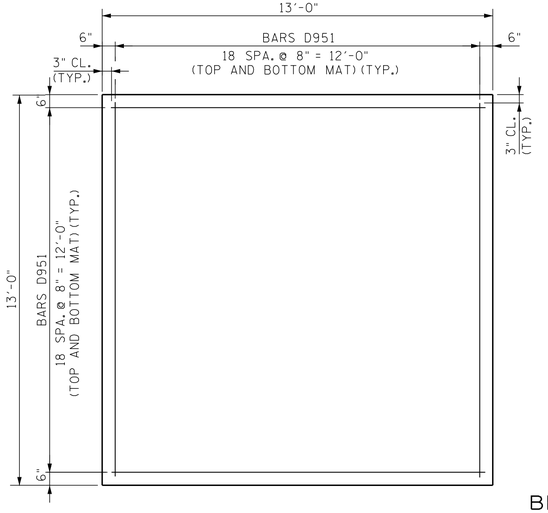

PLAN OF SPREAD FOOTING

ADAM L. PRICE
LICENSED PROFESSIONAL ENGINEER
No. 115
AGRICULTURE
STATE OF TENNESSEE
04-10-2019

STATE OF TENNESSEE
DEPARTMENT OF TRANSPORTATION

BRIDGE NO. 2
BENT NOS. 1 AND 2 DETAILS
STATE ROUTE 115
OVER
STATE ROUTE 168
STATION 143+76.54
KNOX COUNTY
2018

CORRECT
ENGINEER OF STRUCTURES

DESIGNED BY	ALI OMAR	DATE 08-15
DRAWN BY	B. ERVIN	DATE 01-18
SUPERVISED BY	ADAM PRICE	DATE 01-18
CHECKED BY	DAWOD ABDULLAH	DATE 11-17

U-86-132

4/8/2019
P:\Cadd User Group Regions (and 2\Billy Ervin\1180 SR 115 over SR 168, Knox Co, 2017\BP1180.dgn

FF1180.DGN

CONST. NO. 47026-3281-14

PROJECT NO.	YEAR	SHEET NO.
STP/NH-115(27)	2018	

REVISIONS

NO.	DATE	BY	BRIEF DESCRIPTION
1	4-5-19	ALP	GENERAL REVISIONS

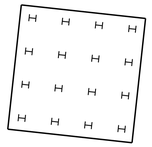

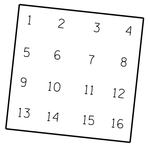

DETAIL "A"

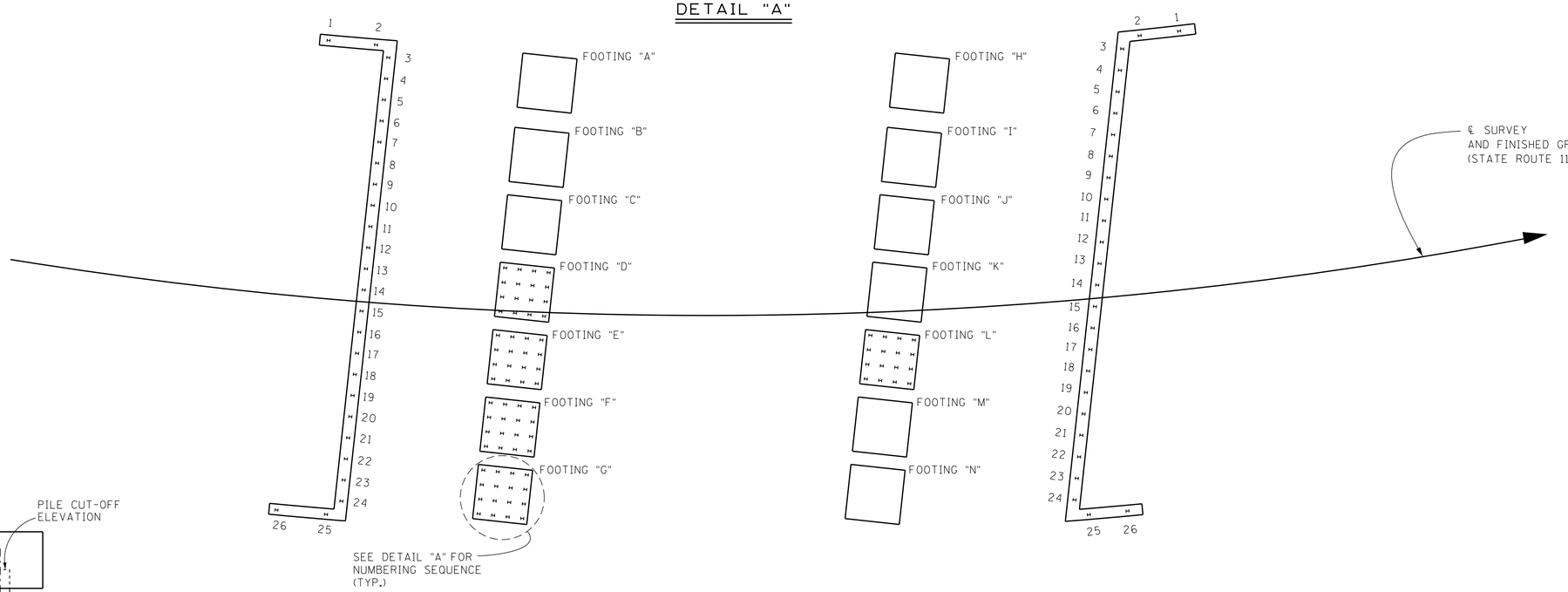

ABUTMENT NO. 1

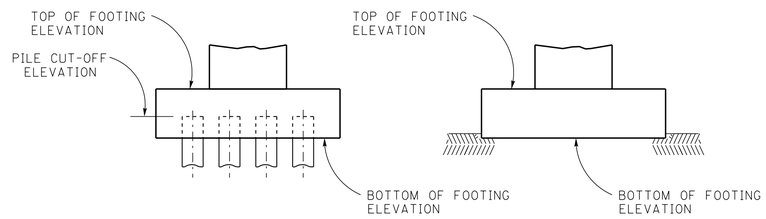

BENT NO. 1

TOP OF FOOTING ELEVATION
FOOTING "D" _____
FOOTING "E" _____
FOOTING "F" _____
FOOTING "G" _____

BOTTOM OF FOOTING ELEVATION
FOOTING "D" _____
FOOTING "E" _____
FOOTING "F" _____
FOOTING "G" _____

TOP OF FOOTING ELEVATION
FOOTING "A" _____
FOOTING "B" _____
FOOTING "C" _____

BOTTOM OF FOOTING ELEVATION
FOOTING "A" _____
FOOTING "B" _____
FOOTING "C" _____

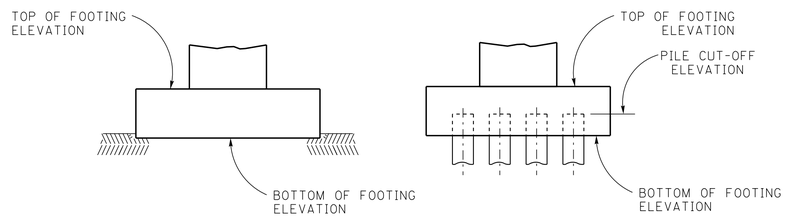

BENT NO. 2

TOP OF FOOTING ELEVATION
FOOTING "H" _____
FOOTING "I" _____
FOOTING "J" _____
FOOTING "K" _____
FOOTING "M" _____
FOOTING "N" _____

BOTTOM OF FOOTING ELEVATION
FOOTING "H" _____
FOOTING "I" _____
FOOTING "J" _____
FOOTING "K" _____
FOOTING "M" _____
FOOTING "N" _____

TOP OF FOOTING ELEVATION
FOOTING "L" _____

BOTTOM OF FOOTING ELEVATION
FOOTING "L" _____

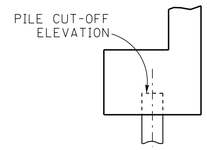

ABUTMENT NO. 2

STATE OF TENNESSEE
DEPARTMENT OF TRANSPORTATION

BRIDGE NO. 2
FINAL FOUNDATION DATA
STATE ROUTE 115
OVER
STATE ROUTE 168
STATION 143+76.54
KNOX COUNTY
2018

1

CORRECT _____ ENGINEER OF STRUCTURES

DESIGNED BY ALI OMAR DATE 08-15
DRAWN BY B. ERVIN DATE 01-18
SUPERVISED BY MARTINKO/PRICE DATE 01-18
CHECKED BY DAWOD ABDULLAH DATE 11-17

U-86-133

4/8/2019
P:\Cadd User Group Regions I and 2\Billy Ervin\180 SR 115 over SR 168, Knox Co. 2017\FF1180.dgn

FF1180.DGN

CONST. NO. 47026-3281-14

PROJECT NO.	YEAR	SHEET NO.
STP/NH-115(27)	2018	

REVISIONS

NO.	DATE	BY	BRIEF DESCRIPTION
1	4-5-19	ALP	GENERAL REVISIONS

TABLE SHOWING PILE NUMBERS, PILE CUT-OFF ELEVATIONS, PILE TIP ELEVATIONS, AND PILE LENGTHS

		1	2	3	4	5	6	7	8	9	10	11	12	13	14	15	16	17	18	19	20	21	22	23	24	25	26
ABUTMENT NO. 1	PILE CUT-OFF ELEV.																										
	PILE TIP ELEV.																										
	IN PLACE PILE LENGTH																										
BENT NO. 1 FOOTING "D"	PILE CUT-OFF ELEV.																										
	PILE TIP ELEV.																										
	IN PLACE PILE LENGTH																										
BENT NO. 1 FOOTING "E"	PILE CUT-OFF ELEV.																										
	PILE TIP ELEV.																										
	IN PLACE PILE LENGTH																										
BENT NO. 1 FOOTING "F"	PILE CUT-OFF ELEV.																										
	PILE TIP ELEV.																										
	IN PLACE PILE LENGTH																										
BENT NO. 1 FOOTING "G"	PILE CUT-OFF ELEV.																										
	PILE TIP ELEV.																										
	IN PLACE PILE LENGTH																										
BENT NO. 2 FOOTING "L"	PILE CUT-OFF ELEV.																										
	PILE TIP ELEV.																										
	IN PLACE PILE LENGTH																										
ABUTMENT NO. 2	PILE CUT-OFF ELEV.																										
	PILE TIP ELEV.																										
	IN PLACE PILE LENGTH																										

NOTE TO CONTRACTOR AND CONSTRUCTION OFFICE:
THE BLANKS ON THIS SHEET AND SHEET U-86-133 ARE TO BE FILLED IN BY THE CONSTRUCTION OFFICE AND/OR FIELD ENGINEER GIVING AS BUILT CONDITIONS. AFTER COMPLETION, IT IS TO BE SENT TO THE DIVISION OF STRUCTURES TO BECOME PART OF FINAL BRIDGE DOCUMENTS.

STATE OF TENNESSEE
DEPARTMENT OF TRANSPORTATION

BRIDGE NO. 2
FINAL FOUNDATION DATA
STATE ROUTE 115
OVER
STATE ROUTE 168
STATION 143+76.54
KNOX COUNTY
2018

CORRECT _____
ENGINEER OF STRUCTURES

DESIGNED BY ALI OMAR DATE 08-15
DRAWN BY B. ERVIN DATE 01-18
SUPERVISED BY MARTINKO/PRICE DATE 01-18
CHECKED BY DAWOD ABDULLAH DATE 11-17

U-86-134

4/8/2019
P:\Cadd User Group Regions 1and 2\Billy Ervin\180 SR 115 over SR 168, Knox Co, 2017\FF180.dgn